

Synthesis, characterization and reactivity of transition metal clusters and their role towards organic transformation

Thesis submitted in partial fulfillment of the requirements for the degree of

Doctor of Philosophy

by

Sumanta Kumar Patel

Under the guidance of

Dr. Saurav Chatterjee



**DEPARTMENT OF CHEMISTRY
NATIONAL INSTITUTE OF TECHNOLOGY, ROURKELA
ROURKELA-769008, ODISHA, INDIA**



CERTIFICATE

This is to certify that the thesis entitled “**Synthesis, characterization and reactivity of transition metal clusters and their role towards organic transformation**” being submitted by Sumanta Kumar Patel to the National Institute of Technology, Rourkela, India, for the award of the degree of **Doctor of Philosophy** is a record of bonafide research work carried out by him under my supervision and guidance. I am satisfied that the thesis has reached the standard fulfilling the requirements of the regulations relating to the nature of the degree. To the best of my knowledge, the matter embodied in the thesis has not been submitted to any other University / Institute for the award of any Degree or Diploma.

Supervisor

Place: Rourkela
Date:

Dr. Saurav Chatterjee,
Department of Chemistry,
National Institute of Technology, Rourkela
Odisha-769008, India

ABSTRACT

Transition metal cluster containing main group atoms as bridging ligands have drawn increased attention in recent years, mainly because of their unusual structures and novel chemical reactivity, as well as for their potential in the field of material science and catalysis. In the last three decades, varieties of synthetic methodologies have been developed for the synthesis of metal clusters containing chalcogens with unique structural features and properties. The chalcogen ligands have been known to act as bridging units and support the metal fragments in various cluster growth reactions. Designing of systematic synthetic routes to clusters containing metal-chalcogen bonds with new geometries and coordination modes led to the development of models and precursors for the synthesis of new materials. Some of these metal-chalcogen containing building blocks have been of great interest due to their unusual structural features and tunable opto-electronic properties. Moreover, mixed-metal clusters have also been of tremendous importance due to their use as valuable precursors for the preparation of supported bimetallic and multimetallic heterogeneous catalysts. In view of the enormous potential of transition metal clusters, we started our investigation to synthesise novel chalcogenide transition metal clusters containing ligands like phosphines, carbonyls, acetylides, alkynes etc. and understand their role in supporting cluster molecules and to explore the reactivity of metal clusters towards cluster growth reactions. Structural diversity of transition metal clusters can be achieved by using different types of ligands that play an important role to support the cluster framework and assist in the tuning of the cluster behaviour. This has prompted us to design transition metal cluster containing diphosphine groups of varied chain length and understand their potential in linking cluster cluster molecule. Furthermore, phosphines are one of the most widely utilized ligands in transition metal complex chemistry due to their extreme versatility in bonding and reactivity. Most of these diphosphine ligands have been found to adopt a variety of bonding modes on the cluster framework, including monodentate with a pendant phosphine center, chelating a single metal atom in the multimetallic cluster, bridging across a metal-metal bond and forming an intermolecular link across two clusters. The bonding modes adopted by these diphosphine ligands are influenced by the flexibility and length of the organic or organometallic backbone. In an effort to prepare novel clusters with structural identity, we sought to explore the possibility of incorporating both diphosphine ligands and chalcogen atoms in the cluster framework and study

their combined effect. We have been able to synthesize several homo- and hetero-metallic transition metal clusters containing chalcogens and diphosphines as supporting ligands. To understand the influence of different diphosphine ligands towards metal chalcogenide clusters we studied the reaction of triiron ditelluride carbonyl cluster and triironditelluride phosphine cluster with two different diphosphine ligands, bis(diphenylphosphino)methane and bis(diphenylphosphino)ethane. Synthesis and characterization of four new iron-palladium mixed metal clusters containing diphosphine ligand have been carried out and shows interesting bonding features and coordination modes. The contrasting results show the difference in reactivity between the cluster species and the influence of phosphines in controlling the cluster synthesis. Our aim has also been to synthesize complexes containing several metal binding sites for the synthesis of multimetallic system. In an effort to synthesize such molecules we have focussed our study on the preparation of dithiocarboxylate-alkyne metal complexes by sunlight mediated reaction process and use them to obtain multimetallic complexes. A variety of organic transformations are supported and catalysed by metal complexes, wherein the necessary steric and electronic requirements for such transformations are offered by the metal centres and ligands. To understand the exact behaviour of the synthesized molecule on this front some investigation on the metal mediated transformation of different alkynes was undertaken.

Keywords: Transition metal cluster, Diphosphine cluster, Carbonyl cluster, Homometallic, Heterometallic, Transformation, Chalcogenide clusters, Metal-metal bonds, Alkyne-cobalt adduct, Cluster growth reaction, Insertion of carbondisulfide.

CONTENTS

	Page
CHAPTER 1 INTRODUCTION	9
1.1 TRANSITION METAL CLUSTERS WITH METAL –METAL BOND	10
1.2 TYPES OF METAL-METAL BOND IN TRANSITION METAL CLUSTER	13
1.2.1 Clusters containing metal-metal single bond	13
1.2.2 Cluster containing metal-metal double bond	14
1.2.3 Cluster containing metal-metal triple bond	15
1.2.4 Cluster having quadruple metal-metal bond	16
1.3 TYPES OF TRANSITION METAL CLUSTERS BASED ON LIGANDS	18
1.3.1 Cluster containing carbonyl ligands	18
1.3.2 Cluster containing hydride ligand	22
1.3.3 Cluster containing phosphine ligand	26
1.3.4 Cluster containing phosphido Ligands	33
1.3.5 Phosphinidene ligands	34
1.3.6 Cluster containing alkenes and alkynes ligand	35
1.3.7 Cluster with cyclopentadienyl ligands	37
1.3.8 Cluster containing oxo ligands	40
1.3.9 Cluster containing acetylide ligands	42
1.3.10 Cluster containing other bridging ligands	45

1.4	TRANSITION METAL CLUSTERS CONTAINING MAIN GROUP ELEMENTS	47
1.5	APPLICATION OF TRANSITION METAL CLUSTER	54
1.5.1	Catalysis by metal cluster compounds	55
1.5.2	Metal cluster mediated Organic transformation	59
1.5.3	Transition metal cluster to Nanocluster	62
1.5.4	Nonlinear Optical Properties	63
1.5.5	Potential use of some metal clusters as hydrogen storage materials	65
1.6	CONCLUSIONS	68
1.7	REFERENCES	69
CHAPTER 2	SYNTHESIS AND CHARACTERIZATION OF HOMOMETALLIC CHALCOGENIDE PHOSPHINE CLUSTERS.	77
2.1.	INTRODUCTION	78
2.2.	RESULTS AND DISCUSSION	83
2.2.1.	Reaction of iron-telluride cluster with Bis-diphenylphosphino methane	83
2.2.2.	Reaction of iron-telluride cluster with Bis-diphenylphosphino ethane (dppe)	86
2.3.	EXPERIMENTAL SECTIONS	91
2.3.1.	General Procedures	91
2.3.2	Reaction of $[\text{Fe}_3\text{Te}_2(\text{CO})_8(\text{PPh}_3)]$ (2) with Bis-(diphenylphosphino)methane	91
2.3.3	Synthesis of $[\text{Fe}_6(\mu_3\text{-Te})_4(\text{CO})_{18}\{\mu\text{-PPh}_2(\text{CH}_2)_2\text{PPh}_2\}]$ (5)	92

2.3.4	Reaction of $[\text{Fe}_3(\mu_3\text{-Te})_2(\text{CO})_8(\text{PPh}_3)]$ (2) with Bis-(diphenylphosphino)ethane	92
2.3.5	Crystal structure determination for 4, 5 and 6	93
2.4	CONCLUSIONS	93
2.5	REFERENCES	96
CHAPTER 3	SYNTHESIS, CHARACTERIZATION AND REACTIVITY OF CHALCOGEN CONTAINING IRON-PALLADIUM MIXED METAL PHOSPHINE CLUSTERS	98
3.1	INTRODUCTION	99
3.2	RESULTS AND DISCUSSIONS	104
3.3	EXPERIMENTAL SECTIONS	110
3.3.1	General Procedures	110
3.3.2	Reaction of $[\text{Fe}_3\text{Y}_2(\text{CO})_9]$ (Y = S, Se, Te) with $\text{Pd}(\text{PPh}_3)_4$ in presence of $\text{TMNO} \cdot 2\text{H}_2\text{O}$	111
3.3.3	Reaction of $[\text{Fe}_2\text{Y}_2\text{Pd}(\text{CO})_6(\text{PPh}_3)_2](\text{Y}=\text{Se},\text{Te})$ with Bis-diphenylphosphino)methane	112
3.3.4	Reaction of $[(\text{CO})_6\text{Fe}_2(\mu_3\text{-Y})_2\text{Pd}(\text{PPh}_3)_2](\text{Y}=\text{Se}, \text{Te})$ with Bis-(diphenylphosphino)ethane	112
3.3.5	Crystal structure determinationfor 6, 9 and10	113
3.4	CONCLUSIONS	114
3.5	REFERENCES	116

CHAPTER 4	SUNLIGHT DRIVEN SYNTHESIS OF METAL DITHIOCARBOXYLATE-ALKYNE COMPLEXES AND THEIR SPECTROSCOPIC AND STRUCTURAL CHARACTERIZATION	120
4.1	INTRODUCTION	121
4.2	RESULTS AND DISCUSSION	125
4.2.1.	DFT Calculations	130
4.2.1.1	Molecular Geometry Optimization of 6	130
4.2.1.2	Electronic Spectrum and its Correlation with Spectroscopic Transitions	131
4.2.1.3	Electron Charge Density Calculation	134
4.3	EXPERIMENTAL SECTIONS	135
4.3.1	General Procedures	135
4.3.2.	Reaction of $[LM(CO)_n C \equiv CR] \{L = \eta^5-C_5H_5, \eta^5-C_5Me_5; M = Mo, W, Fe;$ $R = -C(CH_3)=CH_2, Ph; n = 3, 2\}$ with CS_2	135
4.3.3	Crystal structure determination for 5 and 6	136
4.3.4	Computational details	136
4.4	CONCLUSIONS	139
4.5	REFERENCES	139
CHAPTER 5	SYNTHESIS OF TRIMETALLIC- DITHIOCARBOXYLATE COMPLEX AND METAL MEDIATED TRANSFORMATIONS OF FERROCENYL AND DITHIOCARBOXALATE-ALKYNES	143
5.1	INTRODUCTION	144
5.2	RESULTS AND DISCUSSION	149

5.2.1	Reaction of dithiocarboxylate-alkyne with $\text{Co}_2(\text{CO})_8$	149
5.2.2	Transformation of $[(\eta^5\text{-C}_5\text{Me}_5)\text{Fe}(\text{CO})(\eta^2\text{-S}_2\text{C})\text{C}\equiv\text{CPh}]$ (4) to a dithioleheterocycle	151
5.2.3	Coupling of ferrocenyl alkynes by $[(\text{CO})_8\text{Fe}_3\text{Se}_2(\text{PPh}_3)]$ cluster	153
5.3	EXPERIMENTAL SECTIONS	155
5.3.1	General Procedures	155
5.3.2	Reaction of $[\text{LM}(\text{CO})_n(\eta^2\text{-S}_2\text{C})\text{C}\equiv\text{CR}]$; $\{\text{L}=\eta^5\text{-C}_5\text{H}_5, \text{M} = \text{W}, \text{R} = \text{-C}(\text{CH}_3)=\text{CH}_2, n = 2\}$ (3); $\{\text{L}=\eta^5\text{-C}_5\text{Me}_5, \text{M} = \text{Fe}, \text{R} = \text{Ph}, n = 1\}$ (4)] with dicobaltoctacarbonyl	155
5.3.3	Reaction of $[(\eta^5\text{-C}_5\text{Me}_5)\text{Fe}(\text{CO})(\eta^2\text{-S}_2\text{C})\text{CCPh}(\text{Co}_2\text{CO}_6)]$ (6) with triphenylphosphine	156
5.3.4	Synthesis of dithione-thioleheterocycle	156
5.3.5	Photolytic reaction of ferrocenyl alkynes with $[(\text{CO})_8\text{Fe}_3\text{Se}_2(\text{PPh}_3)]$	156
5.3.6	Crystal structure determination for 8.	157
5.4	CONCLUSIONS	157
5.5	REFERENCES	159
	SUMMARY	162
	ACKNOWLEDGEMENTS	165
	BIODATA	166

CHAPTER 1
INTRODUCTION

1.1. TRANSITION METAL CLUSTER WITH METAL –METAL BONDS

In transition metal cluster two or more metal atoms are bound together by direct and substantial metal-metal bonds to form a three dimensional polyhedral geometry. A large variety of organometallic transition metal clusters are known containing homo or hetero metal atoms, a range of terminal and bridging ligands and with numerous unique structural geometry. Cluster compounds are of immense interest because of their structural diversity and potential applications in the field of catalysis and material science. Transition metal clusters play a fundamental role in bridging the gap between homogeneous and heterogeneous catalysis to improve the activity and selectivity of the catalysts.¹ In the last two decades, polynuclear metal clusters have proved to be useful precursors for the preparation of novel catalyst. Some cluster complexes have been reported for their presence in biological environment, for example in enzymes such as nitrogenase and their activity in biocatalysis.² Interest has also been known in the area of material science and in advanced opto-electronic materials for their non-linear optical property.³

Organometallic clusters are mostly rich in carbonyl ligands and have been found to bind with metals in a variety bonding modes. Cluster containing other ligands like phosphines, isocyanides, hydrides etc. are also known extensively. Some transition metal clusters contains π -donor ligand for example cyclopentadienyl, alkene, alkyne and usually termed as π -donor cluster have interesting and varied structural features. Whereas, ligands like carbonyl and phosphines having π -accepter property often, create the most favorable condition for metal-metal bond formation and substantial overlap between the atomic orbital of the metals. Cluster chemistry has also been important for the cluster–surface analogy, in which the cluster complexes resemble the surface chemistry of metal particles due to the presence of arrays of metal atoms in both cluster and metal surface. The metal-metal bonds are often comparable to those in metal particles, but the presence of ligand environment in transition metal cluster increases the effective interaction among the metals.

Bimetallic clusters with two identical metals consist of metal-metal bonds involving d_z^2 , d_{xy} , d_{xz} , d_{yz} and $d_{x^2-y^2}$ orbitals for the metal – metal interaction. Different types of d- orbital interactions are possible depending on the number of valence electrons available in these orbitals

such as coaxial (σ) interaction, lateral (π and δ) interactions as shown in(Figure 1.1. The d_z^2 orbital of each metal coaxially overlap to make the σ bond whereas d_{xz} and d_{yz} orbitals of each metal can laterally overlap to give rise to π bonds. The d_{xy} and $d_{x^2-y^2}$ orbitals can overlap according to lateral mode to form the δ bond.

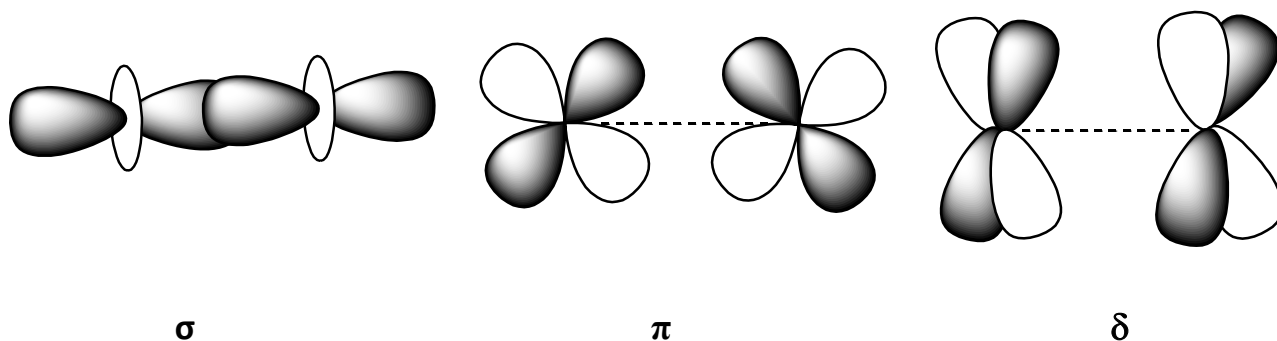


Figure 1.1

The δ bond type overlap is much weaker than the other ones, and the energy of the molecular orbital involved is higher than those of the σ and π molecular orbitals (Figure 1.2).

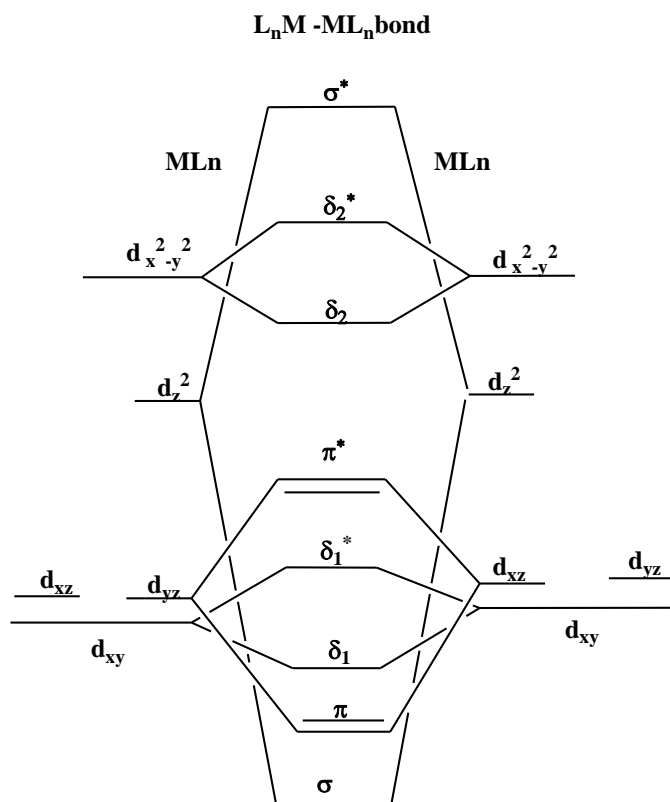


Figure 1.2 Molecular orbital diagram for the metal-metal bond in bimetallic complexes

The order of the metal-metal bond depends upon the number of electrons and the sequence of filling of the orbital levels as shown in Table 1.1.

Table 1.1

n	Electronic structure	Bond type			Bond Order
		σ	π	δ	
2	$(\sigma)^2$	1	0	0	1
4	$(\sigma)^2(\pi)^2$	1	1	0	2
6	$(\sigma)^2(\pi)^4$	1	2	0	3
8	$(\sigma)^2(\pi)^4(\delta)^2$	1	2	1	4
10	$(\sigma)^2(\pi)^4(\delta)^2(\delta)^*$	1	2	0	3
12	$(\sigma)^2(\pi)^4(\delta)^2(\delta^*)^2(\pi^*)^2$	1	1	0	2
14	$(\sigma)^2(\pi)^4(\delta)^2(\delta^*)^2(\pi^*)^4$	1	0	0	1

Formation of single metal-metal bond can be possible with metals each having 1 or 7 valence electrons, a double bond with metals each containing 2 or 6 electrons, a triple bond with metals possessing 3 or 5 electrons and a quadruple bond with metals each having 4 electrons. The metal - metal bond distances can vary between 2 Å and 3.5 Å depending upon the ligands and the structural integrity of the metal cluster. The nature of the ligands and of the metal has a strong influence on the intermetallic distance. However, shortening of the metal-metal distances in quadruple bonds may not be observed due to the weak nature of the δ bond.⁴

In addition, clusters can behave as "electron reservoirs" because they have access to multiple redox states and presence of more number of metals. Clusters have also been shown to undergo rearrangement through the breaking of the metal-metal bond. This property will allow for the organic substrate to react with an accessible coordination site on the metal leading to organic transformations.⁵ Clusters have also shown to effectively catalyze reactions in biphasic medium in which the metal fragments remains in the aqueous phase and the organic substrates in the organic phase.⁶

1.2. TYPES OF METAL-METAL BOND IN TRANSITION METAL CLUSTER

1.2.1. Clusters containing metal-metal single bond

Transition metal cluster involving metal –metal single bond are very common and a variety of examples are known including homo and hetero-metallic bonds. A tetrametallic iron cluster shown in Figure 1.4. has been recently synthesised with a butterfly geometry and provides a promising reaction site for the reductive coupling of unsaturated molecules. The bond distances of the five iron–iron bonds are in the range of 2.4963(3) Å -2.6177(3) Å revealing that all the Fe-Fe bonds are having single bond character. The cluster also involves two isonitrile ligands triply bridged to three of the four iron atoms and four η^5 -cyclopentadienyl groups attached to each of the four iron atom (Figure 1.3).⁷

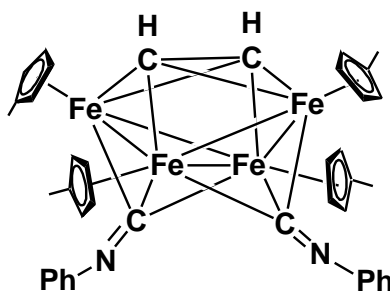


Figure 1.3 $[(\eta^5\text{-C}_5\text{H}_4\text{Me})_4\text{Fe}_4(\mu_3\text{-CH})_2(\mu_3\text{-CNPh})_2]$

Mild pyrolysis of an arachno cluster $[\text{Cp}^*\text{RuCO})_2\text{B}_2\text{H}_6]$, ($\text{Cp}^* = \eta^5\text{-C}_5\text{Me}_5$), with $\text{Fe}_2(\text{CO})_9$ led to the formation of a mixed-metal tetrahedral cluster, $[\text{Cp}^*\text{Ru}(\text{CO})_2(\mu\text{-H})\{\text{RuFe}_3(\text{CO})_9\}]$. The molecular structure involves one $\text{Cp}^*\text{Ru}(\text{CO})_2$ fragment, one ruthenium metal atom and three $\text{Fe}(\text{CO})_3$ fragments, which are linked by metal-metal single bonds. One of the most striking features is the occurrence of a strong metal-metal bond as evidenced by the short Ru-Ru distance of 2.5049(6) Å. The molecule contains a RuFe_3 metal atom core, with an average Ru-Fe bond length of 2.2960 Å and Fe-Fe bond length of 2.647 Å (Figure 1.4).⁸

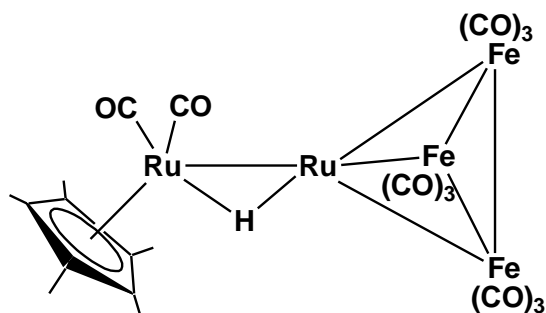


Figure 1.4 $[\text{Cp}^*\text{Ru}(\text{CO})_2(\mu\text{-H})\{\text{RuFe}_3(\text{CO})_9\}]$

1.2.2. Cluster containing metal-metal double bond

Transition metal cluster with metal-metal double bond are known to some extent and the stability is largely dependent upon the coordinating ligands. A methoxycarbonyl-bridged complex $[\text{Mo}_2\text{Cp}_2(\mu\text{-COMe})(\mu\text{-PCy}_2)(\mu\text{-CO})]$ has a reactive Mo_2C center and it reacts with selenium at room temperature to give the diselenide complex $[\text{Mo}_2\text{Cp}_2(\mu\text{-PCy}_2)\{\mu\text{-}\kappa^1, \eta^1: \kappa^1, \eta^1\text{-SeC}(\text{O})\text{C}(\text{OMe})\}(\mu\text{-}\kappa^1: \kappa^1\text{-Se}_2)]$ in high yield. The intermetallic Mo-Mo distance is 2.709(1) Å, which is quite short, considering the size of the bridging atoms. The bond length is in consistent with the formulation of a double Mo-Mo bond (Figure 1.5).⁹

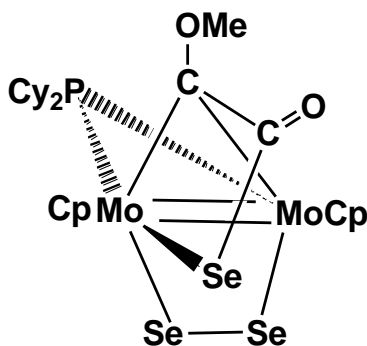


Figure 1.5 $[\text{Mo}_2\text{Cp}_2(\mu\text{-PCy}_2)\{\mu\text{-SeC}(\text{O})\text{C}(\text{OMe})\}(\mu\text{-Se}_2)]$

Treatment of a diruthenium tetrahydrido complex, $[\text{Cp}^*\text{Ru}(\mu\text{-H})_4\text{RuCp}^*]$ ($\text{Cp}^* = \eta^5\text{-C}_5\text{Me}_5$) with a slightly excess amount of 1,3-cyclohexadiene at an ambient temperature resulted in the formation of a $\mu\text{-}\eta^2: \eta^2\text{-cyclohexadiene}$ complex, $[\{\text{Cp}^*\text{Ru}(\mu\text{-H})\}_2(\mu\text{-}\eta^2: \eta^2\text{-C}_6\text{H}_8)]$ with the elimination of dihydrogen. The two Cp^* groups are attached to the metal centers in a cis

geometry with respect to the metal-metal bond. The Ru-Ru distance of 2.6922 Å in the cluster corresponds to the Ru=Ru double bond and each ruthenium atom contains 18 valence electrons (Figure 1.6).¹⁰

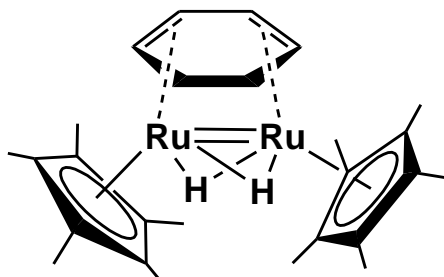


Figure 1.6 [$\{\text{Cp}^*\text{Ru}(\mu\text{-H})\}_2(\mu\text{-}\eta^2:\eta^2\text{-C}_6\text{H}_8)$]

1.2.3 Cluster containing metal-metal triple bond

The anionic heterometallic cluster, $[\text{Au}_2\text{Mo}_2\text{Cp}_2(\mu\text{-PCy}_2)(\text{CO})_2(\text{PR}_3)_2][\text{PF}_6]$ obtained from a dimolybdenum cluster $[\text{Mo}_2\text{Cp}_2(\mu\text{-PCy}_2)(\mu\text{-CO})_2]^-$ exhibits a regular tetrahedral Mo_2Au_2 core containing $\text{Mo}\equiv\text{Mo}$ triple bond. The two $\text{CpMo}(\text{CO})$ fragments are bridged by a dicyclohexylphosphide and two $\text{Au}(\text{P}^i\text{Pr})_3$ cations eventually coupled with each other. The Mo-Mo triple bond is found to be at a distance of 2.5673(3) Å (Figure 1.7).¹¹

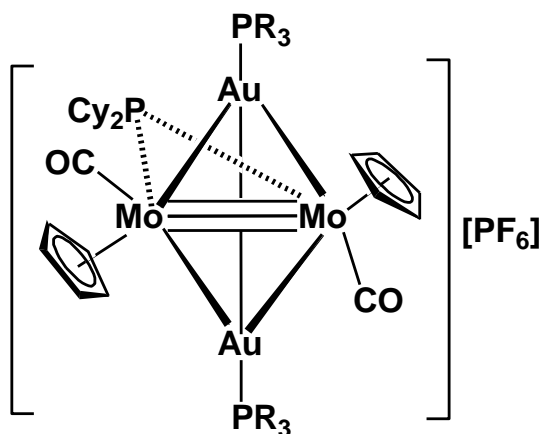


Figure 1.7 $[\text{Au}_2\text{Mo}_2\text{Cp}_2(\mu\text{-PCy}_2)(\text{CO})_2(\text{PR}_3)_2][\text{PF}_6]$

Another example of cluster with metal - metal triple bond was obtained when a trimetallic cluster $[\text{Cp}_2\text{Mo}_3(\mu_3\text{-CH})(\mu\text{-PCy}_2)(\text{CO})_6\{\text{P}(\text{OMe})_3\}]$ was thermally degraded to give selectively a 30-electron methylidyne derivative $[\text{Mo}_2\text{Cp}_2(\mu\text{-CH})(\mu\text{-PCy}_2)(\mu\text{-CO})]$. The structure of the methylidyne complex $[\text{Mo}_2\text{Cp}_2(\mu\text{-CH})(\mu\text{-PCy}_2)(\mu\text{-CO})]$ consists of two CpMo units symmetrically bridged by dicyclohexylphosphide, carbonyl and methylidyne ligands. The Mo-Mo intermetallic distance is 2.467 Å and consistent with the metal-metal triple bond bond distances found in the literature (Figure 1.8).¹²

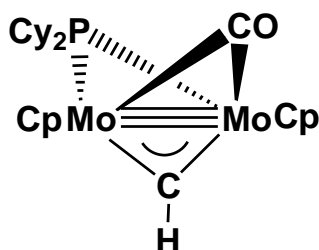


Figure 1.8 $[\text{Mo}_2\text{Cp}_2(\mu\text{-CH})(\mu\text{-PCy}_2)(\mu\text{-CO})]$

Other bimetallic clusters with metal metal triple bond includes a cyclopentadienyl dimolybdenum cluster $[\text{Cp}_2\text{Mo}_2(\text{CO})_4]$ and $[\text{Mo}_2(\text{NMe}_2)_4]$ as shown in Figure 1.9.

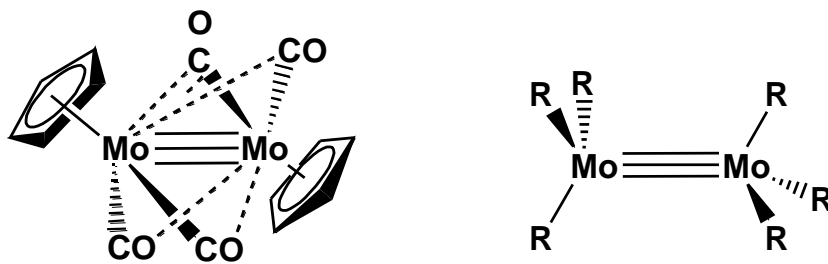


Figure 1.9

1.2.4 Cluster containing metal-metal quadruple bond

Quadruple metal-metal bonds are less common and are mostly found for bimetallic system with bigger sized metals. A tetrachlorotetrakis(1,3,5-triaza-7-phosphaadamantane)dimolybdenum(II), $[\text{Mo}_2\text{Cl}_4(\text{PTA})_4]$ complex with quadruply bonded molybdenum(II)–molybdenum(II) has been synthesized recently by reaction of 1,3,5-triaza-7-

phosphaadamantane (PTA) with $K_4[Mo_2Cl_8]$ in refluxing methanol. The Mo–Mo separation in the molecular structure has been found to be 2.13 Å (Figure 1.10).¹³

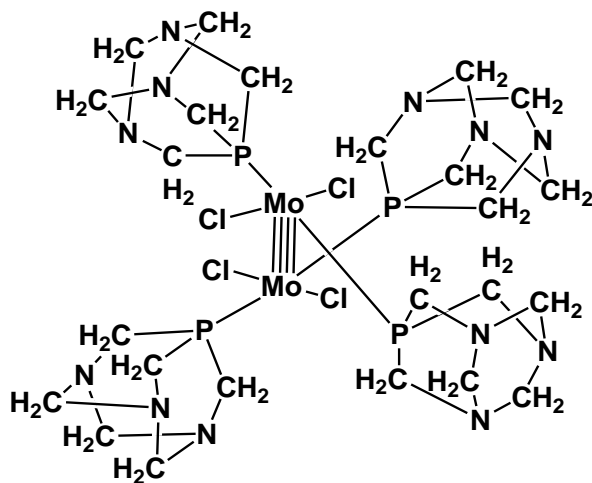


Figure 1.10 $[Mo_2Cl_4(PTA)_4]$, (PTA = 1,3,5-triaza-7-phosphaadamantane)

Another cluster with quadruple M-M bond has been prepared by the treatment of $K_4Mo_2Cl_8$ with 2 equivalents of the sterically hindered amidinates, $Li[RC(N-2,6-i-Pr_2C_6H_3)_2]$ (R = H, Ph) in tetrahydrofuran solvent. The clusters $[Mo_2(\mu-Cl)\{Cl_2Li(OEt_2)\}\{\mu-\eta^2-RC(N-2,6-i-Pr_2C_6H_3)_2\}_2]$, (R = H, Ph) contain a Mo-Mo quadruple bond and adopt a paddle wheel structure supported by two amidinates. It also contains one bridging chloro ligand and a Cl-Li-Cl linkage spanning the Mo-Mo bond. The Mo-Mo bond length of 2.0875(4) Å and 2.0756(8) Å indicates typical Mo-Mo quadruple bonds (Figure-1.11).^{14, 15} The two amidinates and a Cl-Li-Cl groups are playing a vital role to stabilize the Mo-Mo quadruple bonded cluster.

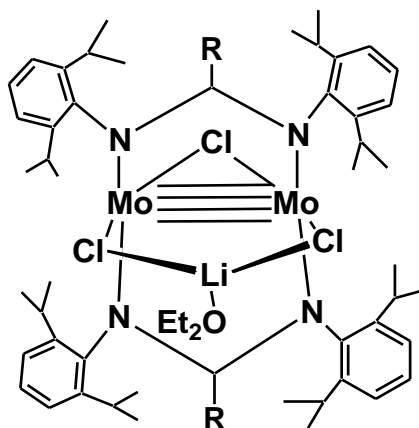


Figure 1.11 $[Mo_2(\mu-Cl)\{Cl_2Li(OEt_2)\}\{\mu-\eta^2-RC(N-2,6-i-Pr_2C_6H_3)_2\}_2]$ (R = H, Ph)

A dirhenium cluster, $[\text{Re}_2(\text{C}_7\text{H}_4\text{NS}_2)_4\text{Cl}_2]$, involving bridging *N,S*-benzothiazole-2-thiolate ligands and axially bonded chloride ligands has been reported recently. The molecule adopts staggered conformation with a Re-Re quadruple bond distance of 2.2716 (3) Å (Figure 1.12).¹⁶

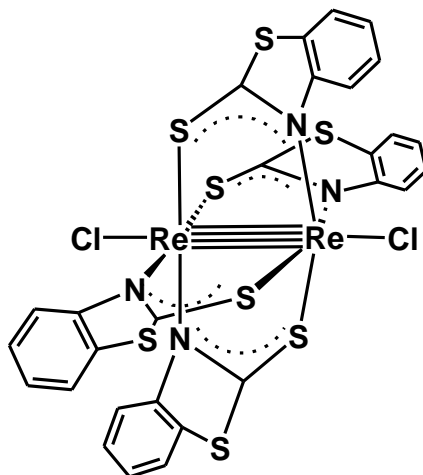


Figure 1.12 $[\text{Re}_2(\text{C}_7\text{H}_4\text{NS}_2)_4\text{Cl}_2]$

1.3. TYPES OF TRANSITION METAL CLUSTER BASED ON LIGANDS

1.3.1. Cluster containing carbonyl ligands

The most widely found ligand in π -acceptor clusters is the carbonyl ligand, which can adopt terminal, edge-bridging, or face-capping bonding modes in a multimetallic cluster compounds. All the three bonding types are considered as two-electron donors (Figure 1.13).¹⁷ It is one of the most important ligand in transition metal cluster chemistry owing to its versatility, range of bonding modes exhibited, stabilizing metals in low oxidation states and also due its small size which allows a large number of carbonyls to surround the metal core. In addition, CO has been found to bond in a variety of bonding modes as illustrated in Figure 1.13. Bridging carbonyls are generally better π - acceptors than terminal carbonyls because of the effective overlap between the d orbitals of two metals with the π^* orbitals of the carbonyls and the increased π^* back-bonding is reflected in the ν_{CO} values which are lower than those of the terminal ligands.^{18,19,20}

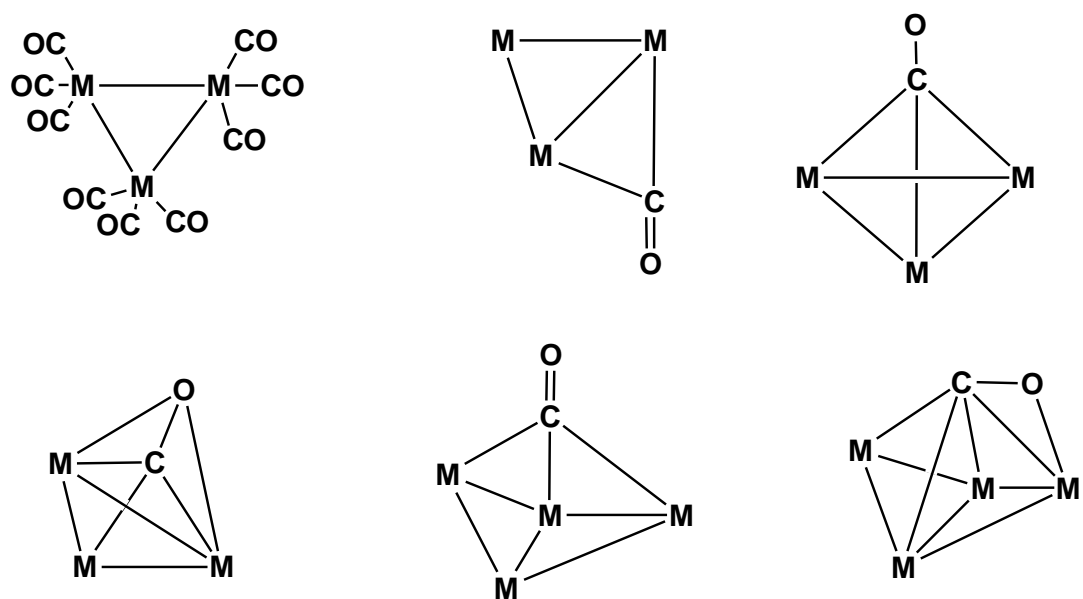


Figure 1.13 Various bonding modes of CO.

During the last 40 years, many efforts have been devoted to prepare transition metal carbonyl cluster complexes in a rational and systematic ways.^{21, 22} A large number of transition metal carbonyl cluster compounds have been reported with unique structural and bonding features. Recently, Adams et al. have prepared a two dimensional transition metal carbonyl cluster containing one iridium and six ruthenium metal atoms that may form the basis for a series of new complexes that also exhibits interesting optical and reactivity properties (Figure 1.14).²³

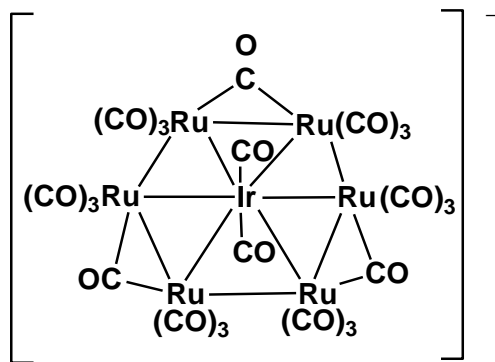


Figure 1.14 $[\text{IrRu}_6(\text{CO})_{23}]^-$

Treatment of $[\text{Ru}_3(\text{CO})_{12}]$ with 2-aminopyridine (H_2apyH) in refluxing xylene for one hour resulted in the formation of a hexaruthenium carbonyl cluster complex, $[\text{Ru}_6(\mu^3\text{-H})_2(\mu^5\text{-}\eta^2\text{-apyH})(\mu\text{-CO})_2(\text{CO})_{14}]$ with a basal edge-bridged square pyramidal metallic core and containing sixteen carbonyl ligands. Each of the six ruthenium atoms satisfy the 18 electron count (Figure 1.15).²⁴

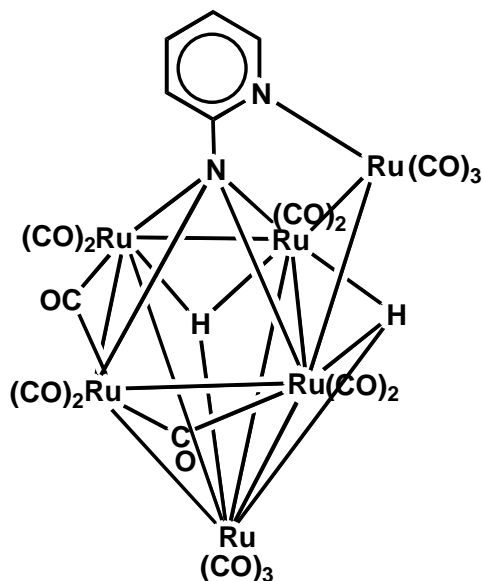


Figure 1.15 $[\text{Ru}_6(\mu^3\text{-H})_2(\mu^5\text{-}\eta^2\text{-apyH})(\mu\text{-CO})_2(\text{CO})_{14}]$

Dimeric metal carbonyl clusters of group 8 and 9 transition metals have been synthesized by using silicon containing diyne ligands. Thus, treatment of $[\text{Co}_2(\text{CO})_8]$ with $\text{HC}\equiv\text{C}-(\text{CH}_3)_2\text{Si}(\text{CH}_3)-\text{C}\equiv\text{CH}$ led to the formation of a tetranuclear cobalt cluster (Figure 1.16). Structurally, each of the tetracobalt species displays two Co_2C_2 cores adopting the pseudo-tetrahedral geometry with the alkyne bond lying essentially perpendicular to the $\text{Co}-\text{Co}$ bond. While the reaction of $[\text{Ru}_3(\text{CO})_{12}]$ with the same ligand in 2:1 molar ratio in refluxing THF led to formation of a different $\text{Si}(\text{CH}_3)_2$ bridged hexanuclear ruthenium carbonyl cluster (Figure 1.17). The hexanuclear ruthenium clusters consist of two trinuclear metal cores with the $\mu_3\text{-}\eta^2,\eta^2$ bonding mode for the acetylene group.²⁵

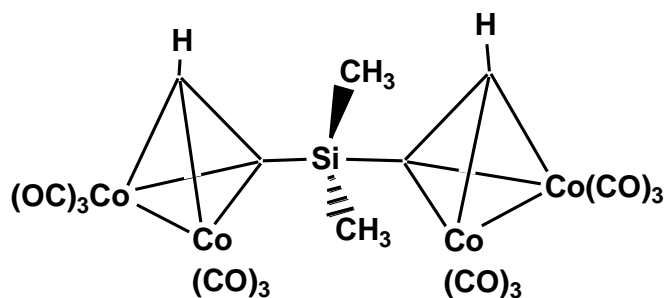


Figure 1.16

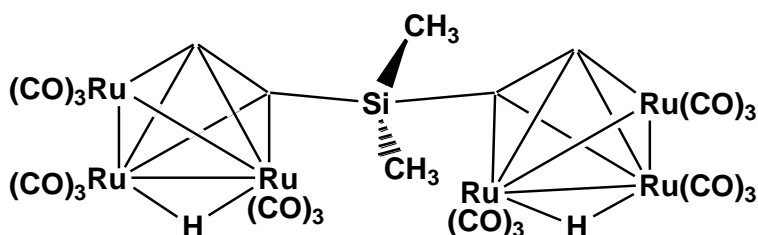


Figure 1.17

Treatment of $\text{Co}_3(\mu_3\text{-Br})(\mu\text{-dppm})(\text{CO})_7$ with zinc dust in refluxing thf afforded a Co_6 – cluster, $[\text{Co}_6(\mu_6\text{-C}_2)(\mu\text{-dppm})_2(\mu\text{-CO})(\text{CO})_{12}]$ structurally confirmed by single-crystal X-ray structural determination technique. In this cluster complex, the two Co_3 clusters have been linked by a further long Co-Co bond (2.6788(6) Å) at the expense of loss of one of the CO ligands. This Co-Co bond is bridged by a CO group, while the C_2 fragment also links the two clusters by interacting with all six metal atoms. The two dppm ligands bridge Co-Co edges of the triangular faces.²⁶ The cluster contains two types of carbonyl groups linked to cobalt atoms, one terminally bonded metal carbonyl and the other, doubly bridged metal carbonyl (Figure 1.18).

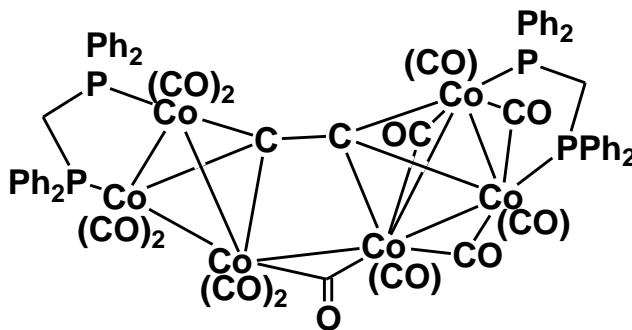


Figure 1.18 $[\text{Co}_6(\mu_6\text{-C}_2)(\mu\text{-dppm})_2(\mu\text{-CO})(\text{CO})_{12}]$

Reaction of $[(PPh_2C_5H_4)Cp_3Fe_4(CO)_4]$ with $(CO)_4W(CH_3CN)_2$ at ambient temperature affords $[(CO)_4W(PPh_2C_5H_4)Cp_3Fe_4(CO)_4]$ as the major product. X-ray diffraction study shows that it contains an interesting μ_4, η^2 -CO ligand, where two electrons donated by the carbon atom are involved to bridge a Fe_3 face and two electrons from oxygen are donated to the tungsten atom (Figure.1.19). While the other carbonyl ligands form either triply bridged or terminally bonded metal carbonyl moieties.²⁷

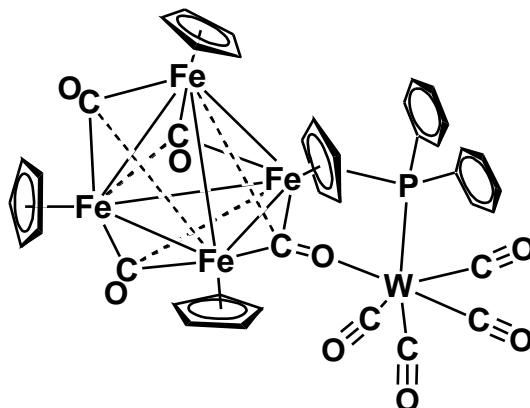


Figure 1.19 $[(CO)_4W(PPh_2C_5H_4)Cp_3Fe_4(CO)_4]$

1.3.2. Cluster containing hydride ligands

Hydrides are found to bind with metals by forming terminal, doubly bridging (μ -H), and face capping triply bridging (μ_3 -H) modes. Sometimes they can also occupy interstitial coordination sites mostly in tetrahedral μ_4 -H or octahedral μ_6 -H clusters (Figure 1.20).

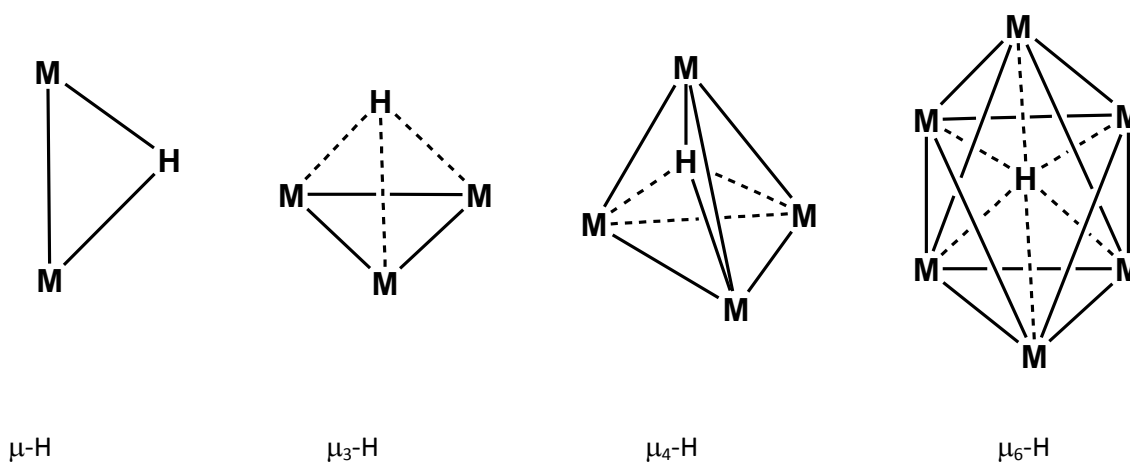


Figure 1.20 Bonding modes of hydride ligand

The M-H bond in terminally attached hydride ligands can be considered to be a localized two-centre interaction, whereas a delocalized bonding picture has been obtained when the hydride interacts with more metals. A novel heterotrimetallic polyhydrido complexes containing ruthenium and group 6 metals, $[(\text{Cp}'\text{Ru})_2(\text{Cp}'\text{M})(\mu\text{-H})_5]$, ($\text{M} = \text{Mo}, \text{W}$) have been synthesized by the reaction of dimeric ruthenium methoxo complex $(\text{Cp}'\text{RuO}(\text{Me})_2)$ with dinuclear polyhydrido complexes $\text{Cp}'\text{Ru}(\mu\text{-H})_3\text{MH}_3\text{Cp}'$ ($\text{M} = \text{Mo}, \text{W}$) in thermal reaction condition. These cluster complexes have similar triangular metal cores, two short M-M bonds in the range 2.5-2.6 Å and one long M-M bond (3.0-3.1 Å). The short M-M bond is bridged by the two hydrido ligands, and the long M-M bond is singly bridged by a hydride ligand (Figure 1.21). Other than hydride ligands, the cluster also contains three cyclopentadienyl group attached to each of the metal atom.²⁸

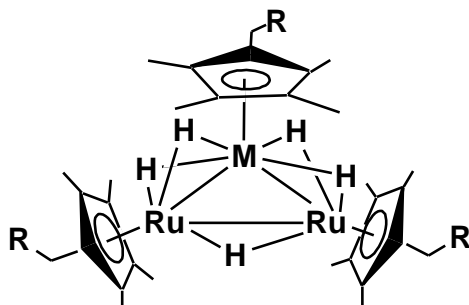


Figure 1.21 $[(\text{Cp}'\text{Ru})_2(\text{Cp}'\text{M})(\mu\text{-H})_5]$ ($\text{M} = \text{Mo}, \text{W}$), ($\text{R} = \text{H}, \text{Me}$)

The treatment of ruthenium tetrahydride $[\text{Cp}^*\text{Ru}(\mu\text{-H})_4\text{RuCp}^*]$ with a slight excess amount of Cp^*OsH_5 in toluene at 100 °C resulted in the formation of trinuclear heterometallic pentahydrido complex, $[(\text{Cp}^*\text{Ru})_2(\text{Cp}^*\text{Os})(\mu\text{-H})_5]$ in reasonable yield. This cluster has five doubly bridging hydrido ligands. Two of these ligands bridge the two Os atoms, two bridge the Os and Ru atoms, and the remaining ligand locates the remaining Os-Ru edge (Figure 1.22).²⁹

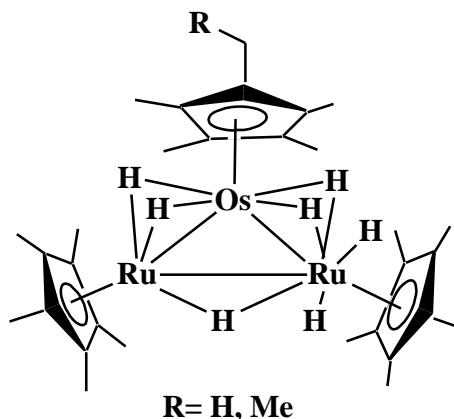


Figure 1.22 $[(\text{Cp}^*\text{Ru})_2(\text{Cp}^*\text{Os})(\mu\text{-H})_5]$

Recently, synthesis of a bridged hydride cluster complex, $[\text{Ir}(1,5\text{-COD})(\mu\text{-H})_4]$ has been reported by Finke et al. containing Ir_4H_4 core and four cyclooctadiene ligand. This cluster molecule is composed of a distorted tetrahedral Ir_4 core of D_{2d} geometry. Each Ir center is bonded to two olefinic groups of a 1,5-COD moiety and two edge-bridging hydrides. The two Ir–Ir distances are long (2.90728 and 2.91138 Å) and four Ir–Ir distances are comparatively short in the range 2.7868 Å–2.7879 Å. The hydrides are located between two Ir atoms connected by short Ir–Ir bonds (Figure 1.23).³⁰

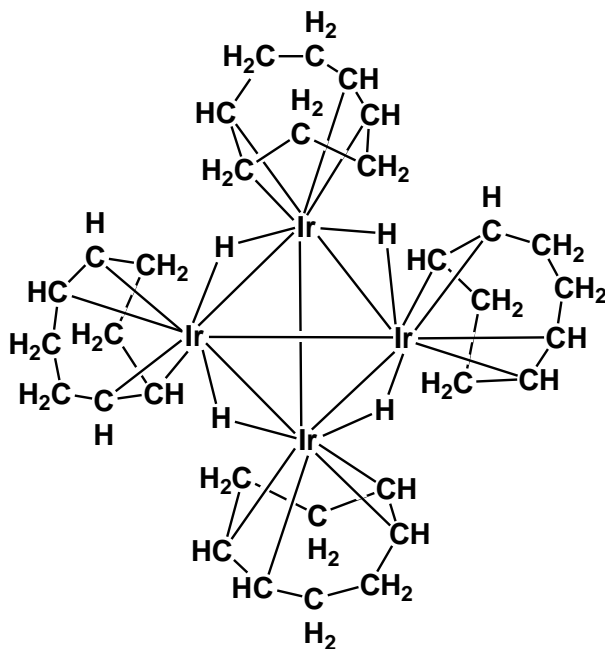


Figure 1.23 $[\text{Ir}(1,5\text{-COD})_4(\mu\text{-H})_4]$

The carbonyl hydride cluster $[\text{Ir}_4\text{H}_8(\text{CO})_4(\text{PPh}_3)_4]$ has been formed in high yield by heating a mixture of $\text{Ir}_4(\text{CO})_{12}$ and PPh_3 in toluene at 90°C under hydrogen at atmospheric pressure. X-ray diffraction studies show that in the solid state one hydrogen, one carbonyl and one triphenylphosphane ligand are terminally bonded to each iridium atom, whereas four hydride ligands are bridging. All the hydrogen atoms were directly located by X-ray analysis at an average H–Ir distance of 1.55 \AA (for the terminal H) and 1.75 \AA (for the bridged H) (Figure 1.24).³¹

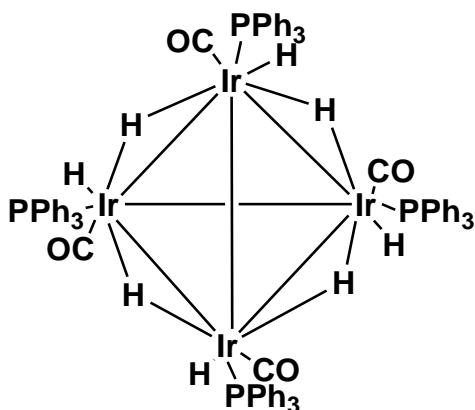


Figure 1.24 $[\text{Ir}_4\text{H}_8(\text{CO})_4(\text{PPh}_3)_4]$

Thermal reaction of $[\text{Ru}_4\text{Pt}_2(\text{CO})_{18}]$ with $[\text{Ru}_4(\text{CO})_{13}(\mu\text{-H})_2]$, yielded a decanuclear platinum ruthenium carbonyl cluster complex $[\text{Pt}_2\text{Ru}_8(\text{CO})_{23}(\mu_3\text{-H})_2]$, found to consist of edge-fused bi-octahedral clusters with platinum atoms along the edge-sharing sites. There are strong metal-metal bonds between the apices of the adjacent octahedra. This cluster compound is electron deficient, and one of the Ru–Ru bonds is unusually short with a bond distance of 2.580 \AA . The hydrides are present in triply bridging modes as shown in the Figure 1.25.³²

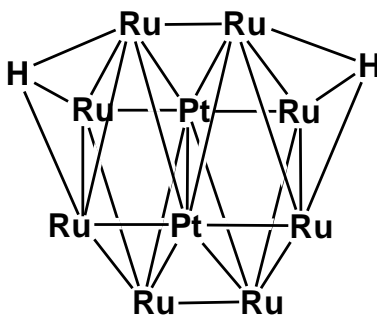


Figure 1.25 $[\text{Pt}_2\text{Ru}_8(\text{CO})_{23}(\mu_3\text{-H})_2]$
(Carbonyls are omitted for clarity)

1.3.3. Cluster containing phosphine ligand

Phosphines are one of the most widely utilized ligands in transition metal cluster chemistry due to their extreme versatility in bonding and reactivity. The electronic and steric properties of the metal clusters containing phosphine ligands can be modified in a systematic and predictable manner by varying the substituents on the phosphorus atom.^{18, 33} They are broadly classified as monodentate phosphine with only one phosphorus atom binding to the metal center and polydentate phosphine, where more than one phosphorus atoms are linked to metal atoms. The chemistry of transition metal carbonyl clusters containing diphosphines has been extensively studied due to their unusual coordination features. Diphosphines contain two phosphine group linked by a backbone unit, the most common being $-(\text{CH}_2)_n-$, $-(\text{C}_6\text{H}_4)-$, $-\text{CH}=\text{CH}-$, $-\text{C}\equiv\text{C}-$ and $-(\text{C}_5\text{H}_4)\text{Fe}(\text{C}_5\text{H}_4)-$. The diphosphine ligand has been found to adopt a variety of bonding modes on the cluster, including monodentate with a pendant phosphine center, chelating a single metal atom in the multimetallic cluster, bridging across a metal-metal bond and forming an intermolecular link across two clusters (Figure 1.26). The bonding modes adopted by these diphosphine ligands are influenced by the flexibility and length of the organic or organometallic backbone.

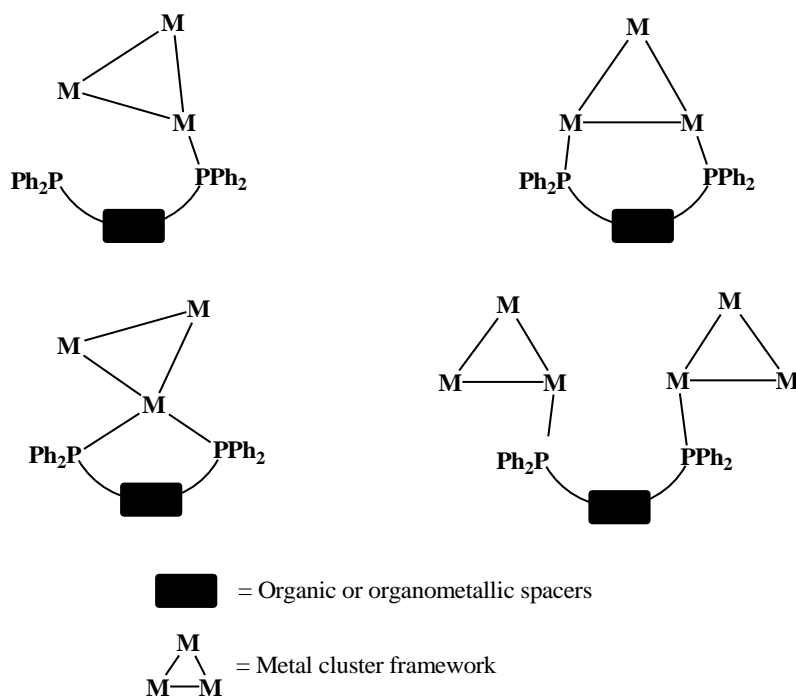


Figure 1.26 Different types of diphosphine coordination to metal clusters

Phosphine ligand can bind with metal using various coordination and can be sub-classed into terminally bonded, chelating mode of coordination and bridging mode of bonding. Examples of some metal cluster compounds with different types of coordination behavior have been described below:

(a) *Cluster with terminally bonded phosphine*

Heterometallic platinum-osmium cluster complex, $[\text{Pt}_2\text{Os}_3(\text{CO})_{10}(\text{P}^t\text{Bu}_3)_2]$ has been synthesized by the reaction of $\text{Os}_3(\text{CO})_{10}(\text{NCMe})_2$ with $\text{Pt}(\text{P}^t\text{Bu}_3)_2$ at 0 °C and involves five metal atoms in the cluster framework in a trigonal bipyramidal geometry with the three osmium atoms in the trigonal plane and the two platinum atoms in the axial positions. Each platinum atom contains one terminally bonded $\text{P}^t(\text{Bu})_3$ ligand with a Pt-P bond length of 2.3426 Å. Presence of six platinum-osmium bonds and three osmium-osmium bonds have also been revealed by structural characterization (Figure 1.27).³⁴

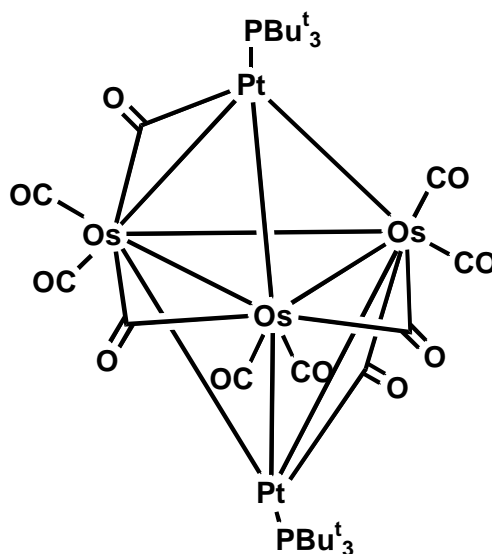


Figure 1.27 $[\text{Pt}_2\text{Os}_3(\text{CO})_{10}(\text{P}^t\text{Bu}_3)_2]$

Recently, Blanco et al. reported a highly luminicent gold- silver cluster with terminal phosphine ligands obtained by the reaction of $[\text{Au}(\text{C}\equiv\text{CPh})(\text{PPh}_3)]$ and $[\text{Ag}(\text{PPh}_3)_2]\text{OTf}$, (OTf = trifluoromethylsulfonate) (Figure.1.28). The $^{31}\text{P}\{^1\text{H}\}$ NMR spectra of the complex shows broad peak at room temperature while at low temperature the peaks were split into two, arising from the two types of phosphorus atoms that are assigned to PPh_3 bonded to the gold centre at δ 39.9 and another peak arising from the fragments $\text{Ag}(\text{PPh}_3)_2$. The latter signal splits into two doublets

because of the coupling of the phosphorus with the magnetically active ^{107}Ag and ^{109}Ag isotopes of the silver center (δ 8.8 ppm).³⁵

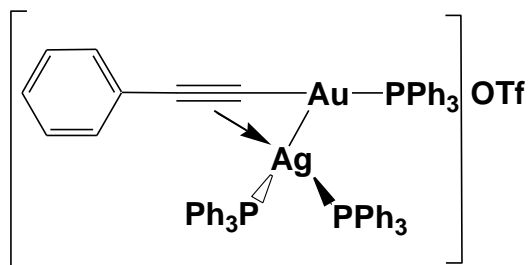


Figure.1.28 $[\text{AuAg}(\text{C}\equiv\text{CPh})(\text{PPh}_3)_3]\text{OTf}$

Reaction of $(\text{PPh}_2)\text{C}_{60}\text{H}$ with $[\text{Os}_3(\text{CO})_{11}(\text{NCMe})]$ affords a triosmium carbonyl cluster $[\text{Os}_3(\text{CO})_{11}((\text{PPh}_2)\text{C}_{60}\text{H})]$ containing diphenylfullerene phosphine fragment terminally bonded with one of the Osmium atoms. The molecular structure of the cluster, shown in Figure.1.29, reveals the $\text{Os}_3(\text{CO})_{11}$ moiety with a phosphine ligand attached to one osmium atom. The Os-P bond is slightly tilted from the trimetallic plane by 4.4° . The Os_3 unit forms an isosceles triangle with one of the Os-Os distance (2.9139 \AA) being slightly longer than the other two Os-Os bonds.³⁶

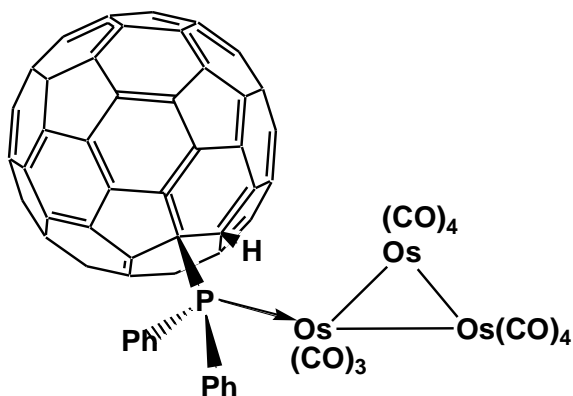


Figure.1.29 $[\text{Os}_3(\text{CO})_{11}(\text{PPh}_2)\text{C}_{60}\text{H}]$

(b) Clusters with chelating phosphine ligand

The diphosphine ligand, 1,2-bis(diphenylphosphino)benzene (dppbz) reacts with the activated cluster $1,2\text{-Os}_3(\text{CO})_{10}(\text{MeCN})_2$ at room temperature to give a triosmium cluster $1,1\text{-Os}_3(\text{CO})_{10}(\text{dppbz})$ as one of the products (Figure.1.30). Single crystal X-ray diffraction analysis

shows that the Os-Os bond distances are in the range 2.9092(5) Å - 2.9263(5) Å. The observed bond angle of 84.90° for the P-Os-P atoms shows the chelating nature of the ancillary dppbz ligand and is comparable to the bite angle for similar chelated coordination reported in the literature.³⁷

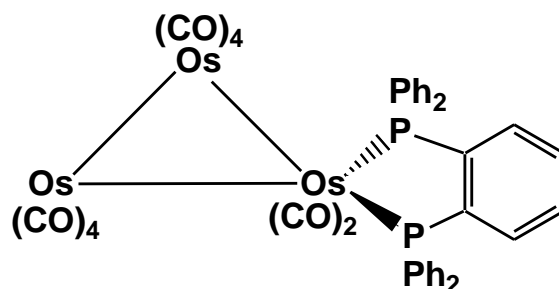


Figure 1.30 [1,1-Os₃-(CO)₁₀(dppbz)]

Tricobalt cluster, [PhCCO₃(CO)₉] undergoes facile ligand substitution with 1,8-bis(diphenylphosphino)naphthalene (dppn) under thermal and in presence of Me₃NO to afford cluster containing a chelating dppn ligand, [PhCCO₃(CO)₄(μ-CO)₃(dppn)] involving three bridging CO groups in the solid state structure. The two Co-P bond distances are 2.2544 Å and 2.1998(9) Å and the bite angle, P-Co-P, has been found to be 88.62° (Figure 1.31).³⁸ The three triangular cobalt atoms are also linked by a triply bridged CPh unit giving extra stability to the cluster core.

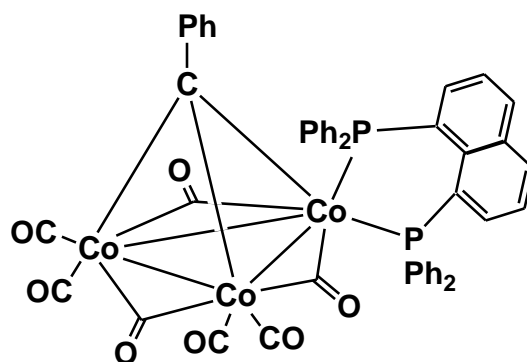


Figure 1.31 [PhCCO₃(CO)₄(μ-CO)₃(dppn)]

Another diphosphine chelated metal carbonyl cluster [Cp₂Fe₃(CO){η²-Ph₂P(CH₂)PPh₂}(μ-CO)(μ₃-CO)(μ-η¹,η²,η²-CF₃C₂CF₃)] has been obtained by the thermal

reaction of $[\text{Cp}_2\text{Fe}_3(\text{CO})_5(\mu_3\text{-CF}_3\text{C}_2\text{CF}_3)]$ with bis(diphenylphosphino)methane (dppm). The cluster has been spectroscopically characterized to contain one terminal metal carbonyls, two bridging metal carbonyls and a chelating dppm ligand attached to iron atom (Figure 1.32).³⁹

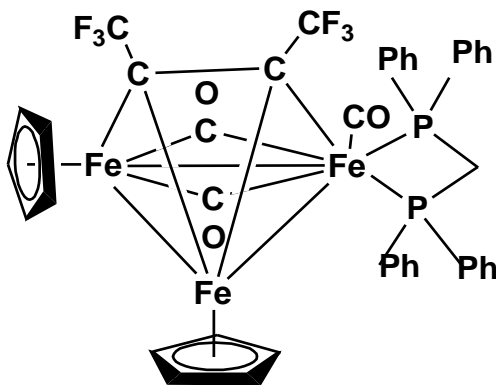


Figure 1.32 $[\text{Cp}_2\text{Fe}_3(\text{CO})\{\eta^2\text{-Ph}_2\text{P}(\text{CH}_2)\text{PPh}_2\}(\mu\text{-CO})(\mu_3\text{-CO})(\mu\text{-}\eta^1, \eta^2, \eta^2\text{-CF}_3\text{C}_2\text{CF}_3)]$

(c) Cluster with bridging diphosphine ligand

Diphosphine ligands can bridge across a metal – metal bond in a cluster molecule in which the two phosphorus atoms of the diphosphine ligand are linked to two transition metals of the same cluster unit. Thermal reaction of $[\text{Os}_3(\text{CO})_{12}]$ with dppf {dppf = 1,1'-bis(diphenylphosphino)ferrocene} in the presence of Me_3NO in benzene furnishes triosmium cluster compound $[\text{Os}_3(\text{CO})_{10}(\mu\text{-dppf})]$ containing a dppf ligand bridging the Os-Os edge. The inter-nuclear P-P distance has been found to be 5.20 Å while $^{31}\text{P}\{^1\text{H}\}$ NMR spectra shows a singlet at δ -5.0, which reveals the presence of equivalent phosphorus nuclei in the cluster molecule (Figure 1.33).⁴⁰

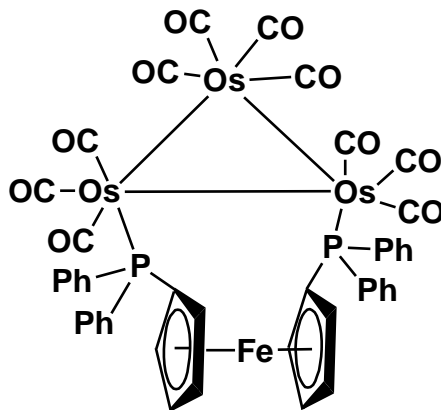


Figure 1.33 $[\text{Os}_3(\text{CO})_{10}(\mu\text{-dppf})]$

A mixed metal cluster $[\text{Fe}_3\text{Pt}(\mu_4\text{-Y})(\text{CO})_9(\text{dppm})]$, isolated from the reaction of $\text{K}_2[\text{Fe}_3\text{Y}(\text{CO})_9]$ ($\text{Y} = \text{Se}, \text{Te}$) with $[(\text{dppm})\text{PtCl}_2]$ shows a diphosphine ligand bridging across an iron-platinum bond. The two phosphorus atoms of the dppm ligand are bonded to two different metal atoms of the same cluster moiety. The cluster also contains a selenium atom quadruply bridged to Fe_3Pt unit and nine terminally bonded metal carbonyl groups attached to iron and platinum atoms (Figure 1.34).⁴¹

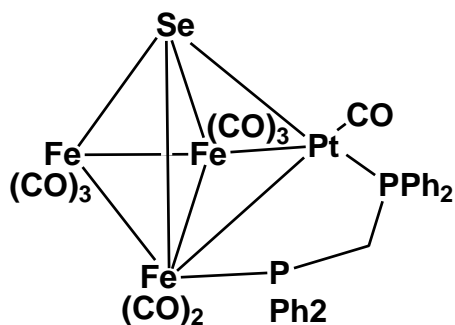


Figure.1.34 $[\text{Fe}_3\text{Pt}(\mu_4\text{-Se})(\text{CO})_9(\text{dppm})]$

(d) Diphosphine bridging two cluster fragments

Some diphosphine ligands have been found to bind with metal atoms from two separate cluster units and form intermolecular link between the two cluster framework. Room temperature reaction of 1,2,4,15- $(\text{PPh}_2)_2(\text{H})_2\text{C}_{60}$ and two equivalent of $\text{Os}_3(\text{CO})_{10}(\text{NCMe})_2$ in toluene results in substitution of the labile acetonitrile ligands to form a double-cluster complex $[\{\text{Os}_3(\text{CO})_{10}\}_2(\mu, \mu, \eta^3, \eta^3\text{-}(\text{PPh}_2)_2(\text{H})_2\text{C}_{60})]$. The diphosphine, $[(\text{PPh}_2)_2(\text{H})_2\text{C}_{60}]$ is linked to two $\text{Os}_3(\text{CO})_{10}$ clusters through the phosphine group and two $\text{C}=\text{C}$ double bonds in a μ, μ, η^3, η^3 -bonding fashion. The Os-P bond lengths are in the range of 2.361 Å - 2.363 Å and the angle Os-P-C = 114.3(2)°. The ^{31}P NMR peaks for the two non equivalent phosphorus atoms has been found at δ 37.37 and δ 30.80 region (Figure 1.35).⁴²

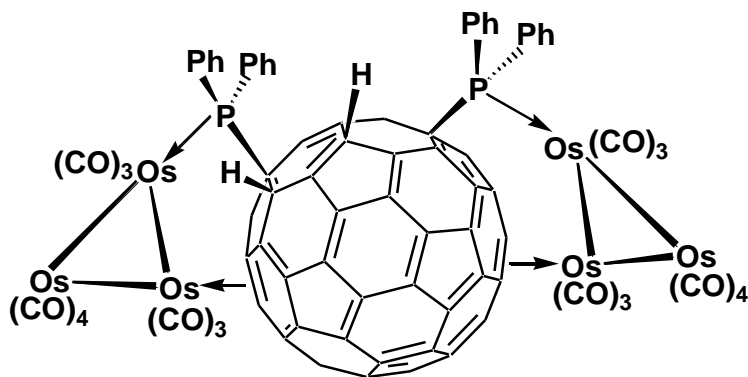


Figure 1.35 $[\{\text{Os}_3(\text{CO})_{10}\}_2-(\mu, \mu, \eta^3, \eta^3-(\text{PPh}_2)_2(\text{H})_2\text{C}_{60})]$

Reaction of a trinuclear iron cluster $[\text{Cp}_2\text{Fe}_3(\text{CO})_5(\mu_3\text{-CF}_3\text{C}_2\text{CF}_3)]$ with the bis(phosphino) ligand dppe yields an hexanuclear cluster $[\{\text{Fe}_3\text{Cp}_2(\text{CO})_4(\mu_3\text{-}\eta^1, \eta^1, \eta^2\text{-CF}_3\text{C}_2\text{CF}_3)\}_2\{\mu\text{-Ph}_2\text{P}(\text{CH}_2)_2\text{PPh}_2\}]$ in which the two tri-iron cluster units are linked by a diphosphine group (Figure 1.36). The ^{31}P NMR spectrum of the cluster compound exhibits a singlet at δ 51.6 ppm due to the presence of equivalent phosphorus atoms. The two Fe–P bond lengths are in the range 2.305 Å– 2.310 Å.³⁹

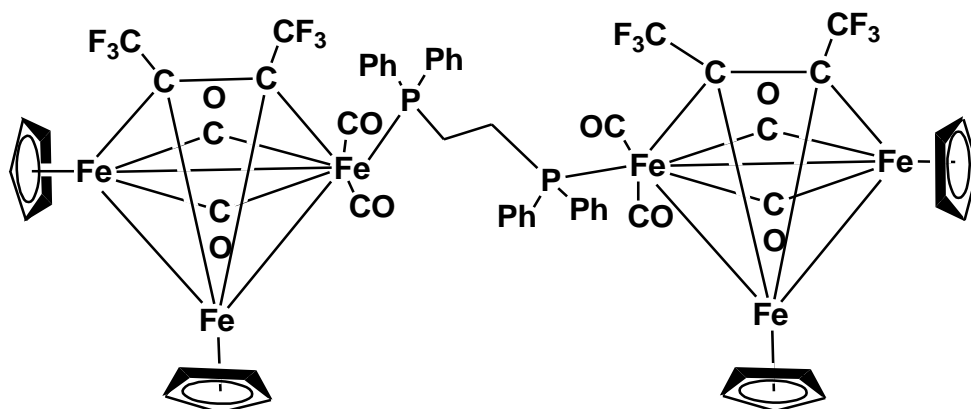


Figure.1.36 $[\{\text{Fe}_3\text{Cp}_2(\text{CO})_2(\mu\text{-CO})(\mu_3\text{-CO})-(\mu_3\text{-}\eta^1, \eta^1, \eta^2\text{-CF}_3\text{C}_2\text{CF}_3)\}_2\{\mu\text{-Ph}_2\text{P}(\text{CH}_2)_2\text{PPh}_2\}]$

Bridging of two diphosphine ligands in between two cluster units has also been observed during the formation of macrocyclic complex $[\{\text{Ru}_3(\text{CO})_7(\mu_3\text{-CMe})(\mu\text{-H})_3\}_2(\mu\text{-dppm})_2]$. The cluster molecule contains two dppm ligand bridging two triruthenium clusters. Each phosphorus atom of the dppm is coordinated to a different Ru_3 cluster core (Figure 1.37).⁴³

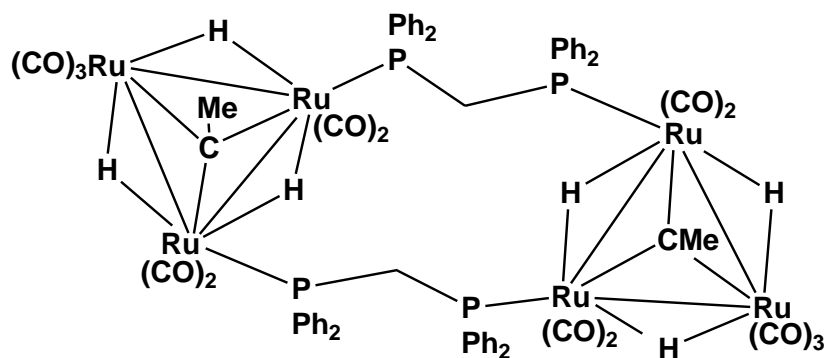


Figure 1.37 [$\{\text{Ru}_3(\text{CO})_7(\mu_3\text{-CMe})(\mu\text{-H})_3\}_2(\mu\text{-dppm})_2$]

1.3.4 Cluster containing phosphido ligands

Phosphido ligands $\mu\text{-PR}_2$ are formed by the loss of one of the R group from coordinated phosphine and binds with metal in bridging mode involving three electrons. Nishibayashi et al. synthesized a tetraruthenium cluster bridged by phosphido, sulfido and chloro ligands. Each one of the two phosphido groups is doubly bridged to ruthenium centres with a Ru–P bond distance of 2.28 Å (Figure 1.38). Each of the two triply bridged sulfido ligand attached to three ruthenium atoms is acting as a clamp to stabilize the molecule.⁴⁴

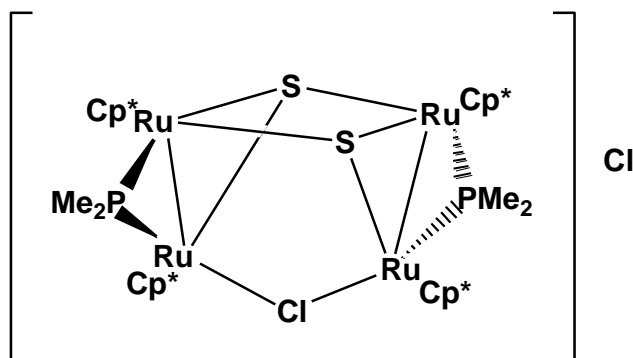


Figure 1.38 [$\{\text{Cp}^*\text{Ru}(\mu\text{-PMe}_2)\text{RuCp}^*\}_2(\mu^3\text{-S})_2(\mu\text{-Cl})$] Cl

Thermolysis of $\text{Os}_3(\text{CO})_{10}(\mu, \eta^3\text{-}(\text{PPh}_2)\text{C}_{60}\text{H})$ in refluxing chlorobenzene led to ortho-metalation of one phenyl group and C-H bond activation of the $(\text{PPh}_2)\text{C}_{60}\text{H}$ ligand to afford the phosphido cluster $[(\mu\text{-H})_2\text{Os}_3(\text{CO})_9(\mu_3, \eta^2\text{-PPh}(\text{C}_6\text{H}_4))]$. The cluster contains triply bridging $\text{PPh}(\text{C}_6\text{H}_4)$ ligand, two bridging hydride groups and terminally bonded carbonyl atoms linked to osmium metal atoms. While the phosphorus atom of the phosphido group is linked to two osmium atoms, the third Os atom is attached to the aromatic carbon (Figure 1.39).⁴⁵

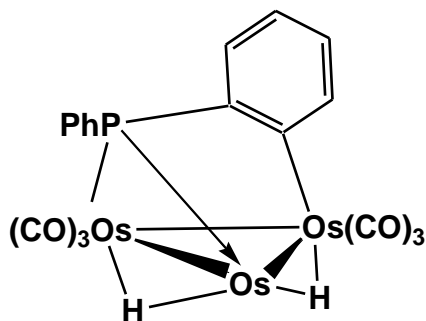
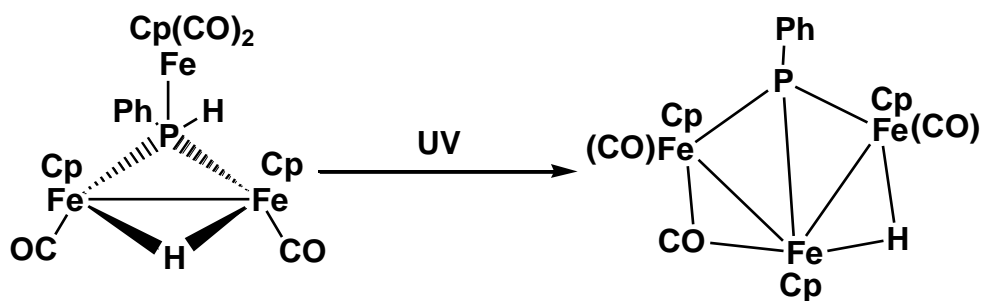


Figure 1.39 $[(\mu\text{-H})_2\text{Os}_3(\text{CO})_9(\mu_3, \eta^2\text{-PPh}(\text{C}_6\text{H}_4))]$

1.3.5. Cluster containing phosphinidene ligands

Phosphinidene ligands (PR) is obtained by the loss of two organic substituent from the phosphine moiety and has been found to donate 4-electron to form mostly triply or quadruply bridging face capping ligand ($\mu_3\text{-PR}$ or $\mu_4\text{-PR}$). Room temperature reaction of phosphine complexes $[\text{Fe}_2\text{Cp}_2(\mu\text{-CO})_2(\text{CO})(\text{PH}_2\text{Ph})]$ with the cluster $[\text{Fe}_2\text{Cp}_2(\mu\text{-CO})_2(\text{CO})(\text{NCMe})]$ in dichloromethane gives the triiron phosphinidene derivative $[\text{Fe}_3\text{Cp}_3(\mu\text{-H})(\mu_3\text{-PPh})(\text{CO})_4]$. Irradiation of toluene solutions of this tetracarbonyl cluster $[\text{Fe}_3\text{Cp}_3(\mu\text{-H})(\mu_3\text{-PPh})(\text{CO})_4]$ with UV-visible light gave another phosphinidene derivative $[\text{Fe}_3\text{Cp}_3(\mu\text{-H})(\mu_3\text{-PPh})(\mu\text{-CO})(\text{CO})_2]$ in quantitate yields (Scheme 1.1). The cluster is built from three metal fragments bridged by a phosphinidene ligand and forming a V-shaped metal core. A carbonyl and a hydride ligand are forming doubly bridged mode of bonding while three cyclopentadienyl groups and two terminal carbonyls are attached to the iron atoms.⁴⁶



Scheme 1.1

Treatment of an electronically unsaturated cluster $[(\mu\text{-H})\text{Os}_3(\text{CO})_8\{\text{Ph}_2\text{PCH}_2\text{P}(\text{Ph})\text{C}_6\text{H}_4\}]$ with primary phosphines PPhH_2 results in the formation of a phosphido bridged cluster compound $[(\mu\text{-H})\text{Os}_3(\text{CO})_8(\mu\text{-PPhH})(\mu\text{-dppm})]$, which on thermolysis forms the phosphinidene compound $[(\mu\text{-H})_2\text{Os}_3(\text{CO})_7(\mu_3\text{-PPh})(\mu\text{-dppm})]$. The three Os atoms with the phosphinidene unit constitute a trigonal pyramidal geometry with two hydride ligands and one diphosphine group forming a bridge across Os-Os bonds (Figure.1.40). ^{31}P NMR spectrum of the cluster contains three equal intensity doublet of doublets for the three magnetically non-equivalent phosphorus atoms.⁴⁷

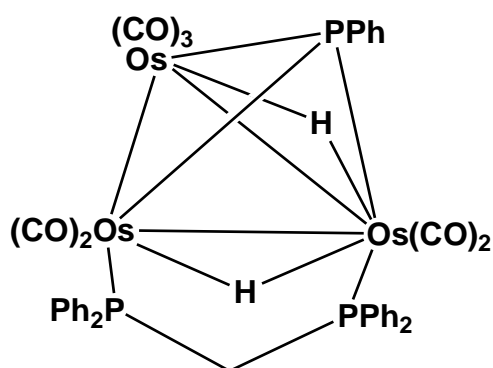


Figure.1.40 $[(\mu\text{-H})_2\text{Os}_3(\text{CO})_7(\mu_3\text{-PPh})(\mu\text{-dppm})]$

1.3.6. Cluster containing alkene and alkyne ligands

Alkenes and alkynes exhibit a wide variety of bonding modes through π - bonds donated towards metal centers. Their geometry is drastically affected upon coordination to a metal cluster due to the back donation of the electron-density from the metals into the π^* orbitals of the ligand. The coordination of alkynes to metal clusters depends on both the metal and the substituents on the alkyne. The variety of bonding interaction of a single alkyne molecule (HC_2R , RC_2R or $\text{RC}_2\text{R}'$) with two to four metal centers is summarized in Figure 1.41.⁴⁸

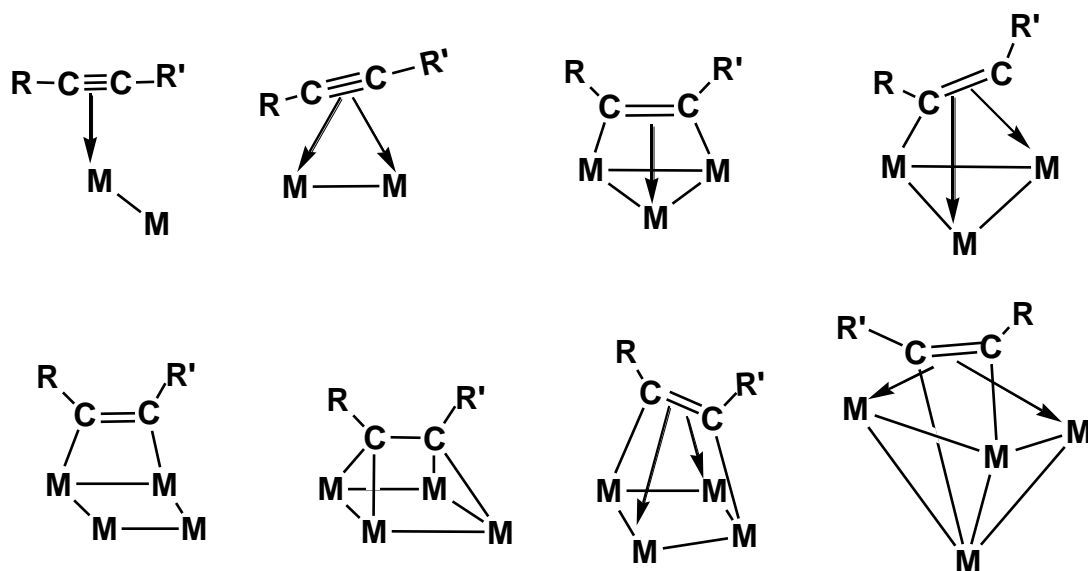


Figure 1.41 Some modes of alkyne interaction with metal centers

Moreno et al. have reported a synthetic method for the preparation of alkyne coordinated cluster $[\text{Os}_3(\mu\text{-H})(\text{CO})_9\{\mu_3, \eta^1:\eta^3:\eta^1\text{-RC}_2\text{COHC}\equiv\text{CR}\}]$ ($\text{R} = \text{C}_4\text{H}_9\text{S}$), containing a bridging hydride unit by the reaction of $\text{RC}\equiv\text{CC}\equiv\text{CR}$ ($\text{R} = \text{C}_4\text{H}_9\text{S}$), with $[\text{Os}_3(\text{CO})_{11}(\text{CH}_3\text{CN})]$ in dichloromethane solvent at room temperature, in the presence of water. The three osmium atoms in the cluster are coordinated to one of the two $\text{C}\equiv\text{C}$ triple bond in a μ_3, η^2 mode. As a result the coordinated C-C bond has increased in length to that in single bond length (Figure.1.42).⁴⁹

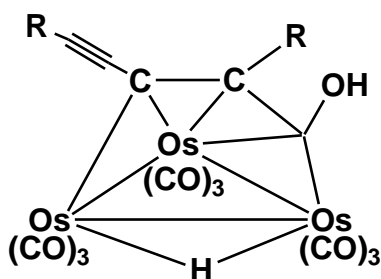


Figure.1.42 $[\text{Os}_3(\mu\text{-H})(\text{CO})_9\{\mu_3, \eta^1:\eta^3:\eta^1\text{-RC}_2\text{COHC}\equiv\text{CR}\}]$ ($\text{R} = \text{C}_4\text{H}_9\text{S}$)

Thermolysis of $[(\text{Cp}^*\text{Ru})_3(\mu_3\text{-CH})(\mu_3\text{-}\eta^2(\parallel)\text{-MeCCH})(\mu\text{-H})_2]$ in benzene at 180°C for 12 h resulted in the exclusive formation of the (\perp)-phenylmethylacetylene complex $(\text{Cp}^*\text{Ru})_3(\mu_3\text{-CH})(\mu_3\text{-}\eta^2:\eta^2(\perp)\text{-PhCCMe})$. X-ray diffraction study shows that the phenylmethylacetylene

ligand is coordinated to the Ru-Ru edge in a perpendicular mode and bisects the Ru₃ triangle (Figure 1.43).⁵⁰

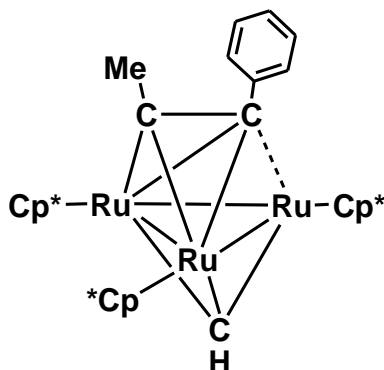


Figure.1.43 [Cp*Ru]₃(μ₃-CH)(μ₃-η²:η²(⊥)-PhCCMe)]

The photolysis of a hexane solution containing ferrocenylacetylene and an excess of tungsten hexacarbonyl at -10°C, resulted in the formation of a ditungsten-1,4,5,8-ferrocenylcyclodecatetraene [W₂{μ-η¹η²,η²,η²- (Fc)C(H)=C(H)=C(Fc)C(Fc)=C(H)C(H)=C(Fc)}(CO)₆] (Figure 1.44).⁵¹

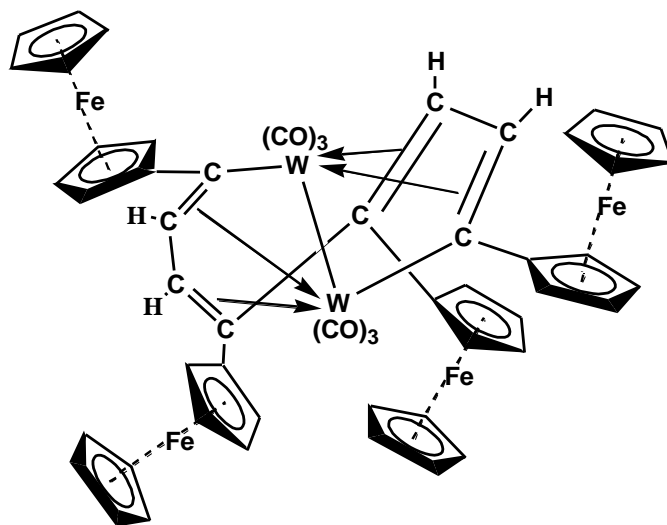


Figure 1.44 [W₂{μ-η¹η²,η²,η²- (Fc)C(H)=C(H)=C(Fc)C(Fc)=C(H)C(H)=C(Fc)}(CO)₆]

1.3.7. Cluster with cyclopentadienyl ligands

Cyclopentadienyl ligands [C₅H₅]⁻ are common throughout organometallic chemistry and metal cluster chemistry. In most of the cyclopentadienyl ring containing cluster compounds the Cp ring is bonded in η⁵ mode, in which all five carbon atoms π- bonded to a single metal centre

act as a five electron donor. However, other hapticity like η^3 and η^1 are also known (Figure 1.45).

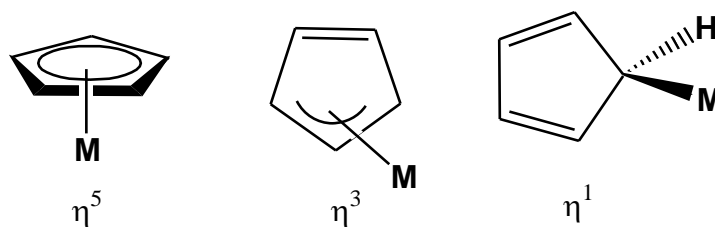


Figure 1.45

Cyclopentadienyl ligands rarely undergo reaction themselves and often simply act only to occupy coordination sites. The most interesting property of cyclopentadienyl ligand is their ability to enforce different geometry to the cluster framework. The ability of cyclopentadienyl ligands to stabilize favored geometries despite unusual electron counts enables some clusters to act like electron reservoir. Cluster with cyclopentadienyl ligand often shows multiple oxidation state resulting in compounds containing unusual properties. Some recent examples of metal clusters containing cyclopentadienyl ligands has been described. Refluxing of the trinuclear cluster $[\text{Cp}_3\text{Rh}_3(\mu\text{-CO})_3]$ with the ethylene complex $[\text{RhCp}(\text{C}_2\text{H}_4)_2]$ in *m*-xylene affords a neutral tetranuclear cluster $[\text{Rh}_4\text{Cp}_4(\mu_3\text{-CO})_2]$ as a major product and a dicationic hexanuclear cluster $[\text{Rh}_6\text{Cp}_6(\mu_6\text{-C})]^{2+}$ with interstitial carbon atom as a minor product. The molecular structure of the neutral cluster complex $[\text{Rh}_4\text{Cp}_4(\mu_3\text{-CO})_2]$, shows a tetrahedral Rh_4 core with a η^5 -cyclopentadienyl ligand coordinated to each rhodium atom while the two opposite Rh_3 faces are bridged by $\mu_3\text{-CO}$ ligands (Figure.1.46). Similarly, the geometry of cationic $[\text{Rh}_6\text{Cp}_6(\mu_6\text{-C})]^{2+}$ consists of six rhodium atoms with a η^5 -cyclopentadienyl ligand coordinated to each rhodium atom. Hexanuclear core of this cluster presents a regular Rh_6 octahedron with the interstitial carbon.⁵² Although, the rhodium metal atoms are coordinated to ligands like Cp and carbonyl groups, the cluster remains electron deficient with the total electron count less than a precise cluster complex.

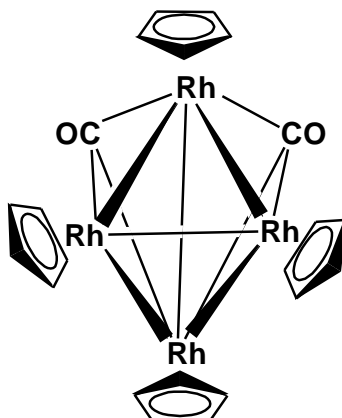


Figure.1.46 $\text{Rh}_4\text{Cp}_4(\mu_3\text{-CO})_2$

The reaction of $[\text{Cb}^*\text{Co}(\text{CO})_2]$ ($\text{Cb}^* = \text{tetramethylcyclobutadiene}$) with the $[\text{Cp}_2\text{Cr}_2(\text{SCMe}_3)_2\text{S}]$ complex gave the heterometallic cluster, $[\text{Cb}^*\text{Co}(\mu_3\text{-S})_2\text{Cr}_2\text{Cp}_2](\mu\text{-SCMe}_3)$. The X-ray diffraction study showed that this cluster complex contains a triangular Cr_2Co core along with two μ_3 -sulfide bridges and cyclopentadienyl and *tert*-butylthiolate ligands at the chromium atoms and a tetramethylcyclobutadiene ligand at the cobalt atom (Figure 1.47).⁵³

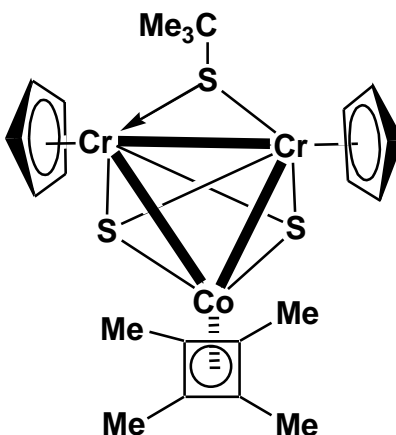


Figure 1.47 $[\text{Cb}^*\text{Co}(\mu_3\text{-S})_2\text{Cr}_2\text{Cp}_2](\mu\text{-SCMe}_3)$

Treatment of $[(\eta^5\text{-C}_5\text{H}_4\text{Me})_4\text{Fe}_4(\text{HCCH})(\mu_3\text{-CH})(\mu_3\text{-CNH}^t\text{Bu})](\text{PF}_6)_2$ with 1,8-diazabicyclo[5.4.0]-undec-7-ene (DBU) in acetonitrile afforded a tetra-iron cluster $[(\eta^5\text{-C}_5\text{H}_4\text{Me})_4\text{Fe}_4(\text{HCCH})(\mu_3\text{-CH})(\mu_3\text{-}\eta^1\text{-CN}^t\text{Bu})](\text{PF}_6)$ in quantitative yield. X-ray crystallography confirmed the existence of five iron-iron bonds and a $\mu_3\text{-}\eta^1$ -isonitrile ligand. Each metal centre in the cluster is coordinated to a cyclopentadienyl ring (Figure 1.48).⁵⁴

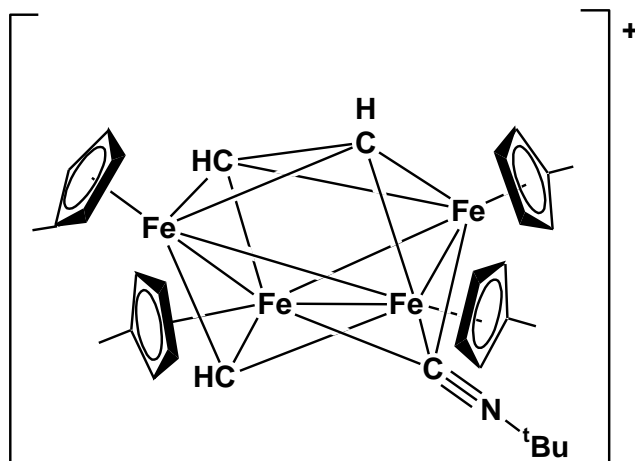


Figure 1.48 $[(\eta^5\text{-C}_5\text{H}_4\text{Me})_4\text{Fe}_4(\text{HCCH})(\mu_3\text{-CH})(\mu_3\text{-}\eta^1\text{-CN}^t\text{Bu})](\text{PF}_6)^+$

1.3.8. Cluster containing oxo ligands

An oxo ligand is an oxygen atom bound only to one or more metal centre. These ligands can exist as terminal or as bridging atom (Figure 1.49). Although oxo ligands stabilizes high oxidation state of a metal, examples are known where oxo ligands are present with low oxidation state metals.⁵⁵

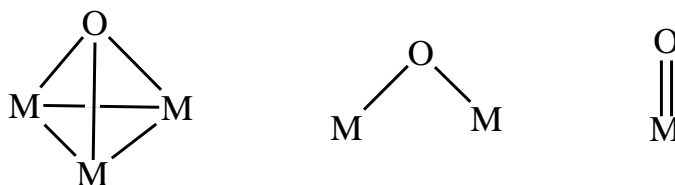


Figure 1.49 Modes of Oxo ligand bonding

The reaction of the dinuclear trihydrido-bridged complex $[\text{H}_3\text{Ru}_2(\text{C}_6\text{Me}_6)(p\text{-Pri-MeC}_6\text{H}_4)]^+$ with the well-known mononuclear triaqua complex $[\text{Ru}(\text{C}_6\text{H}_6)(\text{H}_2\text{O})_3]^{2+}$ in aqueous solution, gives a cationic oxo-capped tetrahedral trinuclear ruthenium cluster $[\text{H}_3\text{Ru}_3(\text{C}_6\text{H}_6)(\text{C}_6\text{Me}_6)(p\text{-Pri-MeC}_6\text{H}_4)(\text{O})]^+$ containing a chiral Ru_3O tetrahedral framework. Due to the four chemically different vertices of the tetrahedron formed by the three arene ruthenium units and the oxo capping in the cluster, the three hydride ligands are non-equivalent (Figure 1.50).⁵⁶

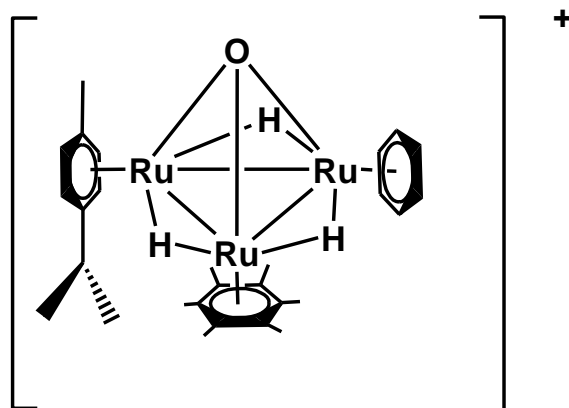


Figure 1.50. $[\text{H}_3\text{Ru}_3(\text{C}_6\text{H}_6)(\text{C}_6\text{Me}_6)(p\text{-Pr}^i\text{MeC}_6\text{H}_4)(\text{O})]^+$

Reaction of $\text{Fe}_3(\text{CO})_{12}$ with 1,8-bis(diphenylphosphino)naphthalene (dppn) yields a tetranuclear oxo cluster $[\text{Fe}_4(\text{CO})_{10}(\mu_4\text{-O})(\kappa^2\text{-dppn})]$. The molecule consists of a butterfly arrangement of four iron atoms, with the oxide nestled between the wings. The diphosphine is symmetrically bound in a chelating fashion to one of the wingtip atoms, which also carries a single carbonyl ligand, while the other three iron atoms are bound to three terminally bonded carbonyl ligands (Figure 1.51).⁵⁷

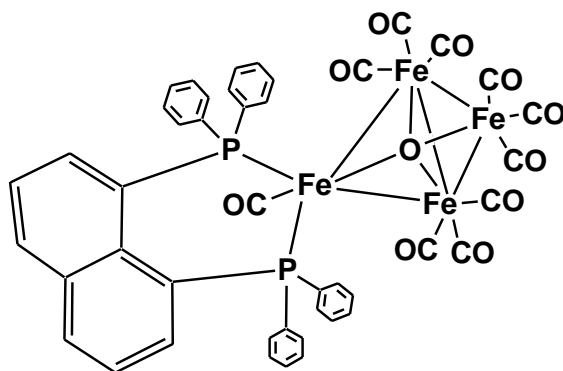


Figure 1.51 $[\text{Fe}_4(\text{CO})_{10}(\mu_4\text{-O})(\kappa^2\text{-dppn})]$

Mathur et al. have reported that in presence of low concentration of oxygen, 2.5-5% O_2 , $[\text{Fe}_2\text{Mo}(\text{CO})_{10}(\mu_3\text{-Se})_2]$ reacts with an acetylide, $[(\eta^5\text{-C}_5\text{Me}_5)\text{W}(\text{CO})_3\text{C}\equiv\text{CPh}]$ to form a selenido and acetylide-bridged oxo cluster $[(\eta^5\text{-C}_5\text{Me}_5)\text{MoWFe}_2(\text{O})(\mu_3\text{-Se})(\mu_4\text{-Se})(\text{CO})_8(\text{CCPh})]$ (Figure 1.53). In another reaction, the sulfur analogue $[\text{Fe}_2\text{Mo}(\text{CO})_{10}(\mu_3\text{-S})_2]$ reacts with $[(\eta^5\text{-C}_5\text{Me}_5)\text{W}(\text{CO})_3\text{C}\equiv\text{CPh}]$ to form a cluster $[(\eta^5\text{-C}_5\text{Me}_5)\text{W}\text{Mo}_2(\mu\text{-O})_2(\mu\text{-S})(\mu^3\text{-$

CCPh) $\{\text{Fe}_2(\text{CO})_6(\mu^3\text{-S})_2\}_2$] containing two bridging oxo ligands linking the acetylide tungsten metal atom with the cluster molybdenum atom (Figure 1.52). Both the oxo ligands are acting as bridges between two Fe_2Mo cluster units resulting in the formation of higher nuclear species.⁵⁸

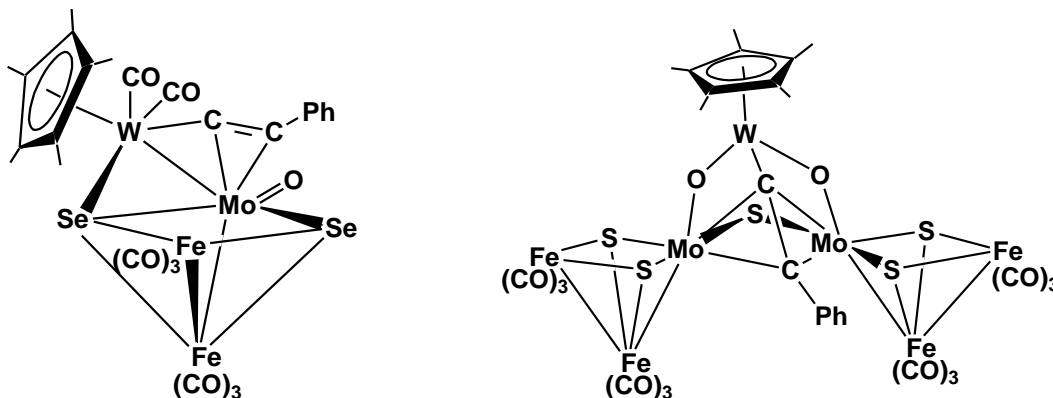


Figure.1.52 $[(\eta^5\text{-C}_5\text{Me}_5)\text{MoWFe}_2(\text{O})(\mu_3\text{-Se})(\mu_4\text{-Se})(\text{CO})_8(\text{CCPh})]$ and $[(\eta^5\text{-C}_5\text{Me}_5)\text{WMo}_2(\mu\text{-O})_2(\mu\text{-S})(\mu^3\text{-CCPh})\{\text{Fe}_2(\text{CO})_6(\mu^3\text{-S})_2\}_2]$

1.3.9. Cluster containing acetylide ligands

The acetylide group ($-\text{C}\equiv\text{CR}$) is an extremely versatile ligand, which can bind to two or more transition metal centers in a variety of coordination modes, while donating up to five electrons in bonding to the metal framework.⁵⁹⁻⁶² Some examples of coordination of the acetylide unit in complexes of the type $[\text{M}]_m(\mu_n\text{-C}_2)$ are shown in Figure 1.53.

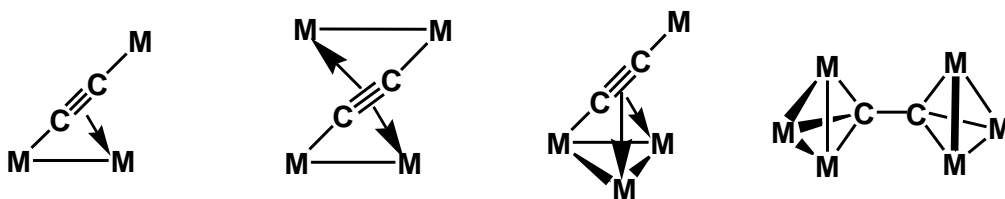


Figure 1.53

Transition metal acetylides have attracted considerable interest for numerous reasons that include their reactivity towards a variety of small molecules to give unusual organometallic compounds.⁶³⁻⁶⁹ In the previous section, some examples containing both oxo and acetylide ligands have been described, the later playing the role of linking metal units together. In this section we will depict some examples of metal clusters containing acetylide fragments either

pendant or coordinated. The reaction of $\{\text{Ar}'\text{Fe}(\mu\text{-Br})\}_2$ ($\text{Ar}' = \text{C}_6\text{H}_3\text{-2,6-(C}_6\text{H}_3\text{-2,6-}^i\text{Pr}_2)_2$) with $\text{LiC}\equiv\text{CPh}$ afforded the unusual 1,3-butadiene-1,4-diyl iron-coordinated derivative $[\text{Fe}_2\{\text{Ar}'\text{C}=\text{C}(\text{Ph})\text{-C}(\text{Ph})=\text{CAr}'\}]$ (Figure 1.54). In this cluster the dimeric structure is a result of Ar' group transfer to the iron-bound carbon of the acetylide ligand and subsequent dimerization via coupling of the phenyl-substituted carbons.⁷⁰

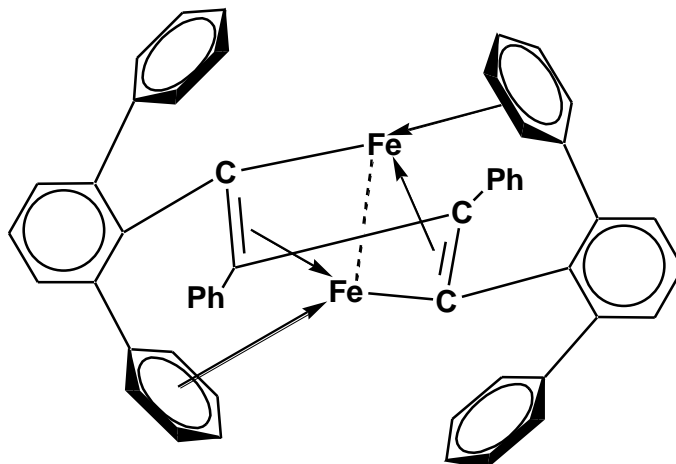


Figure 1.54 $[\text{Fe}_2\{\text{Ar}'\text{C}=\text{C}(\text{Ph})\text{C}(\text{Ph})=\text{CAr}'\}]$ ($\text{Ar}' = \text{terphenyl group}$)

A heteronuclear cluster acetylide with unique bonding environment has been synthesized by Mathur et. al. from a reaction between iron chalcogen cluster and mononuclear metal acetylide in presence of trimethylamine-oxide (Figure 1.55).⁷¹

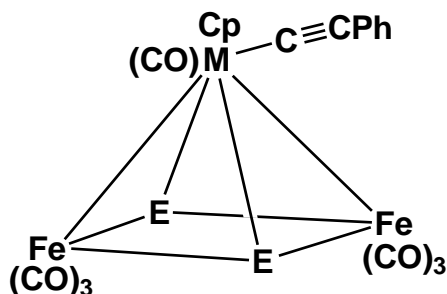


Figure.1.55 $[\text{CpM}(\text{CO})\text{C}\equiv\text{C-Ph}]$, ($\text{E}=\text{Se,Te}$; $\text{M}=\text{Mo, W}$)

The above cluster has been used for the coordination of pendant acetylide unit with dicobaltoctacarbonyl which led to the formation of multimetallic clusters as shown in Figure 1.56.

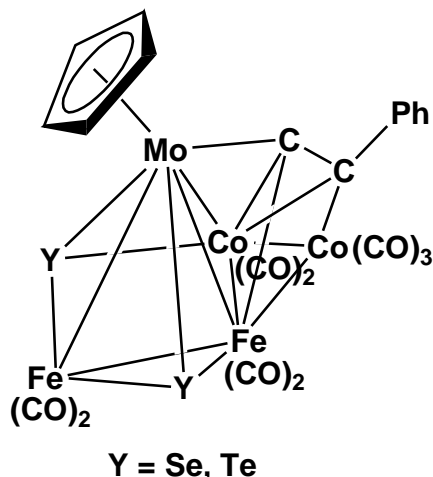


Figure 1.56

Photolytic reaction of a benzene solution of $[\text{Fe}(\text{CO})_5]$ and $[(\eta^5\text{-C}_5\text{R}_5)\text{Mo}(\text{CO})_3(\text{C}\equiv\text{CPh})]$ ($\text{R} = \text{H}, \text{Me}$) under continuous bubbling of argon results in a rapid formation of $[(\eta^5\text{-C}_5\text{R}_5)\text{Fe}_2\text{Mo}(\text{CO})_8(\mu_3\text{-}\eta^1:\eta^2:\eta^2\text{-CCPh})]$ ($\text{R}=\text{H}$, Figure 1.57) and $[(\eta^5\text{-C}_5\text{H}_5)\text{Fe}_3\text{Mo}(\text{CO})_{11}(\mu_4\text{-}\eta^1:\eta^1:\eta^2:\eta^1\text{-CCPh})]$ (Figure 1.58) (Scheme 41).⁶⁷ The structure in Figure 1.57 consists of a MoFe_2 triangle and a $\mu_3\text{-}\eta^1,\eta^2,\eta^2$ acetylide ligand, whereas in Figure 1.58 an open Fe_3Mo butterfly arrangement with an acetylide group bonded in $\mu_3\text{-}\eta^1$ mode has been observed.⁷²

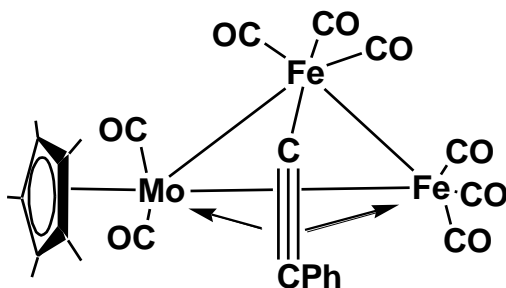


Figure 1.57 $[(\eta^5\text{-C}_5\text{R}_5)\text{Fe}_2\text{Mo}(\text{CO})_8(\mu_3\text{-}\eta^1:\eta^2:\eta^2\text{-CCPh})]$ ($\text{R} = \text{H}, \text{Me}$)

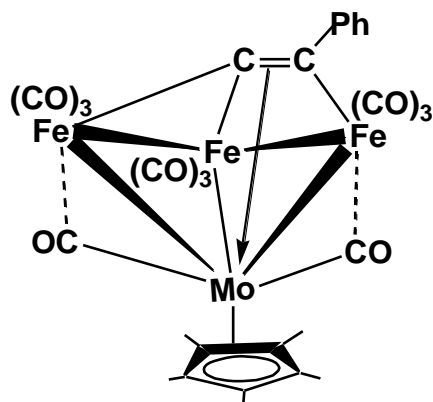


Figure 1.58 $[(\eta^5\text{-C}_5\text{H}_5)\text{Fe}_3\text{Mo}(\text{CO})_{11}(\mu_4\text{-}\eta^1:\eta^1:\eta^2:\eta^1\text{-CCPh})]$

1.3.10. Cluster containing other bridging ligands

A large number of transition metal clusters have been known to form complexes involving different types of other bridging ligands. Ligation of carbon chains of various lengths to metal clusters led to the formation of a variety of carbon chain supported cluster framework. One such example include a substituted allylidene coordinated diiron cluster, recently reported by the treatment of $[\text{Fe}_2\{\mu\text{-}\eta^1:\eta^3\text{-C}(\text{Me})\text{C}(\text{H})\text{C}=\text{N}(\text{Me})(\text{Xyl})\}\{\mu\text{-CO}\}(\text{CO})(\text{Cp})_2][\text{SO}_3\text{CF}_3]$ (Xyl = 2,5- $\text{C}_6\text{H}_3\text{Me}_2$) with NaH in the presence of $\text{H}_2\text{C}=\text{C}=\text{CMe}_2$. The structure of this complex can be described as being composed of a $\text{cis-Fe}_2(\text{Cp})_2(\mu\text{-CO})$ unit to which is bound a bridging allylidene ligand ($\text{C}^1\text{-C}^2\text{-C}^3$), containing one amino and one carboxylate substituent. The bridging C_3 unit is σ -coordinated to Fe_2 and η^3 -coordinated to Fe_1 in an allyl-like fashion (Figure 1.59).¹⁰⁰

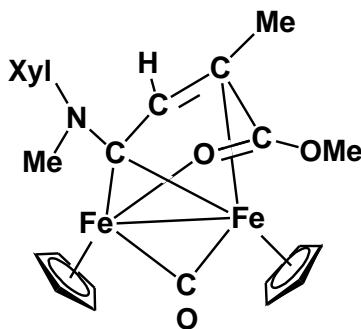


Figure 1.59 $[\text{Fe}_2\{\mu\text{-}\eta^1:\eta^3\text{-C}(\text{Me})\text{C}(\text{H})\text{CN}(\text{Me})(\text{Xyl})\}\{\mu\text{-CO}\}(\text{CO})(\text{Cp})_2][\text{SO}_3\text{CF}_3]$ (Xyl = 2,5- $\text{C}_6\text{H}_3\text{Me}_2$)

Transition metal clusters are known to coordinate with N-donor ligand forming a multidentate coordination. Figure 1.60 shows an amino benzothiazole ligand bridged to osmium metal centres obtained by the thermolysis of $[\text{Os}_3(\mu\text{-H})(\text{CO})_{10}(\mu\text{-C}_8\text{H}_7\text{N}_2\text{S})]$ which results in the elimination of one carbonyl ligand to yield another triosmium cluster $[\text{Os}_3(\mu\text{-H})(\text{CO})_9(\mu_3\text{-}\eta^2\text{-C}_8\text{H}_7\text{N}_2\text{S})]$.¹⁰¹

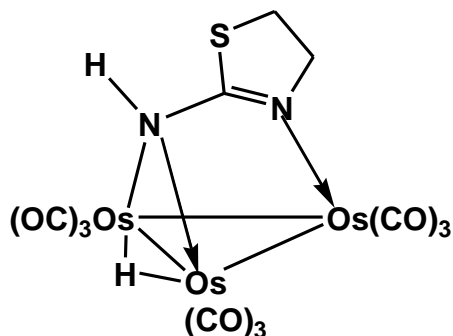


Figure 1.60 $[\text{Os}_3(\mu\text{-H})(\text{CO})_9(\mu_3\text{-}\eta^2\text{-C}_8\text{H}_7\text{N}_2\text{S})]$

An unique quadruply bridged transition metal cluster $[\text{Ru}_4(\mu_4\text{-}\eta^4\text{-dmpu})(\text{CO})_{10}]$, $\text{H}_2\text{dmpu} = \text{N,N}'\text{-bis(6-methylpyrid-2-yl)urea}$, has been prepared by treating $[\text{Ru}_3(\text{CO})_{12}]$ with H_2dmpu in toluene at reflux temperature. X-ray diffraction study has determined that this cluster has a butterfly metallic skeleton linked by a doubly-deprotonated $\text{N,N}'\text{-bis(6-methylpyrid-2-yl)urea}$ ligand (dmpu). This quadruply bridging ligand has the pyridine N atoms attached to the wing-tip ruthenium atoms and the amido N atoms spanning Ru–Ru wing-edges (Figure 1.61).¹⁰²

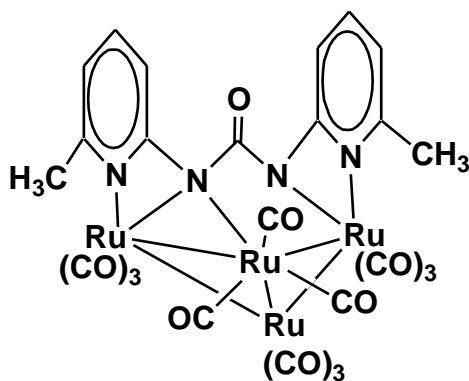


Figure 1.61 $[\text{Ru}_4(\mu_4\text{-}\eta^4\text{-dmpu})(\text{CO})_{10}]$

Another quadruply bridged CH coordinated cluster was synthesized when compound $[\text{Mo}_2\text{Cp}_2(\mu\text{-CH}_3)(\mu\text{-PCy}_2)(\text{CO})_2]$ reacts with $[\text{Fe}_2(\text{CO})_9]$ under photochemical conditions to give

the methylidyne-bridged compound $[\text{Fe}_2\text{Mo}_2\text{Cp}_2(\mu_4\text{-CH})(\mu\text{-PCy}_2)(\text{CO})_8]$. The CH ligand forms a bridge between the four metal atoms (Figure 1.62).¹⁰³

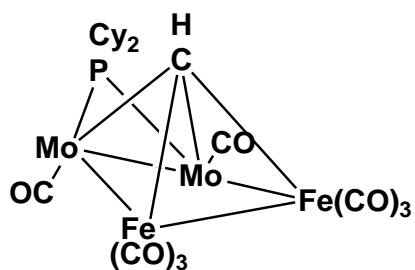


Figure 1.62 $[\text{Fe}_2\text{Mo}_2\text{Cp}_2(\mu_4\text{-CH})(\mu\text{-PCy}_2)(\text{CO})_8]$

1.4. TRANSITION METAL CLUSTER CONTAINING MAIN GROUP ELEMENTS

Heteronuclear transition metal cluster complexes have been known to exhibit unusual properties and are of particular interest as models of heterogeneous bimetallic alloy catalysts. Due to the presence of polar metal-metal bonds, these type of clusters frequently decompose and are converted to the monometallic species. Incorporation of main group elements into the metal clusters can often stabilize the cluster framework considerably. The main group elements act as a clamp and help to stabilize the overall cluster framework.⁷³ Group 13-16 atoms of the Periodic Table have been widely used for supporting cluster growth and stabilization purposes.⁷⁴ In the last two decades a large diversity of structural geometries have been observed for transition metal clusters containing Group 13-16 elements.⁷⁵⁻⁷⁸

Some recent reports includes the synthesis of transition metal homo and hetero nuclear clusters with main group atoms acting as bridging species between two or more metal atoms. $\text{Pt}(\text{P}^t\text{Bu}_3)_2$ reacts with the complex $[\text{Re}_3(\text{CO})_{12}(\mu\text{-BiPh}_2)(\mu\text{-H})_2]$ under heating condition to give a bismuth bridged cluster $[\text{trans-Pt}_2\text{Re}_5(\text{CO})_{22}\{\text{P}(\text{t-Bu})_3\}_2(\mu\text{-H})_3(\mu_4\text{-Bi})_2]$ containing two platinum-rhenium bonds and one rhenium-rhenium bond. Two quadruply-bridging spiro bismuth atoms are playing the role to link four different types of metal fragments (Figure 1.63).⁷⁹

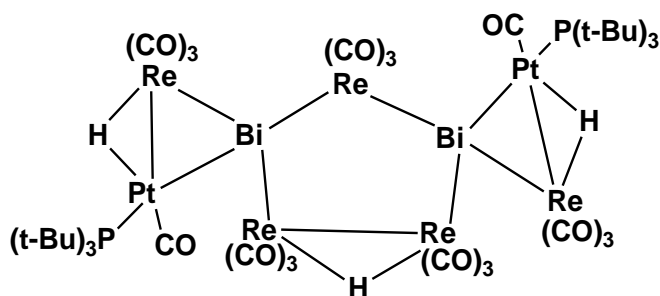


Figure 1.63 [*trans*-Pt₂Re₅(CO)₂₂{P(*t*-Bu)₃}₂(μ-H)₂(μ₄-Bi)₂]

Tellurium bridged cluster, [Ru₄(CO)₁₁(μ₄-Te)₂] has been prepared by refluxing a benzene solution containing [Fe₃(CO)₉(μ₃-Te)₂] and Ru₃(CO)₁₂.⁸⁰ The molecular structure reveals a octahedron with four basal ruthenium atoms and two tellurium atoms occupying the tip of the octahedron. Each of the tellurium atoms are quadruply bridged to four ruthenium metals, while one carbonyl ligand is doubly bridged and ten carbonyl groups are present as terminally bonded to metal atoms (Figure 1.64).

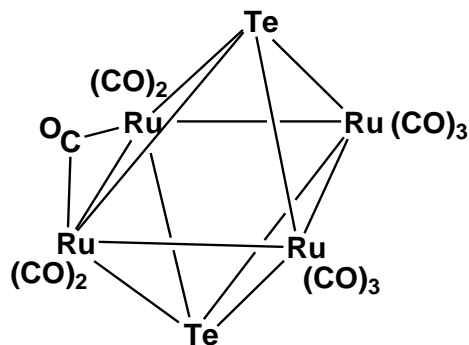


Figure 1.64 [Ru₄(CO)₁₁(μ₄-Te)₂]

Cluster containing bridging indium atom, [Re₄(CO)₁₂(μ₃-InRe(CO)₅)₄] has been recently and synthesized by the thermal reaction of Indium with [Re₂(CO)₁₀].⁸¹ The structure consists of a tetrahedral Re₄ fragment, each triangles of which are capped with a μ₃-InRe(CO)₅ group (Figure 1.65).

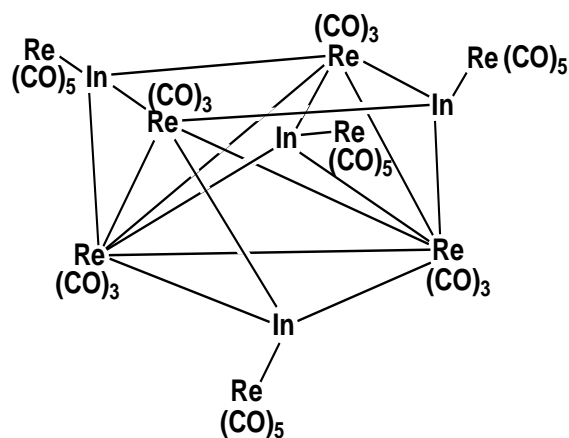


Figure 1.65 $[\text{Re}_4(\text{CO})_{12}(\mu_3\text{-InRe}(\text{CO})_5)_4]$

A thallium capped cluster $[\text{Re}_7\text{C}(\text{CO})_{21}\text{Tl}]^{2-}$ has been obtained on reaction of TlPF_6 with an anionic cluster, $[\text{Re}_7\text{C}(\text{CO})_{21}]^{3-}$. The presence of a thallium atom symmetrically capped to an octahedral face was revealed by single crystal X-ray study. The molecule consists of a Re_6 octahedron in which two of the octahedral faces are capped by thallium atom and a $\text{Re}(\text{CO})_3$ moiety and also contains a carbon atom at the center of the octahedron (Figure 1.66).⁸²

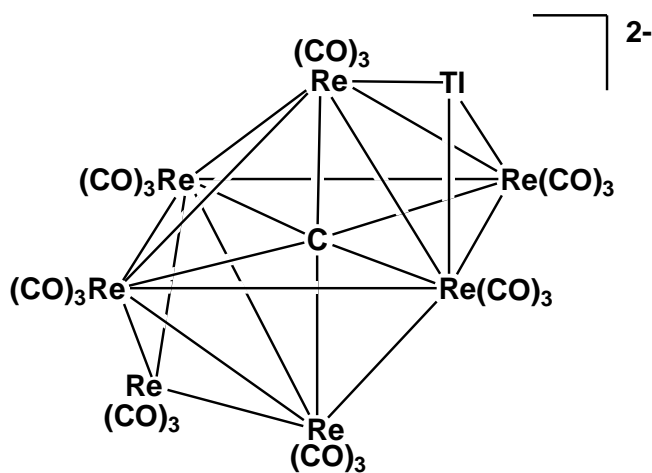


Figure 1.66 $[\text{Re}_7\text{C}(\text{CO})_{21}\text{Tl}]^{2-}$

Heterometallic spiro M_4E type cluster compounds with germanium as a single atom and bridged ligand has been reported in $[\text{Ge}\{\text{Fe}_2(\text{CO})_8\}\{(\text{MeC}_5\text{H}_4)\text{MnFe}(\text{CO})_6\}]$.⁸³ Cluster $[\text{Ge}\{\text{Fe}_2(\text{CO})_8\}\{(\text{MeC}_5\text{H}_4)\text{MnFe}(\text{CO})_6\}]$ has been prepared from the reaction of $[(\eta^5\text{-CH}_3\text{C}_5\text{H}_4)(\text{CO})_2\text{Mn}=\text{Ge}=\text{Mn}(\text{CO})_2(\eta^5\text{-CH}_3\text{C}_5\text{H}_4)]$ and $\text{Fe}_2(\text{CO})_9$ and contains an iron-iron and an iron-manganese bond (Figure 1.67).

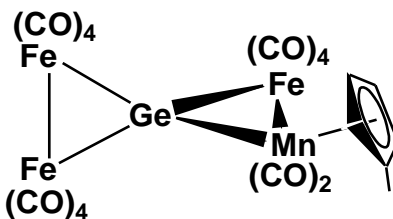


Figure 1.67 $[\text{Ge}\{\text{Fe}_2(\text{CO})_8\}\{(\text{MeC}_5\text{H}_4)\text{MnFe}(\text{CO})_6\}]$

Synthesis of a nona-coordinate bridging selenido ligand in a tricapped trigonal prismatic geometry, $[\text{Cu}_{11}(\mu_9\text{-Se})(\mu_3\text{-Br})_3\{\text{Se}_2\text{P}(\text{OPr}^i)_2\}_6]$ (Figure 1.68) has been reported along with the formation of a closed-shell ion-centered Cu_8 cubes, $[\text{Cu}_8(\mu_8\text{-Se})\{\text{Se}_2\text{P}(\text{OPr}^i)_2\}_6]$ and $[\text{Cu}_8(\mu_8\text{-Br})\{\text{Se}_2\text{P}(\text{OPr}^i)_2\}_6(\text{PF}_6)]$, from the low temperature reaction of $[\text{NH}_4\text{Se}_2\text{P}(\text{OPr}^i)_2]$, $[\text{Cu}(\text{CH}_3\text{CN})_4\text{PF}_6]$ and Bu_4NBr .⁸⁴

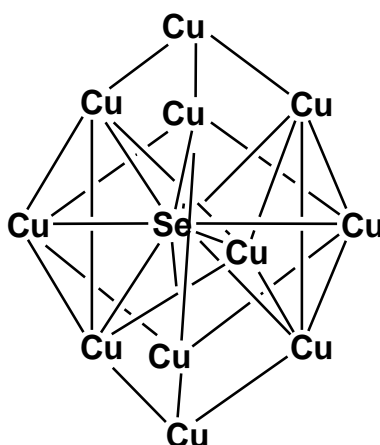


Figure 1.68 Core structure of $[\text{Cu}_{11}(\mu_9\text{-Se})(\mu_3\text{-Br})_3\{\text{Se}_2\text{P}(\text{OPr}^i)_2\}_6]$

A paramagnetic hexamanganese carbonyl selenide cluster $[\text{Se}_6\text{Mn}_6(\text{CO})_{18}]^{4+}$ was prepared by the treatment of selenium with $\text{Mn}_2(\text{CO})_{10}$ in KOH/MeOH solution. The cluster reacts with molecular oxygen under mild condition to afford a O-inserted cluster and led to the activation of O_2 . The structure composed of two $\text{Mn}_3\text{Se}_2(\text{CO})_9$ units linked together by a $\mu_4\text{-Se}_2$ ligand (Figure 1.69).⁸⁵

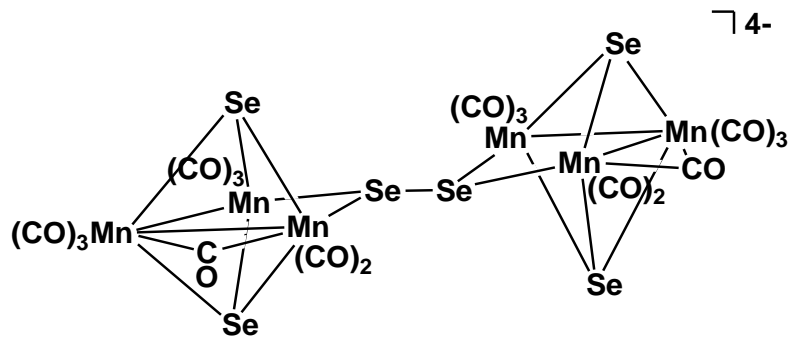


Figure 1.69

Recently, the group 16 elements, commonly known as chalcogens, have been used extensively for the stabilization of some unusual cluster geometries by either forming bridging units or capping ligands.^{86, 87} Sulphur, selenium or tellurium bridged clusters with various bonding modes and unique structural features have been obtained by different synthetic techniques (Figure 1.70)⁸⁸. The elements themselves act as 4-electron donors by either capping triangular metal faces (μ_3 -E) or square metal faces (μ_4 -E). Quadruply bridging chalcogen atoms can serve either as 4 or 6-electron donors.

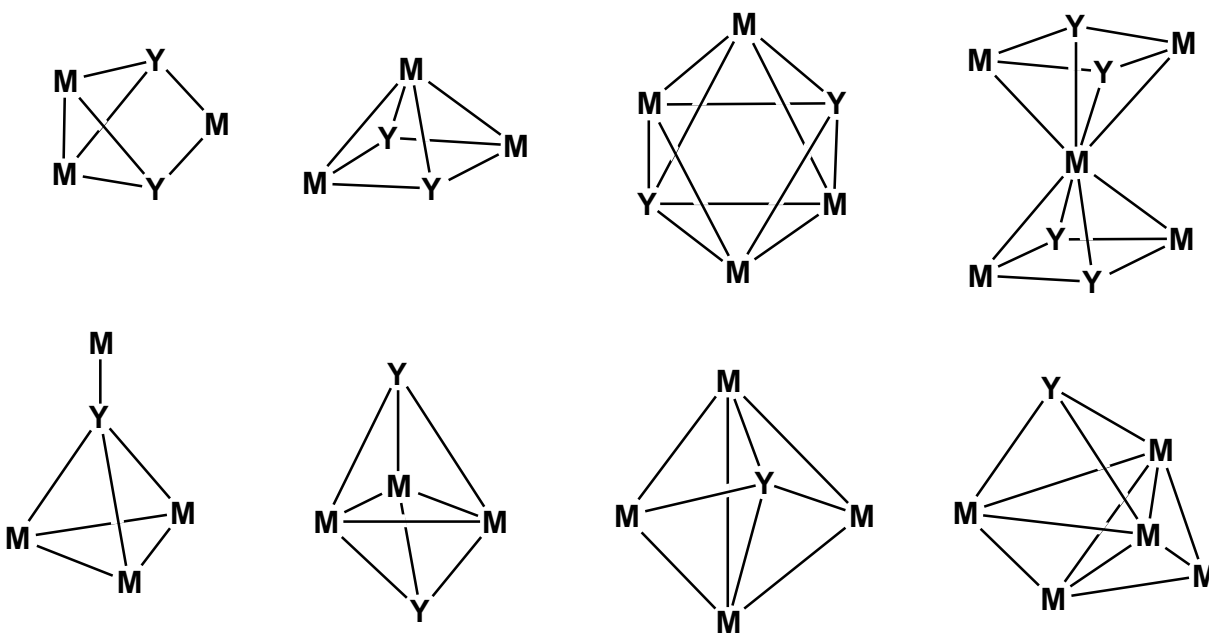


Figure 1.70 Various bonding modes exhibited by chalcogens

The chalcogen ligands have been known to act as bridging ligands and support the metal fragments in various cluster growth reactions. Designing of systematic synthetic routes to clusters containing metals -chalcogen bonds with new geometries and coordination modes led to the development of models and precursors for the synthesis of new materials.^{89, 90} Some of these metal-chalcogen containing building blocks has been of great interest due to their unusual structural features and tunable optoelectronic properties.⁹¹⁻⁹⁴

Formation of $[\text{Cp}_2\text{Mo}_2\text{Fe}_2(\text{CO})_6(\mu_4\text{-Te})(\mu_3\text{-Se})(\mu_3\text{-S})]$ (Figure 1.71) provides an example of mixed-metal cluster containing all three different types of chalcogen ligands in one cluster framework.⁹⁵ The larger chalcogen atom like tellurium occupies the μ_4 -bonding site, while the sulfur and selenium forms the triply bridging bonding with metals. The basic geometry consists of two FeMo_2 triangular arrays with a common Mo_2 edge. Each FeMo_2 plane has μ_3 -bonded chalcogen atom above it and in addition there is a third chalcogen atom quadruply bonded to all four metal atoms. The Mo-Mo bond distance can be tuned depending upon the size of the μ_3 -chalcogen atom.⁹⁶

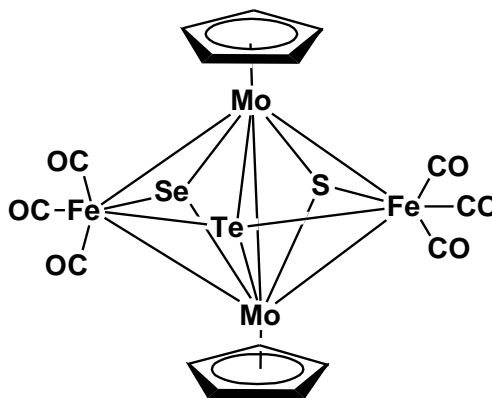


Figure 1.71 $[\text{Cp}_2\text{Mo}_2\text{Fe}_2(\text{CO})_6(\mu_4\text{-Te})(\mu_3\text{-Se})(\mu_3\text{-S})]$

Formation of higher nuclear mixed metal cluster was observed when an iron telluride anionic cluster, $[\text{TeFe}_3(\text{CO})_9]^{2-}$ was treated with 4 equivalents of CuCl at room temperature. The resulting cluster $[\{\text{TeFe}_3(\text{CO})_9\}_2\text{Cu}_4\text{Cl}_2]^{2-}$ contains a Cu_4Cl_2 fragment linked to two $\text{TeFe}_3(\text{CO})_9$ fragments in such a way that each TeFe_3 moiety are bridged and capped by two covalently bonded Cu atoms in which the two TeFe_3Cu_2 clusters were further connected by two Cl atoms (Figure 1.72).⁹⁷

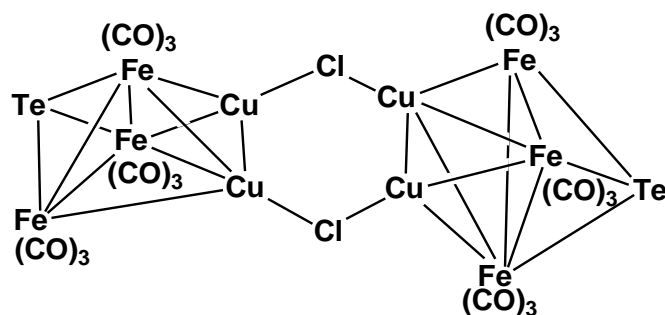


Figure 1.72 $[\{\text{TeFe}_3(\text{CO})_9\}_2\text{Cu}_4\text{Cl}_2]^{2-}$

Among the three group-16 elements, sulphur has the most extensive use in the cluster growth reactions with its diverse bonding modes in cluster complexes. Adams et al. reported a sulphur bridged cluster, $[\text{Mn}_4\text{Ni}_2\text{S}_4(\text{Cp})_2(\text{CO})_{14}]$ (Figure 1.73), containing two Mn-Ni metal metal bond and two MnNiS_2 fragments linked together via two $\text{Mn}(\text{CO})_4$ units.⁹⁸

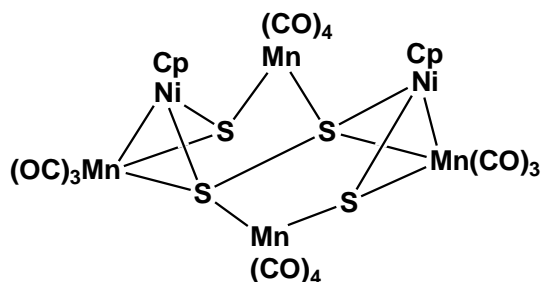


Figure 1.73 $[\text{Mn}_4\text{Ni}_2\text{S}_4(\text{Cp})_2(\text{CO})_{14}]$

Mixed chalcogen containing clusters are less explored than only for a specific chalcogen-containing cluster. Mathur's group synthesized mixed chalcogen containing iron-molybdenum cluster $[\text{Cp}_2\text{Mo}_2\text{Fe}_2\text{STe}(\text{CO})_7]$ (Figure 1.74) by the thermal reaction of $\text{Fe}_3\text{STe}(\text{CO})_9$ and $\text{Cp}_2\text{Mo}_2(\text{CO})_6$.⁹⁹ This cluster contains two Fe and two Mo-atoms bonded to triply bridged sulphur and tellurium atoms. Presence of Cyclopentadienyl ring attached to molybdenum atoms also play some role to stabilize the multimetallic cluster. The cluster also contains carbonyl ligands in three different bonding modes, terminally bonded, doubly bridging and semi-triply bridging.

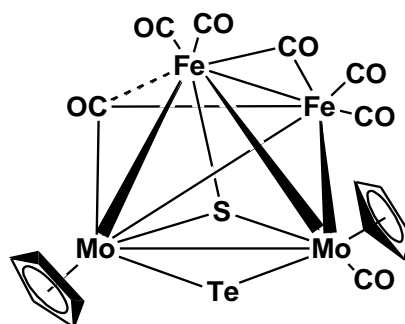


Figure 1.74 [Cp₂Mo₂Fe₂STe(CO)₇]

1.5. APPLICATION OF TRANSITION METAL CLUSTER

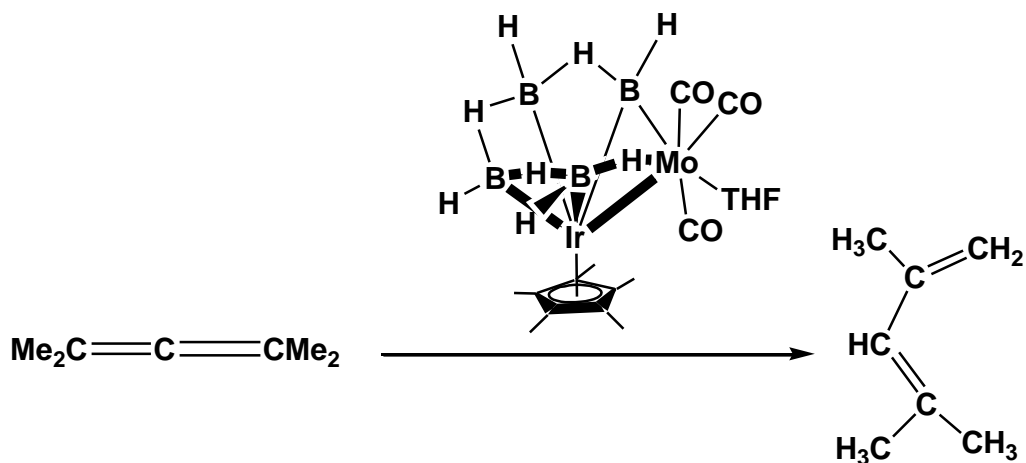
Transition Metal clusters have recently received significant attention for their use as potential catalyst and as precursor to catalyst in several catalytic reactions. Studies in this field have primarily used transition metal carbonyl cluster compounds deposited on a variety of metal oxide supports. Metal clusters have the ability to tune their properties by altering the controlling factors such as cluster framework, choice of ligands, formal oxidation state and varying the metal itself. The potential advantage of this polynuclear compounds is related to the fact that several metal atoms linked together can provide specific sites of interaction between organic molecules and clusters¹⁰⁴⁻¹⁰⁶ Furthermore, in comparison to mononuclear compounds, metal clusters are more advantageous because of their ability to catalyze the multielectron process and to bind small molecules by way of multiple metal ligand bonds. As a result clusters like Ru₃(CO)₁₂ and Ir₄(CO)₁₂ catalyze the water gas shift reaction and Rh₆(CO)₁₆ catalyzes the conversion of carbon monoxide into hydrocarbons.

Clusters have been commonly used as catalysts in the biological environment, for example, the iron-sulfur proteins, which are involved with electron-transfer and catalyses certain transformations. Nitrogen is reduced to ammonia at a Fe-Mo-S cluster at the core of the enzyme nitrogenase. CO is oxidized to CO₂ by the Fe-Ni-S cluster of carbon monoxide dehydrogenase while the hydrogenase enzyme uses Fe₂ and NiFe cluster framework for enzymatic action.¹⁰⁷ Metal clusters have also been used as valuable precursors for preparation of bimetallic and multimetallic heterogenous catalysts. These are very useful for activation of organic molecules

and catalysis. These are of immense interest due to their diverse structural property and potential applications in the field of material science.

1.5.1. Catalysis by metal cluster compounds

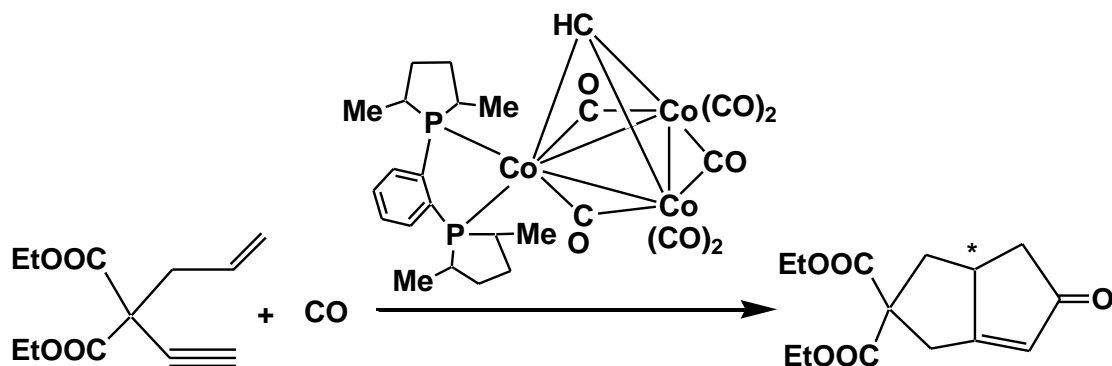
Clusters with well defined structures are excellent models for catalytic studies, and size effects seem to be crucial in determining their reactivity.¹⁰⁸ O'Hair's group first demonstrated that dimeric $[\text{Mo}_2\text{O}_6(\text{OH})]^-$ anion efficiently catalyzes the gas-phase transformation of methanol to formaldehyde while its mononuclear $[\text{MoO}_3(\text{OH})]^-$ congener is not active.¹⁰⁹ Gas phase tungsten (VI) oxide trimers with a proposed $[\text{W}_3(\mu\text{-O})_3\text{O}_4]$ structure deposited over TiO_2 surface have also been investigated as models for the catalytic oxidation of alcohols where 2-propanol is efficiently converted to propene.¹¹⁰ Cluster nido-dimetallahexaborane, $[1\text{-Cp}^*\text{-}2,2,2\text{-(CO)}_3\text{-}2\text{-THF-nido-}1,2\text{-IrMoB}_4\text{H}_8]$ has been recently found to be a catalyst precursor for the isomerization of olefins, for example, for the conversion of tetramethyl allene to 2,4-dimethylpenta-1,3-diene (Scheme 1.2).¹¹¹



Scheme 1.2

Phosphine derivatives of alkylidyne tricobalt carbonyl clusters have been tested as catalysts in several Pauson–Khand reactions (Scheme 1.3). A number of new phosphine derivatives of the tricobalt alkylidyne clusters $[\text{Co}_3(\mu_3\text{-CR})(\text{CO})_9]$ ($\text{R} = \text{H}, \text{CO}_2\text{Et}$) were prepared and characterized. The clusters $[\text{Co}_3(\mu_3\text{-CR})(\text{CO})_{9-x}(\text{PR}'_3)_x]$ ($x = 1\text{-}3; \text{R} = \text{CO}_2\text{Et}, \text{H}; \text{R}' = \text{Et},$

PMe_2Ph), $[\text{Co}_3(\mu_3\text{-CR})(\text{CO})_7(\text{P-P})]$ ($\text{P-P} = \text{dppe, dppm}$) and $[\text{Co}_3(\mu_3\text{-CH})(\text{CO})_7(\text{P-P})]$ [$\text{P-P} = (\text{R,R})\text{-Me-DUPHOS}$] were assayed as catalysts for intermolecular and intramolecular Pauson–Khand reactions. The phosphine-substituted tricobalt clusters proved to be viable catalysts/catalyst precursors that gave moderate to very good yields.¹¹²



Scheme 1.3

Phosphine coordinated iridium clusters $[\text{Ir}_4(\text{CO})_8(\mu_3\text{-}\eta^2\text{-HCCPh})(\mu\text{-PPh}_2)_2]$ and $[\text{Ir}_4(\text{CO})_9(\mu_3\text{-}\eta^3\text{-Ph}_2\text{PC(H)CPh})(\mu\text{-PPh}_2)]$ were investigated as catalyst precursors for the selective hydrogenation of 1,5-cyclooctadiene (Figure 1.75). The results reveals the increased activity and high selective nature of the catalyst for the monohydrogenated product cyclooctene and the isomerisation products 1,3-COD and 1,4-COD, with almost complete suppression of the total hydrogenation reaction to cyclooctane.¹¹³

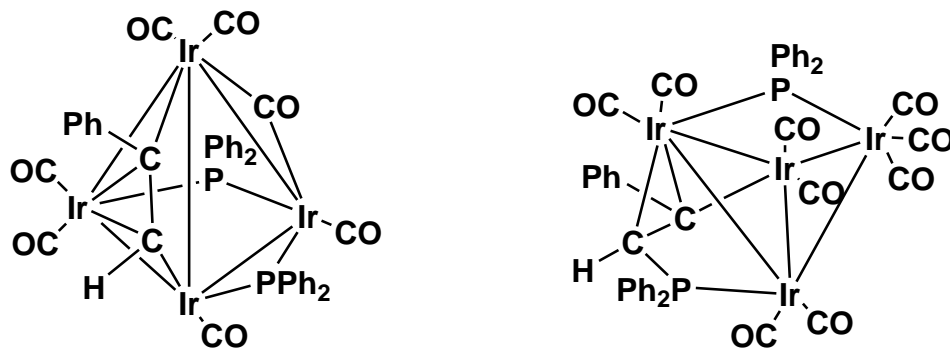
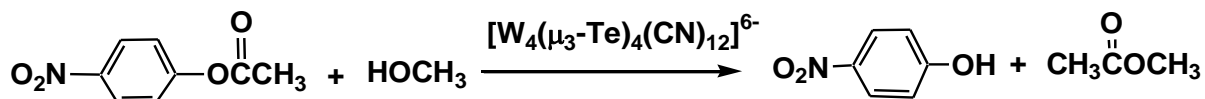


Figure 1.75 $[\text{Ir}_4(\text{CO})_8(\mu_3\text{-}\eta^2\text{-HCCPh})(\mu\text{-PPh}_2)_2]$ and $[\text{Ir}_4(\text{CO})_9(\mu_3\text{-}\eta^3\text{-Ph}_2\text{PC(H)CPh})(\mu\text{-PPh}_2)]$

A compound containing a cubane tungsten chalcogenide cluster $[\text{W}_4(\mu_3\text{-Te})_4(\text{CN})_{12}]^{6-}$ with Ca^{2+} complex counter cation, obtained by the reaction of aqueous solution of $\text{K}_6[\text{W}_4(\mu_3\text{-Te})_4(\text{CN})_{12}]\cdot 5\text{H}_2\text{O}$ with a solution of a $\text{Ca}(\text{NO}_3)_2$ and phen(1,10 phenanthroline) in a solvent mixture of $\text{H}_2\text{O}/\text{EtOH}$, interestingly showed heterogeneous catalytic activity in the transesterification of a range of esters with methanol under mild conditions (Scheme 1.4).¹¹⁴



Scheme 1.4

The catalytic hydrodefluorination of pentafluoropyridine in the presence of arylsilanes is catalyzed by the tungsten and molybdenum(IV) cluster hydrides $[\text{M}_3\text{S}_4\text{H}_3(\text{dmpe})_3]^+$, (M=W, Mo; dmpe=1,2-(bis)dimethylphosphinoethane) (Figure 1.76). The reaction proceeds regioselectively at the 4-position under microwave radiation to yield the 2,3,5,6-tetrafluoropyridine. Catalytic activity is higher for the tungsten complexes with a turnover numbers close to 100, while reactions catalyzed by molybdenum compounds are faster.¹¹⁵

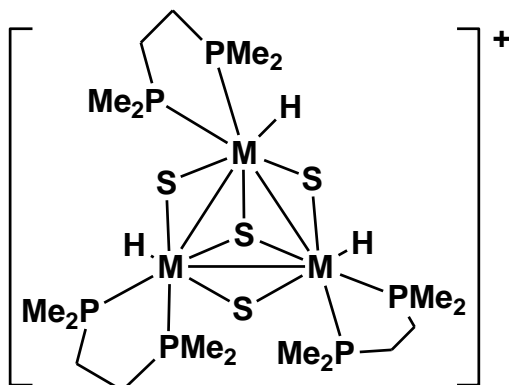
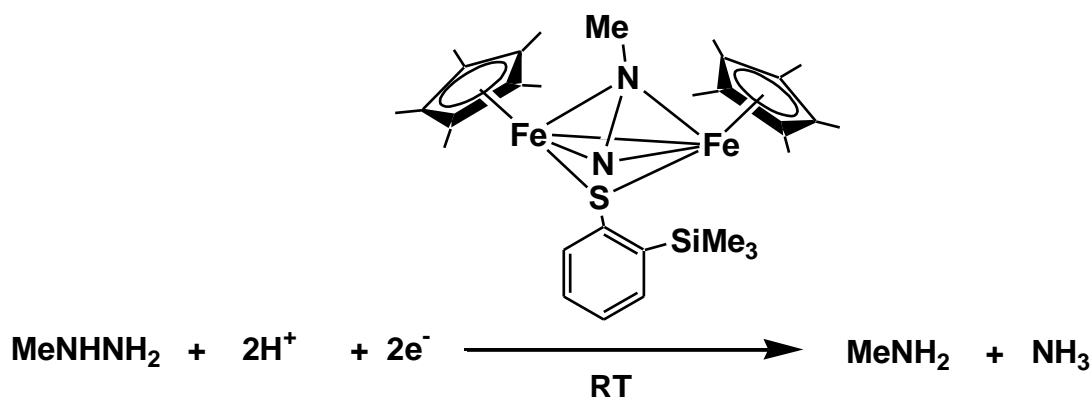


Figure 1.76 $[\text{M}_3\text{S}_4\text{H}_3(\text{dmpe})_3]^+$,
(M=W, Mo; dmpe=1,2-(bis)dimethylphosphinoethane)

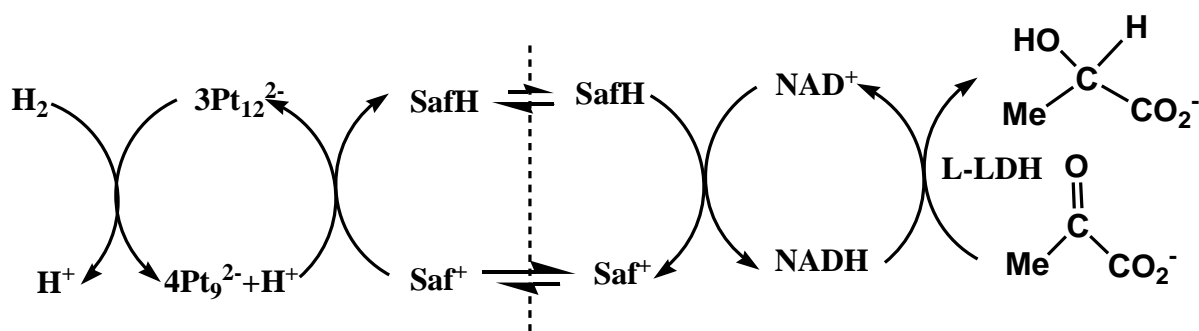
An interesting thiolate-bridged diiron complex bearing diazenido and diazene ligands in a side-on manner have been prepared and characterized structurally by X-ray analysis. These

sulfur-bridged diiron complex works as effective catalysts toward the reduction of hydrazines into amines and ammonia at room temperature (Scheme 1.5).¹¹⁶



Scheme 1.5

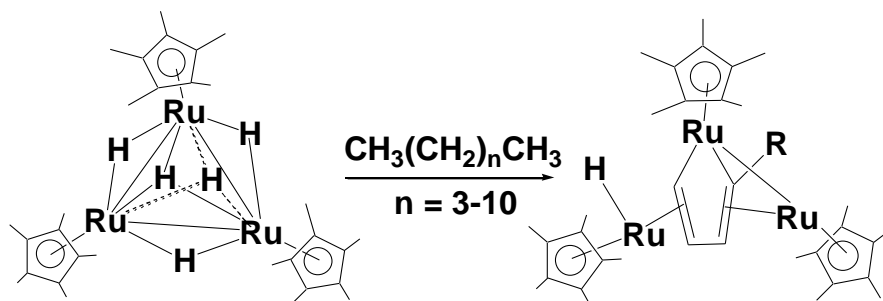
The use of a platinum cluster $[\text{Pt}_9(\text{CO})_{18}]^{2-}$ for the catalytic reduction of NAD^+ to NADH by dihydrogen has been recently established. By using the enzyme L-lactate dehydrogenase (L-LDH) the scope of this reaction has been extended to include reduction of pyruvate to L-lactate. Since both NAD^+ and L-LDH are soluble only in water, and the carbonyl cluster is soluble only in organic solvents, a biphasic system consisting of water and dichloromethane has been used. The cluster catalyzes the reduction of a redox active dye, Safranin O (Saf^+ , 3,7-diamino-2,8-dimethyl-5-phenylphenazinium), by dihydrogen in the organic phase. The oxidized (Saf^+) and the reduced (SafH) dye shuttles across the phase boundary and facilitates the transfer of two electrons and one proton resulting in catalytic redox process (Scheme 1.6).⁶



Scheme 1.6

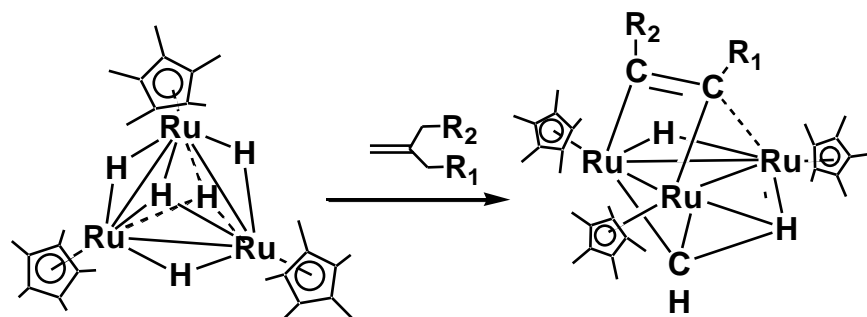
1.5.2. Metal cluster mediated Organic transformation

The reactivity of transition metal cluster complexes has been of special interest in the area of recent organometallic chemistry because of their potential applicability to organic synthesis. The advantageous properties of a multimetallic system over a monometallic one in the substrate activation step are its capability of multiple coordination of the substrate to the metal clusters. Transition metal clusters have been intensively investigated to develop effective organic transformations by the support of the metal centers. A large number of studies on the reactivity of clusters have been reported which leads to the transformation of organic species.¹¹⁷ Recently, metal carbonyls and metal hydride clusters have been widely reported for various organic transformation. It has been understood that due to the presence of higher electron density at the metal centers in metal hydride clusters, these are expected to be much more active than the metal-carbonyl cluster toward oxidative addition of substrates. Liberation of hydride or other ligands from the metal cluster gives rise to vacant coordination sites on the metal centers, and the substrate interacts with the resulting vacant metal centers and gives rise to activation of organic molecule.¹¹⁸ Suzuki et al. have dealt with C-H bond activation of alkane on the multimetallic site and found that triruthenium pentahydride cluster, $[(C_5Me_5)Ru]_3(\mu-H)_3(\mu_3-H)_2$ effectively activate alkanes in a thermal reaction (Scheme 1.7).^{119, 120}



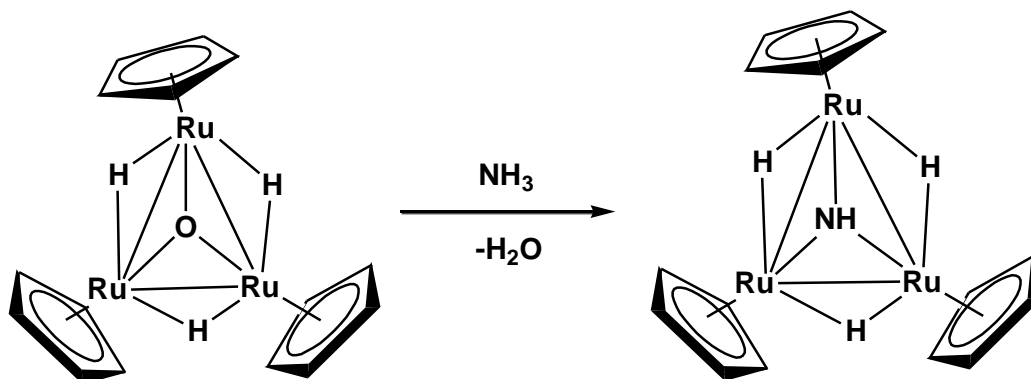
Scheme 1.7

In comparison to the C-H bond cleavage reactions, there have been a relatively small number of successful examples of C-C bond cleavage mediated by mononuclear transition metal complexes. However, the remarkable properties of a multimetallic system and its capability of multiple coordination and multielectron transfer enabled activation of a C-C single bond and a double bond by the triruthenium pentahydride cluster, $[(C_5Me_5)Ru]_3(\mu-H)_3(\mu_3-H)_2$ (Scheme 1.8).^{121, 122}



Scheme 1.8

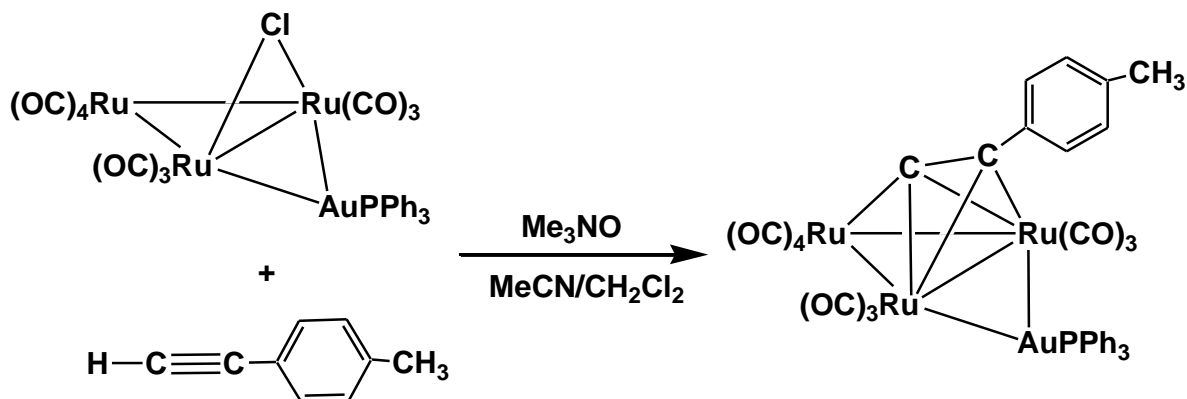
Another important bond activation are the N–H bonds of ammonia which are chemically inert under neutral conditions due to their high bond dissociation energies; therefore, activation of these bonds is a long-standing challenge for both organometallic and inorganic chemists. Recently, a triply bridging oxo cluster $[(Cp^*Ru)_3(\mu-H)_3(\mu_3-O)]$ containing three Ru–Ru bonds readily reacts with ammonia at 1 atm. pressure and at room temperature to yield μ_3 -imido complex with the release of water molecule (Scheme 1.9).¹²³ The cluster also contains three hydride bridging across metal – metal bond and each of the ruthenium atom is attached to a cyclopentadienyl group.



Scheme 1.9

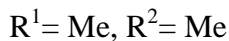
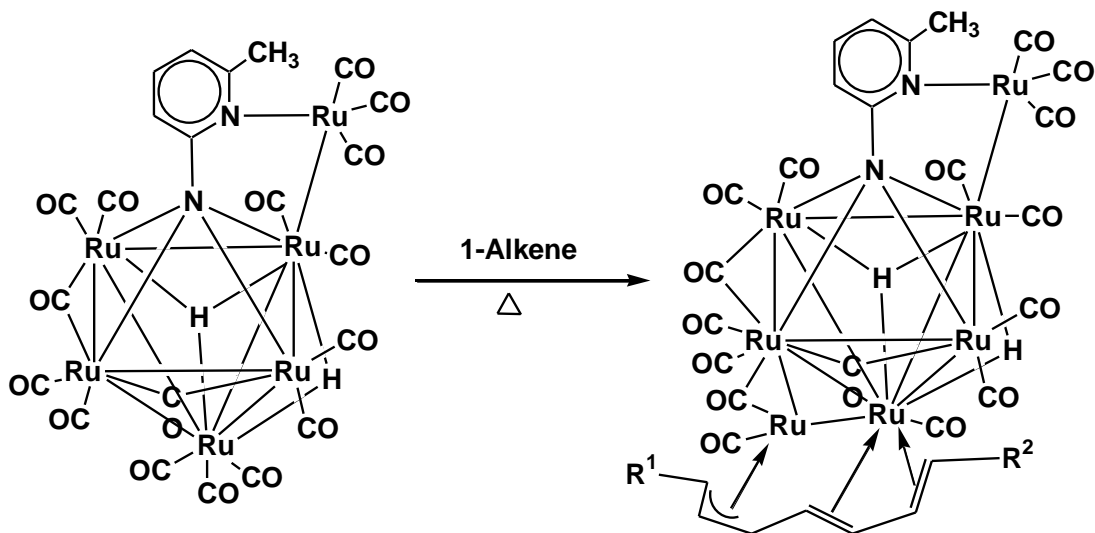
The reaction of compound $[Ru_3(CO)_{10}(\mu-Cl)(\mu-AuPPh_3)]$ with terminal alkynes $HC\equiv CR$; ($R = C_6H_4-CH_3$) under very mild conditions yielded cluster compound $[Ru_3(CO)_9(\mu-AuPPh_3)(\mu_3-\eta^2-\perp-C\equiv CR)]$ ($R = C_6H_4-CH_3$) (Scheme 1.10). The synthesis of this type of compounds shows

the ease of activation of $C_{(sp)}-H$ and $C_{(sp)}-C_{(sp)}$ bonds in alkynes promoted by a heterometallic ruthenium-gold cluster. The activation happens through the rupture of the C-H bond and the re-hybridization of the acetylenic carbon atoms.¹²⁴



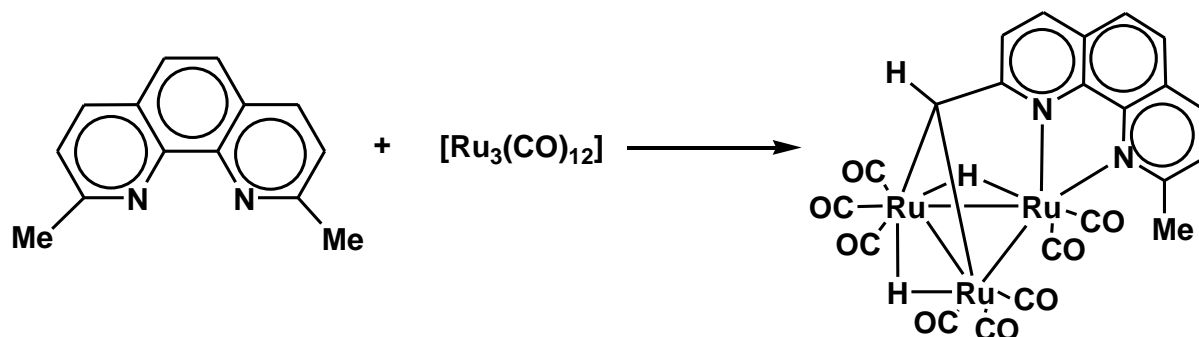
Scheme 1.10

Cabeza et al. reported ruthenium cluster mediated transformation of linear alkenes into trienyl Ligands. The treatment of $[Ru_6(\mu_3-H)_2(\mu_5-\kappa^2-ampy)(CO)_{16}]$ ($H_2ampy = 2$ -amino-6-methylpyridine) with 1-octene, 1-nonene and 1-decene affords heptanuclear derivatives containing trienyl ligands that arise from the unusual activation of five C-H bonds of linear alkenes (Scheme 1.11).¹²⁵



Scheme 1.11

The treatment of $[\text{Ru}_3(\text{CO})_{12}]$ with 6,6'-dimethyl-2,2'-bipyridine (Me_2bipy) or 2,9-dimethyl-1,10-phenanthroline (Me_2phen) in THF at reflux temperature gives the trinuclear dihydride complexes $[\text{Ru}_3(\mu\text{-H})_2(\mu_3\text{-L}^1)(\text{CO})_8]$ ($\text{L}^1 = \text{HCbipyMe}$ or HCphenMe), which result from the activation of two C-H bonds of a methyl group (Scheme 1.12).¹²⁶



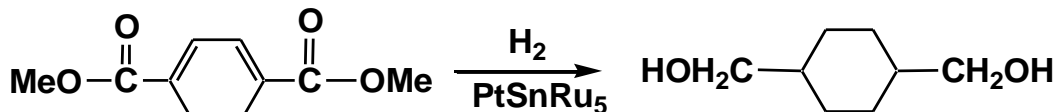
Scheme 1.12

1.5.3. Transition metal cluster to Nanocluster

Small metal particles called colloids or nano-particles have found uses for many years, for example, medieval red stained glass contains colloidal gold. Very striking advances have been made in recent years in their controlled synthesis, better characterization and in the identification of new commercial applications in nanotechnology. Traditional aqueous metal colloids has been easily obtained by reducing a metal salt in the presence of protective polymer such as polyvinyl alcohol (PVA), which absorbs on the surface. More recently, large ligand stabilized particles have been prepared that are intermediate between clusters and nano-particles.¹²⁷

Chaudret et. al. has shown that the metal-organic precursor $\text{Fe}[\text{N}(\text{SiMe}_3)_2]_2$ can be reduced by hydrogen in the presence of $n\text{-C}_{16}\text{H}_{33}\text{NH}_2$ to give iron nano-particles of definite shape and size cubes of 7Å edge length. They even “crystallize” into a cube super lattice, as known from the electron micrographs.¹²⁸ Similarly, mixed-metal cluster complexes containing platinum, ruthenium, palladium, rhodium etc. can form heterogeneous nanoparticle which can serve as hydrogenation catalysts with exceptionally high activity and selectivity when deposited on mesoporous supports and thermally activated to remove their ligands.¹²⁹ Trimetallic nano-catalyst $[\text{PtSnRu}_5]$ as 1–2 nm particles prepared from cluster complex $[\text{PtRu}_5(\text{SnPh}_2)(\text{CO})_{15}(\mu_6\text{-C})]$ on a mesoporous silica support were found to be excellent catalysts for the single-step

hydrogenation of dimethylterephthalate to cyclohexanedimethanol at 100 °C and 20 atm pressure of hydrogen (Scheme 1.13).¹³⁰



Scheme 1.13

A giant palladium cluster was synthesized by Moiseev and co-workers from H₂ and Pd(OAc)₂ and dipyriddy was used to stabilize the Pd colloid.¹³¹ The colloids are catalytically active for O₂ or peroxide oxidation of ethylene, propylene and toluene to vinyl acetate or benzyl acetate. Electron microscopy reveals that it has a 25 Å particle size distribution. Particle size can be easily varied by judiciously changing the synthetic parameters. Thus, 35 Å Pd colloid was stabilized by using polymeric hydrosilanes and has substantially different selectivity than either Pd/C or homogeneous Pd catalysts in hydrogenation and hydrolysis reactions. Giant clusters can also be obtained as pure compounds by different synthetic methodologies. One of the largest clusters that can be crystallized for X-ray studies and are found to be of a defined nuclearity are now in the M100 range, e.g. the closed packed [Pd₆₉(CO)₃₆(PEt₃)₁₈] which shows unusual physical properties.¹³² These preliminary results reveal that metal cluster compounds are potential candidates for nanomaterials with different size and integrity. The most important parameter which the metal clusters have are their tuning ability by changing the metal core and ligand coordination. However, a large number of studies on this front is required to understand the structure-property relationships of various nanosized particles.

1.5.4. Nonlinear Optical Properties

Research into nonlinear optical (NLO) materials has become increasingly intensive because of their potential applications in optical fibers, data storage, optical computing, image processing, optical switching and optical limiting devices.¹³³ Thus, the design and synthesis of new materials with large NLO capability represents an active field in modern chemistry, physics and materials science.¹³⁴ Metal clusters are reported to be excellent candidates for NLO

materials¹³⁵ since they involve $d\pi$ - $p\pi$ delocalized systems and $d\pi$ - $d\pi$ conjugated systems.¹³⁶ These compounds have been found to be structurally unique and the diverse electronic properties can be tuned by virtue of the coordinated metals.¹³⁷ Metal clusters can also extend the p -conjugated length, which is one of the many methods used to increase molecular NLO susceptibilities $\{\chi(3)\}$ values. Moreover, the NLO properties of metal clusters can be enhanced by the introduction of metal \rightarrow ligand and ligand \rightarrow metal charge-transfer states.¹³⁸ Although many methods can be used to promote the NLO properties of metal clusters, the origination of the NLO properties is the delocalization of the π -electron cloud.¹³⁹ This delocalization in metal clusters is mainly brought about by metal ions constructing the skeleton and organic ligands fixing the skeleton, thus both the metal ions and the organic ligands should be important for the nonlinear optical properties of the clusters. However, some studies reveals that heavy-metal ions play a very important roles on the third-order NLO properties of metal clusters because their incorporation introduces more sublevels into the energy hierarchy, which permits more allowed electronic transitions to take place and hence a larger NLO effect to be produced.¹⁴⁰ To investigate whether the metal ions or ligands play more important roles in the NLO properties Hou et al. have reported the unique crown like cluster $[Ag_{10}(dcapp)_4] \cdot 2(OH) \cdot 12H_2O$, (H_2dcapp = 2,6-dicarboxamido-2-pyridylpyridine) and obtained strong nonlinear absorption property (Figure 1.77).¹⁴¹

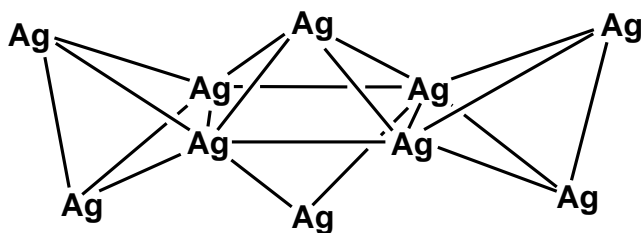


Figure 1.77 Core structure of $[Ag_{10}(dcapp)_4] \cdot 2(OH) \cdot 12H_2O$
(Ligands are omitted for clarity)

In the search for better nonlinear material for the process of optical limiting, recently some clusters have been investigated.¹⁴² It has been well known that C_{60} was shown to be a good optical limiting material. Recently the nonlinear optical properties of some inorganic clusters have been studied which display significant nonlinearities. Mathur et al. have initiated studies to

explore optical nonlinearity in a class of transition-metal, non-metal clusters and have recently demonstrated that the nonlinearity in these clusters can far exceed that of C_{60} .¹⁴³ They have shown by measuring the real and imaginary parts of the third order susceptibility, $\chi(3)$, that the cluster $[Fe_4Se_2(\mu-Se_2PCBu_7)(CO)_{11}]$ displays significant nonlinear property (Figure 1.78). It was also shown that the imaginary part of $\chi(3)$ which leads to nonlinear absorption is significantly larger.¹⁴⁴

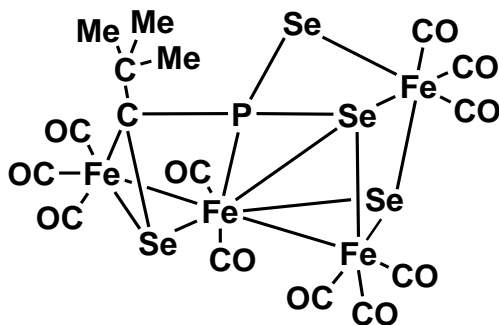
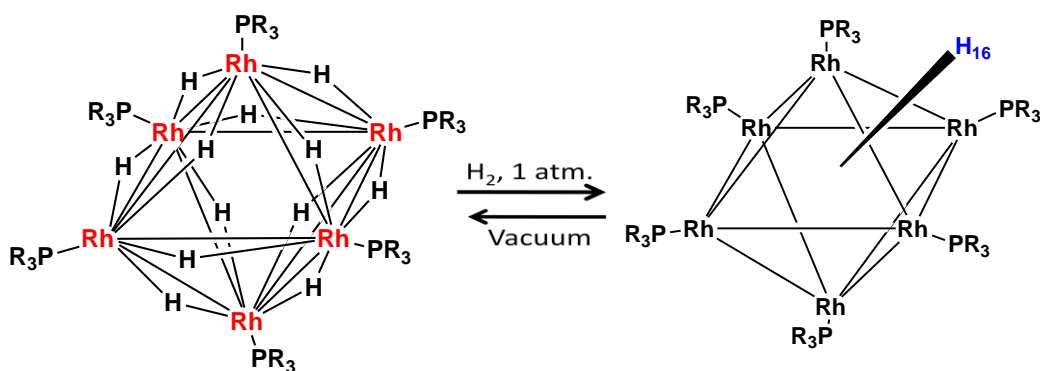


Figure 1.78 $[Fe_4Se_2(\mu-Se_2PCBu_7)(CO)_{11}]$

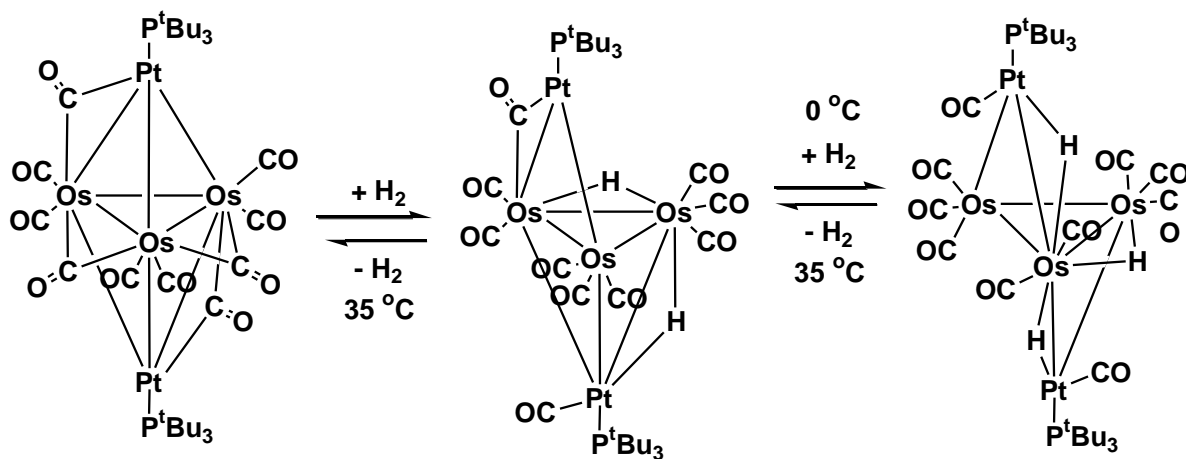
1.5.5. Potential use of some metal clusters as hydrogen storage materials

A global increase in population and need for extra energy has led to several social and environmental problems in everyday life. Excessive use of fossil fuel has made a deep impact on natural energy reserves. Use of solar cells as non-conventional energy resources has been employed. Hydrogen, the third most abundant element on earth is an environmental friendly energy carrier in the automobile industry and a good substitute for fossil fuel resources. The limited use of the gas is primary due to lack of appropriate materials for physical storage of hydrogen. The stability of the hydrogen-trapped complexes also achieves some thermodynamic support from the negative change in energy values. Recently, metal cages and rings are applied as trapping materials for hydrogen for use as future fuel reserve. Interestingly, a rhodium metal cluster, $[Rh_6(PR_3)_6H_{12}][B\{C_6H_3(CF_3)_2\}_4]_2$, ($R=iPr$, Cy) has been capable of adding two equivalents of hydrogen reversibly under very mild conditions (Scheme 1.14).¹⁴⁵



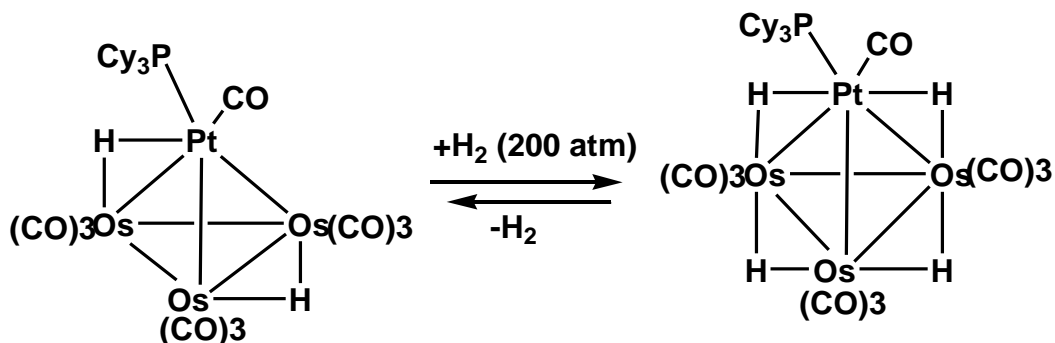
Scheme 1.14

In another such development, Adams et al. prepared a 68-electron heteronuclear five-metal cluster complex $[\text{Pt}_2\text{Os}_3(\text{CO})_{10}(\text{PtBu}_3)_2]$ from the reaction of $[\text{Os}_3(\text{CO})_{10}(\text{NCMe})_2]$ with $[\text{Pt}(\text{PtBu}_3)_2]$. The molecule contains a trigonal-bipyramidal cluster of five metal atoms, where the platinum atoms occupy the axial position and a triangular osmium atoms defines the equatorial plane. This cluster complex is also electron-deficient, and sequentially add two equivalents of hydrogen reversibly to form the di and tetrahydrido cluster complexes $[\text{Pt}_2\text{Os}_3(\text{CO})_{10}(\text{PtBu}_3)_2(\mu\text{-H})_2]$ and $[\text{Pt}_2\text{Os}_3(\text{CO})_{10}(\text{PtBu}_3)_2(\mu\text{-H})_4]$ (Scheme 1.15) even at 0°C .¹⁴⁶



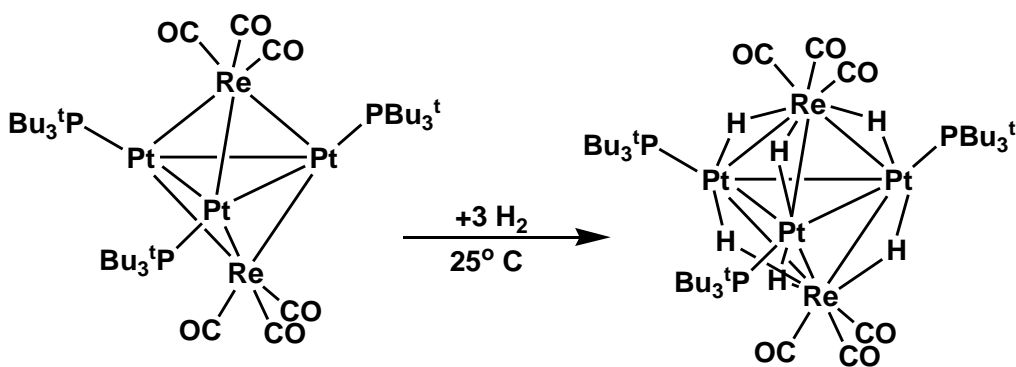
Scheme 1.15

Stone and co-workers showed that the unsaturated 58-electron complex $[\text{PtOs}_3(\text{CO})_{10}(\text{PCy}_3)(\mu\text{-H})_2]$ adds hydrogen reversibly to yield the tetrahydrido complex $[\text{PtOs}_3(\text{CO})_{10}(\text{PCy}_3)(\mu\text{-H})_4]$, but the addition reaction requires a pressure of 200 atm H_2 as shown in Scheme 1.16.¹⁴⁷



Scheme 1.16

In a recent study, Adams et al. have shown that it is possible to prepare electronically unsaturated bi-metallic cluster complexes that are able to add significant amounts of hydrogen under mild conditions. A 62-electron cluster complex $\text{Pt}_3\text{Re}_2(\text{CO})_6(\text{P}^t\text{Bu}_3)_3$ adds three equivalents of hydrogen at room temperature to yield the hexahydrido complex $\text{Pt}_3\text{Re}_2(\text{CO})_6(\text{P}^t\text{Bu}_3)_3(\mu\text{-H})_6$, as shown in Scheme 1.17.¹⁴⁸



Scheme 1.17

1.6. CONCLUSIONS

Transition metal cluster complexes continue to be a special area of recent organometallic chemistry because of their potential applicability in various fields, from organic synthesis to advanced electronic material. We have discussed the various aspects of transition metal clusters mainly on the synthesis, reactivity and application of different types of metal cluster and their future scope in chemical sciences. A large variety of organometallic transition metal clusters have been known containing homo or hetero metal atoms, a range of terminal and bridging ligands and with unique structural geometries. Facile synthesis and stability of higher nuclear transition metal clusters with unusual properties have been a key challenge for the development of cluster chemistry. In spite of that, some methodologies for obtaining novel mixed metal clusters of desired structural and reactivity features have been developed in current years. We have been equally interested to explore the reactivity of metal clusters towards cluster growth reactions and recognize the effect of 'naked' chalcogen atoms and other bridging groups in stabilization of the cluster framework. Subsequent chapters describes the synthesis, characterization and reactivity of homo- and hetero-metallic diphosphine bridged clusters and focuses on the study of the reactivity of metal acetylide compounds in designing polycarbon framework for the synthesis of novel transition metal cluster complexes. We have also been interested to explore and understand the possibility of transition metal mediated organic transformations of different alkynes.

1.7. REFERENCES

1. (a) K. H. Whitmire, *J. Coord. Chem.* 17 (1988) 95; (b) G. Hüttner, K. Knoll, *Angew. Chem. Int. Ed. Engl.* 26 (1987) 743.
2. (a) B. K. Burgess, D. J. Lowe, *Chem. Rev.* 96 (1996) 2983; (b) B. E. Smith, *Adv. Inorg. Chem.* 47 (1999) 159.
3. (a) H. S. Nalwa, *Appl. Organomet. Chem.* 5 (1991) 349; (b) S. Banerjee, G. R. Kumar, P. Mathur, P. Sekar, *Chem. Commun.* (1997) 299; (c) P. Mathur, S. Ghose, M. M. Hossain, C. V. V. Satyanarayana, S. Banerjee, G. R. Kumar, P. B. Hitchcocks, J. F. Nixon, *Organometallics* 16 (1997) 3815.
4. D. Astruct, *Organometallic Chemistry and Catalysis*, Springer–Verlag, Berlin, 2007.
5. B. H. S. Thimmappa, *Coord. Chem. Rev.* 143 (1995) 1.
6. S. Bhaduri, P. Mathur, P. Payra, K. Sharma, *J. Am. Chem. Soc.* 120 (1998) 12127.
7. M. Okazaki, K. Suto, N. Kudo, M. Takano, F. Ozawa, *Organometallics*, 31 (2012) 4110.
8. K. Geetharani, S. K. Bose, S. Ghosh, *Organometallics* 30 (2011) 191.
9. D. G. Vivó, M. E. García, M. A. Ruiz., *Organometallics*.27 (2008) 169.
10. T. Takao, N. Obayashi, B. Zhao, K. Akiyoshi, H. Omori, H. Suzuki. *Organometallics* 30 (2011) 5057.
11. M. A. Alvarez, *J. Organomet. Chem.* 695 (2010) 36.
12. M. A. Alvarez, M. E. García, D. G. Vivo, M. E. Martínez, M. A. Ruiz., *Organometallics* 30 (2011) 2189.
13. B. J. Frost, S. B. Miller, K. O. Rove, D. M. Pearson, J. D. Korinek, J. L. Harkreader, C. A. Mebi, J. Shearer, *Inorg. Chim. Acta* 359 (2006) 283.
14. Y. C. Tsai, H. Z. Chen, C. C. Chang, J. S. K. Yu, G. H. Lee, Y. Wang, T. S. Kuo, *J. Am. Chem. Soc.* 131 (2009) 12534.
15. C. W. Hsu, J. S. K. Yu, C. H. Yen, G. H. Lee, Y. Wang, Y. C. Tsai, *Angew. Chem. Int. Ed.* 47 (2008) 9933.
16. K. T. Horne, G. L. Powell, L. M. Daniels, *Acta Crystallographica Section C, Crystal Structure Communications* 58 (2002) 292.
17. B. F. G. Johnson, *Transition Metal Clusters*, J. Wiley: New York, 1980.

18. R.H. Crabtree, *The Organometallic Chemistry of the Transition Metals*, 3rd Edition John Wiley & Sons Inc.: New York; Singapore, 2001.
19. K. Farmery, M. Kilner, R. Greatrex, N. N. Greenwood, *J. Chem. Soc. [Section] A: Inorganic, Physical, Theoretical*, (1969) 2339.
20. W. Clegg, N. Feeder, S. Nahar, P. R. Raithby, G. P. Shields, S. J. Teat, *New J. Chem*, 22 (1998) 1111.
21. R. D. Adams, *The Chemistry of Metal Cluster Complexes*, ed. D. F. Shriver, H. D. Kaesz and R. D. Adams, VCH, New York, 1990, Ch. 3, p. 121.
22. P. J. Dyson, J. S. McIndoe, *Transition Metal Carbonyl Cluster Chemistry*, Gordon & Breach, Amsterdam, 2000, Ch. 6, p. 73.
23. R. D. Adams, *J. Am. Chem. Soc.* 133 (2011) 15950.
24. J. A. Cabeza, *Dalton Trans.* (2003) 2808.
25. C. K. Wong, *J. Clust. Sci.* 21 (2010) 461.
26. M. I. Bruce, *Organometallics* 25 (2006) 4817.
27. H. F. Dai, W. Y. Yeh, *Inorg. Chim. Acta.* 363 (2010) 925.
28. J. I. Ito, T. Shima, H. Suzuki, *Organometallics* 25 (2006) 1333.
29. H. Kameo, T. Shima, Y. Nakajima, H. Suzuki, *Organometallics* 28 (2009) 2535.
30. K. H. Yih, I. K. Hamdemir, J. E. Mondloch, E. Bayram, S. Ozkar, R. Vasić, A. I. Frenkel, O. P. Anderson, R. G. Finke, *Inorg. Chem.* 51 (2012) 3186.
31. L. Garlaschelli, F. Greco, G. Peli, M. Manassero, M. Sansoni, R. Gobetto, L. Salassa, R. D. Pergola, *Eur. J. Inorg. Chem.* (2003) 2108.
32. R. D. Adams, Z. Li, J. C. Lii, W. Wu, *Organometallics* 11 (1992) 4001.
33. C. A. Tolman, *Chem. Rev.* 77 (1977) 313.
34. R. D. Adams, B. Captain, L. Zhu, *J. Am. Chem. Soc.* 129 (2007) 2454.
35. M. C. Blanco, J. C. Amara, M. C. Gimeno, P. G. Jones, A. Laguna, J. M. L. Luzuriaga, M. E. Olmos, M. D. Villacampa, *Organometallics* 31 (2012) 2597.
36. Wen-Yann Yeh, K. Y. Tsai, *Organometallics* 29 (2010) 604.
37. X. Zhang, S. Kandala, L. Yang, W. H. Watson, X. Wang, D. A. Hrovat, W. T. Borden, M. G. Richmond, *Organometallics* 30 (2011) 1253
38. W. H. Watson, S. Kandala, M. G. Richmond. *J. Organomet Chem.* 692 (2007) 968.

39. F. Y. Pétilion, F. R. Guen, R. Rumin, P. Schollhammer, J. Talarmin, K. W. Muir. J. Organomet. Chem. 691 (2006) 2853.
40. N. Begum, U. K. Das, M. Hassan, G. Hogarth, S. E. Kabir, E. Nordlander, M. A. Rahman, D. A. Tocher, Organometallics 26 (2007) 6462.
41. N. A. Pushkarevsky, S. N. Konchenko, M. Scheer, J. Clust. Sci.18 (2007) 606.
42. Y. Y. Wu, W. Y. Yeh, Organometallics 30 (2011) 4792.
43. R. D. Adams, Y. Kan, Q. Zhang, M. B. Hall, E. Trufan, Organometallics 31 (2012) 50.
44. Y. Miyake, T. Moriyama, Y. Tanabe, S. Endo, Y. Nishibayashi, Organometallics 31 (2012) 3292.
45. W. Y. Yeh, K. Y. Tsai, Organometallics 29 (2010) 604.
46. C. M. Alvarez, M. A. Alvarez, M. E. García, R. Gonzalez, A. Ramos, M. A. Ruiz, Inorg. Chem. 50 (2011) 10937.
47. S. M. Azad, K. A. Azam, S. E. Kabir, M. S. Saha, G. M. G. Hossain, J. Organomet. Chem. 690 (2005) 4206.
48. E. Sappa, S. Tiripicchio, P. Braunstein, Chem. Rev. 83 (1983) 203.
49. A. A. C. Moreno, M. L. Marcos, J. G. Velasco, C. Pastor, R. M. Medina, M. J. Macazaga, Organometallics 30 (2011) 1838.
50. T. Takao, M. Moriya, M. Kajigaya, H. Suzuki. Organometallics 29 (2010) 4770.
51. P. Mathur, S. Chatterjee, A. Das, S. M. Mobin, J. Organomet. Chem. 692 (2007) 819.
52. D. V. Muratov, F. M. Dolgushin, S. Fedi, P. Zanello, A. R. Kudinov, Inorg Chim Acta 374 (2011) 313.
53. A. A. Pasynskii, I. V. Skabitskii, S. S. Shapovalov, A. R. Galustyan, Yu. V. Torubaev, Zh. V. Dobrokhotova, V. A. Grinberg, E. V. Mutseneck, A. R. Kudinov, Russian Chemical Bulletin, Int. Ed. 56 (2007) 1731
54. M. Okazaki, T. Tsuchimoto, Y. Nakazawa, M. Takano, F. Ozawa, Organometallics 30 (2011) 3487.
55. W. A. Nugent, J. M. Mayer, "Metal-Ligand Multiple Bonds" John Wiley & Sons, New York, 1988.
56. L. V. Petit, G. Süß-Fink, B. Therrien, T. R. Ward, H. Stoeckli-Evans, G. Labat, L. K. BreLOT, A. Neels, T. Bürgi, R. G. Finke, C. M. Hagen. Organometallics 24 (2005) 6104.

57. S. Ghosh, G. Hogarth, S. E. Kabir, A. I. Latif Miah, L. Salassa, S. Sultana, C. Garino. *Organometallics* 28 (2009) 7047
58. P. Mathur, S. Mukhopadhyay, G. K. Lahiri, C. Thöne. *Organometallics* 21 (2002) 5209.
59. R. Nast., *Coord. Chem. Rev.* 47 (1982) 89.
60. A. J. Carty, *Pure Appl. Chem.* 54 (1982) 113.
61. E. Sappa, A. Tiripicchio, P. Braunstein, *Coord. Chem. Rev.* 65 (1985) 219.
62. P. R. Raithby, M. J. Rosales, *Adv. Inorg. Chem.* 29 (1985) 169.
63. C. S. Yi, N. H. Liu, A. L. Rheingold, L. M. Liable-Sands, I. A. Guzei, *Organometallics* 16 (1997) 3729.
64. F. G. Kirchbauer, P. M. Pellny, H. S. Sun, V. V. Burlakov, P. Arndt, W. Baumann, A. Spannenberg, U. Rosenthal, *Organometallics* 20 (2001) 5289.
65. M. I. Bruce, M. J. Liddell, M. R. Snow, E. R. T. J. Tiekink, *J. Organomet. Chem.* 352 (1988) 199.
66. P. Mathur, A. K. Ghosh, S. Mukhopadhyay, Ch. Srinivasu, S. M. Mobin, *J. Organomet. Chem.* 678 (2003) 142.
67. P. Mathur, A. K. Bhunia, Ch. Srinivasu, S. M. Mobin, *Phosphorus, Sulfur, Silicon Relat. Elem.* 179 (2004) 899.
68. P. Mathur, Ch. Srinivasu, M. O. Ahmed, V. G. Puranik, S. B. Umbarkar, *J. Organomet. Chem.* 659 (2002) 196.
69. Y. Chi, C. H. Wu, S. M. Peng, G. H. Lee, *Organometallics* 9 (1990) 2305.
70. N. Chengbao, G. J. Long, P. P. Power. *Organometallics* 28 (2009) 5012.
71. P. Mathur, A. K. Bhunia, A. Kumar, S. Chatterjee, S. M. Mobin, *Organometallics*, 21 (2002) 2215.
72. P. Mathur, A. K. Bhunia, S. M. Mobin, V. K. Singh, Ch. Srinivasu, *Organometallics* 23 (2004) 3694.
73. P. Mathur, S. Ghose, M. M. Hossain, C. V. V. Satyanarayana, R. K. Chadha, S. Banerjee, G. R. Kumar, *J. Organomet. Chem.* 568 (1998) 197.
74. (a) K. H. Whitmire, *Adv. Organomet. Chem.*, 42 (1998) 1; (b) P. Mathur, *Adv. Organomet. Chem.* 41 (1997) 243; (c) K. H. Whitmire, *J. Coord. Chem.*, 17 (1988) 9.
75. P. Mathur, S. Chatterjee, Y. V. Torubaev, *J. Cluster Sci.*, 18 (2007) 505.
76. P. Mathur, S. Chatterjee, V. D. Avasare, *Adv. Organomet. Chem.* 55 (2008) 201.

77. P. Mathur, S. Chatterjee, S. Ghose, M. F. Mohan J. Organomet. Chem 587 (1999) 93.
78. R. D. Adams, E. Boswell, Organometallics 27(2008) 2021.
79. R. D. Adams, W. C. Pearl Jr., J. Organomet Chem. 696 (2011) 1198.
80. P. Mathur, B. H. S. Thimmappa, A. L. Rheingold, Inorg. Chem. 29 (1990) 4658.
81. H. J. Haupt, F. Neumann, H. Preut, J. Am. Chem. Soc. 99 (1975) 439
82. U. Brand, J. R. Shapley, Inorg. Chem. 36 (1997) 253.
83. D. Melzer, E. Weiss, J. Organomet. Chem. 255 (1983) 335.
84. K. Guo, C. W. Liu, C. M. Huang, H. C. Chen, J. C. Wang, T. C. Keng, Chem. Commun. (2000) 1897.
85. M. Shieh, C. H. Ho, W. S. Sheu, H. W. Chen, J. Am. Chem. Soc. 132 (2010) 4032.
86. H. Vahrenkamp, Angew. Chem. Int. Ed. 87 (1975) 363.
87. L. C. Roof, J. W. Kolis, Chem. Rev. 93 (1993) 1037.
88. K. H. Whitmire, J. Coord. Chem. 17 (1988) 95.
89. M. L. Steigerwald, Polyhedron 13 (1994) 1245.
90. P. Mathur, M. M. Hossain, P. B. Hitchcock, J. F. Nixon, Organometallics 14 (1995) 3101.
91. D. T. T. Tran, L. M. C. Beltran, C. M. Kowalchuk, N. R. Trefiak,; N. J. J. Taylor, J. F. Corrigan, Inorg. Chem. 41 (2002) 5693.
92. M. W. D. Groot, N. J. J. Taylor, J. F. Corrigan, Inorg. Chem. 44 (2005) 5447.95.
93. G. Henkel, B. Krebs, Chem. Rev. 104 (2004) 801.
94. B. Tirloni; D. F. Back, R. A. Burrow, G. N. M. de Oliveira, M. A. Villetti, E. S. Lang, J. Braz. Chem. Soc. 21 (2010).
95. P. Mathur, M. M. Hossain, S. B. Umbarkar, C. V. V. Satyanarayana, A. L. Rheingold, L. M. Liable-Sands, G. P. A. Yap, Organometallics 15 (1996) 1898.
96. P. Mathur, Adv. Organomet. Chem. 41 (1997) 243.
97. B. G. Chen, C. H. Ho, C. J. Lee, M. Shieh, Inorg. Chem. 48 (2009) 10757.
98. R. D. Adams, S. Miao, M. D. Smith, H. Farach, C. E. Webster, J. Manson, M. B. Hall Inorg. Chem. 43 (2004), 2515.
99. P. Mathur, S. Chatterjee, G. K. Lahiri, S. Chakraborty, J. H. Kaldis, M. J. McGlinchey, J. Organomet. Chem. 689 (2004) 122.
100. F. Renili, F. Marchetti, S. Zacchini, V. Zanotti, J. Organomet. Chem. 696 (2011) 1483.

101. L. D'Ornelas, T. Castrillo, L. Hernández de B., A. Narayan, R. Atencio. *Inorg. Chim. Acta.* 342 (2003) 1.
102. J. A. Cabeza, I. del Río, L. M. Méndez, D. Miguel, J. Organomet. Chem. 692 (2007) 4407.
103. M. A. Alvarez, M. E. García, M. E. Martínez, M. I. A. Ruiz. *Organometallics* 29 (2010) 904
104. J. A. Cabeza, P. Braunstein, L. A. Oro, P. R. Raithby (Eds.), *Metal Clusters in Chemistry*, vol. II, Wiley VCH, Germany, 1999, pp. 715-740 and references therein.
105. Y. Li, W. eT Wong, *Eur. J. Inorg. Chem.* (2003) 2651.
106. P. Braunstein, J. Rosé, P. Braunstein, L. A. Oro, P. R. Raithby (Eds.), *Metal Clusters in Chemistry*, vol. II, Wiley-VCH, Germany, 1999, pp. 617-677 (and references therein).
107. *Bioorganometallics: Biomolecules, Labeling, Medicine*; G. Jaouen, Ed. Wiley-VCH: Weinheim, 2006.
108. T. F. Beltrana, M. Feliz, R. Llusara, V. S. Safonta, C. Vicentc, *Catalysis Today* 177 (2011) 72.
109. T. Waters, R. A. J. O'Hair, A. G. Wedd, *J. Am. Chem. Soc.* 125 (2003) 3384.
110. Y. K. Kim, R. Rousseau, B. D. Kay, J. M. White, Z. Dohnalek, *J. Am. Chem. Soc.* 130 (2008) 5059.
111. F. Montigny, R. Macias, B. C. Noll, T. P. Fehlner, K. Costuas, J. Saillard, J. F. Halet, *J. Am. Chem. Soc.* 129 (2007) 3392.
112. V. Moberg, M. A. Mottalib, D. Sauer, Y. Poplavskaya, D. C. Craig, S. B. Colbran, A. J. Deeming, E. Nordlander, *Dalton Trans.* (2008) 2442.
113. F. C. C. Moura, E. N. dos Santos, R. M. Lago, M. D. Vargas, M. H. Araujo, *J. Molecular Catalysis A: Chemical* 226 (2005) 243.
114. J. Y. Kwon, Y. Kim, S. J. Kim, S. H. Lee, H. Kwak, C. Kim, *Inorganica Chimica Acta* 361 (2008) 1885.
115. T. F. Beltrán, M. Feliz, R. Llusar, J. A. Mata, V. S. Safont. *Organometallics* 30 (2011) 290.
116. M. Yuki, Y. Miyake, Y. Nishibayashi, *Organometallics* 31 (2012) 2953.
117. *Topics in Organometallic Chemistry: Activation of Unreactive Bonds and Organic Synthesis* (Ed.: S. Murai), Springer, Heidelberg, 1999, p. 97.
118. (a) Y. Ohki, H. Suzuki, *Angew. Chem. Int. Ed.* 39 (2000) 3120; (b) Y. Ohki, T. Kojima, M. Oshima, H. Suzuki, *Organometallics* 20 (2001) 2654.
119. A. Inagaki, T. Takemori, M. Tanaka, H. Suzuki, *Angew. Chem. Int. Ed.* 39 (2000) 404.

120. K. Matsubara, A. Inagaki, M. Tanaka, H. Suzuki, *J. Am. Chem. Soc.* 121 (1999) 74
121. Y. Ohki, H. Suzuki, *Angew. Chem. Int. Ed.* 39 (2000) 3463.
122. T. Takemori, A. Inagaki, H. Suzuki, *J. Am. Chem. Soc.* 123 (2001) 1762.
123. H. Kameo, Y. Nakajima, K. Namura, H. Suzuki, *Organometallics* 30 (2011) 6703
124. M. H. Sandoval, F. J. Zuno-Cruz, M. J. Rosales-Hoz, M. A. Leyva, N. Andrade, V. Salazar, G. S. Cabrera, *J. Organomet. Chem.* 696 (2011) 4070.
125. J. A. Cabeza, I. D. Río, P. G. Alvarez, D. Miguel, *Organometallics* 26 (2007) 2482.
126. J. A. Cabeza, I. Rio, L. M. Mendez, D. Miguel, *Chem. Eur. J.* 12 (2006) 1529
127. C. Femoni, M. C. Iapalucci, F. Kaswalder, G. Longoni, S. Zacchini, *Coord. Chem. Rev.* 250 (2006) 1580.
128. B. Chaudret, *J. Organomet. Chem.* 16 (2005) 233.
129. J. M. Thomas, B. F. G. Johnson, R. Raja, G. Shankar, P. A. Midgley, *Acc. Chem. Res.*, 36 (2003) 20.
130. A. B. Hungria, R. D. Adams, B. Captain, J. M. Thomas, P. A. Midgley, V. Golvenko, B. F. G. Johnson, *Angew. Chem.* 118 (2006) 4900; *Angew. Chem. Int. Ed.* 45 (2006) 4782.
131. (a) B. M. Trost, *Pure. Appl. Chem.*, 68 (1996) 779; (b) J. W. Faller, K. H. Chao, *Organometallics*, 3 (1984) 927.
132. (a) N. T. Tran, L. F. Dahl, *Angew. Chem. Int. Ed.* 42 (2003) 3533; (b) B. C. Gates, *Chem. Rev.* 95 (1995) 511.
133. (a) T. S. Wang, Z. L. Ahmadi, T. C. Green, A. Henglein, M. A. Elsayed, *Science* 272 (1996) 1924; (b) J. W. Perry, K. Mandour, I. Y. S. Lee, X. L. Wu, P. V. Bedworth, C. T. Chen, D. Ng, S. R. Marder, P. Miles, T. Wada, M. Tian, H. Sasabe, *Science* 273 (1996) 1533.
134. (a) J. G. Qin, D. Y. Liu, C. Y. Dai, *Coord. Chem. Rev.* 188 (1999) 23 ;(b) J. L. Bredas, C. Adant, *Tackx. Chem. Rev.* 94 (1994) 243; (c) R. Signorini, M. Zerbetto, M. Meneghetti, R. Bozio, M. Maggini, C. D. Faveri, M. Prato, G. Scorrano, *Chem. Commun.* (1996); (d) M. Spassova, V. Enchev, *Chem. Phys.* 298 (2004) 29.
135. (a) S. Vagin, M. Barthel, D. Dini, M. Hanack, *Inorg. Chem.* 42 (2003) 2683; (b) S. Shi, W. Ji, S. H. Tang, J. P. Lang, X. Q. Xin, *J. Am. Chem. Soc.* 116 (1994) 3615; (c) W. F. Sun, M. M. Bader, T. Carvalho, *Opt. Commun.* 215 (2003) 185.
136. K. Mashima, M. Tanaka, Y. Kaneda, A. Fukumoto, H. Mizomoto, K. Tani, H. Nakano, A. Nakamura, T. Sakaguchi, K. Kamada, K. Ohta, *Chem. Lett.* (1997) 411.

- 137.(a) V. Carcia, P. J. V. Koningsbruggen, H. Kooijman, A. L. Spek, J. G. Haasnoot, O. Kahn, *Eur. J. Inorg. Chem.* (2000) 307; (b) A. V. A. Gerard, C. G. Reinier, G. H. Jaap, L. Martin, L. S. Anthony, R. Jan, *Eur. J. Inorg. Chem.* (2000) 121; (c) E. F. Marchetti, C. Pettinari, B.W. Skelton, A. H. White, *Inorg. Chem.* 42 (2003) 112.
- 138.(a) C. E. Powell, J. P. Morrall, S. A. Ward, M. P. Cifuentes, E. G. Notaras, A. M. Samoc, M. G. Humphrey, *J. Am. Chem. Soc.* 126 (2004) 12234; (b) N. J. Long, *Angew. Chem.* 107 (1995), 37; *Angew. Chem. Int. Ed. Engl.* 34. (1995) 21.
- 139.(a) T. Wada, L. Wang, H. Okawa, T. Masuda, M. Tabata, M. Wan, M. Kakimoto, Y. Lmai, H. Sasabe, *Mol. Cryst. Liq. Cryst. Sci. Technol. Sect. A* 294 (1997) 250; (b) C. Francis, K. White, G. Boyd, R. Moshrefzadeng, *Chem. Mater.* 5 (1993) 506; (c) S. Morina, T. Yamashita, K. Horie, T. Wada, H. Sadabe, *Rec. Func. Polymer* 44 (2000) 183; (d) H. S. Nalwa, *Adv. Mater.* 5 (1993) 341.
140. (a) W. B. Lin, Z. Y. Wang, L. Ma, *J. Am. Chem. Soc.* 121 (1999) 11249; (b) H.W. Hou, X. R. Meng, Y. L. Song, Y. T. Fan, Y. Zhu, H. J. Lu, C. X. Du, W. H. Shao, *Inorg. Chem.* 41 (2002) 4068; (c) H. Chao, R. H. Li, B. H. Ye, H. Li, X. L. Feng, J. W. Cai, J. Y. Zhou, L. N. Ji, *J. Chem. Soc. Dalton Trans.* (1999) 3711.
141. H. Hou, Y. i. Wei, Y. Song, L. Mi, M. Tang, L. Li, Y. Fan, *Angew. Chem. Int. Ed.* 44 (2005) 6067
142. L. W. Tutt, T. F. Boggess, *Prog. Quantum Electron.* 17 (1993) 299.
143. S. Banerjee, G. R. Kumar, P. Mathur, P. Sekar, *Chem. Commun.* (1997) 299.
144. P. Mathur, S. Ghose, M. M. Hossain, C. V. V. Satyanarayana, S. Banerjee, G. R. Kumar, P. B. Hitchcock, J. F. Nixon. *Organometallics* 16 (1997) 3815.
145. R. D. Adams, B. Captain, *Angew. Chem. Int. Ed.* 47 (2008) 252.
146. R. D. Adams, B. Captain, L. Zhu, *J. Am. Chem. Soc.* 129 (2007) 2454.
147. L. J. Farrugia, M. Green, D. R. Hankey, A. G. Orpen, F. G. A. Stone, *J. Chem. Soc. Chem. Commun.* (1983) 310.
148. R. D. Adams, B. Captain, *Angew. Chem., Int. Ed.* 44 (2005) 2531.

CHAPTER 2

**SYNTHESIS AND CHARACTERIZATION OF
HOMOMETALLIC CHALCOGENIDE
PHOSPHINE CLUSTERS**

2.1. INTRODUCTION

Transition metal cluster containing non-metal atoms as bridging element have drawn increased attention in recent years, mainly because of their unusual structures and novel chemical reactivity, as well as for their potential in the field of material science and catalysis.¹⁻⁴ Among main group atoms, chalcogen displays a wide variety of bonding modes when these are incorporated in transition metal carbonyl cluster frameworks and lead to compounds with novel structural and reactivity features and play a key role in stabilizing the bonding network in the transition metal, non-metal clusters. In the last two decades, metal clusters with unique structural features and unusual reactivities have been obtained by using chalcogen atoms as bridging ligands.^{5,6} In recent times, smaller nuclear iron chalcogenide clusters, $[\text{Fe}_3(\text{CO})_9(\mu\text{-E}_2)]$ and $[\text{Fe}_2(\text{CO})_6(\mu\text{-E})_2]$ (E= S, Se, Te) have been extensively used as convenient starting materials for several cluster growth reactions.⁷⁻¹⁰ In contrast to sulfur and selenium-transition metal clusters, tellurium containing metal clusters have attracted much attention, particularly because of the pronounced effect of the tellurium element on the entire metal skeleton. However, study into the potential use of tellurium as a stabilizing ligand for metal clusters has been limited and its use in the cluster formation has been largely unexplored. The ability of telluride metal clusters to function as building blocks for metal expansion reactions in terms of the effect of tellurium and transition metals is of great interest and is a challenge because of their potential uses in the preparation of mixed metal nanoparticles in nanotechnology. It has been well understood that other ligands attached to metals are also important to maintain structural geometries, which provides interesting properties to the cluster unit. Carbonyl ligands are one of most common ligands in metal cluster chemistry leading to stabilization of low oxidation state metal cluster compounds. Other ligands like phosphines, PR_3 , also constitute one of the few series of ligands in which electronic and steric properties can be altered in a systematic and predictable way over a very wide range by varying the organic group (R).¹¹ During the last three decades extensive research has been focused on the synthesis of transition metal clusters containing phosphine ligands, obtained mostly by ligand substitution reaction of the carbonyl analogue.¹²⁻¹⁶ Bidentate ligands like diphosphines either provide support to the multimetallic framework or help to attach two or more cluster fragments resulting in cluster stability and structural diversity of higher nuclear cluster. Some of these phosphine ligands play a major role for the synthesis of polynuclear metal clusters by linking two or more cluster fragments.^{17, 18}

Literature survey reveals that in recent years a handful of metal clusters have been designed which contain both chalcogen and diphosphine ligands playing a vital role in stabilizing the multimetallic framework.¹⁹⁻²¹ This has prompted us to design of synthetic strategies required for the preparation of transition metal clusters containing both chalcogen atom and diphosphine ligands.

Recent reports show the formation of ruthenium–telluride diphosphine cluster, $[\text{Ru}_3(\text{CO})_7(\text{dppm})\text{Te}_2]$ and hexa-ruthenium selenide clusters $[\text{Ru}_6(\mu_3\text{-Se})_4(\text{CO})_{12}(\mu\text{-dppm})_2]$ (Figure 2.1 & Figure 2.2) where the chalcogen atoms act as clamp to form the internal core of the structure while diphosphine (dppm) ligand provide support from the outer portion of the cluster core. Both the clusters contain Ru_3Y_2 , (Y = Se, Te) square pyramidal core attached bridging diphosphine ligand and terminally bonded metal carbonyl groups.

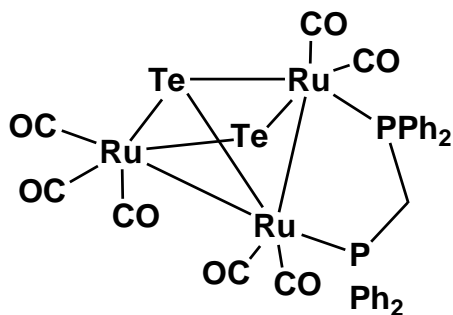


Figure 2.1 $[\text{Ru}_3(\text{CO})_7(\text{dppm})\text{Te}_2]$

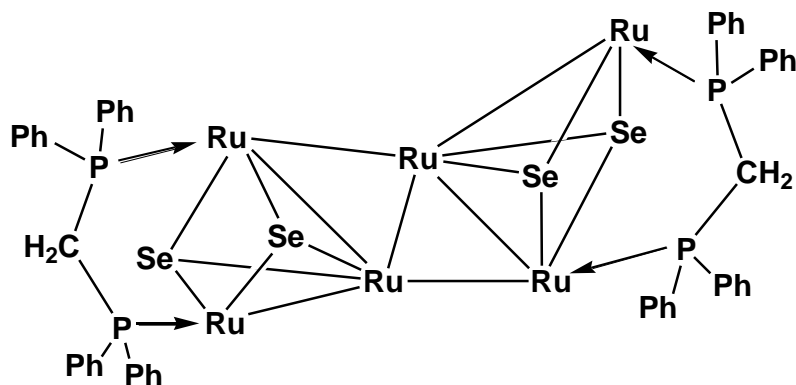


Figure 2.2 $[\text{Ru}_6(\mu_3\text{-Se})_4(\text{CO})_{12}(\mu\text{-dppm})_2]$

Kabir et al. studied the reactivity of $M_3(CO)_12$ ($M = Ru, Fe$) with a series of long chain diphosphine chalcogenide ligands such as $dpphSe_2$ (1,6-bis(diphenylphosphino)hexane) diselenide), $dpphS_2$ (1,6-bis(diphenylphosphino hexane)disulfide), $dpppeSe_2$ (1,5-bis(diphenylphosphino) pentane)diselenide) and $dpppeS_2$ (1,5-bis(diphenylphosphino)pentane-disulfide) to obtain a variety of triruthenium-selenide diphosphine compounds as shown in Figure 2.3. One of the cluster, $[Ru_3(CO)_7(\mu-CO)(\mu_3-Se)(\mu-dpph)]$ contains a triangular tri-ruthenium core with one capping selenium atom, one bridging diphosphine ($dpph$), one doubly bridging carbonyl and seven terminal carbonyl ligands, while, another cluster complex have a square-pyramidal structure with two metal and two selenium atoms forming the basal plane and the third metal atom at the apex of the pyramid. This cluster belongs to the family of nido clusters with seven skeletal electron pairs.²³

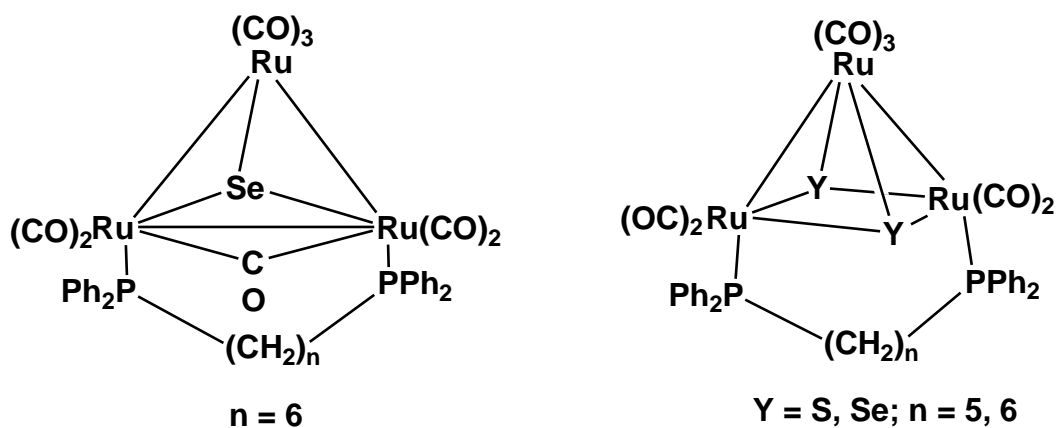


Figure 2.3 $[Ru_3(CO)_7(\mu-CO)(\mu_3-Se)(\mu-dpph)]$ and $[Ru_3(CO)_7(\mu_3-Y)_2(\mu-L)]$, ($L = dpppe, dpph$)

An unusual isomerization of diphosphine ligand from bridging-to-chelating coordination has been observed for a triosmium diphosphine cluster as reported by Zhang et al.²⁴ The diphosphine ligand 1,2-bis(diphenylphosphino)benzene ($dppbz$) reacts with the cluster $1,2-Os_3(CO)_{10}(MeCN)_2$ at room temperature to furnish a mixture of the triosmium clusters $1,2-Os_3(CO)_{10}(dppbz)$ and $1,1-Os_3(CO)_{10}(dppbz)$. The $dppbz$ -bridged cluster $1,2-Os_3(CO)_{10}(dppbz)$ irreversibly transforms to the corresponding chelated isomer at ambient temperature (Figure 2.4). The factor that the bridged $dppbz$ ligand in $1,2-Os_3(CO)_{10}(dppbz)$ is thermodynamically less

favourable than the chelation isomer $1,1\text{-Os}_3(\text{CO})_{10}(\text{dppbz})$ forms the driving force for the facile isomerizations.²⁵

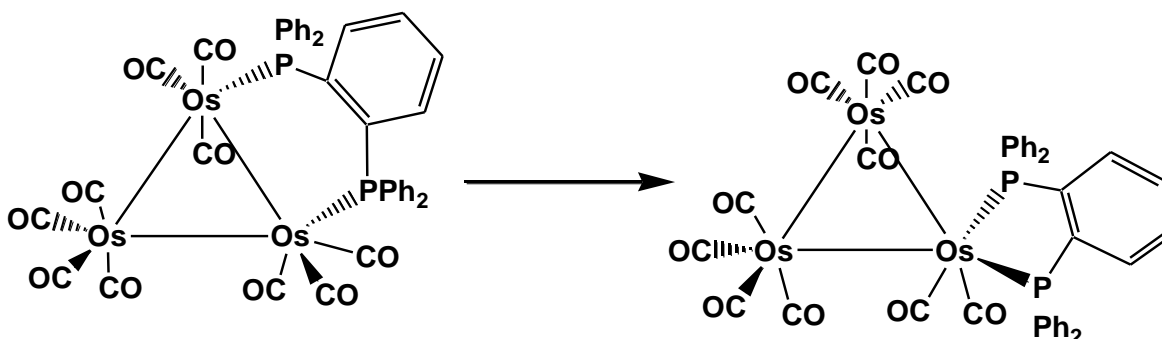


Figure 2.4 Isomerization from bridging to chelating coordination

Among chalcogens the much larger tellurium has been used as a bridge between different metal fragments in cluster synthesis, with a prediction that the tellurium-containing clusters will be structurally and chemically different from those containing sulphur or selenium. Mathur et al. reported the synthesis of a tetra-ruthenium cluster with bridging tellurium and diphosphine ligands, $[\text{Ru}_4(\text{CO})_9(\mu\text{-dppm})(\mu_4\text{-Te})_2]$, by reacting $[\text{Ru}_4(\text{CO})_{10}(\mu\text{-CO})(\mu_4\text{-Te})_2]$ with bis(diphenylphosphino)methane (dppm) at room temperature (Figure 2.5).²⁶ X-ray diffraction analysis shows that the molecule consists of a distorted octahedral Ru_4Te_2 framework in which two Ru-Ru bonds are bridged by a carbonyl group and a dppm ligand. Each of the four ruthenium atoms also contains two terminally bonded carbonyl ligands satisfying the 18 electron count.

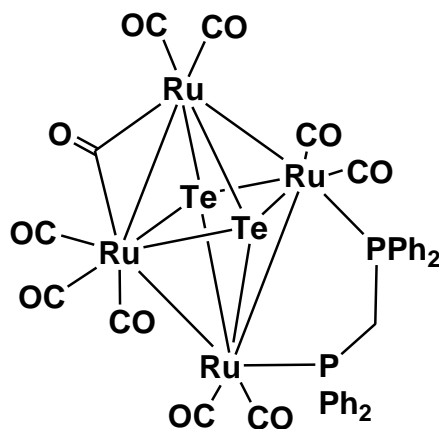


Figure 2.5 $[\text{Ru}_4(\text{CO})_9(\mu\text{-dppm})(\mu_4\text{-Te})_2]$

Presence of bidentate phosphine ligands and main group atoms like chalcogen can play the role of stabilizing the cluster framework, thus generating structural diversity in transition metal cluster compounds. Moreover, diphosphine containing clusters displays versatile bonding properties and fascinating structural as well as reactivity features when bonded to two or more metal units.

The flexible diphosphine, 1,1'-bis(diphenylphosphino)ferrocene (dppf), is an important member of the ferrocenylphosphine family. Most commonly, dppf chelates to a single metal atom, but it can also act as a monodentate ligand or as a bridge across a metal-metal bond. Two isomeric nido-clusters $[\text{Ru}_3(\mu_3\text{-Se})_2(\text{dppf})(\text{CO})_7]$ and $[\text{Ru}_3(\mu_3\text{-Se})_2(\text{CO})_7(\mu\text{-dppf})]$ containing a dppf ligand in chelating and bridging mode have been obtained by a reaction of 1,1'-bis(diphenylphosphino)ferrocene diselenide (dppfSe₂) with $[\text{Ru}_3(\text{CO})_{12}]$ at reflux temperature. The kinetically controlled chelated compound can be converted to the more stable bridged cluster at high temperature (Figure 2.6).^{26b}

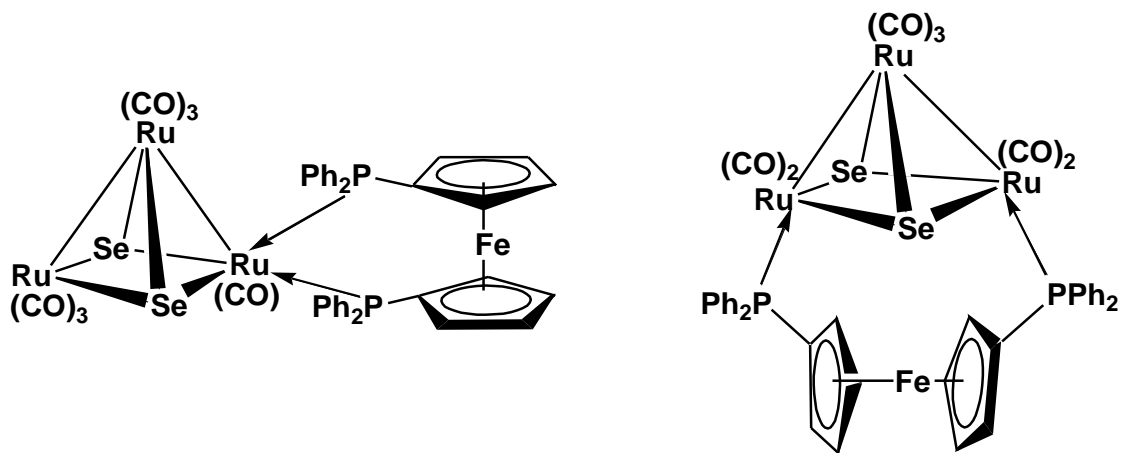


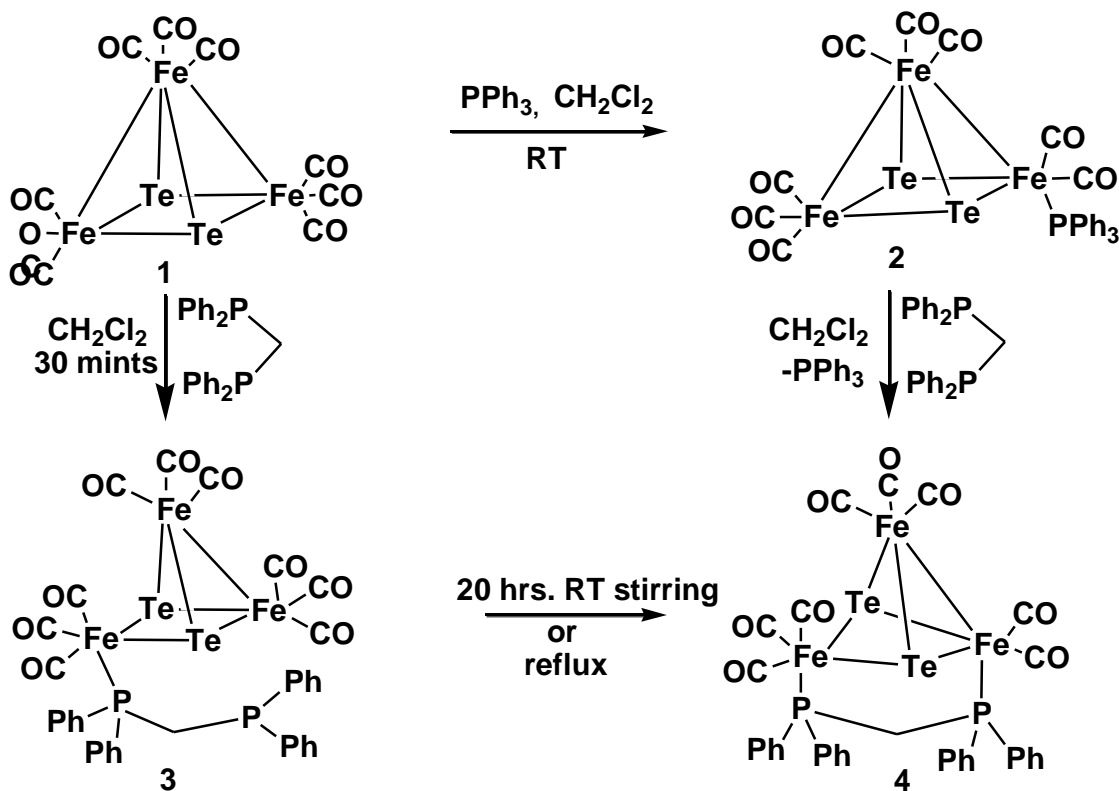
Figure 2.6 $[\text{Ru}_3(\mu_3\text{-Se})_2(\text{dppf})(\text{CO})_7]$ in chelating and bridging mode

In view of their uniqueness and to understand the influence of different diphosphine ligands towards metal chalcogenide clusters we studied the reaction of triiron dithiolene carbonyl cluster and triiron dithiolene phosphine cluster with two different diphosphine ligands, bis(diphenylphosphino)methane and bis(diphenylphosphino)ethane. In this chapter, synthesis and characterization of some diphosphine coordinated iron telluride clusters have been described and their molecular structures have been established by single crystal X-ray crystallography.

2.2. RESULTS AND DISCUSSION

2.2.1. Reaction of iron-telluride cluster with Bis-diphenylphosphino methane

Room temperature reaction of $[\text{Fe}_3\text{Te}_2(\text{CO})_8(\text{PPh}_3)]$ (**2**) with Bis-(diphenylphosphino)methane in dichloromethane solvent results in the formation of a dppm bridged triiron –tellurium cluster, $[\text{Fe}_3\text{Te}_2(\text{CO})_8(\mu\text{-dppm})]$ (**4**) (Scheme 2.1). The formation of compound **4** was also observed in very low yield by the reaction of $[\text{Fe}_3\text{Te}_2(\text{CO})_9]$ (**1**) with dppm which first gave an intermediate adduct $[\text{Fe}_3\text{Te}_2(\text{CO})_9(\text{dppm})]$ (**3**) which on stirring for 20 hrs converted to the dppm bridged open cluster $[\text{Fe}_3\text{Te}_2(\text{CO})_8(\mu\text{-dppm})]$ (**4**). It has been previously reported that $[\text{Fe}_3\text{Te}_2(\text{CO})_9]$ reacts with triphenylphosphine or dppm ligand to obtain compounds **2** and **3** respectively.²⁷



Scheme 2.1

Compound **4** has been characterized by FTIR and ^1H and ^{31}P NMR spectroscopy. Compound **3** was identified on the basis of comparison of its FTIR spectra with that of compound

reported earlier.²⁷ FTIR spectrum of compound **4** shows peaks in the region 1930-2036 cm⁻¹ due to the presence of terminal metal carbonyl groups. ¹H NMR spectrum shows peaks in the aromatic region, δ7.15 - δ7.65, for phenyl groups and a triplet at δ 3.16 for CH₂ - group of dppm ligand. The two non-equivalent phosphorus atoms attached to iron centres have been detected by ³¹P NMR spectroscopy, one at δ 51.06 (doublet) and the other at δ 45.47 (doublet) with a coupling constant of ²J_{P-P} = 63 Hz (Figure 2.7).

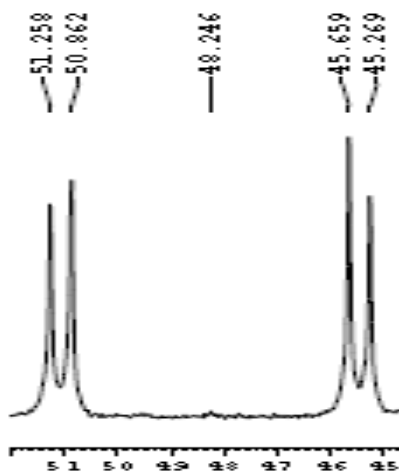


Figure 2.7 ³¹P{H} NMR of **4**

Single crystals of compound **4** have been grown from dichloromethane–hexane solvent mixture at -10°C. Structural characterization of compound **4** shows an open tri-iron cluster with a bridging dppm ligand between Fe1 and Fe2 iron centres. One phosphorus atom of the dppm ligand is attached to Fe1 with a bond length of 2.1860(15) Å and the other phosphorus atom is linked to Fe2 center (Fe2-P2 = 2.2928 (15)Å). Eight terminal carbonyl groups are attached to three iron atoms as shown in the Figure 2.8.

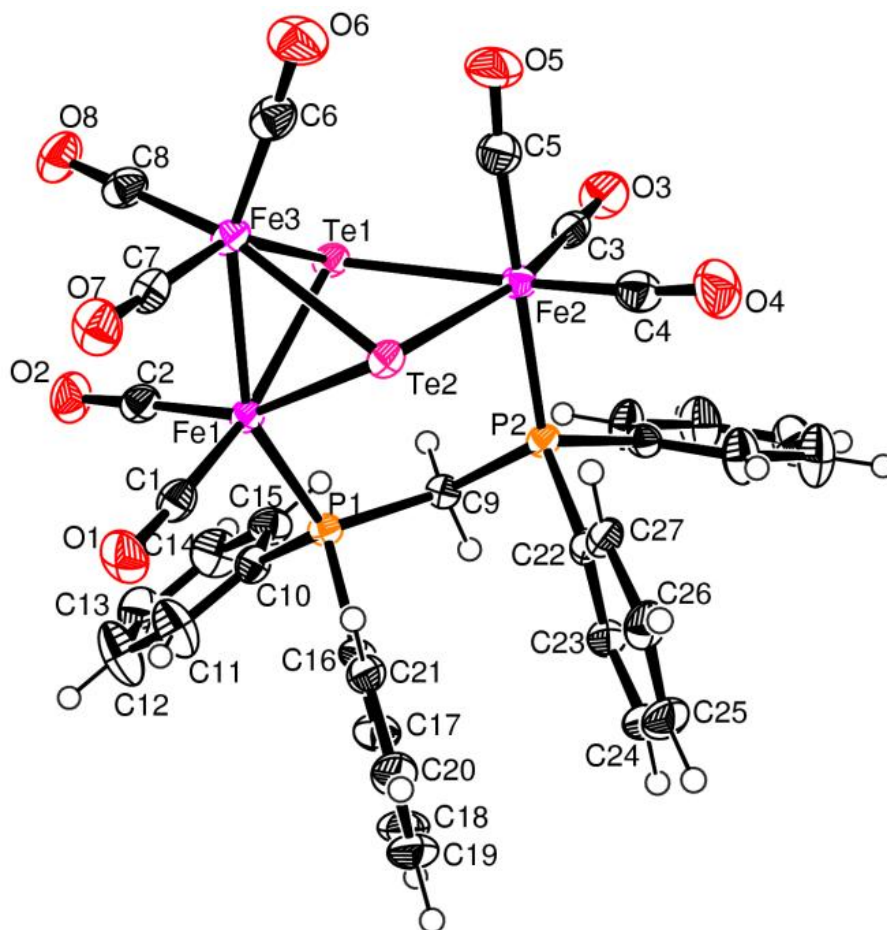


Figure 2.8 Molecular structure of $[\text{Fe}_3\text{Te}_2(\text{CO})_8(\mu\text{-dppm})]$ (**4**).

A possible reaction pathway can be proposed for the transformation of compound **2** to compound **4** in which the first step is the substitution of triphenylphosphine group in compound **2** by one of the phosphorus atoms of dppm ligand, followed by bond formation of the other phosphorus atom of the dppm ligand with the basal iron center and subsequent Fe-Fe bond breaking to satisfy the 18 electron rule. The replacement of triphenylphosphine group by a dppm ligand is preferred over replacement of carbonyl group, which results in the formation of compound **4**.

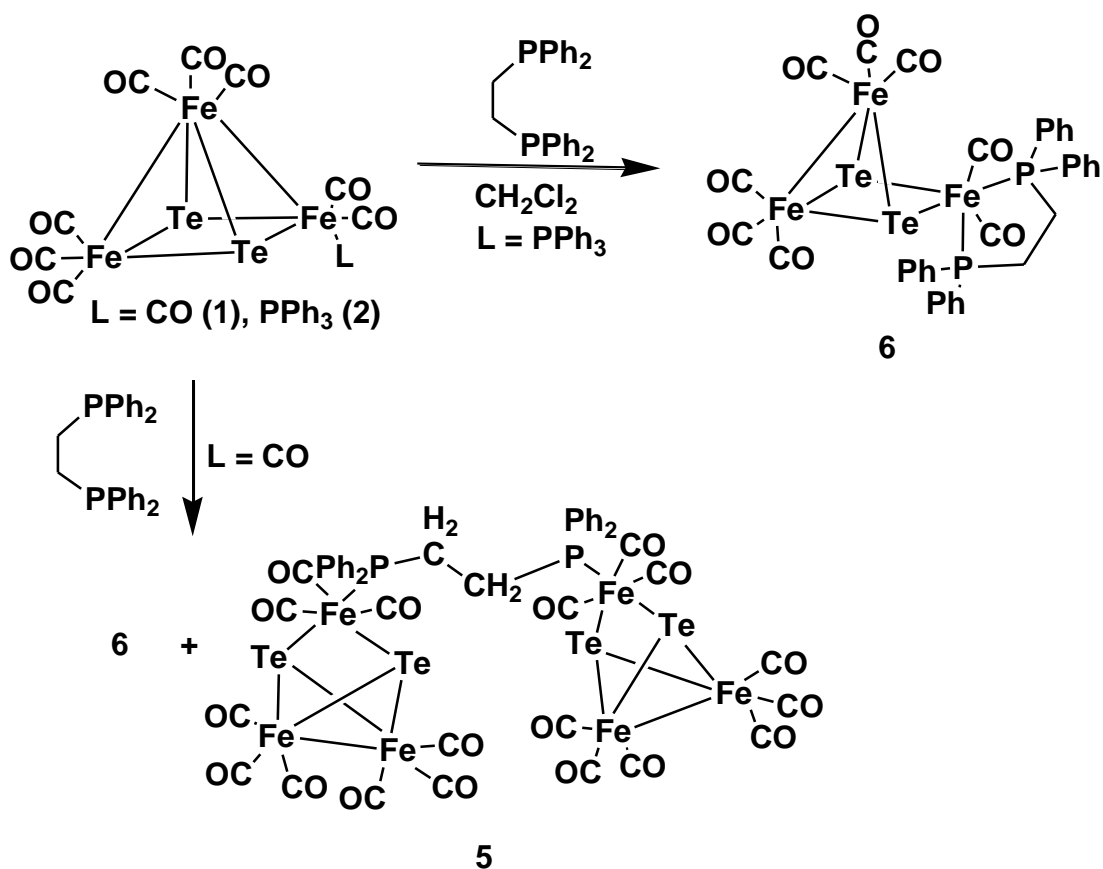
Table 2.1: Selected bond lengths (Å) and angles (deg) for **4**

Compound 4			
Fe(1)-Fe(3)	2.5732(10)	Fe(1)-Te(2)	2.5699(8)
Fe(1)-P(1)	2.1860(15)	Fe(1)-Te(1)	2.5665(8)
Fe(2)-P(2)	2.2928(15)	Fe(3)-Te(2)	2.5685(8)
Fe(2)-C(4)	1.799(6)	Fe(2)-Te(2)	2.6642(8)
Fe(2)-Te(1)	2.6818(8)	Fe(3)-Te(1)	2.5768(8)
Te(1)-Te(2)	3.1473(5)	Fe(2)-Te(2)	2.6642(8)
Te(2)-Fe(2)-Te(1)	72.13(2)	Fe(3)-Te(1)-Fe(2)	97.33(2)
Te(2)-Fe(3)-Fe(1)	59.97(2)	Fe(1)-Te(1)-Te(2)	52.260(18)
C(7)-Fe(3)-Te(1)	150.40(19)	Fe(3)-Te(1)-Te(2)	52.170(18)
C(8)-Fe(3)-Te(1)	89.30(18)	Fe(2)-Te(1)-Te(2)	53.675(18)
C(6)-Fe(3)-Te(1)	109.45(19)	Fe(3)-Te(2)-Fe(1)	60.10(2)
Te(2)-Fe(3)-Te(1)	75.42(2)	Fe(3)-Te(2)-Fe(2)	97.98(3)
Fe(1)-Fe(3)-Te(1)	59.78(2)	Fe(1)-Te(2)-Fe(2)	97.97(2)
Fe(1)-Te(1)-Fe(2)	97.60(2)	Fe(3)-Te(2)-Te(1)	52.409(18)
Fe(1)-Te(2)-Te(1)	52.164(18)	C(9)-P(2)-Fe(2)	117.43(18)
Fe(2)-Te(2)-Te(1)	54.192(18)	Fe(1)-Te(1)Fe(3)	60.04(2)
C(9)-P(1)-Fe(1)	116.60(17)	P(1)-Fe(1)-Te(2)	103.55(5)
C(9)-P(2)-C(28)	101.1(2)	Te(1)-Fe(1)-Te(2)	75.58(2)
C(9)-P(2)-C(22)	104.8(2)	P(1)-Fe(1)-Fe(3)	154.33(5)
P(2)-C(9)-P(1)	118.2(3)	Te(1)-Fe(1)-Fe(3)	60.18(2)
P(1)-Fe(1)-Te(1)	98.16(4)	Te(2)-Fe(1)-Fe(3)	59.92(2)
P(2)-Fe(2)-Te(2)	90.45(4)	C(3)-Fe(2)-Te(1)	91.72(18)
C(4)-Fe(2)-Te(1)	168.5(2)	P(2)-Fe(2)-Te(1)	96.18(4)
C(5)-Fe(2)-Te(1)	83.9(2)		

2.2.2. Reaction of iron-telluride cluster with Bis-diphenylphosphino ethane (dppe)

Reaction of $[\text{Fe}_3(\mu_3\text{-Te})_2(\text{CO})_9]$ (**1**) with Bis(diphenylphosphino)ethane for 20 hrs. under inert atmospheric condition results in the formation of a high-nuclearity cluster $[(\text{CO})_{18}\text{Fe}_6(\mu_3\text{-$

$\text{Te}_4\{\mu\text{-PPh}_2(\text{CH}_2)_2\text{PPh}_2\}$ (**5**) and trace amount of $[\text{Fe}_3(\mu_3\text{-Te})_2(\text{CO})_8\{\text{PPh}_2(\text{CH}_2)_2\text{PPh}_2\}]$ (**6**). Compound **6** has been obtained in higher yields by the reaction of $[\text{Fe}_3(\mu_3\text{-Te})_2(\text{CO})_8\text{PPh}_3]$ (**2**) with dppe at room temperature (Scheme 2.2). Compounds **5** and **6** have been characterized by FTIR, NMR and single crystal diffraction studies. Although the synthesis of compound **5** has been reported earlier,²⁷ the structural identity was uncertain. Therefore, we carried out its detailed structural characterization to confirm the structural parameters. Infrared spectroscopy of compounds **5** and **6** consist of vibration peaks in the range of 2052 - 1940 cm^{-1} that reveals the presence of terminally bonded carbonyls attached to the iron atoms. ^1H NMR shows peaks corresponding to twenty phenyl protons in the range $\delta 7.22\text{-}\delta 7.73$ and four CH_2 protons for each of the compounds **5** and **6** at $\delta 2.18$ and $\delta 2.53$ region respectively. A single ^{31}P NMR peak at $\delta 40.43$ reveals the presence of equivalent phosphorus atoms bonded to iron centre for **5** and at $\delta 69.2$ for **6**. The variation of ^{31}P NMR peaks in compounds **5** and **6** is due to the different types of bonding modes of dppe with the metal atom.



Scheme 2.2

The molecular structure of compound **5** was confirmed by single crystal X-ray crystallography. It consists of two Fe_3Te_2 cluster fragments linked together by a bridging dppe unit. Each of the two phosphorus atoms of the bridging diphosphine unit is bonded to the iron atom of the metal cluster. The two Fe_3Te_2 units are directed in the same side and forms a cis oriented geometry. The structure also consists of two Fe-Fe bonds and a total of eighteen carbonyl groups attached to six iron atoms (Figure 2.9). A similar diphosphine bridged cluster, $[\{\text{Fe}_3\text{Se}_2(\text{CO})_8\}_2(\text{dppe})]$ with four Fe-Fe bonds and 16 carbonyl groups reported previously shows two Fe_3Se_2 units linked together via a dppe ligand and are oriented opposite to each other forming a trans geometry.²⁸

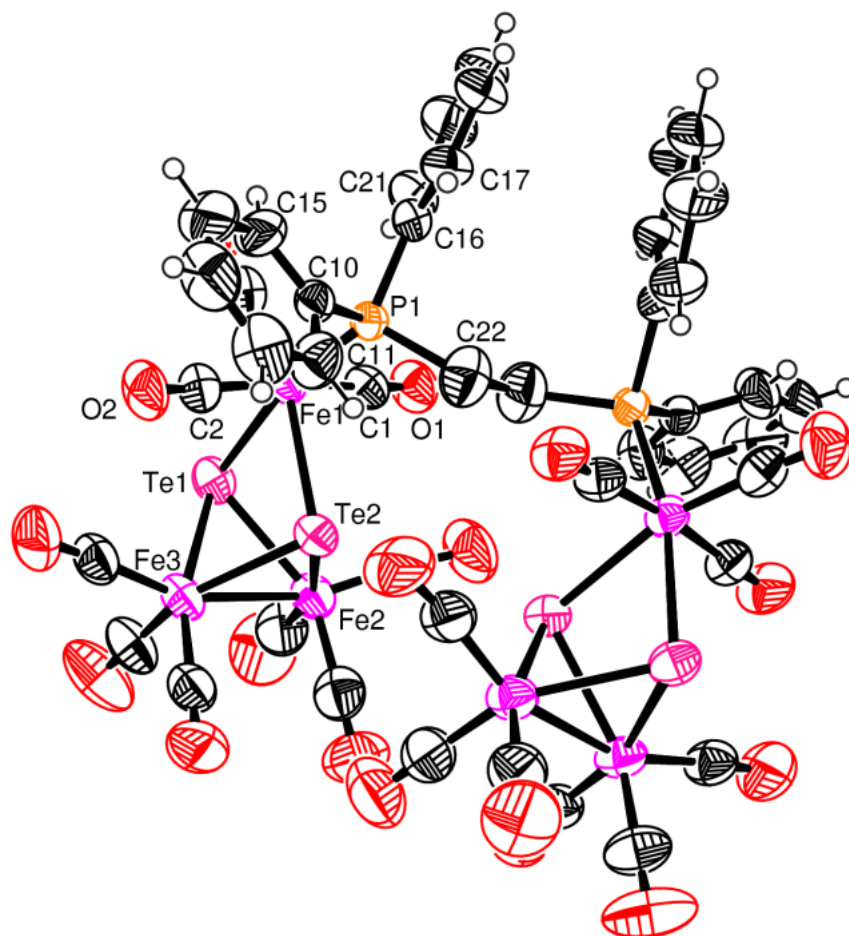


Figure 2.9: Molecular structure of $[(\text{CO})_{18}\text{Fe}_6(\mu_3\text{-Te})_4\{\mu\text{-PPh}_2(\text{CH}_2)_2\text{PPh}_2\}]$ (**5**).

Structural characterization of compound **6** has been performed to confirm the structure which we first thought to be an analogue of $[\text{Fe}_3(\mu_3\text{-Te})_2(\text{CO})_8(\mu\text{-dppm})]$ (**4**), synthesized from

the reaction between $[\text{Fe}_3(\mu_3\text{-Te})_2(\text{CO})_8\text{PPh}_3]$ and dppe. The structure of compound **6** unexpectedly came out to be different which consists of a Fe_3Te_2 unit linked to eight terminal iron carbonyl and a dppe ligand forming a chelate with one of the basal iron atom (Figure 2.10). Selected bond lengths and angles for compounds **5** and **6** are collected in Table 2.2. The dppe ligand serving as bidentate chelate is very rare in multimetallic system and often tends to form bridging ligands between two metal atoms. Although three iron atoms are present in **6**, the dppe ligand chose to form a bidentate chelating coordination with one iron atom and not a bridging ligand. A possible reaction pathway can be proposed for the formation of compound **6**, in which the initial step may be the substitution of PPh_3 group attached to the basal iron atom of compound **2** by one of the phosphorus atom of a dppe ligand. Subsequently, the other phosphorus atom of the diphosphine ligand attacks the same iron centre and breaking of a Fe-Fe bond takes place resulting in compound **6**. Whereas, reaction of **1** with dppe, results in the formation of **5** probably by the attack of dppe phosphorus atoms to two different Fe_3Te_2 units with the breaking of Fe-Fe bonds.

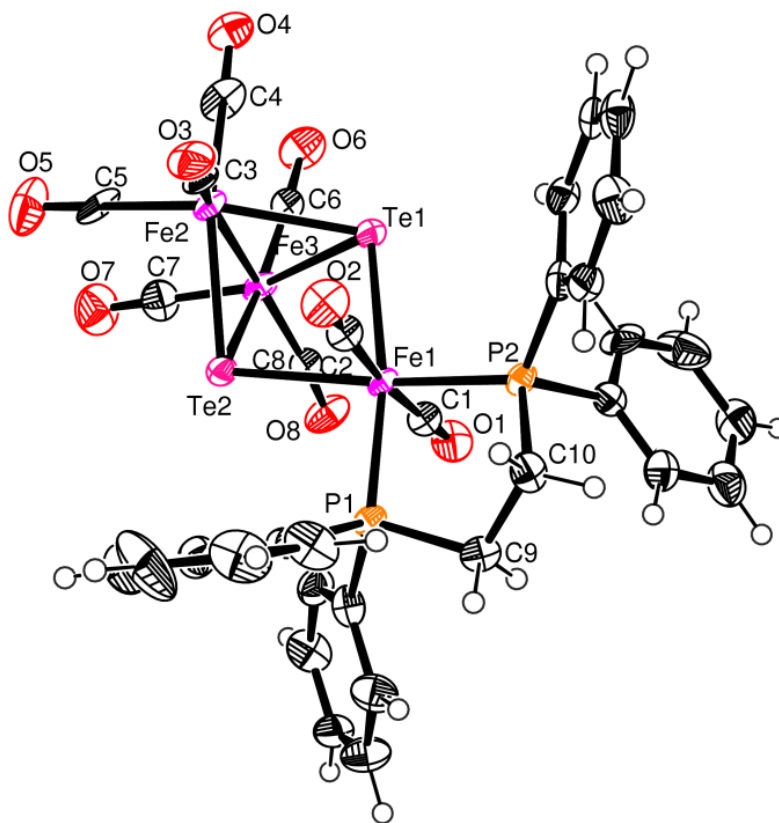


Figure 2.10: Molecular structure of $[\text{Fe}_3(\mu_3\text{-Te})_2(\text{CO})_8\{\text{PPh}_2(\text{CH}_2)_2\text{PPh}_2\}]$ (**6**).

Table 2.2: Selected bond lengths (Å) and angles (deg) for **5** and **6**

Compound 5			
Te(1)-Fe(3)	2.5628(16)	Te(2)-Fe(2)	2.5647(15)
Te(1)-Fe(2)	2.5805(17)	Te(2)-Fe(3)	2.5836(15)
Te(1)-Fe(1)	2.6491(14)	Te(2)-Fe(1)	2.6813(15)
Te(1)-Te(2)	3.1715(9)	P(1)-C(22)	1.848(8)
Te(2)-Fe(3)-Fe(2)	59.36(5)	Fe(3)-Te(1)-Fe(2)	60.62(5)
Fe(3)-Te(2)-Fe(1)	96.79(5)	Fe(3)-Te(1)-Fe(1)	98.11(5)
Fe(2)-Te(2)-Te(1)	52.17(4)	Fe(2)-Te(1)-Fe(1)	96.45(5)
Fe(3)-Te(2)-Te(1)	51.66(4)	Fe(3)-Te(1)-Te(2)	52.25(3)
Fe(1)-Te(2)-Te(1)	53.02(3)	Fe(2)-Te(1)-Te(2)	51.72(4)
P(1)-Fe(1)-Te(1)	166.95(9)	Fe(1)-Te(1)-Te(2)	53.96(3)
P(1)-Fe(1)-Te(2)	94.61(7)	Fe(2)-Te(2)-Fe(3)	60.56(5)
Te(1)-Fe(1)-Te(2)	73.02(4)	Fe(2)-Te(2)-Fe(1)	96.03(5)
Te(2)-Fe(2)-Te(1)	76.11(5)	Te(2)-Fe(2)-Fe(3)	60.08(5)
C(6)-Fe(2)-Fe(3)	104.5(4)	Te(1)-Fe(2)-Fe(3)	59.35(5)
C(4)-Fe(2)-Fe(3)	156.7(4)	Te(1)-Fe(3)-Te(2)	76.08(4)
C(5)-Fe(2)-Fe(3)	91.3(4)	Te(1)-Fe(3)-Fe(2)	60.02(5)
Compound 6			
Fe(1)-P(1)	2.223(4)	Fe(2)-Te(2)	2.567(2)
Fe(1)-P(2)	2.232(4)	Fe(2)-Fe(3)	2.586(3)
Fe(1)-Te(1)	2.6325(19)	Fe(3)-Te(2)	2.564(2)
Fe(1)-Te(2)	2.638(2)	Fe(3)-Te(1)	2.586(2)
Fe(2)-Te(1)	2.564(2)	Te(1)-Te(2)	3.1736(13)
P(1)-C(9)	1.849(14)	P(2)-C(10)	1.830(14)
Te(1)-Fe(2)-Te(2)	76.41(6)	Fe(3)-Te(1)-Fe(1)	95.39(6)
Te(1)-Fe(2)-Fe(3)	60.27(7)	Fe(2)-Te(1)-Te(2)	51.83(5)
Te(2)-Fe(2)-Fe(3)	59.69(6)	Fe(3)-Te(1)-Te(2)	51.65(5)
Te(2)-Fe(3)-Te(1)	76.09(6)	Fe(1)-Te(1)-Te(2)	53.06(5)
Te(2)-Fe(3)-Fe(2)	59.79(6)	Fe(3)-Te(2)-Fe(2)	60.53(6)
Te(1)-Fe(3)-Fe(2)	59.45(6)	Fe(3)-Te(2)-Fe(1)	95.76(7)

Fe(2)-Te(1)-Fe(3)	60.28(6)	Fe(2)-Te(2)-Fe(1)	97.04(7)
Fe(2)-Te(1)-Fe(1)	97.25(7)	P(1)-Fe(1)-Te(1)	168.30(12)
P(2)-Fe(1)-Te(1)	102.88(11)		

2.3. EXPERIMENTAL SECTIONS

2.3.1. General Procedures

All reactions and manipulations were carried out under an inert atmosphere of dry, pre-purified argon or nitrogen using standard schlenk line techniques. Solvents were purified, dried and distilled under an argon atmosphere prior to use. Infrared spectra were recorded on a Perkin Elmer Spectrum RX-I spectrometer as dichloromethane solutions in 0.1 mm path lengths NaCl cell and NMR spectra on a 400 MHz Bruker spectrometer in CDCl₃. Elemental analyses were performed on a Vario El Cube analyser. TLC plates (20x20 cm, Silica gel 60 F254) were purchased from Merck. [Pd(PPh₃)₄] and TMNO.2H₂O was purchased from Sigma Aldrich. [Fe₃Y₂(CO)₉] (Y = S, Se, Te), [Fe₃Te₂(CO)₈(PPh₃)] were prepared following reported procedures.^{27, 29, 30}

2.3.2. Reaction of [Fe₃Te₂(CO)₈(PPh₃)] (2) with Bis-(diphenylphosphino)methane

Dichloromethane solution of [Fe₃Te₂(CO)₈(PPh₃)] (2) (91 mg, 0.1 mmol) and Bis-(diphenylphosphino)methane (39 mg, 0.1 mmol) was subjected to room temperature reaction under stirring condition and N₂ atmosphere for 4 hrs. After the completion of the reaction the solution was vacuum dried and the residue was subjected to chromatographic work-up using preparative TLC with dichloromethane / hexane (20:80 v/v) solvent mixture. The compounds obtained on subsequent elution are trace amount of unreacted [Fe₃Te₂(CO)₈(PPh₃)] followed by the orange product [Fe₃Te₂(CO)₈(μ-dppm)] (4). (Yield=78 mg, 78 %)

4: IR(ν_{CO} , cm⁻¹, CH₂Cl₂): 2036(s), 1973.4(vs,br), 1931(s, br). ¹H NMR(δ , CDCl₃): 3.157 (t, 2H, -CH₂), 7.15-7.65 (m, 20H, C₆H₅). ³¹P{¹H}NMR(δ): 45.47 (d, ²J_{P-P}= 63 Hz), 51.06 (d, ²J_{P-P}= 63 Hz). ¹³C NMR(δ , CDCl₃) = 29.7 (s, CH₂), 128.4-131 (m, C₆H₅).

2.3.3 Synthesis of $[Fe_6(\mu_3-Te)_4(CO)_{18}\{\mu-PPh_2(CH_2)_2PPh_2\}]$ (**5**)

A dichloromethane solution of $[Fe_3(\mu_3-Te)_2(CO)_9]$ (**1**) (135 mg, 0.2 mmol) was reacted with Bis-(diphenylphosphino)ethane (40 mg, 0.1 mmol) at room temperature under continuous stirring condition and argon atmosphere for 20 hours. The reaction was monitored by TLC. On completion of the reaction the solution was dried under vacuum and the residue was dissolved in dichloromethane solvent and subjected to chromatographic work-up using preparative TLC. Elution with dichloromethane / hexane (30:70 v/v) solvent mixture separated the following compounds: unreacted $[Fe_3(\mu_3-Te)_2(CO)_9]$ (15 mg), orange coloured $[Fe_6(\mu_3-Te)_4(CO)_{18}\{\mu-PPh_2(CH_2)_2PPh_2\}]$ (**5**) (Yield= 125 mg, 79 %) and $[Fe_3(\mu_3-Te)_2(CO)_8\{PPh_2(CH_2)_2PPh_2\}]$ (**6**) (Yield= 8 mg). Trace amount of decomposition was also observed during the workup.

5: Anal. calcd. (found): C, 30.22 (30.07); H, 1.37 (1.49). IR(ν_{CO} , cm^{-1} , CH_2Cl_2): 2052(m), 2036(s), 2011(s), 1987(m), 1971(s). 1H NMR(δ , $CDCl_3$): 2.18-2.15 (m, 4H, $-CH_2$), 7.22-7.58 (m, 20H, C_6H_5). $^{31}P\{^1H\}$ NMR(δ): 40.43 (s, $J_{P-Te} = 38$ Hz). ^{13}C NMR(δ , $CDCl_3$) = 29.7 (s, CH_2), 129.3-132.1 (m, C_6H_5), 206.9 (s, CO), 209.6 (s, CO), 213.2 (s, CO).

2.3.4. Reaction of $[Fe_3(\mu_3-Te)_2(CO)_8(PPh_3)]$ (**2**) with Bis-(diphenylphosphino)ethane

In a two necked round bottomed flask dichloromethane solution of $[Fe_3(\mu_3-Te)_2(CO)_8(PPh_3)]$ (**2**) (91mg, 0.1 mmol) was taken and reacted with Bis-(diphenylphosphino)ethane (40 mg, 0.1 mmol) at room temperature under argon atmosphere for 4 hrs. After the completion of the reaction the solution was vacuum dried and the residue was dissolved in minimum volume of dichloromethane solvent and subjected to preparative TLC. Elution with dichloromethane / hexane (30:70 v/v) solvent mixture separated trace amount of unreacted $[Fe_3(\mu_3-Te)_2(CO)_8(PPh_3)]$ and an orange compound $[Fe_3(\mu_3-Te)_2(CO)_8\{PPh_2(CH_2)_2PPh_2\}]$ (**6**). (Yield= 86 mg, 82 %). Trace amount of decomposition was also observed.

6: Anal. calcd. (found): C, 39.05 (39.32); H, 2.30 (2.37). IR(ν_{CO} , cm^{-1} , CH_2Cl_2): 2035(s), 2019(vs), 1975(vs), 1956(s), 1940(s). 1H NMR(δ , $CDCl_3$): 2.528 (d, 4H, $-CH_2$, $J = 14.4$ Hz),

7.44-7.73 (m, 20H, C₆H₅). ³¹P{¹H} NMR(δ): 69.2 (s). ¹³C NMR(δ, CDCl₃) = 29.5 (s, CH₂), 128.7-132 (m, C₆H₅), 212.4 (s, CO).

2.3.5. Crystal structure determination for **4**, **5** and **6**

Single crystal X-ray structural studies of **4**, **5** and **6** were performed on a CCD Oxford Diffraction XCALIBUR-S diffractometer equipped with an Oxford Instruments low-temperature attachment. Data were collected at 150(2) K using graphite-monochromated Mo K α radiation ($\lambda_{\alpha} = 0.71073$ Å). The strategy for the Data collection was evaluated by using the CrysAlisPro CCD software. The data were collected by the standard 'phi-omega scan techniques, and were scaled and reduced using CrysAlisPro RED software. The structures were solved by direct methods using SHELXS-97 and refined by full matrix least-squares with SHELXL-97, refining on F^2 .³¹ The positions of all the atoms were obtained by direct methods. All non-hydrogen atoms were refined anisotropically. The remaining hydrogen atoms were placed in geometrically constrained positions and refined with isotropic temperature factors, generally $1.2U_{eq}$ of their parent atoms. The crystallographic details are summarized in Table 2.3.

2.4. CONCLUSION

Synthesis of bis(diphenylphosphino)methane coordinated triiron tellurium cluster, [Fe₃Te₂(CO)₈(μ -dppm)] (**4**) and two new bis(diphenylphosphino)ethane coordinated clusters [(CO)₁₈Fe₆(μ_3 -Te)₄{ μ -PPh₂(CH₂)₂PPh₂}] (**5**) and [Fe₃(μ_3 -Te)₂(CO)₈{PPh₂(CH₂)₂PPh₂}] (**6**) have been carried out by a room temperature facile reaction condition. Among the three homometallic clusters, compound **4** has a bridging diphosphine ligand between metals from the same cluster framework, while **5** contains a diphosphine ligand bridged between two cluster entities, and cluster **6** has a chelating diphosphine group. The variation in cluster coordination has been attributed to different factors like diphosphine chain length, metallic framework and strain in between the phosphorus atoms of a diphosphine unit.

Table 2.3: Crystal data and structure refinement parameters for compounds **4**, **5** and **6**.

	4	5	6
Empirical formula	C ₃₃ H ₂₂ Fe ₃ O ₈ P ₂ Te ₂	C ₄₄ H ₂₄ Fe ₆ O ₁₈ P ₂ Te ₄	C ₃₄ H ₂₄ Fe ₃ O ₈ P ₂ Te ₂
Formula weight	1031.20	1748.04	1045.22
Crystal system	Triclinic,	Monoclinic	Monoclinic,
Space group	<i>P</i> -1	<i>C</i> 2/c	<i>P</i> 2 ₁ /n
<i>a</i> , Å	10.7508(3)	25.125(2)	11.6944(4)
<i>b</i> , Å	12.1314(3)	14.6248(12)	19.7638(8)
<i>c</i> , Å	16.6082(6)	21.762(3)	15.5663(6)
α deg	95.626(3)	90	90
β deg	91.898(2)	122.651(4)	93.576(3)
γ deg	107.027(2)	90	90
<i>V</i> , Å ³	2056.80(11)	6732.7(12)	3590.8(2)
<i>Z</i>	2	4	4
D _{calcd} , Mg m ⁻³	1.665	1.721	1.933
abs coeff, mm ⁻¹	2.554	3.060	2.927
F(000)	992	3288	2016
Cryst size, mm	0.32 x 0.28 x 0.23	0.32 x 0.28 x 0.23	0.33 x 0.29 x 0.21
θ range, deg	3.38 to 25.00	2.01 to 25.00	3.34 to 32.91
index ranges	-12<= <i>h</i> <=12, -12<= <i>k</i> <=14, - 19<= <i>l</i> <=19	-29<= <i>h</i> <=27, -14<= <i>k</i> <=17, - 25<= <i>l</i> <=25	-17<= <i>h</i> <=16, -30<= <i>k</i> <=22, - 21<= <i>l</i> <=23
reflections collected/ unique data/ restraints / parameters	15403 / 7223 [R(int) = 0.0185] 7223 / 0 / 433	23175 / 5927 [R(int) = 0.0448] 5927 / 0 / 334	42902 / 12300 [R(int) = 0.0980] 12300 / 39 / 424
goodness-of-fit on F ²	1.145	1.101	1.107
Final R indices[I>2 σ (I)]	R1 = 0.0324, wR2 = 0.1247	R1 = 0.0489, wR2 = 0.1691	R1 = 0.1222, wR2 = 0.2484
R indices (all data)	R1 = 0.0378, wR2 = 0.1285	R1 = 0.0780, wR2 = 0.1972	R1 = 0.1746, wR2 = 0.2639

largest diff peak and hole, eÅ ⁻³	2.838 -0.483	1.421 -0.970	3.483 -3.459
---	-----------------	-----------------	-----------------

2.5. REFERENCES

1. (a) P. Mathur, S. Chatterjee, Y. V. Torubaev, *J. Cluster Sci.* 18 (2007) 505; (b) M. Shieh, *J. Clust. Sci.* 10 (1999) 3.
2. M. Scheer, S. B. Umbarkar, S. Chatterjee, R. Trivedi, P. Mathur, *Angew. Chem. Int. Ed. Eng.* 40 (2001) 376.
3. R. D. Adams, E. Boswell, *Organometallics* 27 (2008) 2021.
4. (a) G. W. Drake, J. W. Kolis, *Coord. Chem. Rev.* 137 (1994) 131; (b) M. Di Vaira, P. Stoppioni, *Coord. Chem. Rev.* 120 (1992) 259.
5. (a) L. C. Roof, W. Kolis, *Chem. Rev.* 93 (1994) 1037; (b) P. Mathur, M. M. Hossain, S. B. Umbarkar, C. V. V. Satyanarayana, A. L. Rheingold, L. M. Liable-Sands, G. P. A. Yap, *Organometallics* 15 (1996) 1898; (c) P. Mathur, S. Ghose, M. M. Hossain, C. V. V. Satyanarayana, M. F. Mahon, *J. Organomet. Chem.* 543 (1997) 189; (d) J. Wachter, *Eur. J. Inorg. Chem.* (2004) 1367.
6. (a) C. W. Pin, Y. Chi, C. Chung, A. J. Carty, S. M. Peng, G. H. Lee, *Organometallics* 17 (1998) 4148; (b) A. J. Carty, G. D. Enright, G. Hogarth, *Chem. Commun.* (1997) 1883; (c) E. Delgado, Y. Chi, W. Wang, G. Hogarth, P. J. Low, G. D. Enright, S.M. Peng, G.-H. Lee, A. J. Carty, *Organometallics* 17 (1998) 2936; (d) V. P. Fedin, *Russ. J. Coord. Chem.* 30 (2004) 151; (e) S. Nagao, H. Seino, M. Hidai, Y. Mizobe, *J. Organomet. Chem.* 669 (2003) 124; (f) M. Shieh, *J. Clust. Sci.* 10 (1999) 3.
7. P. Mathur, *Adv. Organomet. Chem.* 41 (1997) 243.
8. (a) P. Mathur, B. H. S. Thimmappa, A. L. Rheingold, *Inorg. Chem* 29 (1990) 4658; (b) P. Mathur, M. M. Hossain, A. L. Rheingold, *Organometallics* 13 (1994) 3909.
9. P. Mathur, P. Sekar, C. V. V. Satyanarayana, *Organometallics* 14 (1995) 2115.
10. P. Michelin-Lausarot, G. A. Vaglio, M. Valle, *J. Organomet. Chem.* 275 (1984) 233.
11. P. Michelin-Lausarot, G. A. Vaglio, M. Valle, *Inorg. Chim. Acta.* 25(1977) L104.
12. M. I. Bruce, M. L. Williams, B. W. Skelton, A. H. White, *J. Organomet. Chem.* 306 (1986) 115.
13. R. D. Adams, I. T. Horváth, L. W. Yang, *J. Am. Chem. Soc.* 105 (1983) 1533.
14. (a) R. D. Adams, S. Wang, *Organometallics* 5 (1985) 1272; (b) M. I. Bruce, P. A. Humphrey, O. B. Shawkataly, M. R. Snow, E. R. T. Tickink, *Organometallics* 9 (1990) 2910.

15. (a) W. Schuh, P. Braunstein, M. B. Nard, M. M. Rohmer, R. Welter, *Angew. Chem. Int. Ed. Eng.* 42 (2003) 2161.
16. P. Braunstein, C. Charles, G. Kickelbick, U. Schubert, *Chem. Commun.* (1997) 2093.
17. P. Braunstein, J. L. Richert, Y. Dusausoy, *J. Chem. Soc., Dalton Trans.* (1990) 3801.
18. S. Chatterjee, S. K. Patel, S. M. Mobin, *J. Organomet. Chem.* 696 (2011) 1782.
19. (a) B. F.G. Johnson, T. M. Layer, J. Lewis, A. Martin, P. R. Raithby, *J. Organomet. Chem.* 429 (1992) C41; (b) Z.-G. Fang, Y.-S. Wen, R. K. L. Wong, S.-C. Ng, L.-K. Liu, T. S. A. Hor, *J. Clust. Sci.* 5 (1994) 327.
20. (a) P. Mathur, B. H. S. Thimmappa, A. L. Rheingold, *Inorg. Chem.* 29 (1990) 4658; (b) F. Fabrizi de Biani, C. Graiff, G. Opromolla, G. Predieri, A. Tiripicchio, P. Zanello, *J. Organomet. Chem.* 637-639 (2001) 586.
21. M. Brandl, H. Brunner, H. Cattey, Y. Mugnier, J. Wachter, M. Zabel, *J. Organomet. Chem.* 659 (2002) 22.
22. D. Cauzzi, C. Graiff, G. Predieri, C. Vignali, A. Tiripicchio, *J. Chem. Soc., Dalton Trans.* (1999) 237.
23. S. E. Kabir, M. ArzuMiah, M. A. Rahim, S. Sultana, G. M. G. Hossain, E. Nordlander, E. Rosenberg, *J. Clust. Sci.*, 16 (2005) 1.
24. Xue Zhang, S. Kandala, L. Yang, W. H. Watson, X. Wang, D. A. Hrovat, W. T. Borden, M. G. Richmond, *Organometallics* 30 (2011) 1253.
25. (a) W. H. Watson, G. Wu, M. G. Richmond, *Organometallics* 24 (2005) 5431; (b) W. H. Watson, B. Poola, M. G. Richmond, *Polyhedron* 26 (2007) 3585.
26. (a) P. Mathur, B. H. S. Thimmappa, A. L. Rheingold, *Inorg. Chem.* 29 (1990) 4658; (b) F. F. de Biani, C. Graiff, G. G. Predieri, A. Tiripicchio, P. Zanello, *J. Organomet. Chem.* 586 (2001) 637.
27. D. A. Lesch, T. B. Rauchfuss, *Organometallics* 1 (1982) 499.
28. D. Cauzzi, C. Graiff, M. Lanfranchi, G. Predieri, A. Tiripicchio, *J. Organomet. Chem.* 536 (1997) 497.
29. (a) W. Hieber, J. Gruber, *Z. Anorg. Allg. Chem.* 296 (1958) 91; (b) D. A. Lesch, T. B. Rauchfuss, *Inorg. Chem.* 20 (1981) 3583;
30. P. Mathur, I. J. Mavunkal, *J. Organomet. Chem.* 350 (1988) 251.
31. G. M. Sheldrick, *Acta Cryst. A* 64 (2008) 112.

CHAPTER 3

**SYNTHESIS, CHARACTERIZATION AND
REACTIVITY OF CHALCOGEN CONTAINING
IRON-PALLADIUM MIXED METAL
PHOSPHINE CLUSTERS**

3.1. INTRODUCTION

Mixed metal clusters are of interest because of their structural uniqueness and as precursors for the preparation of bimetallic heterogeneous catalysts.¹⁻³ The synthesis of mixed-metal cluster complexes by the process of metal-metal exchange usually involves a sequence of two steps, consisting of a metal addition followed by a metal elimination. The chemistry of transition-metal, non-metal cluster compounds has undergone rapid developments, particularly for metal-chalcogenide clusters⁴⁻¹⁰ It has been recently reported that mixed metal cluster complexes can produce more intimately mixed bimetallic nanoparticles¹¹⁻¹². In the last couple of decades, a variety of di- and polynuclear metal clusters containing different supporting ligands have been prepared.¹³⁻¹⁷ Among them metal carbonyl chalcogenide clusters display unusual structural and reactivity patterns. Chalcogens like tellurium and selenium play a vital role to clamp two or more metal units, resulting in the formation of mixed metal bonding interaction and stabilization of heterometallic cluster. Recently, some chalcogenide mixed metal clusters have been used for coupling reaction of metal-acetylide moieties resulting in clusters containing polycarbon units.¹⁸⁻²⁰ Ligand substitution reactions form an interesting aspect of the overall study of reactivity in mixed-metal clusters. Variation of the chalcogen atoms in the cluster amongst the congeners S, Se and Te, could lead to interesting contrasts in the reactivity of the ligand substitution reactions. It has been observed that the tellurium containing clusters have structural features and reactivity that are different from those of sulfur or selenium analogues. On the other hand, diphosphines are an important group of ligands with a versatile bonding modes and tunable properties.²¹⁻²⁹ Diphosphine ligand contains two phosphine moieties linked by a backbone unit, the most common being $-(\text{CH}_2)_n-$ ($n = 1,2,\dots$), $-(\text{C}_6\text{H}_4)-$, $-\text{CH}=\text{CH}-$, $-\text{C}\equiv\text{C}-$ and $-(\text{C}_5\text{H}_4)\text{Fe}(\text{C}_5\text{H}_4)-$. Most of these diphosphine ligands have been found to adopt a variety of bonding modes on the cluster framework, including monodentate with a pendant phosphine centre, chelating a single metal atom in a multimetallic cluster, bridging across a metal-metal bond and forming an intermolecular link across two clusters (Figure 3.1). The bonding modes adopted by these diphosphine ligands are influenced by the flexibility and length of the organic or organometallic backbone. In an effort to prepare novel clusters with structural identity, we sought to explore the possibility of incorporating both diphosphine ligands and chalcogen atoms in the cluster framework and study their combined effect. Literature survey reveals that homo metal chalcogenide clusters containing diphosphine-bridging ligands are

known to some extent while mixed transition metal clusters containing both selenium or tellurium atom and diphosphine ligands are rare³⁰⁻³⁵.

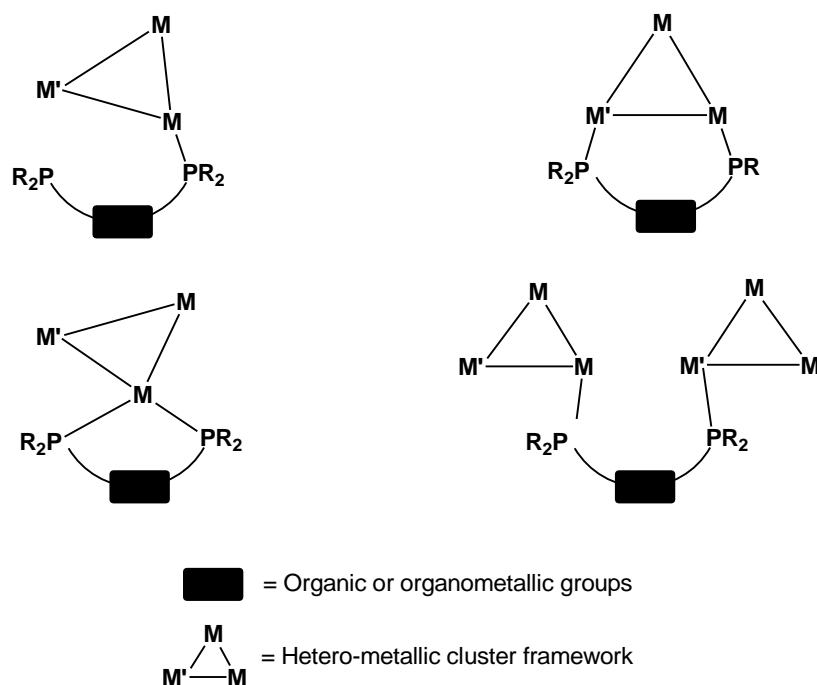


Figure 3.1: Different types of diphosphine coordination to hetero-metal clusters

In order to understand the influence of diphosphine ligands towards metal clusters, the reaction of several transition metal clusters with phosphines was studied. Some reports on the synthesis of diphosphine containing clusters reveals their versatile bonding properties and fascinating structural as well as reactivity features.³⁶⁻⁴⁴ Recently, palladium has been shown to be of great value as a catalyst for the hydrogenation of unsaturated organic molecules.⁴⁵ Studies have shown that improved catalytic activity is also obtained when palladium is combined with other transition metals.^{46, 47} It has also been shown that bimetallic complexes containing palladium can be good precursors to supported bimetallic catalysts.

Adams et al. reported that a new heterometallic tetrahedral osmium cluster containing tert.-butyl phosphine ligand, $[\text{Os}_4(\text{CO})_{12}\{\text{Pd}(\text{P}^t\text{Bu}_3)\}_4]$ was obtained from the reaction of $\text{Os}_3(\text{CO})_{12}$ with $\text{Pd}(\text{P}^t\text{Bu}_3)_2$ in octane solution at reflux temperature (Figure 3.2). The core of the molecule contains four osmium atoms and attached to twelve terminally bonded carbonyl

ligands. The Os-Pd bond distances are in the range 2.809(3) Å – 2.812(3) Å, while the Pd-P bond length is 2.429(5) Å.⁴⁸

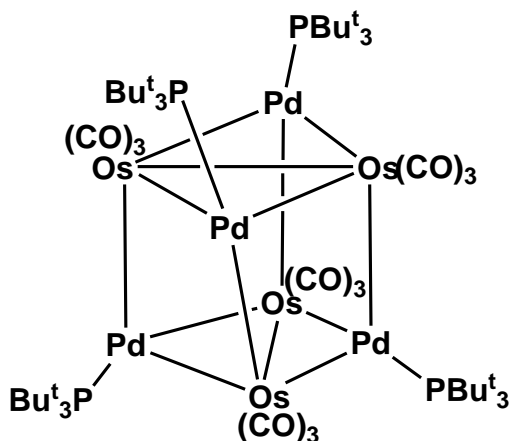


Figure 3.2 $[\text{Os}_4(\text{CO})_{12}\{\text{Pd}(\text{PBu}^t_3)\}_4]$

Braunstein et al. reported the reactivity of some dppm ($\text{Ph}_2\text{PCH}_2\text{PPh}_2$) stabilized palladium-cobalt and other heterometallic cluster system and studied the regioselective synthesis of mixed-metal cluster, $[\text{PdPtCo}_2(\text{CO})_7(\text{dppm})_2]$ by the reaction of $[\text{PdPtCl}_2(\text{dppm})_2]$ with $[\text{Co}(\text{CO})_4]$. The synthesis shows the exclusive insertion of the $\text{Co}(\text{CO})_3$ fragment into the palladium metal centre (Figure 3.3).⁴⁹

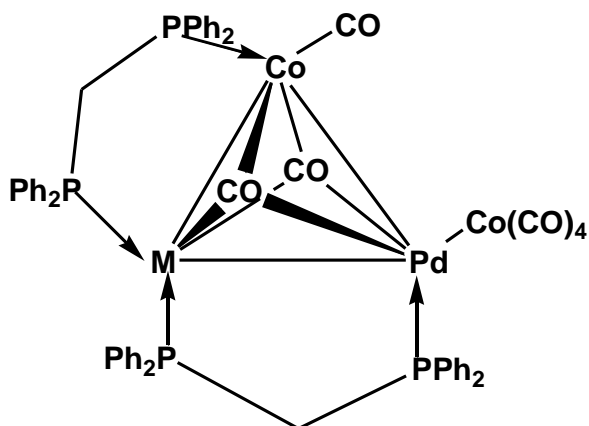


Figure 3.3 $[\text{PdPtCo}_2(\text{CO})_7(\text{dppm})_2]$, (M = Pt, Pd)

Reaction of dppm with the cluster $[\text{Pd}_2\text{Co}_2(\text{CO})_7(\text{dppm})_2]$ in THF at room-temperature resulted in both exocyclic Pd-Co bond cleavage and carbonyl substitution at the cobalt atom,

yielding a tris -dppm mixed metal cluster $[\text{Pd}_2\text{Co}_2(\mu_3\text{-CO})(\mu\text{-dppm})_3][\text{Co}(\text{CO})_4]$ as shown in Figure 3.4.⁴⁹

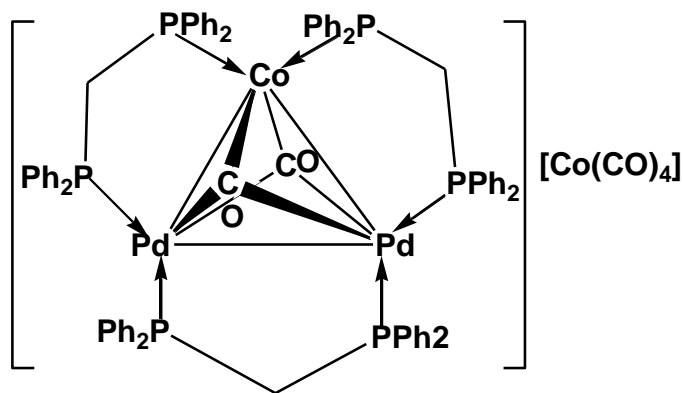


Figure 3.4 $[\text{Pd}_2\text{Co}(\mu_3\text{-CO})_2(\text{dppm})_2][\text{Co}(\text{CO})_4]$

Clusters incorporating main group elements are favourable building blocks in ‘step by-step assembling strategies’ which are used to create larger heteronuclear cluster aggregates from fragments of lower nuclearity.^{50, 51} For instance, the controlled expansion of a cluster core by the addition of electrophilic species to the anionic cluster complexes is much more readily achieved for compounds with bridged main group elements because of their increased stability in comparison with clusters without such elements.⁵² The reactions of the tetrahedral clusters $[\text{Fe}_3(\mu_3\text{-Y})(\text{CO})_9]^{2-}$ ($\text{Y} = \text{S}, \text{Se}, \text{Te}$) with appropriate electrophilic reagents appears to be a useful synthetic method for the preparation of chalcogenide heteronuclear derivatives containing various combinations of the main group elements and/or transition metals.⁵³

It has been found that the reactions of $\text{K}_2[\text{Fe}_3\text{Y}(\text{CO})_9]$ ($\text{Y} = \text{Se}, \text{Te}$) with $[(\text{dppm})\text{PtCl}_2]$ led to the formation new heteronuclear clusters via addition of the electrophilic $[(\text{dppm})\text{Pt}]^{2+}$ moiety to the Fe_2Y face of the $[\text{Fe}_3\text{Y}]$ core. The resulting $[\text{Fe}_3\text{Pt}(\mu_4\text{-Y})(\text{CO})_9(\text{dppm})]$ clusters were isolated in two isomeric forms, which differ in the coordination mode of the dppm ligand: chelating (Figure 3.5) and bridging (Figure 3.6).⁵⁴ The ^{31}P NMR spectrum of the cluster compound where dppm is coordinated in chelating mode contains only one singlet signal at -14 ppm for two equivalent phosphorus atoms bound to Pt, while that of its isomer contains two doublets, caused by the coupling of two non-equivalent phosphorus atoms with each other.

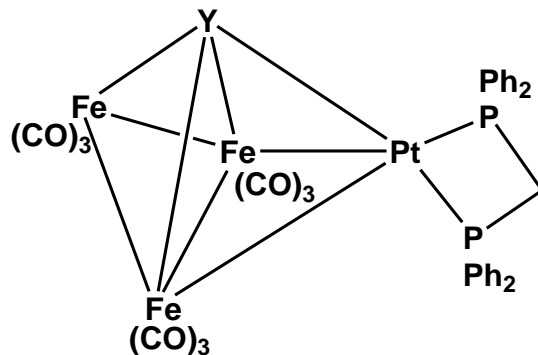


Figure 3.5 $[\text{Fe}_3\text{Pt}(\mu_4\text{-Y})(\text{CO})_9(\text{dppm})]$, (Y = Se, Te)

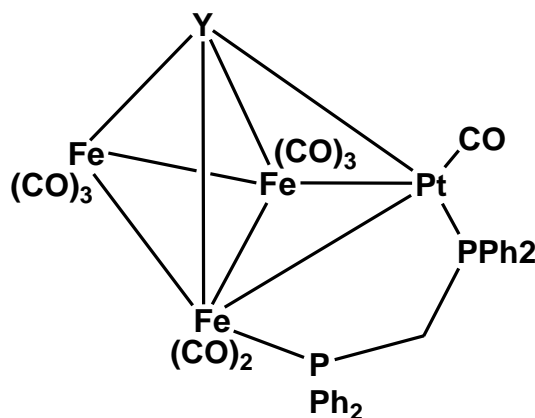


Figure 3.6 $[\text{Fe}_3\text{Pt}(\mu_4\text{-Se})(\text{CO})_9(\text{dppm})]$, (Y = Se, Te)

Ni et al. reported the synthesis of a heteronuclear cluster, $[\text{Pd}_2\{\mu\text{-Pt}(\text{PPh}_3)_2\}\text{Cl}_2(\text{dmpm})_2]$ by the insertion of a $\text{Pt}(\text{PPh}_3)_2$ fragment into Pd-Pd single bond of $\text{Pd}_2\text{Cl}_2(\text{dmpm})$, (dmpm = bis-(dimethylphosphino methane) (Figure 3.7). The ^{31}P NMR spectrum of $[\text{Pd}_2(\mu\text{-Pt}(\text{PPh}_3)_2)\text{Cl}_2(\text{dmpm})_2]$ shows a signal at -34.7 ppm assigned to two PPh_3 ligand coordinated to bridgehead platinum atom. The other signal at -25.2 ppm is assigned to the four dmpm phosphorus nuclei.⁵⁵

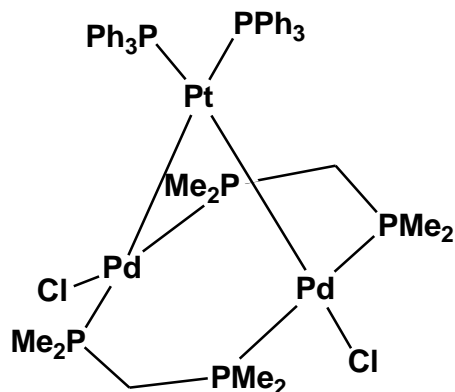
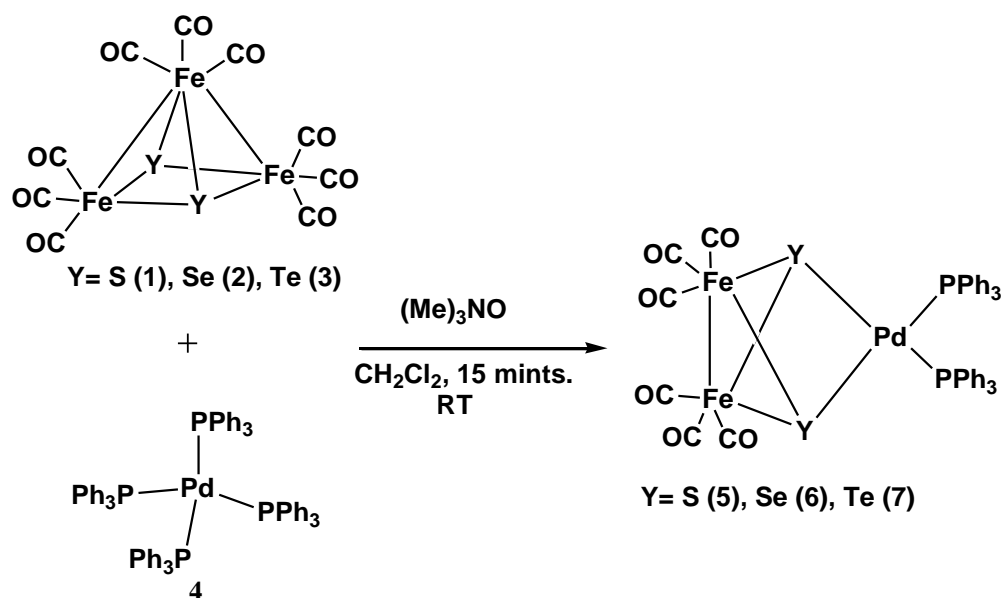


Figure 3.7 $[\text{Pd}_2(\mu\text{-Pt}(\text{PPh}_3)_2)\text{Cl}_2(\text{dmpm})_2]$

In this chapter, we have described the reactivity study with two different types of diphosphines, anticipating the formation of clusters with interesting bonding and structural characteristics. We have reported the synthesis of four new iron-palladium mixed metal clusters containing diphosphine ligand in different bonding modes.

3.2. RESULTS AND DISCUSSION

Iron –palladium mixed metal clusters, $[(\text{CO})_6\text{Fe}_2\text{PdY}_2(\text{PPh}_3)_2]$ (Y= S, Se, Te) (**5-7**), have been synthesized in minutes when a dichloromethane solution of $[\text{Fe}_3\text{Y}_2(\text{CO})_9]$ (Y = S, Se, Te) (**1-3**), was reacted with $[\text{Pd}(\text{PPh}_3)_4]$ (**4**) at room temperature in presence of trimethylamine-N-oxide, dihydrate (Scheme 3.1). Synthetic methods for the preparation of compounds **5-7** were reported previously by the reaction of $[\text{Fe}_3\text{Y}_2(\text{CO})_9]$ (Y= S, Se, Te) with $\text{Pd}(\text{PPh}_3)_4$ and reaction of $[\text{Fe}_2\text{Y}_2(\text{CO})_6]$ (Y= S, Se, Te) with $[\text{Pd}(\text{C}_2\text{H}_4)\text{PPh}_3)_2]$.^{56, 57} Use of trimethylamine-N-oxide results in rapid reaction and better yields for some of the products. This may be due to decarbonylation of one CO by TMNO and subsequent breaking of Fe-Y and Fe-Fe bonds leading to the formation of $[\text{YFe}_2\text{Y}]$ intermediate, which being an unstable species reacts with $\text{Pd}(\text{PPh}_3)_4$ to form compounds **5-7**. All the compounds (**5-7**) have been characterized by FTIR and ^1H and ^{31}P NMR spectroscopy and on the basis of comparison with the compounds reported earlier.^{56, 57} Structural characterization of compound **6** has been achieved from a needle shaped single crystal grown at low temperature in hexane –dichloromethane solvent mixture.



Scheme 3.1

The structure shows the presence of Fe_2Se_2 unit linked to $\text{Pd}(\text{PPh}_3)_2$ via two Se atoms. The Fe-Fe bond distance has been found to be 2.501(4) Å and the Pd-P bond distances are 2.316(3) and 2.330(2) Å. Six terminal carbonyl groups are attached to iron atoms as shown in the Figure 3.8. A sulphur bridged compound $[(\text{CO})_6\text{Fe}_2\text{S}_2\text{Pd}(\text{bipy})]$ has been reported which also contains a $\text{Fe}_2\text{S}_2\text{Pd}$ fragment, analogous to compound **5**.⁵⁸

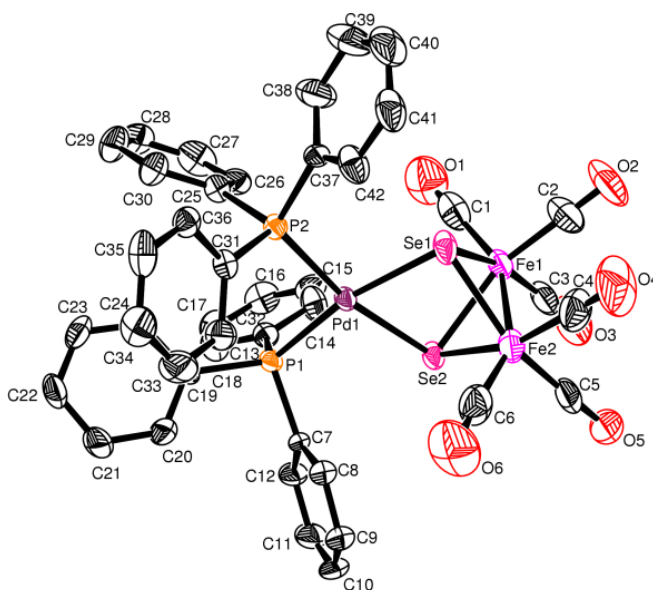
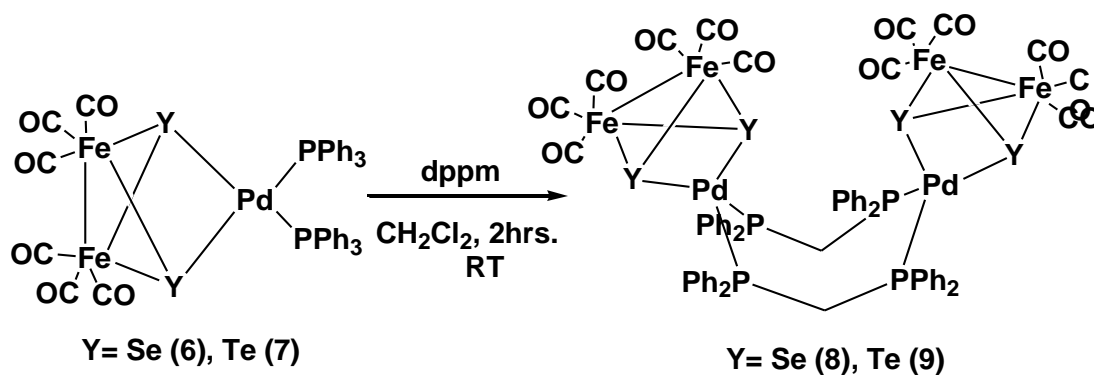


Figure 3.8 Molecular structure of $[(\text{CO})_6\text{Fe}_2\text{Se}_2\text{Pd}(\text{PPh}_3)_2]$ (**6**)

Table 3.1: Selected bond lengths (Å) and angles (deg) for **6**

Compound 6			
Pd(1)-P(2)	2.316(3)	Pd(1)-P(1)	2.330(2)
Pd(1)-Se(1)	2.4085(12)	Pd(1)-Se(2)	2.444(2)
Fe(2)-Se(2)	2.3730(18)	Se(2)-Fe(1)	2.362(2)
Fe(2)-Se(1)	2.380(3)	Fe(2)-Fe(1)	2.501(4)
Se(1)-Fe(1)	2.376(3)	Fe(1)-C(1)	1.798(17)
O(1)-C(1)	1.106(16)	P(1)-C(7)	1.806(9)
P(1)-Pd(1)-Se(1)	165.86(6)	P(2)-Pd(1)-Se(2)	168.05(6)
P(2)-Pd(1)-P(1)	100.88(8)	Se(1)-Pd(1)-Se(2)	75.10(5)
Se(2)-Fe(2)-Se(1)	76.96(6)	Fe(1)-Se(1)-Pd(1)	94.27(7)
Fe(1)-Se(1)-Fe(2)	63.46(9)	P(2)-Pd(1)-Se(1)	93.21(7)
Se(2)-Fe(2)-Fe(1)	57.91(6)	Se(1)-Fe(2)-Fe(1)	58.18(9)

Equimolar amounts of $[(\text{CO})_6\text{Fe}_2\text{Y}_2\text{Pd}(\text{PPh}_3)_2]$ (Y= Se(**6**), Te(**7**)) and Bis-(diphenylphosphino)methane (dppm), when stirred in dichloromethane solvent at room temperature for 2 hrs. under argon atmosphere, give rise to new mixed metal clusters, $[(\text{CO})_{12}\text{Fe}_4\text{Y}_4\text{Pd}_2(\mu\text{-dppm})_2]$ (Y=Se (**8**); Y=Te (**9**)), as shown in Scheme 3.2.



Scheme 3.2

The products were isolated after completion of the reaction and characterized by FTIR, ¹H, ³¹P and ¹³C NMR. The infrared spectra for **8** and **9** show peaks due to terminally bonded

metal carbonyl groups. ^1H NMR spectra for both the compounds reveal the presence of phenyl protons in the region δ 7.2 – 7.7 and a doublet at δ 3.93 for **8** and a doublet at δ 4.085 for **9** due to the presence of $-\text{CH}_2$ groups. $^{31}\text{P}\{^1\text{H}\}$ NMR shows a peak at δ 25.11 for compound **8** and δ 29.31 for **9** confirming that all the phosphorus atoms in each of the compounds are equivalent. After the completion of the reaction triphenylphosphine ligand has been detected in the reaction mixture by $^{31}\text{P}\{^1\text{H}\}$ NMR spectrum (δ -5.2). Single crystal X-ray structural characterization was carried out for compound **9**, which shows the presence of two $\text{Fe}_2\text{Te}_2\text{Pd}$ units linked together by two bridged dppm ligands (Figure 3.9). The Fe-Fe bonds are at the distance of 2.5915(13) Å and the Pd-Te distances are 2.6054(6) Å and 2.6154(6) Å. Twelve terminal carbonyl groups are attached to four iron atoms. The two dppm ligands form bridges in between two palladium centers and show the presence of an eight membered $\text{Pd}_2\text{P}_4\text{C}_2$ –ring forming a basket like conformation. The Pd-P bond lengths are 2.3401(15) Å and 2.3540(15) Å. Compounds **8** and **9** are formed possibly by the replacement of two PPh_3 groups with two dppm ligands and then attaching another fragment, $[(\text{CO})_6\text{Fe}_2\text{Y}_2\text{Pd}]$ of the reactant molecule.

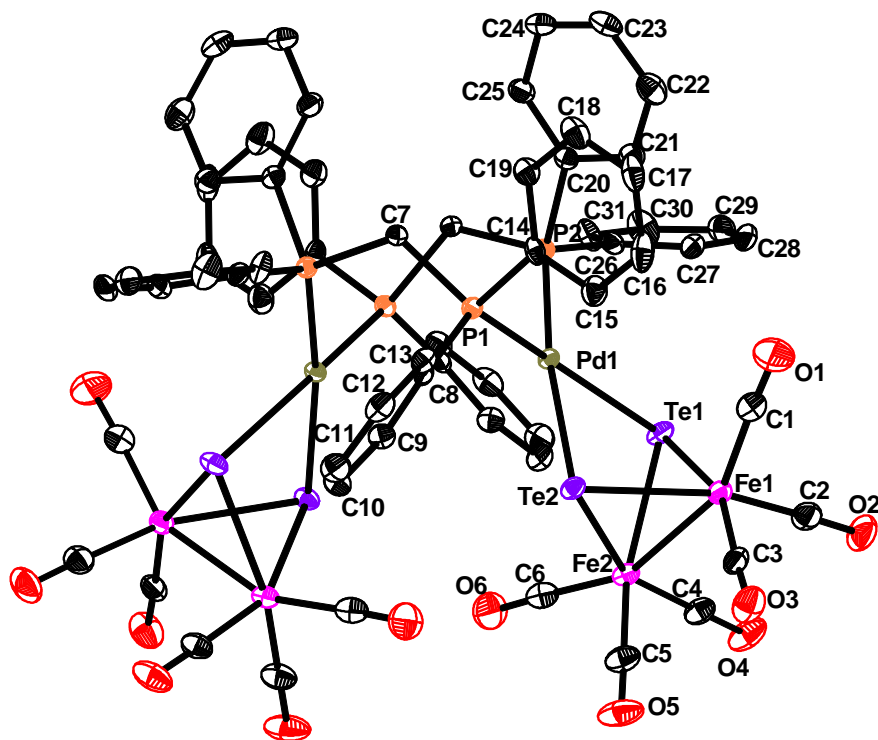
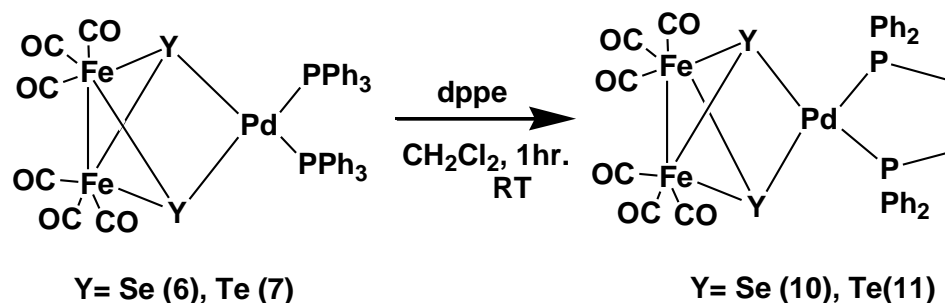


Figure 3.9 Molecular structure of $[(\text{CO})_{12}\text{Fe}_4\text{Te}_4\text{Pd}_2(\text{dppm})_2]$ (**9**)

Table 3.2: Selected bond lengths (Å) and angles (deg) for **9**

Compound 9			
Pd(1)-P(1)	2.3401(15)	Pd(1)-Te(2)	2.6054(6)
Pd(1)-P(2)	2.3540(15)	Pd(1)-Te(1)	2.6154(6)
Fe(1)-Te(2)	2.5668(9)	Fe(1)-Te(1)	2.5669(10)
Fe(1)-Fe(2)	2.5915(13)	Fe(2)-Te(2)	2.5515(9)
Fe(1)-C(3)	1.773(7)	Te(1)-Te(2)	3.0991(5)
Fe(2)-Te(1)	2.5769(10)	P(1)-C(7)	1.848(6)
O(1)-C(1)	1.142(10)	Fe(2)-C(6)	1.791(8)
P(1)-Pd(1)-P(2)	97.45(5)	P(1)-Pd(1)-Te(2)	92.23(4)
P(2)-Pd(1)-Te(2)	170.07(4)	Fe(2)-Te(2)-Fe(1)	60.84(3)
Fe(1)-Te(1)-Pd(1)	95.47(3)	P(1)-Pd(1)-Te(1)	160.91(4)
P(2)-Pd(1)-Te(1)	97.24(4)	Te(2)-Pd(1)-Te(1)	72.829(16)
Te(2)-Fe(1)-Te(1)	74.27(3)	Te(2)-Fe(1)-Fe(2)	59.29(3)
Te(1)-Fe(1)-Fe(2)	59.94(3)	Fe(1)-Te(1)-Fe(2)	60.51(3)
Te(2)-Fe(2)-Fe(1)	59.87(3)	Fe(2)-Te(1)-Pd(1)	99.51(3)
Pd(1)-Te(1)-Te(2)	53.437(14)	Fe(1)-Te(1)-Te(2)	52.86(2)

Diphosphine coordinated heterometallic iron palladium clusters, $[(\text{CO})_6\text{Fe}_2(\mu_3\text{-Y})_2\text{Pd}\{\text{PPh}_2(\text{CH}_2)_2\text{PPh}_2\}]$ (Y=Se (**10**); Y=Te (**11**)) have been obtained when an equimolar amounts of $[(\text{CO})_6\text{Fe}_2(\mu_3\text{-Y})_2\text{Pd}(\text{PPh}_3)_2]$ (Y= Se(**6**), Te(**7**)) and bis-(diphenylphosphino)ethane (dppe) was stirred in dichloromethane solvent at room temperature for 1 hr. under argon atmosphere (Scheme 3.3). The products were isolated after completion of the reaction and characterized by FTIR, ^1H , ^{31}P and ^{13}C NMR spectroscopy. The infrared spectra for **10** and **11** show peaks due to terminally bonded metal carbonyl groups. ^1H NMR spectra for both the compounds reveal the presence of phenyl protons with a multiplet in the region δ 7.36 – 7.70 and a doublet in the region δ 2.26 for **10** and δ 2.3 for **11** due to the presence of $-\text{CH}_2$ groups. $^{31}\text{P}\{^1\text{H}\}$ NMR shows a singlet peak at δ 48.26 for compound **10** and δ 48.33 for **11** confirming that all the phosphorus atoms in each of the compounds are equivalent.



Scheme 3.3

Single crystal X-ray structural characterization was carried out for compound **10**, which shows the presence of one $\text{Fe}_2\text{Se}_2\text{Pd}$ core and a dppe ligand is chelated to the palladium via two phosphorus atoms. It also consists of one Fe-Fe bond and six terminal metal carbonyl groups attached to the iron atoms (Figure 3.10). In comparison to the dppm bridged iron-palladium cluster, $[(\text{CO})_{12}\text{Fe}_4\text{Te}_4\text{Pd}_2(\text{dppm})_2]$ (**9**) where the diphosphines (dppm) form a bridge between two $\text{Fe}_2\text{Te}_2\text{Pd}$ fragments, the structure of compound **10** is unexpected and contains a diphosphine ligand chelated to Pd atom of the cluster fragment. In compound **10** the bond angle P(2)-Pd(1)-P(1) is $84.61(11)^\circ$ as compared to $100.88(8)^\circ$ in $[(\text{CO})_6\text{Fe}_2\text{Se}_2\text{Pd}(\text{PPh}_3)_2]$. The variation in the bond angle is probably due to the strain developed by the chelation of dppe ligand around the palladium atom. The downfield peak in ^{31}P NMR of **10** (δ 48.26) and **11** (δ 48.33) as compared to that in cluster, $[(\text{CO})_6\text{Fe}_2\text{Se}_2\text{Pd}(\text{PPh}_3)_2]$ (δ 29.26) is also related to the chelating mode of coordination of the dppe ligand around the palladium atom in clusters **10** and **11**.

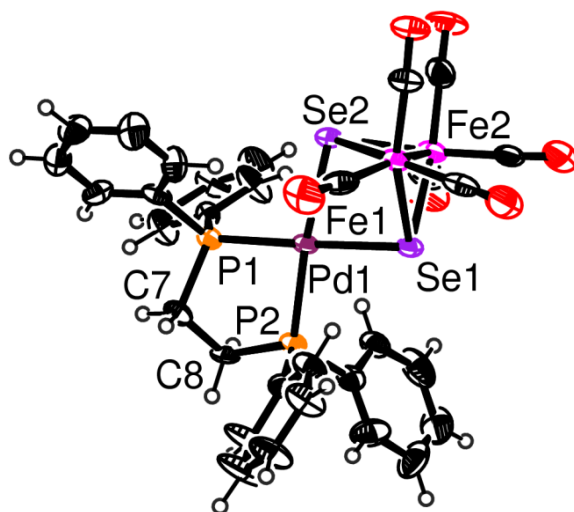


Figure 3.10 Molecular structure of $[(\text{CO})_6\text{Fe}_2(\mu_3\text{-Se})_2\text{Pd}\{\text{PPh}_2(\text{CH}_2)_2\text{PPh}_2\}]$ (**10**).

Table 3.3: Selected bond lengths (Å) and angles (deg) for **10**

Compound 10			
Pd(1)-P(2)	2.273(3)	Fe(1)-Fe(2)	2.532(2)
Pd(1)-Se(1)	2.4354(15)	C(7)-C(8)	1.541(16)
Pd(1)-Se(2)	2.4428(13)	Se(2)-Fe(1)	2.399(2)
Pd(1)-P(1)	2.287(3)	Se(2)-Fe(2)	2.401(2)
Se(1)-Fe(1)	2.4010(19)	Se(1)-Fe(2)	2.4004(19)
Fe(1)-C(3)	1.775(12)	O(1)-C(1)	1.131(15)
P(1)-Pd(1)-Se(2)	100.38(8)	Fe(1)-Se(2)-Fe(2)	63.68(6)
P(2)-Pd(1)-P(1)	84.61(11)	Fe(2)-Se(1)-Fe(1)	63.65(6)
P(2)-Pd(1)-Se(1)	97.02(9)	Fe(2)-Se(1)-Pd(1)	93.91(6)
Se(1)-Pd(1)-Se(2)	77.92(5)	Fe(1)-Se(2)-Pd(1)	89.81(6)
P(1)-Pd(1)-Se(1)	177.79(9)	P(2)-Pd(1)-Se(2)	174.25(9)
Fe(1)-Se(1)-Pd(1)	89.93(6)	Fe(2)-Se(2)-Pd(1)	93.71(6)

Iron – palladium cluster compounds **8**, **9**, **10** and **11** have been formed possibly by the substitution of the two PPh₃ groups by the phosphorus atoms of the respective diphosphine ligands resulting in chelating type of coordination around the palladium metal centre. The downfield character of the ³¹P NMR peaks for compounds **10** and **11** as compared to that in compounds **8** and **9** is perhaps due to the strain developed by the chelation of dppe around the palladium atom. Thus, the two diphosphine ligands, dppe and dppm, gave two different type of diphosphine coordinated products : one chelating (**10**, **11**) and other bridging (**8**, **9**), on reaction of [(CO)₆Fe₂Y₂Pd(PPh₃)₂] with the respective diphosphines. The contrasting results show the difference in reactivity between the cluster species and the influence of phosphines in controlling the cluster synthesis.

3.3. EXPERIMENTAL SECTIONS

3.3.1. General Procedures

All reactions and manipulations were carried out under an inert atmosphere of dry, pre-purified argon or nitrogen using standard schlenk line techniques. Solvents were purified, dried

and distilled under an argon atmosphere prior to use. Infrared spectra were recorded on a Perkin Elmer Spectrum RX-I spectrometer as dichloromethane solutions in 0.1 mm path lengths NaCl cell and NMR spectra on a 400 MHz Bruker spectrometer in CDCl₃. Elemental analyses were performed on a Vario El Cube analyser. TLC plates (20x20 cm, Silica gel 60 F254) were purchased from Merck. [Pd(PPh₃)₄] and TMNO.2H₂O was purchased from Sigma Aldrich. [Fe₃Y₂(CO)₉] (Y = S, Se, Te), [Fe₃Te₂(CO)₈(PPh₃)] were prepared following reported procedures.^{59,60}

3.3.2. Reaction of [Fe₃Y₂(CO)₉] (Y = S, Se, Te) with Pd(PPh₃)₄ in presence of TMNO.2H₂O

A dichloromethane solution (20 ml) of [Fe₃Y₂(CO)₉] (Y = S (49 mg, 0.1 mmol), Se (58 mg, 0.1 mmol), Te (68 mg, 0.1 mmol)) and [Pd(PPh₃)₄] (115 mg, 0.1 mmol) was added to a round bottomed flask under inter atmosphere. TMNO.2H₂O (17 mg, 0.15 mmol) in dichloromethane solvent was added at a time in the reaction mixture. The solution was stirred at room temperature for 15 mints under inter atmosphere until all the reactants disappears as monitored by TLC. The reaction mixture was filtered and dried in vacuum. The residue was subjected to chromatographic work-up using preparative TLC with dichloromethane / hexane (40:60 v/v) solvent mixture. The following compounds were separated in the order of elution: [Fe₂Y₂(CO)₆] {Yields = 12% (Y =S), 10% (Y = Se), 8% (Y = Te)}, [Fe₃Y₂(CO)₈(PPh₃)] {Yields = 9% (Y =S), 8% (Y = Se), 9% (Y = Te)}, trace amount of [Fe₃Y₂(CO)₇(PPh₃)₂] and [(CO)₆Fe₂PdY₂(PPh₃)₂] (Y =S (**5**), 65 mg, 67% ; Y =Se (**6**), 75 mg, 70%; Y = Te (**7**), 84 mg, 72 %). Trace amount of decomposition was also observed during the workup.

5: Anal. calcd. (found): C, 51.75 (52.26); H, 3.08 (3.17). IR(ν_{CO} , cm⁻¹, CH₂Cl₂): 2050(s), 2009 (vs), 1974 (s), 1960 (s). ¹H NMR(δ , CDCl₃): 7.2-7.65 (m, C₆H₅). ³¹P{¹H} NMR(δ): 23.8 (s).

6: Anal. calcd. (found): C, 47.11 (47.52); H, 2.80 (2.66). IR(ν_{CO} , cm⁻¹, CH₂Cl₂): 2037(s), 1995.5(s), 1961(s), 1950(s). ¹H NMR(δ , CDCl₃): 7.2-7.7 (m, C₆H₅). ³¹P{¹H} NMR(δ): 29.16 (s).

7: Anal. calcd. (found): C, 43.24 (42.87); H, 2.57 (2.69). IR(ν_{CO} , cm⁻¹, CH₂Cl₂): 2033(s), 1993(s), 1957(s), 1948(s). ¹H NMR(δ , CDCl₃): 7.23-7.7 (m, C₆H₅). ³¹P{¹H} NMR(δ): 26.5 (s).

3.3.3. Reaction of $[\text{Fe}_2\text{Y}_2\text{Pd}(\text{CO})_6(\text{PPh}_3)_2](\text{Y}=\text{Se}, \text{Te})$ with Bis-(diphenylphosphino)methane

A dichloromethane solution (30ml) of $[\text{Fe}_2\text{Y}_2\text{Pd}(\text{CO})_6(\text{PPh}_3)_2]$ (Y =Se, 107 mg, 0.1 mmol; Te, 117 mg, 0.1 mmol) was taken in a two necked round bottomed flask and Bis-(diphenylphosphino)methane (39 mg, 0.1 mmol) was added under stirring condition and in argon atmosphere. The reaction was carried out for 2 hrs at room temperature with continuous stirring in argon atmosphere. After the completion of the reaction the solution was vacuum dried and the residue was subjected to chromatographic work-up using preparative TLC with dichloromethane / hexane (40:60 v/v) solvent mixture. The compounds obtained on subsequent elution are trace amount of unreacted $[\text{Fe}_2\text{Y}_2\text{Pd}(\text{CO})_6(\text{PPh}_3)_2]$ followed by the product $[\text{Fe}_4\text{Y}_4\text{Pd}_2(\text{CO})_{12}(\text{dppm})_2]$, (Y =Se (**8**), 162 mg, 79 %; Y = Te (**9**), 156 mg, 75%).

8: Anal. calcd. (found): C, 40.01 (39.62); H, 2.38 (2.26). IR(ν_{CO} , cm^{-1} , CH_2Cl_2): 2038 (s), 1992.3(s), 1958 (s, br). ^1H NMR (δ , CDCl_3): 3.93 (d, 4H, CH_2 , $^2\text{J}_{\text{P-H}} = 7$ Hz), 7.2-7.65 (m, 40H, C_6H_5). $^{31}\text{P}\{^1\text{H}\}$ NMR(δ): 25.11 (s). ^{13}C NMR(δ , CDCl_3) = 29.65 (s, CH_2), 128.2-133.6 (m, C_6H_5).

9: IR(ν_{CO} , cm^{-1} , CH_2Cl_2): 2033 (s), 1990.3 (s), 1953 (s, br). ^1H NMR(δ , CDCl_3): 4.085 (d, 4H, CH_2 , $^2\text{J}_{\text{P-H}} = 7$ Hz), 7.2-7.65 (m, 40H, C_6H_5). $^{31}\text{P}\{^1\text{H}\}$ NMR(δ): 29.31 (s). ^{13}C NMR (δ , CDCl_3) = 29.69 (s, CH_2), 128.26-134.5 (m, C_6H_5), 212 (CO).

3.3.4. Reaction of $[(\text{CO})_6\text{Fe}_2(\mu_3\text{-Y})_2\text{Pd}(\text{PPh}_3)_2](\text{Y}=\text{Se}, \text{Te})$ with Bis-(diphenylphosphino)ethane

A dichloromethane solution (15ml) of $[(\text{CO})_6\text{Fe}_2(\mu_3\text{-Y})_2\text{Pd}(\text{PPh}_3)_2]$ (Y =Se, 107 mg, 0.1 mmol; Te, 117 mg, 0.1 mmol) was taken in a two necked round bottomed flask and Bis-(diphenylphosphino)ethane (40 mg, 0.1 mmol) was added. The reaction was carried out for 1 hr. at room temperature with continuous stirring under argon atmosphere. After the completion of the reaction the solution was vacuum dried and the residue was dissolved in dichloromethane solvent. Chromatographic work-up using preparative TLC with dichloromethane / hexane (40:60 v/v) solvent mixture gave trace amount of unreacted $[(\text{CO})_6\text{Fe}_2(\mu_3\text{-Y})_2\text{Pd}(\text{PPh}_3)_2]$

followed by $[(\text{CO})_6\text{Fe}_2(\mu_3\text{-Y})_2\text{Pd}\{\text{PPh}_2(\text{CH}_2)_2\text{PPh}_2\}]$, (Y = Se (**10**), 80 mg, 85 %; Y = Te (**11**), 84 mg, 81%).

10: Anal. calcd. (found): C, 40.76 (40.94); H, 2.55 (2.66). IR(ν_{CO} , cm^{-1} , CH_2Cl_2): 2039.8(vs), 1998.8(vs), 1958.5(vs, br). ^1H NMR (δ , CDCl_3): 2.26 (d, 4H, CH_2 , $J = 19$ Hz), 7.44-7.70 (m, 40H, C_6H_5). $^{31}\text{P}\{^1\text{H}\}$ NMR(δ): 48.26 (s). ^{13}C NMR(δ , CDCl_3) = 27.4 (s, CH_2), 128.5-133.3 (m, C_6H_5), 211.5 (s, CO).

11: Anal. calcd. (found): C, 36.95 (36.71); H, 2.31 (2.25). IR(ν_{CO} , cm^{-1} , CH_2Cl_2): 2031.3(vs), 1989.2(vs), 1952.2(vs, br). ^1H NMR(δ , CDCl_3): 2.3 (d, 4H, CH_2 , $J = 18.8$ Hz), 7.36-7.67 (m, 40H, C_6H_5). $^{31}\text{P}\{^1\text{H}\}$ NMR(δ): 48.33 (s). ^{13}C NMR (δ , CDCl_3) = 28.6 (s, CH_2), 128.9-134.3 (m, C_6H_5), 212.3 (CO).

3.3.5. Crystal structure determination for **6**, **9** and **10**

Single crystal X-ray structural studies of **6**, **9** and **10** were performed on a CCD Oxford Diffraction XCALIBUR-S diffractometer equipped with an Oxford Instruments low-temperature attachment. Data were collected at 150(2) K using graphite-monochromated Mo $K\alpha$ radiation ($\lambda_\alpha = 0.71073$ Å). The strategy for the Data collection was evaluated by using the CrysAlisPro CCD software. The data were collected by the standard 'phi-omega scan techniques, and were scaled and reduced using CrysAlisPro RED software. The structures were solved by direct methods using SHELXS-97 and refined by full matrix least-squares with SHELXL-97, refining on F^2 .⁶¹ The positions of all the atoms were obtained by direct methods. All non-hydrogen atoms were refined anisotropically. The remaining hydrogen atoms were placed in geometrically constrained positions and refined with isotropic temperature factors, generally $1.2U_{eq}$ of their parent atoms. The crystallographic details are summarized in Table 3.4.

3.4. CONCLUSIONS

Synthesis and characterization of four new iron-palladium mixed metal clusters containing diphosphine ligand in different bonding modes have been carried out. The mixed metal clusters, $[(\text{CO})_{12}\text{Fe}_4\text{Y}_4\text{Pd}_2(\text{dppm})_2]$ ($\text{Y} = \text{Se}$ (**8**), Te (**9**)), obtained by the reaction of $[(\text{CO})_6\text{Fe}_2\text{PdY}_2(\text{PPh}_3)_2]$ ($\text{Y} = \text{Se}$ (**6**), Te (**7**)) with bis(diphenylphosphino)methane, contain two diphosphine units forming a bridge between two cluster framework, while the clusters $[(\text{CO})_6\text{Fe}_2(\mu_3\text{-Y})_2\text{Pd}\{\text{PPh}_2(\text{CH}_2)_2\text{PPh}_2\}]$ ($\text{Y}=\text{Se}$ (**10**); $\text{Y}=\text{Te}$ (**11**)) having a chelating type of diphosphine coordination, have been obtained using bis(diphenylphosphino)ethane ligand. The contrasting results show the difference in reactivity between the cluster species and the influence of phosphines in controlling the cluster synthesis.

Table 3.4: Crystal data and structure refinement parameters for compounds **6**, **9** and **10**.

	6 .CH ₂ Cl ₂	9	10
Empirical formula	C ₄₃ H ₃₂ Cl ₂ Fe ₂ O ₆ P ₂ PdSe ₂	C ₆₂ H ₄₄ Fe ₄ O ₁₂ P ₄ Pd ₂ Te ₄	C ₆₄ H ₄₈ Fe ₄ O ₁₂ P ₄ Pd ₂ Se ₄
Formula weight	1153.55	2051.45	1883.94
Crystal system	Monoclinic,	Monoclinic	Monoclinic
Space group	<i>P</i> 2 ₁ / <i>c</i>	<i>C</i> 2/ <i>c</i>	<i>P</i> 2 ₁ / <i>n</i>
<i>a</i> , Å	9.380(11)	21.5570(7)	23.8469(10)
<i>b</i> , Å	24.036(4)	15.247	12.7529(3)
<i>c</i> , Å	19.271(14)	24.8968(2)	24.3883(12)
α deg	90	90.011(4)	90
β deg	92.68(9)	116.7350(10)	107.770(5)
γ deg	90	89.96	90
<i>V</i> , Å ³	4340(6)	7308.3(2)	7063.0(5)
<i>Z</i>	4	8	4
<i>D</i> _{calc} , Mg m ⁻³	1.765	2.081	1.772
abs coeff, mm ⁻¹	2.990	3.184	3.506
<i>F</i> (000)	2272	4368	3676
Cryst size, mm	0.33 x 0.26 x 0.21	0.34 x 0.28 x 0.23	0.33 x 0.26 x 0.21
θ range, deg	3.08 to 25.00	3.31 to 25.00	3.31 to 25.00
index ranges	-7<= <i>h</i> <=11, -28<= <i>k</i> <=28, - 22<= <i>l</i> <=22	-25<= <i>h</i> <=25, -18<= <i>k</i> <=18, - 29<= <i>l</i> <=27	-28<= <i>h</i> <=28, -15<= <i>k</i> <=15, - 29<= <i>l</i> <=29
reflections collected/ unique	31808 / 7628 [R(int) = 0.0939]	26563 / 6428 [R(int) = 0.0265]	52211 / 12402 [R(int) = 0.0707]
data/ restraints / parameters	7628 / 0 / 523	6428 / 0 / 433	12402 / 0 / 811
goodness-of-fit on <i>F</i> ²	1.019	1.058	1.091
Final <i>R</i> indices [<i>I</i> >2 σ (<i>I</i>)]	R1 = 0.0608, wR2 = 0.1335	R1 = 0.0420, wR2 = 0.1098	R1 = 0.0753, wR2 = 0.1817
<i>R</i> indices (all data)	R1 = 0.1244, wR2 = 0.1683	R1 = 0.0478, wR2 = 0.1125	R1 = 0.1124, wR2 = 0.1904
largest diff peak and hole, eÅ ⁻³	1.962 -1.332	2.824 -3.280	2.632 -1.016

3.5. REFERENCES

1. A. Siani, B. Captain, O. S. Alexseev, E. Stafyla, R. D. Adams, M. D. Amiridis, *Langmuir* 22 (2006) 5160.
2. C. Mihut, B. D. Chandler, M. D. Amiridis, *Catal. Commun.* 3 (2002) 91
3. (a) A. Choplin, L. Huang, A. Theolier, P. Gallezot, J. M. Basset, *J. Am. Chem. Soc.* 108 (1986) 4224; (b) J. M. Thomas, R. Raja, W. D. Lewis, *Angew. Chem., Int. Ed. Eng.* 44 (2005) 6456; (c) J. M. Thomas, B. F. G. Johnson, R. Raja, G. Sankar, P. A. Midgley, *Acc. Chem. Res.* 36 (2003) 20; (d) B. F. G. Johnson, *Top. Catal.* 24 (2003) 147.
4. P. Mathur, *Adv. Organomet. Chem.* 41 (1997) 243.
5. L. C. Roof, W. Kolis, *Chem. Rev.* 93 (1994) 1037.
6. P. Mathur, M. M. Hossain, A. L. Rheingold, *Organometallics* 13 (1994) 3909.
7. (a) P. Mathur, M. M. Hossain, S. B. Umbarkar, C.V.V. Satyanarayana, A. L. Rheingold, L. M. Liable-Sands, G. P. A. Yap, *Organometallics* 15 (1996) 1898; (b) J. Wachter, *Eur. J. Inorg. Chem.* (2004) 1367; (c) C. W. Pin, Y. Chi, C. Chung, A. J. Carty, S. M. Peng, G. H. Lee, *Organometallics* 17 (1998) 4148.
8. (a) A. J. Carty, G. D. Enright, G. Hogarth, *Chem. Commun.* (1997) 1883 ; (b) E. Delgado, Y. Chi, W. Wang, G. Hogarth, P.J. Low, G. D. Enright, S. M. Peng, G. H. Lee, A. J. Carty, *Organometallics* 17 (1998) 2936.
9. V. P. Fedin, *Russ. J. Coord. Chem.* 30 (2004) 151.
10. (a) S. Nagao, H. Seino, M. Hidai, Y. Mizobe, *J. Organomet. Chem.* 669 (2003) 124; (b) M. Shieh, *J. Cluster Sci.* 10 (1999) 3.
11. (a) B. F. G. Johnson, *Coord. Chem. Rev.* 192 (1999) 1269; (b) D. S. Shephard, T. Maschmeyer, B. F. G. Johnson, J. M. Thomas, G. Sankar, D. Ozkaya, W. Zhou, R. D. Oldroyd, R. G. Bell, *Angew. Chem., Int. Ed. Eng.* 36 (1997) 2242.
12. (a) M. S. Nashner, A. I. Frenkel, D. Somerville, C. W. Hills, J. R. Shapley, R. G. Nuzzo, *J. Am. Chem. Soc.* 120 (1998) 8093; (b) P. A. Midgley, M. Weyland, J. M. Thomas, B. F. G. Johnson, *Chem. Commun.* (2001) 907.
13. G. W. Drake, J. W. Kolis, *Coord. Chem. Rev.* 137 (1994) 131.
14. P. Mathur, S. Chatterjee, Y. V. Torubaev, *J. Cluster Sci.* 18 (2007) 505.
15. M. Di Vaira, P. Stoppioni, *Coord. Chem. Rev.* 120 (1992) 259.
16. (a) R. D. Adams, B. Captain, W. Fu, M. B. Hall, M. D. Smith, C. E. Webster, *Inorg. Chem.* 43 (2004) 3921; (b) R. D. Adams, B. Captain, W. C. Pearl Jr, *Inorg. Chem.* 45 (2006)

- 8283; (c) E. Brivio, A. Ceriotti, R. D. Pergola, L. Garlaschelli, F. Demartin, M. Manassero, M. Sansoni, P. Zanello, F. Laschi, B. T. Heaton, *J. Chem. Soc., Dalton Trans.* (1994) 3237.
17. (a) A. G. Sykes, V. P. Fedin, M. N. Sokolov, *Comprehensive Coordination Chemistry II*, Oxford: Elsevier, 4 (2003) 1037; (b) R. H. Holm, *Adv. Inorg. Chem.* 38 (1992) 1; (c) D. Coucouvanis, *Acc. Chem. Res.* 24 (1991) 1; (d) R. D. Adams, E. Boswell, *Organometallics* 27 (2008), 2021; (e) L. J. Farrugia, *Adv. Organomet. Chem.* 31 (1990) 301; (f) J. L. Xiao, R. J. Puddephatt, *Coord. Chem. Rev.* 143 (1995) 457.
18. (a) P. Mathur, S. Chatterjee, *Comm. Inorg. Chem.* 26 (2005) 255; (b) P. Mathur, S. Chatterjee, V.D. Avasare, *Adv. Organomet. Chem.* 55 (2008) 201.
19. (a) P. Mathur, S. M. Mukhopadhyay, M. O. Ahmed, G. K. Lahiri, S. Chakraborty, M. G. Walawalkar, *Organometallics* 19 (2000) 5787; (b) P. Mathur, M. O. Ahmed, A. K. Dash, J. H. Kaldis, *Organometallics* 19 (2000) 941.
20. (a) P. Mathur, M. O. Ahmed, J. H. Kaldis, M. J. McGlinchey, *J. Chem. Soc., Dalton Trans.* 2 (2002) 619; (b) P. Mathur, M. O. Ahmed, A. K. Dash, M. G. Walawalkar, V. G. Puranik, *J. Chem. Soc., Dalton Trans.* (2000) 2916.
21. W. Schuh, P. Braunstein, M. B. Nard, M. M. Rohmer, R. Welter, *Angew. Chem. Int. Ed. Eng.* 42 (2003) 2161.
22. P. Braunstein, C. Charles, G. Kickelbick, U. Schubert, *Chem. Commun.* (1997) 2093.
23. B. F. G. Johnson, T. M. Layer, J. Lewis, A. Martin, P. R. Raithby, *J. Organomet. Chem.* 429 (1992) C41.
24. Z. G. Fang, Y. S. Wen, R. K. L. Wong, S. C. Ng, L. K. Liu, T. S. A. Hor, *J. Clust. Sci.* 5 (1994) 327.
25. M. Brandl, H. Brunner, H. Cattey, Y. Mugnier, J. Wachter, M. Zabel, *J. Organomet. Chem.* 659 (2002) 22.
26. R. Bender, C. Okio, R. Welter, P. Braunstein, *J. Chem. Soc., Dalton Trans.* (2009) 4901.
27. S.G. Bott, K. Yang, M.G. Richmond, *J. Organomet. Chem.* 691 (2006) 3771.
28. C. Graiff, G. Predieri, A. Tiripicchio, *Eur. J. Inorg. Chem.* (2003) 1659.
29. L. Li, L. C. Song, M. M. Wang, Q. L. Li, H. B. Song, *Organometallic* 30 (2011) 4899.
30. B. F. G. Johnson, T. M. Layer, J. Lewis, A. Martin, P. R. Raithby, *J. Organomet. Chem.* 429 (1992) C41.
31. Z. G. Fang, Y. S. Wen, R. K. L. Wong, S. C. Ng, L. K. Liu, T. S. A. Hor, *J. Cluster Sci.* 5 (1994) 327.
32. P. Mathur, B. H. S. Thimmappa, A. L. Rheingold, *Inorg. Chem.* 29 (1990) 4658.
33. D. Cauzzi, C. Graiff, G. Predieri, C. Vignali, A. Tiripicchio, *J. Chem. Soc., Dalton*

- Trans. (1999) 237.
34. F. Fabrizi de Biani, C. Graiff, G. Opromolla, G. Predieri, A. Tiripicchio, P. Zanello, J. Organomet. Chem. 637-639 (2001) 586.
35. M. Brandl, H. Brunner, H. Cattey, Y. Mugnier, J. Wachter, M. Zabel, J. Organomet. Chem. 659 (2002) 22.
36. W. Schuh, P. Braunstein, M. B. Nard, M. M. Rohmer, R. Welter, Angew. Chem. Int. Ed. Engl. 42 (2003) 2161.
37. P. Braunstein, C. Charles, G. Kickelbick, U. Schubert, Chem. Commun. (1997) 2093.
38. B. F.G. Johnson, T. M. Layer, J. Lewis, A. Martin, P. R. Raithby, J. Organomet. Chem. 429 (1992) C41.
39. Z. G. Fang, Y. S. Wen, R. K. L. Wong, S. C. Ng, L. K. Liu, T. S. A. Hor, J. Clust. Sci. 5 (1994) 327.
40. M. Brandl, H. Brunner, H. Cattey, Y. Mugnier, J. Wachter, M. Zabel, J. Organomet. Chem. 659 (2002) 22.
41. R. Bender, C. Okio, R. Welter, P. Braunstein, J. Chem. Soc., Dalton Trans. (2009) 4901.
42. S.G. Bott, K. Yang, M.G. Richmond, J. Organomet. Chem. 691 (2006) 3771.
43. C. Graiff, G. Predieri, A. Tiripicchio, Eur. J. Inorg. Chem. (2003) 1659.
44. L. Li, L. C. Song, M. M. Wang, Q. L. Li, H. B. Song, Organometallic 30 (2011) 4899.
45. B. Chen, U. Dingerdissen, J. G. E. Krauter, H. G. J. Lansink Rotgerink, K Möbus, D. J. Ostgard, P. Panster, T. H. Riermeier, S. Seebald, T. Tacke, H. Trauthwein, Appl. Catal. 280 (2005) 17.
46. (a) R. Raja, T. Khimyak, J. M. Thomas, S. Hermans, B. F. G. Johnson, Angew. Chem. Int. Ed. 40 (2001) 4638; (b) J. M. Thomas, B. F. G. Johnson, R. Raja, G. Sankar, P. A Midgley, Acc. Chem. Res. 36 (2003) 20.
47. (a) P. Braunstein, J. Kervennal, J. L. Richert, Angew. Chem., Int. Ed. Engl. 24 (1985) 768.
48. R. D. Adams, E. M. Boswell, B. Captain, Organometallics 27 (2008) 1169.
49. P. Braunstein, C. M. Bellefon, M. Ries. Inorg. Chem. 27 (1988) 1338.
50. D. A. Roberts, G. L. Geoffroy, in G. Sir Wilkinson et al. (eds.), Comprehensive Organometallic Chemistry (Pergamon Press, New York, 1982), Vol. 6, pp 763.
51. D. Fenske, in G. Schmid (ed.), Clusters and Colloids: from Theory to Applications (VCH, WeinheimGermany, 1994), pp 212 .
52. K. H. Whitmire J. Coord. Chem. 17, (1988). 95.
53. M. Shieh, C. H. Ho, W. S. Sheu, H. W. Chen, J. Am. Chem. Soc. 132 (2010) 4032.

54. N. A. Pushkarevsky . S. N. Konchenko . M. Scheer, *J Clust Sci* 18 (2007) 606
55. J. Ni, C. P. Kubiak, *Inorganica Chimica Acta*, 127 (1987) L37
56. (a) V. W. Day, D. A. Lesch, T. B. Rauchfuss, *J. Am. Chem. Soc.* 104 (1982) 1290; (b) P. Mathur, I. J. Mavunkal, V. Rugmini, *J. Organomet. Chem.* 367 (1989) 243
57. P. Mathur, I. J. Mavunkal, *J. Organomet. Chem.* 350 (1988) 251.
58. R. D. Adams, M. Huang, W. Wu, *J. Cluster Sci.* 8 (1997) 115.
59. D. A. Lesch, T. B. Rauchfuss, *Organometallics* 1 (1982) 499.
60. (a) W. Hieber, J. Gruber, *Z. Anorg. Allg. Chem.* 296 (1958) 91; (b) D. A. Lesch, T. B. Rauchfuss, *Inorg. Chem.* 20 (1981) 3583;
- 61 G. M. Sheldrick, *Acta Cryst. A*64 (2008) 112.

CHAPTER 4

**SUNLIGHT DRIVEN SYNTHESIS OF METAL
DITHIOCARBOXYLATE-ALKYNE
COMPLEXES AND THEIR
SPECTROSCOPIC AND STRUCTURAL
CHARACTERIZATION**

4.1. INTRODUCTION

Transition metals coordinated to small organic species like alkyls, aryls, olefins, alkynes etc gives rise to rich chemistry due to their vast number of metal – ligand bonding modes and structural variety.¹⁻³ Such complexes are found to be versatile synthetic intermediates, which facilitate a number of interesting transformations and offer a fascinating perspective for the synthesis of novel organic compounds.⁴⁻⁶ The insertion or activation of molecules such as CO, CO₂, CS₂, COS, olefins, alkynes etc. into metal-hydride, metal-carbon, metal-nitrogen, metal-oxygen and metal-sulfur bonds of transition metal fragments and their subsequent functionalization have drawn much attention due to their potential sources of C₁ chemistry for the generation of useful organic compounds.^{7,8} This area of research, especially insertion of CO₂, has been receiving enormous interest due primarily to their potential for the generation of useful organic compounds from an abundant and inexpensive source of carbon. Being structurally similar to CO₂, the diverse chemistry of CS₂ including coordination, addition, cleavage, and insertion reactions is currently being intensively investigated. Moreover, the transition metal complexes bearing CS₂ may be regarded as model compounds for CO₂ activation and transformation.^{9,10}

Insertion reaction of an unsaturated molecule into M-C bond leads to new metal ligand complexes and can have unusual properties related to catalysis and organic transformation. Insertion reaction depends upon various factors like increase in the nucleophilicity of the external ligand and electrophilicity of the metal center considerably accelerates the reaction. Insertion of CO and olefins are very common as regard to the catalytic steps are concerned and lead to a variety of important compounds. Both CO and olefins insert into metal –alkyl bonds, while insertion of olefins into metal-hydride bonds has been found favorable but rarely in case of CO.

Carbon disulfide is an unsaturated electrophile with an extensive organic and organometallic chemistry.¹¹ Insertion reactions of CS₂ into transition metal-hydride and metal-carbon(sp³) bonds are well known,^{12,13} giving dithioformate and dithiocarboxylate complexes respectively. Varieties of other complexes are also obtained by insertion of CS₂ into transition metal-aryl bonds¹⁴ or metal-oxygen and metal-nitrogen bonds.¹⁵ A range of compounds involving CS₂ insertion into M-C bonds have been synthesized where CS₂ is linked to metal center in η^1 -, η^2 - and η^3 bonding modes.¹⁶⁻²⁴

Literature survey reveals that dithiocarboxylate groups constitute an important class of multidentate ligands known for their unique metal-ligand interaction,²⁵⁻³⁰ organic

transformation and catalysis.³¹⁻³⁵ This type of ligands contain multisite coordination environment and helps to bind metals easily. However, synthesis and reactivity of transition metal dithiocarboxylato complexes have been investigated to a far lesser extent than other dithio ligands like xanthates, thioxanthates and dithiocarbamates. Although, the synthesis and reactivity of a few number of transition metal dithiocarboxylato complexes have been investigated in the last decade,³⁶⁻⁴⁰ study on their derivatization and the possibility to introduce more metal bonding sites on such groups have largely been unexplored. In fact, a small number of article have been found for the synthesis of alkynyl dithiocarboxylate complexes of the type I involving only three transition metals, Mo, Fe and Ru with R as phenyl, tert-butyl or SiMe₃.⁴¹⁻⁴⁴

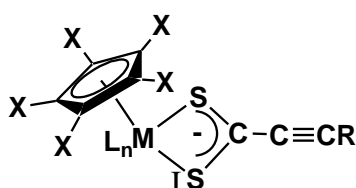


Figure 4.1

Selegue et. al. first reported the electrophilic attack of carbon disulfide on the iron alkynyl complex $[\text{Fe}(\eta^5\text{-C}_5\text{H}_5)(\text{C}\equiv\text{CMe})(\text{dppe})]$, which results in the formation of a complex containing a 2H-thiete-2-thione (Figure 4.2).⁴⁵

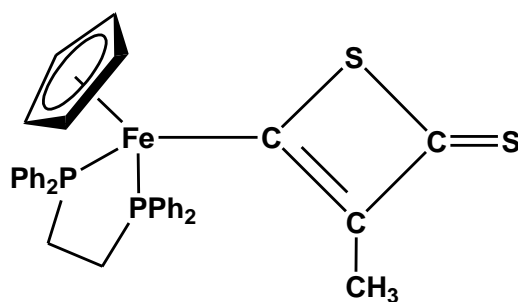
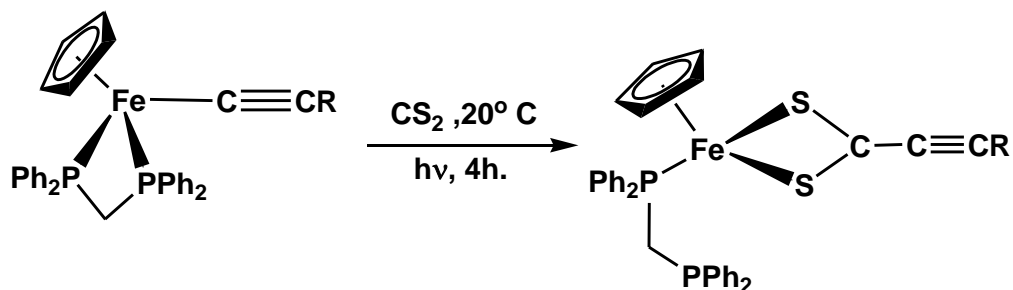


Figure 4.2

Irradiation of a CS₂ solution of $[\text{Fe}(\eta^5\text{-C}_5\text{H}_5)(\text{C}\equiv\text{CR})(\text{dppm})]$ with a UV lamp for 4 hrs. yields alkynyldithiocarboxylate iron(II) complexes, $[\text{Fe}(\eta^5\text{-C}_5\text{H}_5)(\text{S}_2\text{CC}\equiv\text{CR})(\text{dppm-P})]$ (R = Ph or ^tBu) containing a diphosphine ligand with one metal–phosphorus bond (Scheme 4.1).⁴² The ³¹P NMR spectrum shows two well-separated doublets for the phosphorus atoms. One of the doublets is located in the range typical for the coordinated dppm in iron

complexes while the other doublet appears close to that of free dppm and can be assigned to a non-coordinated phosphorus atom. This reaction shows that dithiocarboxylate has a greater tendency to act as a chelating ligand than the diphosphine (dppm) species.



Scheme 4.1

Recently, Mathur et al. reported reactions of molybdenum acetylide complexes with CS₂ under aerobic and anaerobic reaction conditions and in presence of UV radiation.⁴³ It has been described that photolysis of a solution containing [(L)Mo(CO)₃(C≡CPh)] (L= η⁵-C₅H₅, η⁵-C₅Me₅) and CS₂ led to the formation of dithiopropiolato containing complexes, [(L)Mo(CO)₂(η²-S₂CC≡CPh)] (L=η⁵-C₅H₅, η⁵-C₅Me₅). The molecular structure shows that a (S₂CC≡CPh) ligand is bonded to molybdenum atom in η²-bonding mode. The two Mo-S bond lengths are 2.4639(11) Å and 2.4610(12) Å.

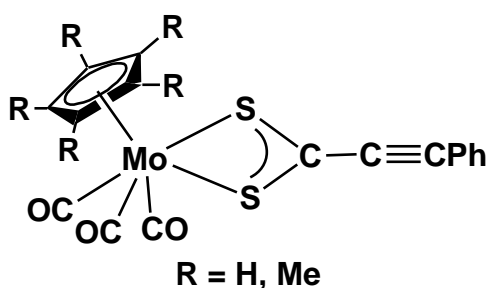
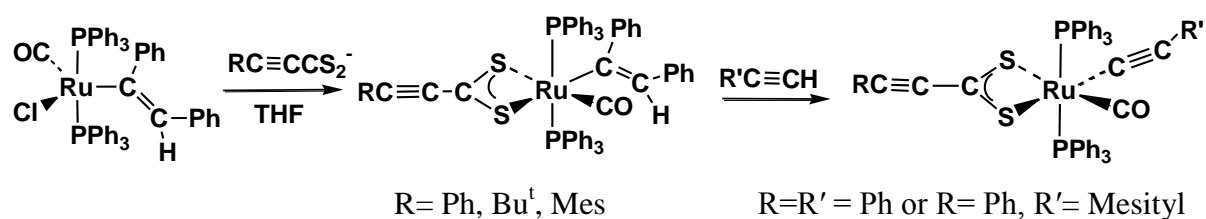


Figure 4.3

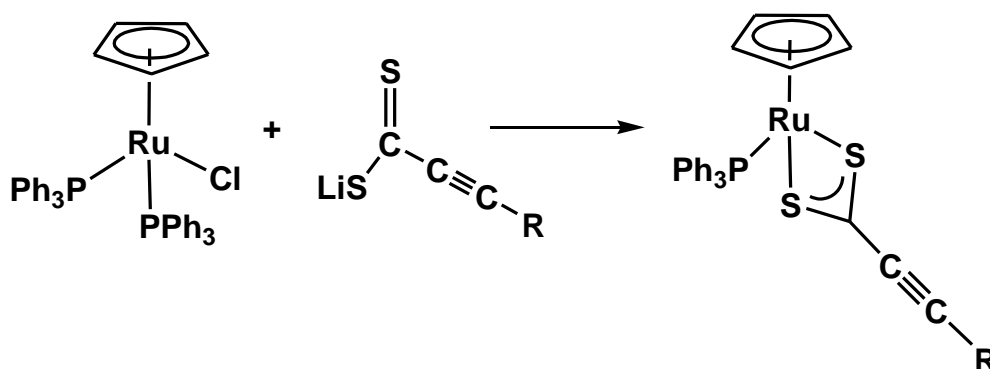
Usual synthetic methods for the preparation of dithiocarboxylate ligands include the reaction of Grignard reagents or lithium aryls with carbon disulfide.⁴⁶⁻⁴⁹ In a recent investigation, it has been found that the addition of alkynyl anions, RC≡C⁻ to CS₂ at low temperature generates the alkynyldithiocarboxylate ligands⁵⁰ which can be converted to several important organic molecules such as dithioesters⁵¹ and 1,2-dithiole-3-thiones.⁵²

Adams et al. reported that alkynyl dithiocarboxylates could be prepared by addition of acetylide anions to CS_2 and stabilizes by coordination to ruthenium. Solutions of the alkynyl dithiocarboxylate anions $\text{RC}\equiv\text{C}-\text{CS}_2^-$ ($\text{R} = \text{Mesityl}, \text{Ph}, \text{Bu}^t$), generated by treatment of the acetylides $\text{LiC}\equiv\text{CR}$ with carbon disulfide, are sufficiently stable to allow reaction with halo-ruthenium complexes.⁵³ They also used vinyl dithiocarboxylate complexes to react with additional terminal alkynes $\text{R}'\text{C}\equiv\text{CH}$ at room temperature to generate a acetylide complexes $[\text{Ru}(\text{CO})(\text{C}\equiv\text{CR}')(\text{S}_2\text{CC}\equiv\text{CR})(\text{PPh}_3)_2]$ (Scheme 4.2).



Scheme 4.2

Using a similar reaction strategy complex $[\text{CpRu}(\text{PPh}_3)_2\text{Cl}]$ was reacted with alkynyl dithiocarboxylate anions in refluxing THF to give Cp based ruthenium-dithiocarboxalate alkyne complexes $[\text{CpRu}(\text{PPh}_3)(\text{S}_2\text{CC}\equiv\text{CR})]$ ($\text{R} = \text{Bu}^t, \text{Bu}^n, \text{Ph}, \text{SiMe}_3$) (Scheme 4.3).⁴⁴ The anionic ligands were prepared by the reaction of the alkynyl anions $\text{RC}\equiv\text{CLi}$ with CS_2 at low temperature. The weak $\text{Ru}-\text{Cl}$ bond has facilitated the reaction to proceed in the forward direction to get the product.



Scheme 4.3

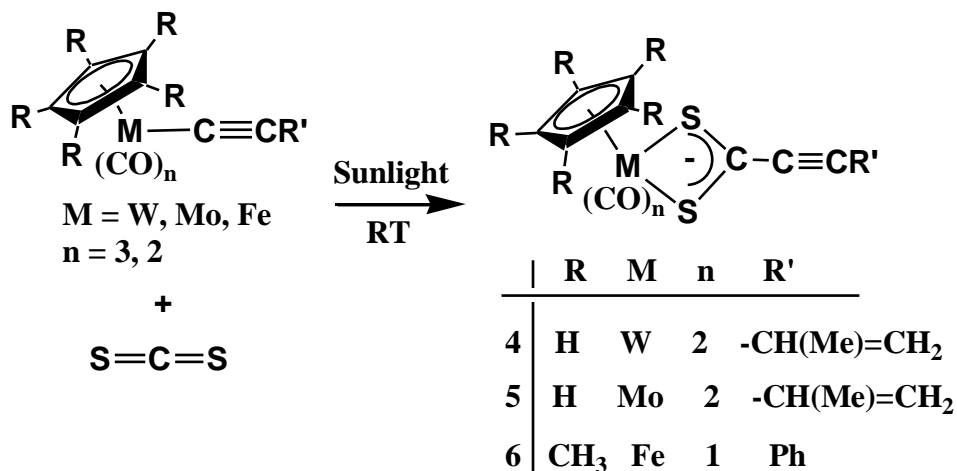
On the other hand, complexes containing acetylide ligands occupies a very important position in the development of di-, tri- and polynuclear organometallic chemistry. In the last decade, transition metal- acetylide compounds have been used for a large number of studies on organic transformations. Some of these acetylides show unique bonding environment and structural framework and are found to be versatile synthetic intermediates for the efficient synthesis of novel organic compounds.⁵⁴ The ability of the alkynyl part of the metal acetylides to bind to the metal centres in a variety of bonding modes enables a large number of acetylide bridged polynuclear complexes to be synthesized.⁵⁵ The presence of metal and electron rich C≡C moiety in acetylide complexes facilitates cluster growth reactions, and provides platform for the coupling of acetylide moieties to form poly carbon chains on cluster frameworks.⁵⁶ Metal acetylide complexes draw attention as precursors for the preparation of useful organometallic compounds and as components in NLO and other opto-electronic materials.

Considering the enormous potential of metal acetylide compounds, we focused our study on the reaction of different metal acetylide compounds using a renewable source of energy like sunlight. Our aim has also been to synthesize complexes containing several metal binding sites for the synthesis of multimetallic system. In an effort to synthesize such molecules we have described, in this chapter, the preparation of dithiocarboxylate-alkyne metal complexes by sunlight mediated reaction process and studied to understand the electronic properties of metal dithiocarboxylato complexes by carrying out calculations based on DFT and electron charge distribution.

4.2. RESULTS AND DISCUSSION

A mixture of carbon-disulfide and metal acetylide, $[LM(CO)_n C \equiv CR]$ [$\{L = \eta^5-C_5H_5, M = W, R = -C(CH)_3=CH_2, n = 3\}; \{L = \eta^5-C_5H_5, M = Mo, R = -C(CH)_3=CH_2, n = 3\}; \{L = \eta^5-C_5Me_5, M = Fe, R = Ph, n = 2\}$] (**1-3**) in n-hexane solvent when exposed to sunlight for a few seconds results in the formation of a blue to violet colored compounds $[LM(CO)_n(\eta^2-S_2C)C \equiv CR]$, [$\{L = \eta^5-C_5H_5, M = W, R = -C(CH)_3=CH_2, n = 3\}; \{L = \eta^5-C_5H_5, M = Mo, R = -C(CH)_3=CH_2, n = 2\}; \{L = \eta^5-C_5Me_5, M = Fe, R = Ph, n = 1\}$] (**4-6**) in quantitative yield (Scheme 4.4). The above insertion reactions have also been observed to takes place in the absence of any solvent. The use of sunlight for a short period of exposure time for the

insertion reaction is unusual and we are presently looking into the possibility of light driven reaction with other organometallic compounds.



Scheme 4.4

All the compounds **4-6** were purified by chromatographic technique and spectroscopic characterizations were performed. FTIR spectra for each of the compounds, **4-6** show a weak intensity peak in the region 2175-2169 cm⁻¹ corresponding to C≡C moiety and peaks in the region 1990-1898 cm⁻¹ corresponding to terminally bonded metal carbonyls. ¹H NMR spectral analysis for **4** and **5** reveals the presence of a η⁵-C₅H₅ unit attached to the metal center in the region δ5.496-δ5.64, and show triplet peaks at δ1.97 and δ1.962 due to the methyl protons, multiplets in the region δ5.47 - δ5.547 due =CH₂. Compound **6** show peaks corresponding to η⁵-C₅Me₅ and phenyl at δ1.35 and δ7.2-7.65 (multiplet) region respectively (Figure .4.4).

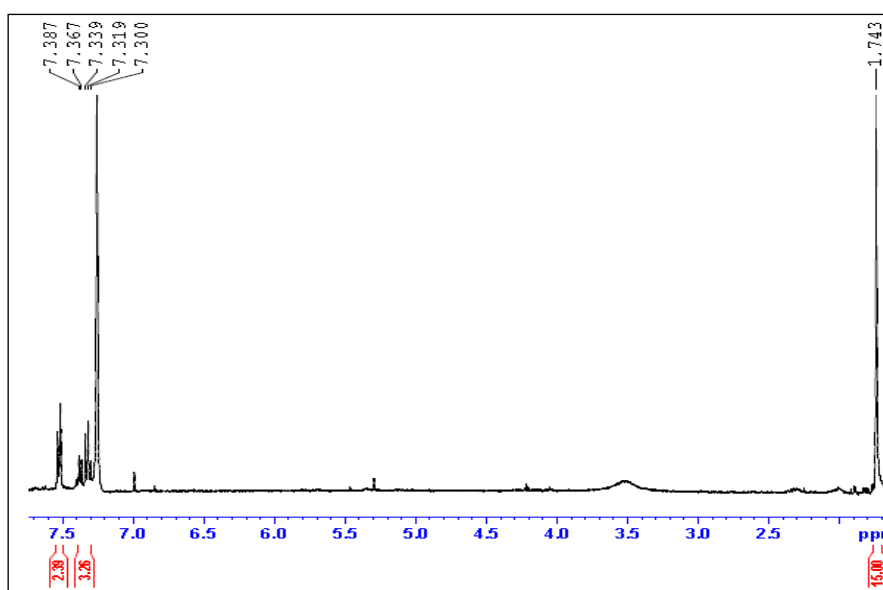


Figure 4.4 ¹H Spectrum of **6**

The UV-Visible spectra for compounds **4-6** show mainly four bands in each of the dithiocarboxylato complexes in the range 227-233 nm, 274-286 nm, 303-322 nm and 526-555 nm (Figure 4.5). The low energy transition has been gradually red shifted as we go from compound **6** to **4**. The observed shifting may be attributed to the variation of group from phenyl to vinyl attached to the dithiocarboxylato ligand (Table 4.1).

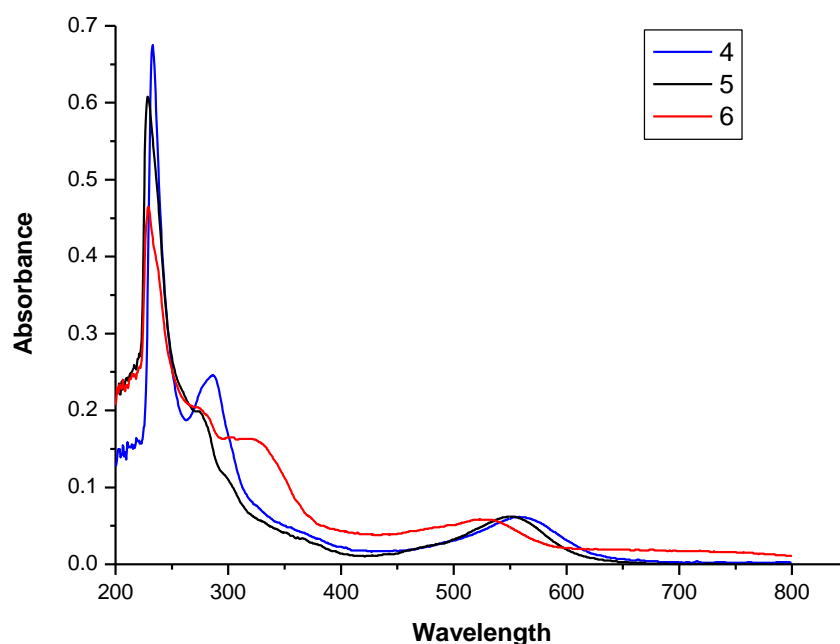


Figure 4.5 UV-Visible spectra for **4-6**

Table 4.1. UV-Visible data for complexes **4-6** in dichloromethane solvent

Compounds	λ_{max} (nm) [$\epsilon(\text{dm}^3 \text{mol}^{-1} \text{cm}^{-1})$]
4	233 (6750), 286 (2460), 304 (1460), 555 (620)
5	228 (6080), 274 (1990), 303 (1030), 550 (620)
6	227 (6560), 282 (2620), 322 (2250), 526 (820)

Single crystal X-ray diffraction studies have been carried out for $[\text{CpMo}(\text{CO})_2\text{S}_2\text{C}-\text{C}\equiv\text{CC}(\text{CH}_3)=\text{CH}_2]$ (**5**) and $[\text{Cp}^*\text{Fe}(\text{CO})\text{S}_2\text{C}-\text{C}\equiv\text{CPh}]$ (**6**) with the respective single crystals, grown from dichloromethane/n-hexane solvent mixture at -10°C . Structural characterization

for both the compound reveals the presence of S_2C_3R unit bonded to the metal center via two sulphur atoms in η^2 bonding mode. In both the structures, one of the metal-sulphur bonds is slightly longer than that of the other. The metals are also attached to a cyclopentadienyl ring and terminal carbonyl groups as shown in Figure 4.6 and 4.7. Compounds **5** and **6** contain an alkyne unit, with $C\equiv C$ bond length of 1.200(3) Å and 1.201(9) Å respectively, which can be used for further ligations with metal fragments through pi type bonding.

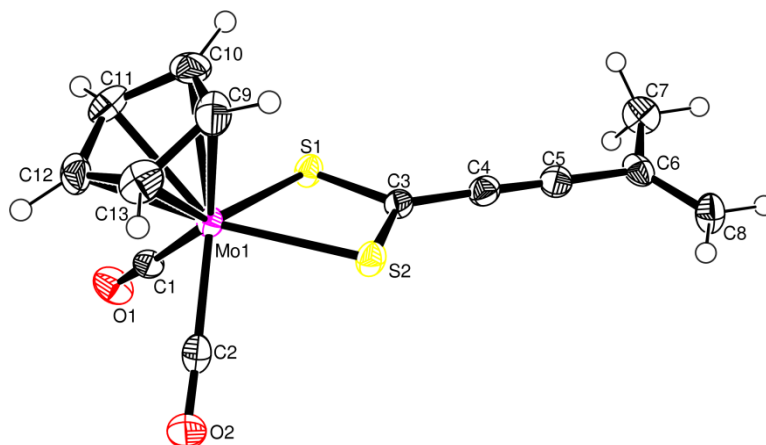


Figure 4.6: Molecular structure of **5**.

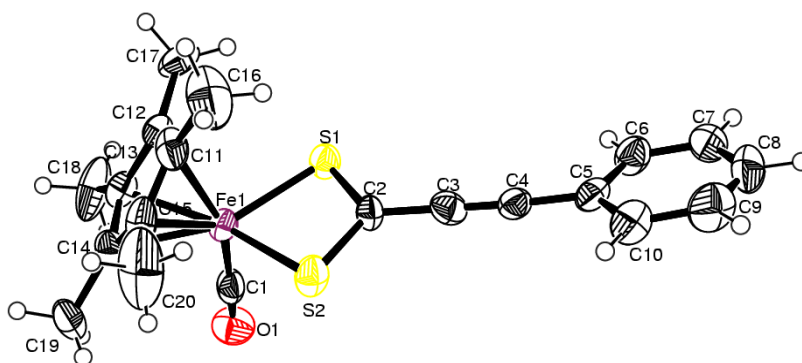


Figure 4.7: Molecular structure diagram of **6**.

Table 4.2: Selected bond lengths (Å) and angles (deg) for **5**

Compound 5			
Mo(1)-S(1)	2.4644(5)	S(1)-C(3)	1.693(2)
Mo(1)-S(2)	2.4607(5)	S(2)-C(3)	1.6924(19)
C(3)-C(4)	1.409(3)	C(4)-C(5)	1.200(3)
Mo(1)-C(1)	1.986(2)	Mo(1)-C(2)	1.991(2)

Mo(1)-C(12)	2.2783(19)	C(5)-C(6)	1.431(3)
C(6)-C(8)	1.372(3)	C(6)-C(7)	1.453(3)
C(9)-C(10)	1.394(3)	C(10)-C(11)	1.406(3)
O(1)-C(1)	1.144(3)	O(2)-C(2)	1.146(3)
C(1)-Mo(1)-S(2)	124.19(6)	C(2)-Mo(1)-S(2)	80.37(6)
C(1)-Mo(1)-S(1)	79.82(5)	C(2)-Mo(1)-S(1)	122.90(5)
S(2)-Mo(1)-S(1)	68.635(16),	S(2)-C(3)-S(1)	110.20(10)
C(5)-C(4)-C(3)	178.8(2)	C(4)-C(3)-S(1)	125.30(15)
C(1)-Mo(1)-C(2)	79.99(8)	C(3)-S(2)-Mo(1)	90.52(7)
C(3)-S(1)-Mo(1)	90.38(6)	O(1)-C(1)-Mo(1)	178.10(17)
C(4)-C(3)-S(2)	124.50(16)	C(4)-C(5)-C(6)	178.4(2)
C(8)-C(6)-C(5)	119.73(19)	C(8)-C(6)-C(7)	123.11(19)
C(5)-C(6)-C(7)	117.14(19)	C(10)-C(9)-C(13)	108.2(2)

Table 4.3: Selected bond lengths (Å) and angles (deg) for **6**

Compound 6			
Fe(1)-S(1)	2.266(2)	Fe(1)-S(2)	2.2615(19)
C(2)-C(3)	1.442(10)	C(3)-C(4)	1.201(9)
S(1)-C(2)	1.674(6)	S(2)-C(2)	1.681(7)
C(2)-C(3)	1.442(10)	O(1)-C(1)	1.168(8)
Fe(1)-C(1)	1.752(8)	Fe(1)-C(12)	2.090(6)
C(5)-C(6)	1.405(10)	C(11)-C(12)	1.395(10)
S(1)-C(2)-S(2)	110.5(4)	S(2)-Fe(1)-S(1)	74.98(7)
C(4)-C(3)-C(2)	179.3(7)	C(2)-S(1)-Fe(1)	87.3(2)
C(2)-S(1)-Fe(1)	87.3(2)	C(2)-S(2)-Fe(1)	87.3(2)
O(1)-C(1)-Fe(1)	177.9(7)	C(3)-C(2)-S(1)	124.6(5)
S(1)-C(2)-S(2)	110.5(4)	C(4)-C(3)-C(2)	179.3(7)
C(12)-C(11)-Fe(1)	70.9(4)	C(12)-C(11)-C(15)	107.7(6)

For a better understanding of the reactivity features and electronic structures of these alkynyl dithiocarboxylato complexes, we carried out DFT calculation on compound **6** and calculated their electron charge density and frontier molecular orbitals. The calculations

were carried out on single crystal x-ray diffraction data of **6** in gas phase and was fully optimized without any constrain. Electron charge density calculation showed that the C≡C is found to be polarized having unequal electron charges on two carbon atoms and the CS bonds are also polarized with positive charge on the sulphur atoms and negative charge on C6 carbon atom. These results shows that further reactions with alkynyl dithiocarboxylato complexes can be undertaken to properly understand the experimental facts.

4.2.1. DFT Calculations

4.2.1.1. Molecular Geometry Optimization of **6**

DFT calculation was carried out on single crystal x-ray diffraction data for compound **6** in gas phase and was fully optimized without any constrain. The DFT calculated geometrical parameters were tabulated in Table 4.4 for the complex along with the experimental values obtained from the Single Crystal X-ray studies. Figure 4.8 depicts the DFT optimized structure of the complex. Calculated Fe-C bond length (1.760 Å), excellently reproduced the experimental value (1.753 Å). Experimental Fe-C(cp), Fe-S and C≡O bond length found to be slightly smaller than the DFT calculated result. The deviations for C-S and C≡C bond length are also found to be quite less (0.085 and 0.031 Å respectively) while S-C-S and S-Fe-S bond angle found to differ only by 2.9° and 1.2°. Other bond length and bond angles agree well within 0.01Å and 1° respectively when compared with crystal structures as shown in Table 4.4. The minor discrepancies between the calculated and experimental geometries are reasonable as the calculated geometry are in gaseous phase while the experimental geometry is for the complex packed in a crystal lattice in presence of intermolecular interactions.

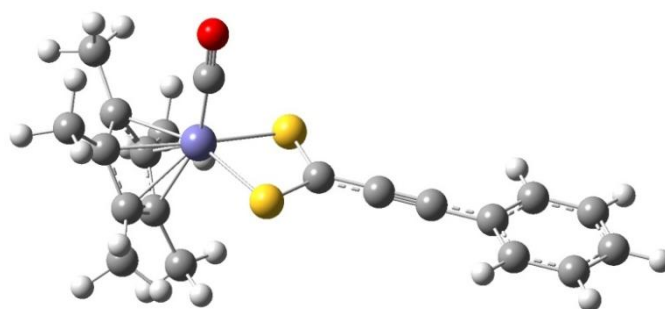


Figure 4.8: DFT optimized structure of compound **6**.

Table 4.4. Experimental and calculated selected bond lengths and bond angles for compound **6** along with the deviation.

Parameters	Experimental data	DFT calculated data	RMS deviation
Fe-C	1.753 Å	1.760 Å	0.007 Å
C≡O	1.167 Å	1.182 Å	0.015 Å
Fe-C(cp)	2.089 Å	2.169 Å	0.08 Å
Fe-S	2.266 Å	2.383 Å	0.117 Å
C-S	1.674 Å	1.759 Å	0.085 Å
C=C	1.442 Å	1.403 Å	0.039 Å
C≡C	1.201 Å	1.232 Å	0.031 Å
S-C-S	110.4°	113.3°	2.9°
S-Fe-S	74.9°	76.1°	1.2°

4.2.1.2. Electronic Spectrum and its Correlation with Spectroscopic Transitions

Absorption spectrum of the compound **6** consists of four bands as shown in Figure 4.5. The strongest band appears in the region of 200-260 nm ($\lambda_{\max} = 229$ nm) along with two humps at around 275 and 320 nm. At longer wavelength, a broad band in 450-600 nm region with $\lambda_{\max} = 527$ nm has also been observed. In order to get deeper understandings of transitions occurring in the complex, TD-DFT calculation has been performed. The calculated absorption bands for the complex in the ground state, corresponding oscillator strengths, energies and the involvement of MO in major transitions occurring at a particular wavelength are tabulated in Table 4.5. The assignment of the calculated electronic transitions to the experimental absorption bands was based on an overview of the contour plots and relative energy of highest occupied (HOMOs) and lowest unoccupied (LUMOs) molecular orbitals involved in the electronic transitions (Figure 4.9). In higher wavelength region (450-600 nm), TD-DFT calculated results show three respective transitions at 556, 511 and 451 nm, among which most intense transition was at 511 nm. The band at 556 nm in the complex corresponds to HOMO to LUMO+1 transition, where HOMO consists of mixture of non-bonding orbital of S and d_{yz} orbital of Fe atom and LUMO+1 consists of $\sigma^*(CS_2)$ and $d_{x^2-y^2}$ orbital of Fe atom. The band at 511 nm corresponds to HOMO-1 to LUMO transition

and assigned as transition between $\pi(S) \rightarrow \pi^*(\text{phenyl ring})$. Band at 370 nm corresponds to the HOMO-3 to LUMO+2 transitions and is assigned as $\pi(C\equiv C \text{ and phenyl ring}) \rightarrow \pi^*$ (phenyl ring and cp). Band with highest oscillator strength found to be at 320nm can be related to HOMO-6 to LUMO+2 transition assigned to be due to $\pi(\text{cp})/n(\text{O}) \rightarrow \pi^*(\text{phenyl})$ electronic transition.

Table 4.5. Selected electronic transitions calculated with TDDFT method.

Wavelength (nm)	Oscillator strength	Energy (eV)	Transitions between MOs
556	0.0306	2.2281	HOMO \rightarrow LUMO+1
547	0.0048	2.2648	HOMO \rightarrow LUMO
511	0.0935	2.4251	HOMO-1 \rightarrow LUMO
451	0.0118	2.7433	HOMO-1 \rightarrow LUMO+2
370	0.1147	3.3430	HOMO-3 \rightarrow LUMO+2
344	0.0782	3.6027	HOMO-5 \rightarrow LUMO
325	0.0088	3.8143	HOMO-7 \rightarrow LUMO
320	0.4915	3.8723	HOMO-6 \rightarrow LUMO
307	0.0100	4.0330	HOMO-2 \rightarrow LUMO+1
281	0.0283	4.4002	HOMO \rightarrow LUMO+6
264	0.100	4.6957	HOMO-1 \rightarrow LUMO+4
255	0.0536	4.8457	HOMO-4 \rightarrow LUMO+1
252	0.0909	4.9138	HOMO-2 \rightarrow LUMO+6
235	0.0271	5.2600	HOMO \rightarrow LUMO+7
228	0.0840	5.4235	HOMO-5 \rightarrow LUMO+2
222	0.0402	5.5646	HOMO-3 \rightarrow LUMO+4
217	0.044	5.6890	HOMO-5 \rightarrow LUMO+5

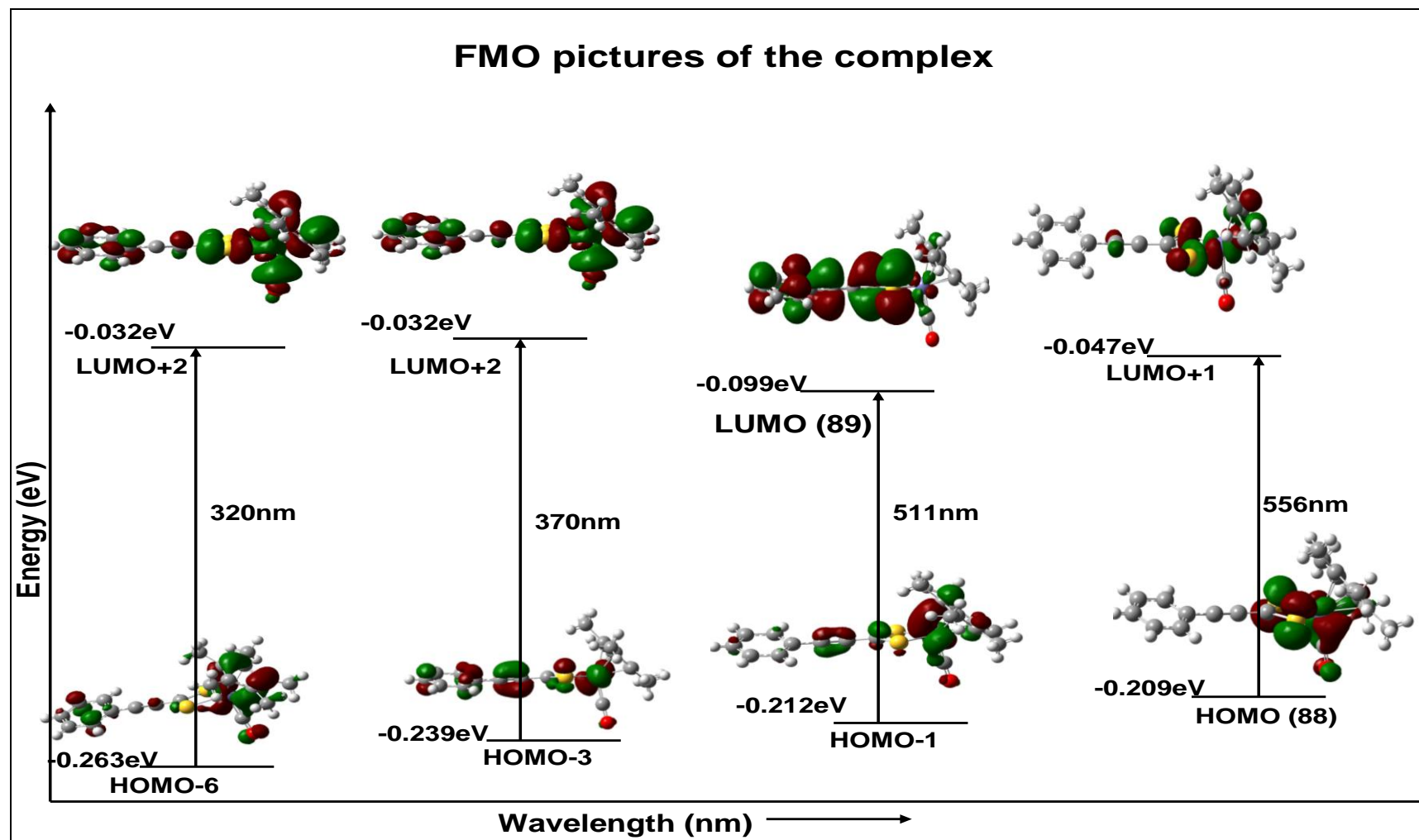


Figure 4.9. Various transitions in compound 6 depicted with Frontier Molecular Orbitals.

4.2.1.3. Electron Charge Density Calculation

The existence of a carbon-carbon triple bond in the complex may provide the opportunity to have a reaction centre. To judge the possibility, electron densities on all the atoms have been calculated and plotted the molecular electrostatic potential surface as shown in Figure 4.10. Mulliken charge distribution on different atoms of the complex are shown in the Table 4.6. The $C\equiv C$ is found to be polarized having unequal electron charges on two carbon atoms. While C7 is largely positive, C8 carries excess charge though small. As expected metal centre (Fe) and carbonyl oxygen holds the highest electron density. The CS bonds are also polarized with positive charge on the sulphur atoms and negative charge on C6 carbon atom.

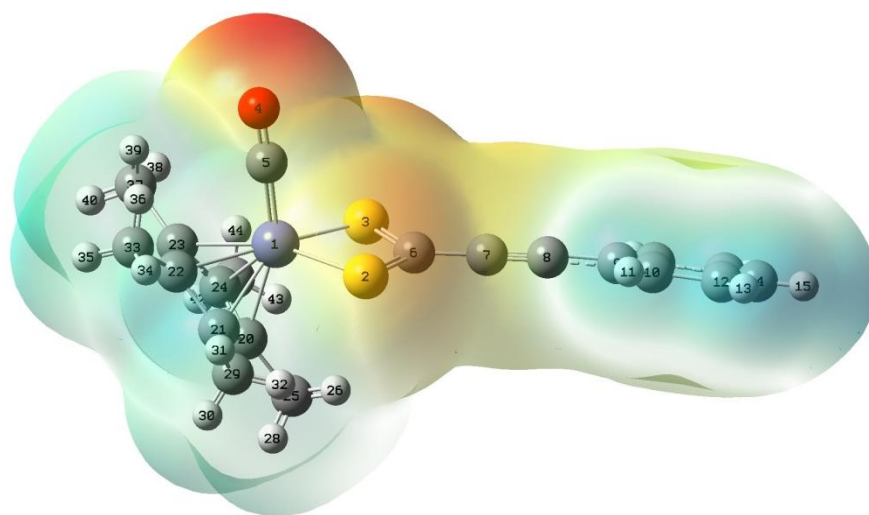


Figure 4.10 Molecular Electrostatic Potential (MEPs) plot of **6** in ground state. (color red to blue shade indicates the electron density in decreasing order.)

Table 4.6. Mulliken charge distribution on different atoms of compound **6**

Atom number	Atom Symbol	Charge distribution
1	Fe	-0.555
2	S	0.156
3	S	0.156
4	O	-0.193

5	C	0.290
6	C	-0.497
7	C	0.136
8	C	-0.017
9	C	0.373
10	C	-0.128

4.3. EXPERIMENTAL SECTIONS

4.3.1. General Procedures

All reactions and manipulations were carried out under an inert atmosphere of dry, pre-purified argon or nitrogen using standard schlenk line techniques. Solvents were purified, dried and distilled under an argon atmosphere prior to use. Infrared spectra were recorded on a Perkin Elmer Spectrum RX-I spectrometer as dichloromethane solutions and NMR spectra on a 400 MHz Bruker spectrometer in CDCl₃. Elemental analyses were performed on a Vario El Cube CHNS analyser. TLC plates (20x20 cm, Silica gel 60 F254) were purchased from Merck. [Cp*Fe(CO)₂C≡CPh], [CpMo(CO)₃C≡CC(CH₃)=CH₂], were prepared following the reported procedures.⁵⁷

4.3.2. Reaction of [LM(CO)_nC≡CR] {L=η⁵-C₅H₅, η⁵-C₅Me₅; M = Mo, W, Fe; R = -C(CH₃)=CH₂, Ph; n = 3, 2} (1-3) with CS₂

An equimolar mixture of [LM(CO)_nC≡CR] [{L=η⁵-C₅H₅, M = W, R = -C(CH₃)=CH₂, n = 3}; {L=η⁵-C₅H₅, M = Mo, R = -C(CH₃)=CH₂, n = 3}; {L=η⁵-C₅Me₅, M = Fe, R = Ph, n = 2}] (1-3) (0.1 mmol) and carbondisulphide (0.1 mmol) in n-hexane solution was exposed to sunlight at room temperature under inert atmosphere and stirring condition. An immediate color change from yellow to blue or violet was observed. The solution was vacuum dried and the residue was subjected to chromatographic work-up using preparative TLC with dichloromethane / hexane (10:90 v/v) solvent mixture. The compound obtained on subsequent elution is the blue to violet coloured compound [LM(CO)_n(η²-S₂C)C≡CR] [{L=η⁵-C₅H₅, M = W, R = -C(CH₃)=CH₂, n =

3});{L= η^5 -C₅H₅, M = Mo, R = -C(CH₃)=CH₂, n = 2};{ L= η^5 -C₅Me₅, M = Fe, R = Ph, n = 1}] (**4-6**). (Yield: **4** (30mg, 82 %); **5** (36 mg, 89 %); **6** (35 mg, 88 %).

4: IR(ν_{CO} , cm⁻¹, CH₂Cl₂): 2063 (w), 1964.5 (vs), 1898 (s, br), 1260 (m), 1094(m), 1022(m), 801 (m). ¹H NMR (δ , CDCl₃): 1.97 (t, 3H, -CH₃, J = 1.2 Hz), 5.47 (m, 1H, =CH₂), 5.54 (m, 1H, =CH₂), 5.64 (s, 5H, η^5 -C₅H₅). MS (ESI): m/z 446 (M)⁺.

5: Anal. calcd. (found): C, 43.58 (43.21); H, 2.79 (2.67); S, 17.88 (18.04). IR(ν_{CO} , cm⁻¹, CH₂Cl₂): 1974(vs), 1913 (s), 1022 (m), 800 (m). ¹H NMR (δ , CDCl₃): 1.962 (t, 3H, -CH₃, J = 1.2 Hz), 5.470 (m, 1H, =CH₂), 5.547 (m, 1H, =CH₂), 5.496 (s, 5H, η^5 -C₅H₅). MS (ESI): m/z 360 (M+2)⁺.

6: Anal. calcd. (found): C, 60.60 (60.22); H, 5.05 (4.94); S, 16.16 (16.4). IR(ν_{CO} , cm⁻¹, CH₂Cl₂): 2175 (m), 1934.5(s), 1026 (m), 975(m), 755 (m). ¹H NMR (δ , CDCl₃): 1.35 (s, 15H), 7.2-7.65 (m, 5H, C₆H₅). MS (ESI): m/z 397 (M+1)⁺.

4.3.3. Crystal structure determination for **5** and **6**.

Single crystal X-ray structural studies of **5** and **6**, was performed on a CCD Oxford Diffraction XCALIBUR-S diffractometer equipped with an Oxford Instruments low-temperature attachment. Data were collected at 150(2) K using graphite-monochromated Mo K α radiation ($\lambda_{\alpha} = 0.71073 \text{ \AA}$). The strategy for the Data collection was evaluated by using the CrysAlisPro CCD software. The data were collected by the standard 'phi-omega scan techniques, and were scaled and reduced using CrysAlisPro RED software. The structures were solved by direct methods using SHELXS-97 and refined by full matrix least-squares with SHELXL-97, refining on F^2 .⁵⁸ The positions of all the atoms were obtained by direct methods. All non-hydrogen atoms were refined anisotropically. The remaining hydrogen atoms were placed in geometrically constrained positions and refined with isotropic temperature factors, generally $1.2U_{eq}$ of their parent atoms. The crystallographic details are summarized in Table 4.7.

4.3.4. Computational details

The Gaussian 03 program was used for the Density Functional Theory (DFT) calculation of the organometallic complex. The basis set already implemented in the program was used for the different types of calculations. The geometry of the organometallic complex was optimized at the Becke's three parameter hybrid method with LYP correlation (B3LYP) level^{59, 60} and

using LanL2DZ basis set. In addition to optimization (starting from the coordinates of single crystal x-ray diffraction data), frequency calculation was done at same level of calculation using the same basis sets. The absence of imaginary vibrational frequencies in calculated vibrational spectrum ensures the presence of a true minimum in the potential energy surface. The spectroscopic and electronic property of this complex has been computed by time dependent DFT (TD-DFT) calculation ⁶¹ at the same B3LYP level in gaseous phase. The nature and the role of the electronic excitation contributions are rationalized in terms of frontier molecular orbitals (FMO).

Table 4.7: Crystal data and structure refinement parameters for compounds **5** and **6**.

	5	6
Empirical formula	C13 H10 Mo O2 S2	C20 H20 Fe O S2
Formula weight	358.27	396.33
Crystal system	Monoclinic	Monoclinic
Space group	<i>P</i> 2 ₁ / <i>c</i>	<i>C</i> 2/ <i>c</i>
<i>a</i> , Å	10.6834(2)	28.782(4)
<i>b</i> , Å	11.2401(2)	9.8247(11)
<i>c</i> , Å	12.1033(2)	15.944(2)
α deg	90	90
β deg	107.308(2)	122.46(2)
γ deg	90	90
<i>V</i> , Å ³	1387.58(4)	3804.3(9)
<i>Z</i>	4	8
<i>D</i> _{calcd} , Mg m ⁻³	1.715	1.384
abs coeff, mm ⁻¹	1.235	1.015
<i>F</i> (000)	712	1648
Cryst size, mm	0.33 x 0.26 x 0.21	0.23 x 0.18 x 0.14
θ range, deg	3.53 to 24.99	3.26 to 25.00
index ranges	-12 \leq <i>h</i> \leq 12, -13 \leq <i>k</i> \leq 12, - 14 \leq <i>l</i> \leq 14	-34 \leq <i>h</i> \leq 34, -11 \leq <i>k</i> \leq 11, - 18 \leq <i>l</i> \leq 18

reflections collected/ unique	9748 / 2449 [R(int) = 0.0223]	13314 / 3349 [R(int) = 0.1056]
data/ restraints / parameters	2449 / 0 / 164	3349 / 0 / 222
goodness-of-fit on F ²	1.072	1.110
Final R indices [I>2σ(I)]	R1 = 0.0178, wR2 = 0.0460	R1 = 0.0677, wR2 = 0.1709
R indices (all data)	R1 = 0.0213, wR2 = 0.0466	R1 = 0.1078, wR2 = 0.1812
largest diff peak and hole, eÅ ⁻³	0.390 -0.322	0.422 -0.415

4.4. CONCLUSIONS

In summary, insertion of CS₂ has been observed into metal –carbon acetylide bond when exposed to mild sunlight to obtain a variety of transition metal dithiolato complexes. We have also been able to understand the electronic properties of iron dithiocarboxylato complexes by carrying out DFT calculations and electron charge distribution studies. Molecular orbitals involved in the electronic transition of iron alkynyl-dithiocarboxylate complexes was determined by TD-DFT calculation. Electron charge density on different atoms was also calculated to understand the charge distribution.

4.5. REFERENCES

1. (a) M. I. Bruce, P. J. Low, *Adv. Organomet. Chem.* 50 (2004) 231; (b) V. W.W. Yam, *Acc. Chem. Res.* 35 (2002) 555.
2. (a) P. Mathur, S. Chatterjee, A. Das, S. M. Mobin, *J. Organomet. Chem.* 692 (2007) 819; (b) Z. P. Qi, S. A. Li, Y. Q. Huang, G. C. Xu, G. X. Liu, L. Y. Kong, W. Y. Sun, *Inorg. Chem. Commun.* 11 (2008) 929.
3. P. Blenkiron, G. D. Enrighta, A. J. Carty, *Chem. Commun.* 483 (1997).
4. C. S. Yi, S. Y. Yun, I. A. Guzei, *J. Am. Chem. Soc.* 127 (2005) 5782.
5. P. Mathur, V. D. Avasare, S. M. Mobin, *J Clust Sci* 20 (2009) 399.
6. P. Mathur, A. K. Singh, S. Chatterjee, V. K. Singh, Shaikh M. Mobin, *J. Organomet. Chem.* 695 (2010) 950.
7. (a) K. K. Pandey, *Coord. Chem. Rev.*, 1995, 140, 37; (b) W. Leitner, *Coord. Chem. Rev.*, 1996, 153, 257; (c) K. Tanaka, *Adv. Inorg. Chem.*, 1995, 43, 409.
8. G. Albertin, S. Antoniutti, E. Del Ministro, E. Bordignon, *J. Chem. Soc., Dalton Trans.* (1994) 1769.
- 9 (a) I. Omae, *Catal. Today* 115 (2006) 33; (b) R. Rossi, A. Marchi, A. Duatti, L. Magon, U. Casellato, R. Graziani, *J. Chem. Soc., Dalton Trans.*, (1988) 899 ; (c) J. M. Sav' eant, *Chem. Rev.*, 108 (2008) 2348.
10. Y. Chen, Y. Peng, P. Chen, J. Zhao, L. Liu, Y. Li, S. Chen , J. Qu, *Dalton Trans.*, 39 (2010) 3020.

11. (a) P.V. Yaneff, *Coord. Chem. Rev.*, 232 (1977) 183; (b) J. Li, R. Hoffmann, C. Mealli, J. Silvestre, *Organometallics* 8 (1989) 1921; (c) L. Linford, H.G. Raubenheimer, *Comments Inorg. Chem.* 12 (1991) 113.
12. R.P. Bums, F.P. McCullough and C.A. McAuliffe, *Adv. Inorg. Chem. Radiochem.* 23 (1980) 211.
13. (a) H. Werner, M.A. Tena, N. Mahr, K. Peters, H. G. Schering, *Chem. Ber.*, 128 (1995) 41; (b) K. K. Pandey, H. Garg S.K. Tewary, *Polyhedron*, 11 (1992) 947; (c) H.G. Raubenheimer, F. Scott, S. Cronje, P. H. Van Rooyen, *J. Chem. Soc., Dalton Trans.* (1992) 1859; (d) S. J. Schauer, D. P. Eyman, R. J. Bemhardt, M. A. Wolff, L. M. Mallis, *Inorg. Chem.*, 30 (1991) 570; (e) W. D. Jones, V. L. Chandler, F. J. Fehrer, *Organometallics*, 9 (1990) 164 (f) G. J. Kruger, S. Cronje, A. Lombard, H. G. Raubenheimer, R. Benn, A. Rufinska, *Organometallics*, 9 (1990) 1071.
14. (a) E. B. Brouwer, P. Legzdins, S. J. Rettig, K. J. Ross, *Organometallics*, 12 (1993) 4234; (b) T.R. Gaffney, J.A. Ibers, *Inorg. Chem.*, 21 (1982) 2062.
15. (a) P. Legzdins, S.J. Rettig, K.J. Ross, *Organometallics* 13 (1994) 569; (b) R.D. Simpson, R.G. Bergman, *Angew. Chem., Int. Ed. Engl.* 31 (1992) 220.
16. L. Ruis-Ramirez, T.A. Stephenson, E.S. Switkes, *J. Chem. Soc. Dalton Trans.* (1973). 1770
17. F.G. Moers, R.W.M. ten Hoedt, J.P. Langhout, *Inorg. Chem.* 12 (1973) 2196.
18. M.P. Yagupsky, G. Wilkinson, *J. Chem. Soc. A* (1968) 2813.
19. M.C. Baird, G. Wilkinson, *J. Chem. Soc. A* (1967) 865.
20. D. A. Brown, F.J. Hughes, *Inorg. Chim. Acta* 1 (1967) 448.
21. S. Sakaki, K. Kitaura, K. Morokuma, *Inorg. Chem.* 21 (1982) 760.
22. C. Mealli, R. Hoffmann, A. Stockis, *Inorg. Chem.* 23 (1984) 56.
23. T. Ziegler, *Inorg. Chem.* 25 (1986) 2721.
24. M. Rosi, A. Sgamellotti, F. Tarantelli, C. Floriani, *Inorg. Chem.* 26 (1987) 3805.
25. M. I. Bruce, T. W. Hambley, M. R. Snow, A. G. Swincer, *J. Organomet. Chem.* 273 (1984) 361.
26. F. Scott, G. J. Kruger, S. Cronje, A. Lombard, H. G. Raubenheimer, R. Benn, A. Rufinska, *Organometallics* 9 (1990) 1071.
27. E. B. Brouwer, P. Legzdins, S. J. Rettig, K. J. Ross, *Organometallics* 12 (1993) 4234.
28. H. Adams, P. E. McHugh, M. J. Morris, S. E. Spey, P. J. Wright, *J. Organomet. Chem.* 619 (2001) 209.

29. (a) A. Campus, N. Marsich, A. M. M. Lanfredi, F. Ugozzoli, *Inorg. Chim. Acta* 175 (1990) 193-202; (b) Z.-U. Rehman, N. Muhammad, S. Shuja, S. Ali, I. S. Butler, A. Meetsma, M. Khan, *Polyhedron* 28 (2009) 3439.
30. (a) A. M. M. Lanfredi, A. Tiripicchio, A. Campus, N. Marsich, *J. Chem. Soc., Chem. Commun.* (1983) 1126-1128; (b) A. K. Hughes, J. M. Malget, A. E. Goeta, *Dalton Trans.* (2001) 1927..
31. L. F. Szczepura, C. P. Galloway, Y. Zheng, P. Han, S. R. Wilson, T. B. Rauchfuss, A. L. Rheingold, *Angew. Chem. Int. Ed.* 34 (1995) 1890.
32. P. Mathur, V. D. Avasare, A. K. Ghosh, S. M. Mobin, *J. Organomet. Chem.* 689 (2004) 1325.
33. Q. Willem, F. Nicks, X. Sauvage, L. Delaude, A. Demonceau, *J. Organomet. Chem.* 694 (2009) 4049.
34. S. K. Maji, A. K. Dutta, P. Biswas, D. N. Srivastava, P. Paul, A. Mondal, B. Adhikary, *App. Catal. A: General* 419– 420 (2012) 170
35. G. Kedarnath, V. K. Jain, S. Ghoshal, G. K. Dey, C. A. Ellis, E. R. T. Tiekink, *Eur. J. Inorg. Chem.* (2007) 1566
36. M. S. Thomas, M. Landman, S. Lotz, E. M. van der Merwe, *Polyhedron* 26 (2007) 3471
37. D. J. Darensbourg, M. J. Adams, J. C. Yarbrough, *Inorg. Chem. Commun.* 5 (2002) 38.
- 38 S. Dilsky, W. A. Schenk, *Z. Naturforsch.* 61b (2006) 570
39. E. M. Matson, W. P. Forrest, P. E. Fanwick, S. C. Bart, *J. Am. Chem. Soc.* 133 (2011) 4948
40. W. J. Mace, L. Main, B. K. Nicholson, M. Hagyard, *J. Organomet. Chem.* 664 (2002) 288
41. M. I. Bruce, M. J. Liddell, M. R. Snow, E. R. T. Tiekink, *J. Organomet. Chem.* 352 (1988) 199
42. V. Cadierno, M. P. Gamasa, J. Gimeno, E. Lastra, *J. Organomet. Chem.* 510 (1996) 207
43. P. Mathur, A.K. Ghosh, S. Mukhopadhyay, C. Srinivasu, S.M. Mobin, *J. Organomet. Chem.* 678 (2003) 142
44. M. El-khateeb, H. Görls, W. Weigand, *J. Organomet. Chem.* 691 (2006) 2055
45. J. P. Selegue, *J. Am. Chem. Soc.*, 104 (1982) 119.
46. D. Coucouvanis, *Prog. Inorg. Chem.* 26 (1979) 301.
47. D. Coucouvanis, *Prog. Inorg. Chem.* 11 (1970) 233.
48. C. Ives, E. L. Fillis, J. R. Hagadorn, *J. Chem. Soc., Dalton Trans.* (2003) 527.
49. K. Ruhlandt-Senge, J.J. Ellison, R. J. Wehmschulte, F. Pauer, P. P. Power, *J. Am. Chem. Soc.* 115 (1993) 11353.

50. K. Hartke, H. D. Gerber, V. Roesrath, *Annalen* 22 (1991) 903
51. K. Takimiya, A. Morikami, T. Otsubo, *Synlett*. (1997) 319.
52. P. Mathur, V. D. Avasare, A. K. Ghosh, S. M. Mobin, *J. Organomet. Chem.* 689 (2004) 1325.
53. H. Adams, P. E. Mcttugh, M. J. Morris, S. E. Spey, P. J. Wright, *J. Organomet. Chem.* 619 (2001) 209.
54. (a) P. Mathur, S. Chatterjee, V. D. Avasare, *Adv. Organomet. Chem.* 55 (2008) 201 and references therein; (b) C. J. Li, *Acc. Chem. Res.* 43 (2010) 581(c) R. J. Madhushaw, C. L. Li, H. L. Su, C. C. Hu, S. F. Lush, R. S. Liu, *J. Org. Chem.* 68 (2003) 1872 (d) U. Rosenthal, *Angew. Chem. Int. Ed.* 42 (2003) 1794; (e) P. Mathur, S. Chatterjee, *Comm. Inorg. Chem.* 26
55. (a) P. Mathur, S. Bodida, S.M. Mobin, *J.Organomet.Chem.* 694 (2009) 3043-3045; (b) P. Mathur, Ipe J. Mavunkal, V. Rugmini, *J. Organomet. Chem.* 367 (1989) 243.
56. (a) P. Baistrocchi, D. Cauzzi, M. Lanfranchi, G. Predieri, A. T. Camellini, *Inorg. Chem. Acta* 235 (1995) 173; (b) P. Mathur, A. K. Singh, S. Chatterjee, V. K. Singh, S. M. Mobin, *J. Organomet. Chem.* 695 (2010) 950; (c) P. Mathur, A. K. Singh, J. R. Mohanty, S. Chatterjee, S.M. Mobin, *Organometallics* 27 (2008) 5094; (d) P. Mathur, S. Chatterjee, A. Das, S. M. Mobin, *J. Organomet. Chem.* 263 (2008) 1919.
57. (a) M. I. Bruce, M. G. Humphrey, J. G. Matisons, S. K. Roy, A. G. Swincer, *Aust. J. Chem.* 37 (1984) 1955 ;(b) M. Akita, M. Terada, S. Oyama, Y. Moro-oka, *Organometallics* 9 (1990) 816-825.
58. G. M. Sheldrick, A short history of *SHELX*, *Acta Cryst. A* 64 (2008) 112-122.
59. A. D. Becke, *J. Chem. Phys.* 98 (1993) 5648-5652.
60. A. Lee, W. Yang, R. G. Parr, *Phys. Rev. B* 37 (1988) 785-789.
61. A. Ghosh, I. Halvorsen, H. J. Nilsen, E. Steene, T. Wondimagegn, R. Lie, E. Caemelbecke, N. Guo, Z. Ou, K. M. Kadish, *Phys. Chem. B* 105 (2001) 8120.

CHAPTER 5

**SYNTHESIS OF TRIMETALLIC-
DITHIOCARBOXYLATE COMPLEX AND
METAL MEDIATED TRANSFORMATIONS
OF FERROCENYL AND
DITHIOCARBOXALATE-ALKYNES**

5.1. INTRODUCTION

Transition metal complexes have been intensively investigated to develop new and effective transformations achieved by the synergic effect of metal centers and ligand entities. The reactivity of transition metal complexes with organic molecules has been of special interest in the area of recent organometallic chemistry because of their potential applicability to organic synthesis. The behavior of organic molecules with metals is of prime importance to understand the mechanism of the catalytic activity in heterogenous and homogeneous system. Transition metals coordinated to small organic species gives rise to a versatile and rich chemistry due to their vast number of metal – ligand bonding modes and structural variety.^{1,2} Such complexes are found to be versatile synthetic intermediates, which facilitate a number of interesting transformations and offer a fascinating perspective for the synthesis of novel organic compounds.³⁻⁶ Recently, mixed-metal clusters have shown to undergo different types of coupling reaction of terminal and functionalized metal-acetylide compounds resulting in clusters containing multisite-bound polycarbon units.³ Literature survey reveals that a variety of organic transformations are supported and catalyzed by metal cluster complexes, wherein the steric and electronic requirements for such transformations are offered by the metal component.³

A large diversity of coordination modes have been known for metal complexes with various organic ligands where, changing a ligand in the coordination sphere can affect the function of the metal fragment. It has been well established that the electronic and/or steric factors can be finely tuned by simple substitution of labile ligands or changing the metal core framework.^{7,8} One such facile tuning of the electronic and optical properties of transition metal π -arene tricarbonyl complexes by carbonyl substitution has been reported recently.⁸

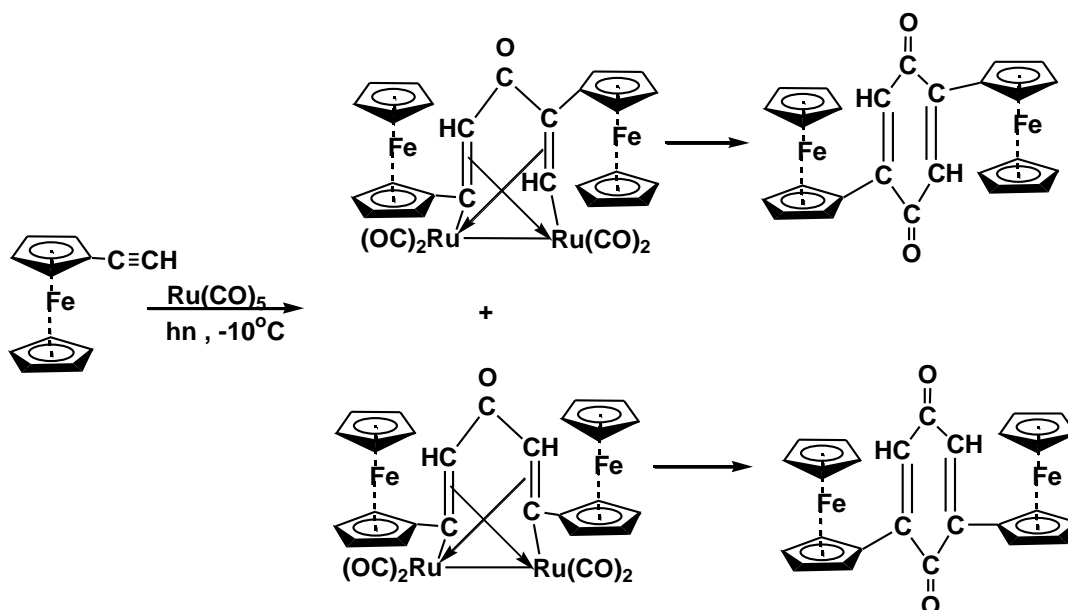
The chemistry of metal-alkyne compounds have grown tremendously since Reppe discovered the cyclomerization of acetylene to get cyclooctatetraene and the pioneering work of Hübel for the organic transformation of alkynes assisted by metal carbonyls.⁹⁻¹³ A range of catalytic activity have been shown by molybdenum and tungsten carbonyl complexes for alkyne metathesis reactions and for the synthesis of macrocyclic compounds.¹⁴⁻¹⁷ Moreover, metal acetylenic systems has been extended for the use of alkynes as bridging ligands in cluster formation and several other coupling reactions on metal framework.¹⁸⁻²¹

In the last decade, reactivity of alkynes has been extended to a variety of applications in organic synthesis such as functionalization, C-H and C-C bond cleavage, C-C bond coupling, oligomerization etc. Studies have shown that the alkyne system becomes an

excellent π acceptor by attaching a strong electron withdrawing group, by which it can also displace other ligands such as phosphines. As a result some of the ynyl and polynyl ligands are very important in the synthesis of the organometallic compounds with different structural and physical properties.²²⁻²⁴ This had prompted to design complexes of different chain length by linking the metal centers via the M-C bonds, which exhibits nonlinear optical and other electronic properties due to the presence of extended conjugated π systems.²⁵ Metal cluster complexes containing poly-carbon ligands has also been synthesized by using higher ynyl ligands.²⁶ Alkynes can be complexed with transition metal through the σ - or π -bond. Recently, σ -acetylide and σ -enynyl metal complexes have attracted much attention as promising candidates for NLO materials.²⁷ It is a general feature of π -alkyne complexes that electrons are back-donated from a metal d-orbital into the ligand LUMO resulting in the formation of more stable metal-alkyne adduct.²⁸ Very recently, a range of dicobaltcarbonyl-alkyne complexes have been synthesized and examined for their non-linear optical properties. These complexes offer the possibility of a new class of NLO chromophore by tuning their optical properties by the substitution of carbonyl groups.²⁹

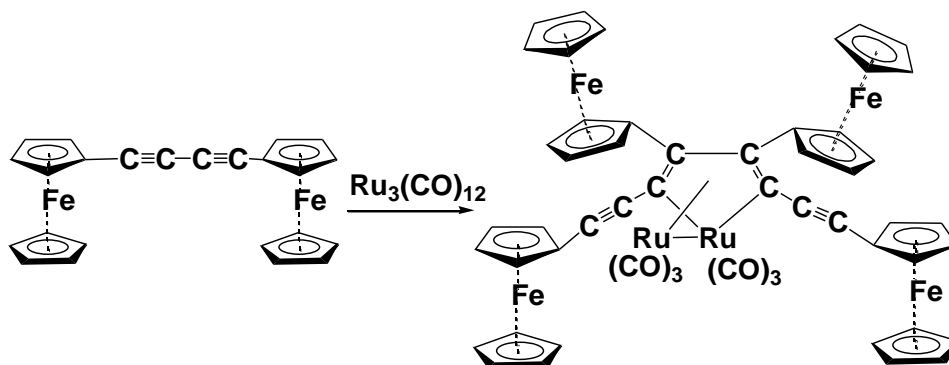
Metal mediated alkyne transformation have attracted a plethora of research activity due to the formation of different organic compounds. Recently, reaction of a number of alkynes with iron pentacarbonyl in presence of trimethylamine-N-oxide and subsequent oxidation by $\text{CuCl}_2 \cdot 2\text{H}_2\text{O}$ led to the formation of cyclobutendiones.³⁰ Cyclo-oligomerisations of ferrocenylacetylenes using metal carbonyls, have been reported to give interesting products. One such reaction of ferrocenylacetylene with $\text{Fe}(\text{CO})_5$ gave three types of coupling products $[\text{Fe}(\text{CO})_2\{\eta^5\text{-}2,5\text{-Fc}_2\text{C}_5\text{H}_2\text{CO}\}\text{C}(\text{Fc})=\text{CH}]$, $[\text{Fe}(\text{CO})_2\{\eta^2:\eta^2\text{-}2,5\text{-Fc}_2\text{C}_4\text{H}_2\text{Fe}(\text{CO})_3\}\mu\text{-CO}]$ and $[\text{Fe}(\text{CO})_3\{\eta^2:\eta^2\text{-}2,5\text{-Fc}_2\text{C}_4\text{H}_2\text{CO}\}]$,³¹ while low temperature photolysis of solutions containing ferrocenylacetylene and iron pentacarbonyl in presence of carbon monoxide forms 2,5- and 2,6-diferrocenylquinones.³²

In another transformation reaction of bulky alkyne, ferrocenylacetylene was photolytically reacted with freshly prepared $[\text{Ru}(\text{CO})_5]$ to obtain two metallalacyclic compounds: $[\text{Ru}_2(\text{CO})_6\{\mu\text{-}\eta^1:\eta^1:\eta^1:\eta^2\text{-}1,4\text{-Fc}_2\text{C}_5\text{H}_2\text{O}\}]$ and $[\text{Ru}_2(\text{CO})_6\{\mu\text{-}\eta^1:\eta^1:\eta^1:\eta\text{-}1,5\text{-Fc}_2\text{C}_5\text{H}_2\text{O}\}]$ which further transformed to 2,5-diferrocenylbenzo-1,4-quinone and 2,6-diferrocenylbenzo-1,4-quinone respectively by the addition of carbonmonoxide (Scheme 5.1).³³



Scheme 5.1

Dialkyne also play similar role with metal fragments and shows unusual coupling products. Mathur et al recently reported a low temperature photolysis of a hexane solution containing $[\text{Ru}_3(\text{CO})_{12}]$ and $\text{FcC}\equiv\text{CC}\equiv\text{CFc}$ which led to the isolation of ruthenacyclopentadiene complex $[\text{Ru}_2(\text{CO})_6\{\text{C}_4\text{Fc}_2\text{-(C}\equiv\text{CFc)}_2\}_2]$ (Scheme 5.2). The molecular structures of comprises of a ruthenacyclopentadiene ring in which the ruthenium atom bears three terminally bonded carbonyl groups and the ring is η^4 -bonded to a Ru(CO)_2 fragment which is also bonded to the ring ruthenium atom.³⁴



Scheme 5.2

They have also synthesized diruthenacycloheptadienone, $\text{Ru}_2(\text{CO})_6[\mu\text{-}\eta^1\text{:}\eta^1\text{:}\eta^2\text{:}\eta^2\text{-}\{\text{FcC}\equiv\text{CC}\equiv\text{C(Fc)-C(O)-C(Fc)CC}\equiv\text{Fc}\}]]$ and $[\text{Ru}_2(\text{CO})_6[\mu\text{-}\eta^1\text{:}\eta^1\text{:}\eta^2\text{:}\eta^2\text{-}\{\text{FcC}\equiv\text{CC}\equiv\text{C(Fc)-C(O)-C(-C}\equiv\text{CFc)C(Fc)}\}]]$ from the reaction of $[\text{Ru}_3(\text{CO})_{10}\{\mu_3\text{-FcC}_2\text{C}\equiv\text{CFc}\}]$ and diferrocenyldiacetylene in thermal reaction condition (Figure 5.1).³⁴

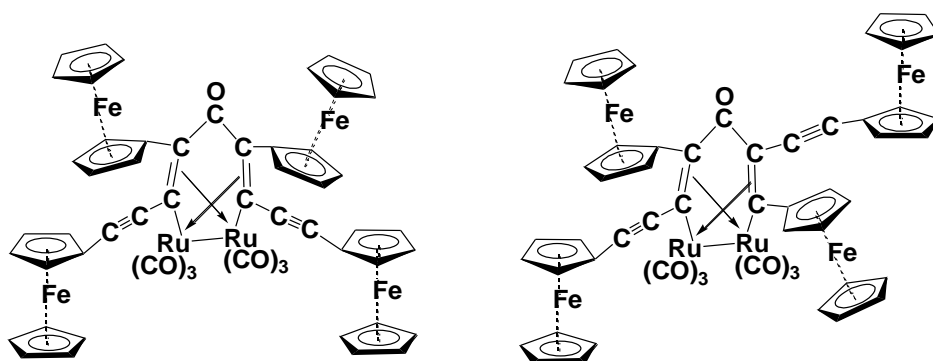
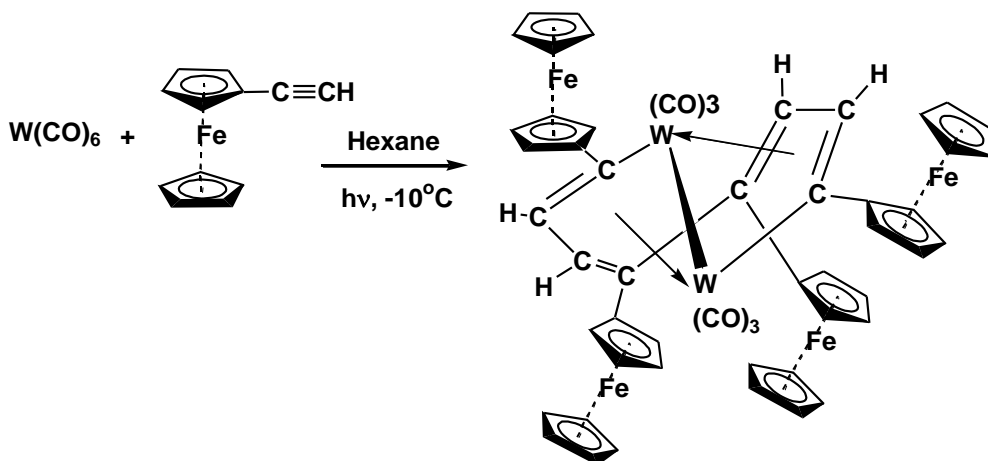


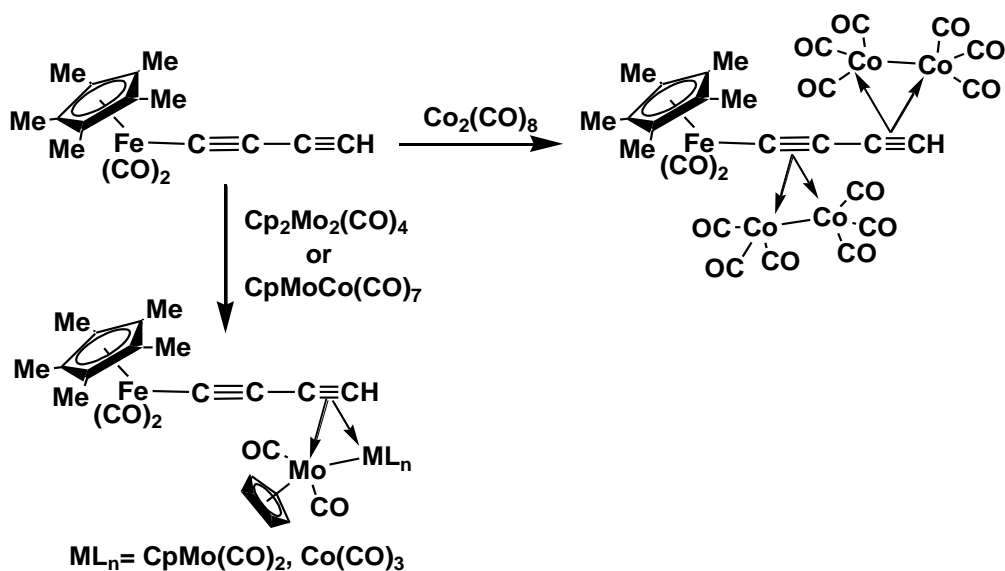
Figure 5.1

Another important metallacyclic compound containing four alkyne units coupled together and coordinated to ditungsten fragment has been obtained when tungsten hexacarbonyl was used to react with excess of ferrocenylacetylene in presence of UV-irradiation (Scheme 5.3).³⁵



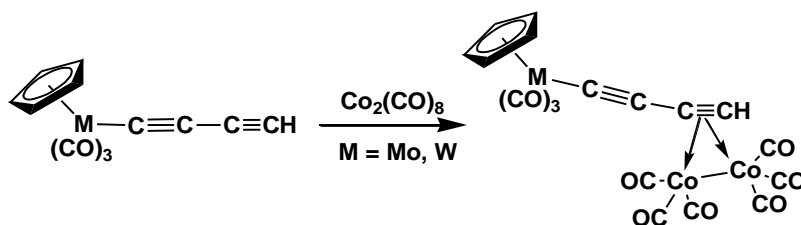
Scheme 5.3

Alkynes, being more electronegative, can bind with metals more strongly than corresponding alkenes. A variety of bonding modes exist where alkynes form adducts with metallic fragments. Akita et. al.³⁶ have reported the formation of several alkyne-metal adduct by the reaction of $[\text{Cp}^*\text{Fe}(\text{CO})_2-\text{C}\equiv\text{C}-\text{C}\equiv\text{C}-\text{H}]$ with $[\text{Co}_2(\text{CO})_8]$, $[\text{Mo}_2\text{Cp}_2(\text{CO})_4]$ or $[\text{CpMoCo}(\text{CO})_7]$ as shown in Scheme 5.4



Scheme 5.4

Similar reactivity has been observed when reaction of $[\text{Co}_2(\text{CO})_8]$ with the acetylide complexes, $[\text{M}(\text{C}\equiv\text{CC}\equiv\text{CR})(\text{CO})_3\text{Cp}]$ ($\text{M} = \text{Mo}, \text{W}$; $\text{R} = \text{H}$) was carried out to afford simple adducts containing a $\text{Co}_2(\text{CO})_6$ group attached to the least sterically-hindered $\text{C}\equiv\text{C}$ triple bond (Scheme 5.5).³⁷



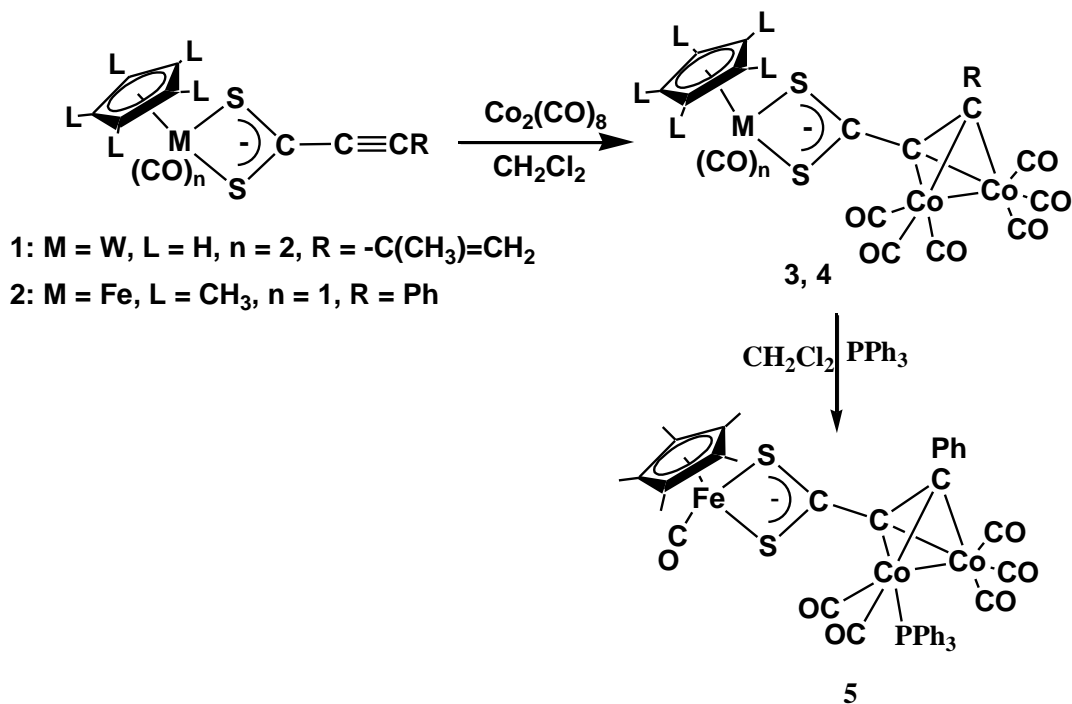
Scheme 5.5

The different facets of the alkyne reactivity have prompted us to undergo reactions with different types of alkynes and understand their behavior. In this chapter, we have described three different types of metal mediated transformations involving dithiocarboxylate-alkynes and ferrocenyl alkynes.

5.2. RESULTS AND DISCUSSION

5.2.1. Reaction of dithiocarboxylate-alkyne with $\text{Co}_2(\text{CO})_8$

Room temperature reaction of compounds $[\text{LM}(\text{CO})_n(\eta^2\text{-S}_2\text{C})\text{C}\equiv\text{CR}]$, [$\{\text{L}=\eta^5\text{-C}_5\text{H}_5, \text{M} = \text{W}, \text{R} = \text{-C}(\text{CH}_3)_3\text{CH}_2, n = 2\}$ (**1**); $\{\text{L}=\eta^5\text{-C}_5\text{Me}_5, \text{M} = \text{Fe}, \text{R} = \text{Ph}, n = 1\}$] (**2**) with dicobalt-octacarbonyl under inert atmospheric condition results in the formation of a dark colored compound, presumed to be the corresponding alkyne-cobalt carbonyl adducts **3** and **4** (Scheme 5.6). Infrared spectral data of **3** and **4** shows three peaks each in the region $2091\text{ cm}^{-1} - 2029.5\text{ cm}^{-1}$, which represents terminally bonded cobalt carbonyls and peaks at 1954 cm^{-1} , 1888 cm^{-1} and 1934 cm^{-1} have been observed due to terminal iron and tungsten carbonyl respectively. The Infrared peaks pattern observed for compound **3** and **4** in the region $2091\text{ cm}^{-1} - 2029.5\text{ cm}^{-1}$ exactly matches with that present in other alkyne-cobalt carbonyl adduct in the literature.^{38, 39} Proton NMR spectrum for **3** show peaks at δ 5.613 corresponding to $\eta^5\text{-C}_5\text{H}_5$, δ 2.221 (triplet) due to CH_3 group, δ 5.385 and δ 5.737 for olefinic protons (Figure 5.2). Spectrum for compound **6** reveals the presence of a methyl peak at δ 1.58 for $\eta^5\text{-C}_5\text{Me}_5$ unit and phenyl protons in the range δ 7.25-7.6. We have not been able to get good quality crystals for the structural evaluation of compounds **3** and **4** after several attempts to grow crystals in different solvent medium. Therefore, the proposed structures are based upon infrared, NMR and ESI-Mass spectroscopic data.



Scheme 5.6

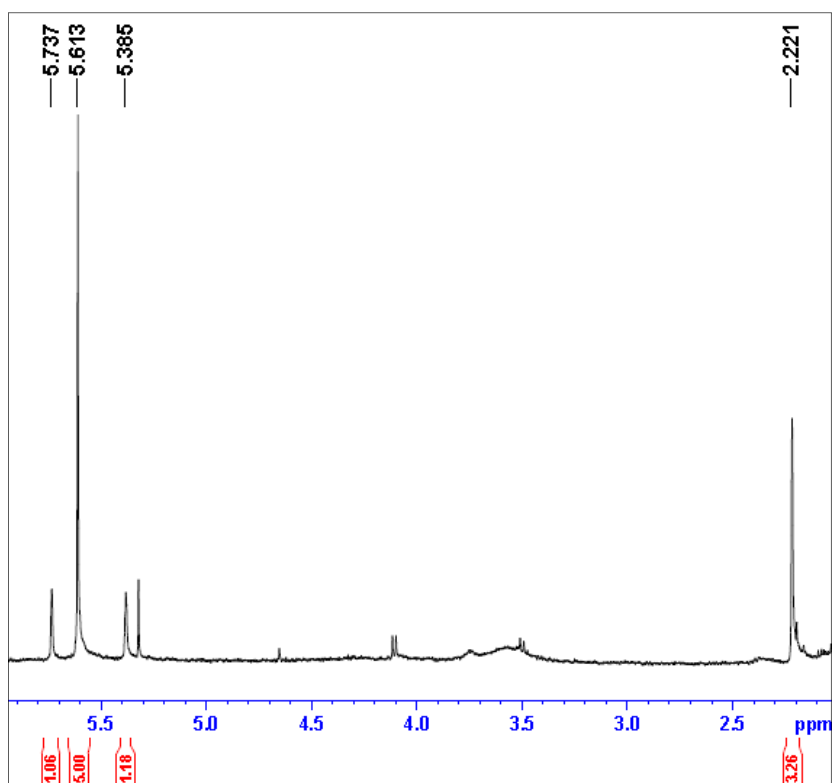


Figure 5.2 ^1H NMR Spectrum of **3**

To establish the proposed structure of **4**, we performed carbonyl substitution reaction with equimolar amount of triphenylphosphine. Room temperature stirring reaction of compound **4** with equivalent amount of PPh_3 for 24 hours led to the formation of a black colored compound (**5**) with a phosphine unit attached to one of the cobalt atom. The terminally bonded carbonyl attached to the iron with a ν_{CO} value at 1920 cm^{-1} remains intact as revealed by spectroscopic characterization. The Infrared spectral data shows the presence of peaks at $2061(\text{vs})$, $2019(\text{vs})$, $2004(\text{vs})$, $1970(\text{m})$ and 1920 cm^{-1} region. The peaks from 2061 cm^{-1} - 1970 cm^{-1} are due to the carbonyl groups attached to cobalt and peak at 1920 cm^{-1} reveals the presence of a carbonyl attached to iron atom. The IR peak pattern is similar to other phosphine substituted alkyne-cobalt compounds like $[\text{HCC}\{\text{Co}_2(\text{CO})_5(\text{PPh}_3)\}\text{CH}=\text{CH}-\text{C}_6\text{H}_4-\text{NO}_2]$ ³⁸ and $[\text{HCC}\{\text{Co}_2(\text{CO})_5(\text{PPh}_3)\}\text{CH}_2\text{-o-menthyl}]$ ⁴⁰. Proton NMR of **5** shows the presence of one $\eta^5\text{-C}_5\text{Me}_5$ and four phenyl groups at δ 1.613 and δ 6.92-7.3 region respectively and ^{31}P NMR peak was obtained at δ 43.3 corresponding to the triphenylphosphine attached to one of the cobalt atom (Figure 5.3).

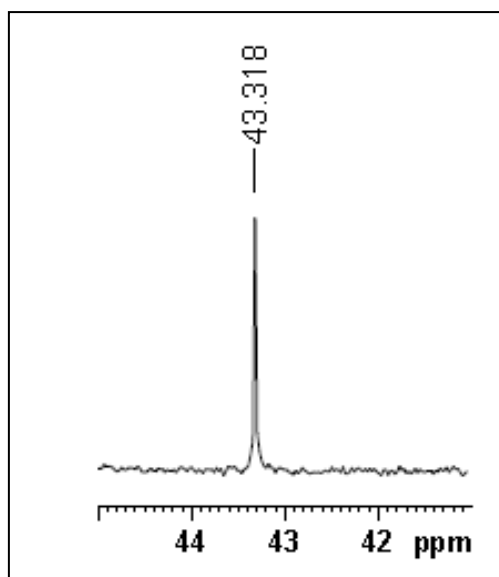
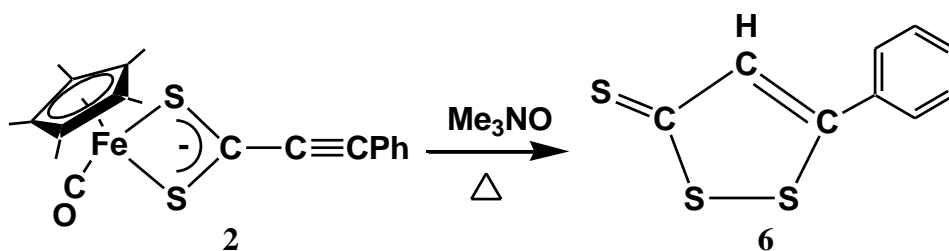


Figure 5.3 ^{31}P NMR Spectrum of **5**

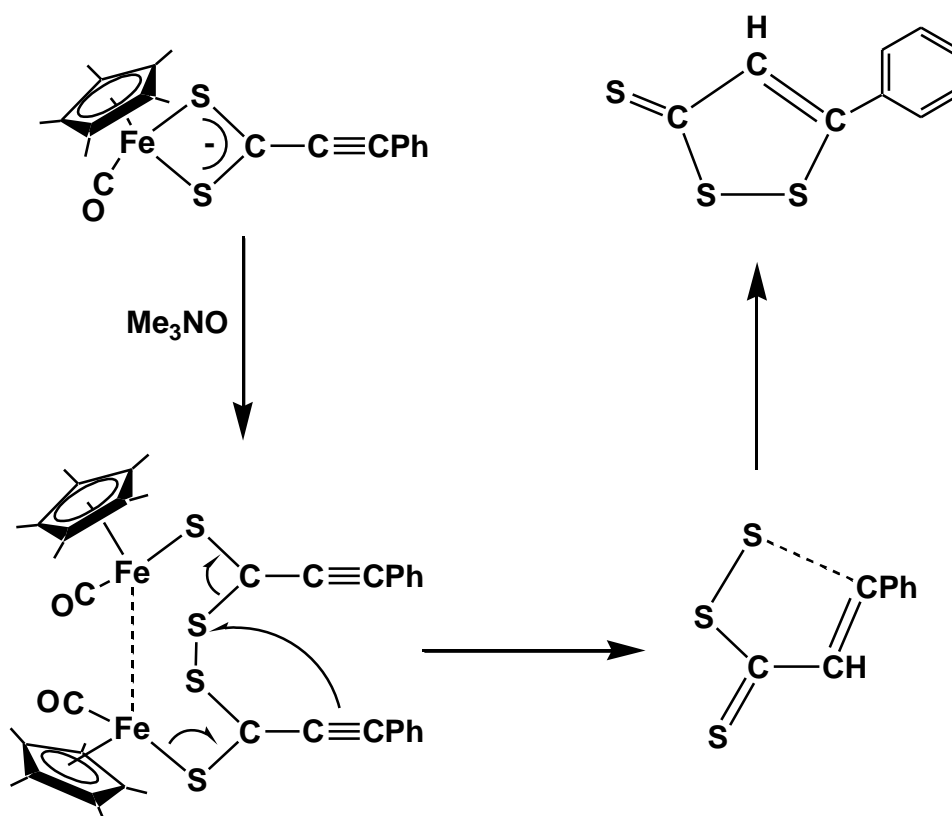
5.2.2. Transformation of $[(\eta^5\text{-C}_5\text{Me}_5)\text{Fe}(\text{CO})(\eta^2\text{-S}_2\text{C})\text{C}\equiv\text{CPh}]$ (**2**) to a dithiole heterocycle

Treatment of the iron-dithiocarboxylate-alkyne complex with trimethylamine N-oxide in thermal reaction condition results in the formation of a yellow colored compound, $[\text{C}(\text{S})\text{C}(\text{H})=\text{C}(\text{Ph})\text{S}_2]$ (**6**) (Scheme 5.7). The compound was isolated by preparative TLC and characterized by IR and NMR spectroscopy. IR spectra reveals the presence of C=S group with a peak at 1736 cm^{-1} while ^1H NMR spectral shows the presence of phenyl and =CH moieties in the region δ 7.0-7.4. Although, the NMR and IR data of compound **6** was compared with the literature value, we could able to confirm the compound. Therefore, we carried out low temperature crystallization method to obtain good quality single crystal for X-ray crystallographic study. Crystal structure of the same compound has been reported earlier by Mathur et. al.⁴¹



Scheme 5.7

The structural characterization was carried out with a single crystal obtained at -10°C with hexane/acetonitrile solvent mixture to confirm the structural identity. The structure shows the presence of a five membered ring containing a dithiole unit with a S-S bond distance of $2.053(3)\text{ \AA}$ and an olefinic group with a C=C bond distance of $1.357(11)\text{ \AA}$. A thiole unit is also linked to one of carbon atom having a double bond character (CS = $1.673(9)\text{ \AA}$) (Figure 5.4). The structure of compound **6** is similar to the earlier reported molecular structure by Mathur et. al.⁴¹ Although, the exact mechanism for the formation of the heterocycle is not known, but a tentative pathway can be predicted or proposed. It has been understood that two molecules of the metal dithiocarboxyle species are involved to give the product. The first step may be the initial rupture of Fe-S bond and formation intermolecular S-S bond. The formation iron-iron bond after the breaking of Fe-S bond cannot be ruled out to electronically saturate the metal fragment. Subsequently cyclization takes place involving two sulphur and three carbon units, resulting in the formation of dithione-thiole heterocycle (Scheme 5.8).



Scheme 5.8

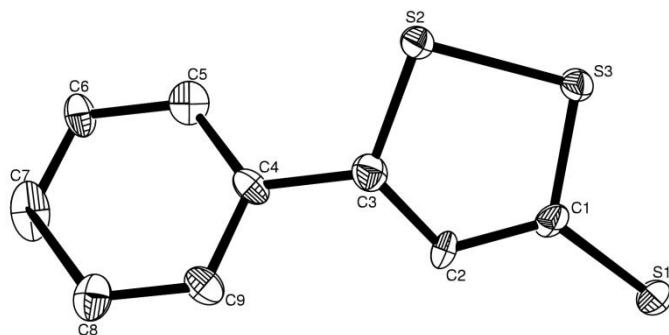
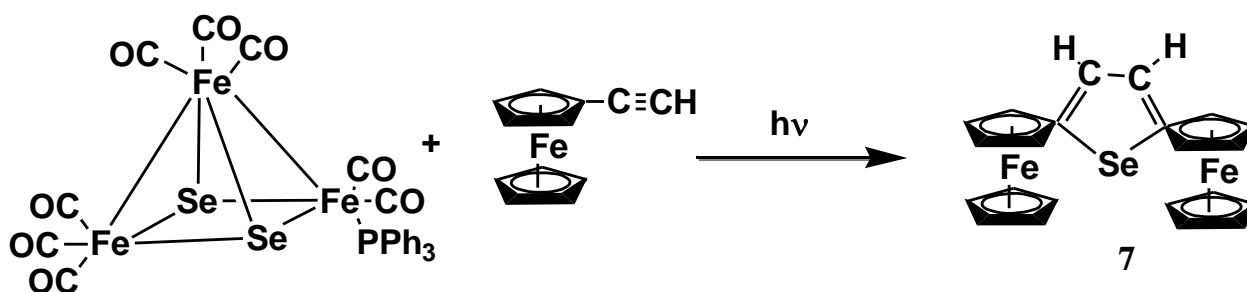


Figure 5.4: Molecular structure of **6**

5.2.3. Coupling of ferrocenyl alkynes by $[(CO)_8Fe_3Se_2(PPh_3)]$ cluster

Photolytic reaction of Ferrocenyl acetylene with iron –phosphine selenido cluster, $[(CO)_8Fe_3Se_2(PPh_3)]$ led to the formation of a yellow, diferrocenylselenophene compound in major amount. Trace amount of other compounds has been detected by TLC, but could not be isolated or characterized due to less yield of the products (Scheme 5.9). The major product was isolated by preparative TLC in n-hexane/ dichloromethane solvent mixture and characterized by NMR and ESI-MS spectroscopic technique. The 1H NMR spectrum of **7** has been compared with the literature value³¹ and reveals the presence of two ferrocenyl groups in the region δ 4.11-4.51, while the olefinic CH protons have been detected at δ 6.94 region (Figure 5.5). Two types of ferrocenyl Cp protons, one unsubstituted and another substituted Cp's, have been confirmed from the NMR spectrum. The spectrum also reveals the presence of 2,4 –isomer of diferrocenyl selenophene in trace amount, which could not be separated by TLC. The ESI mass spectrum shows M^+ ion peak at m/z 499.8 (Figure 5.6).



Scheme 5.9

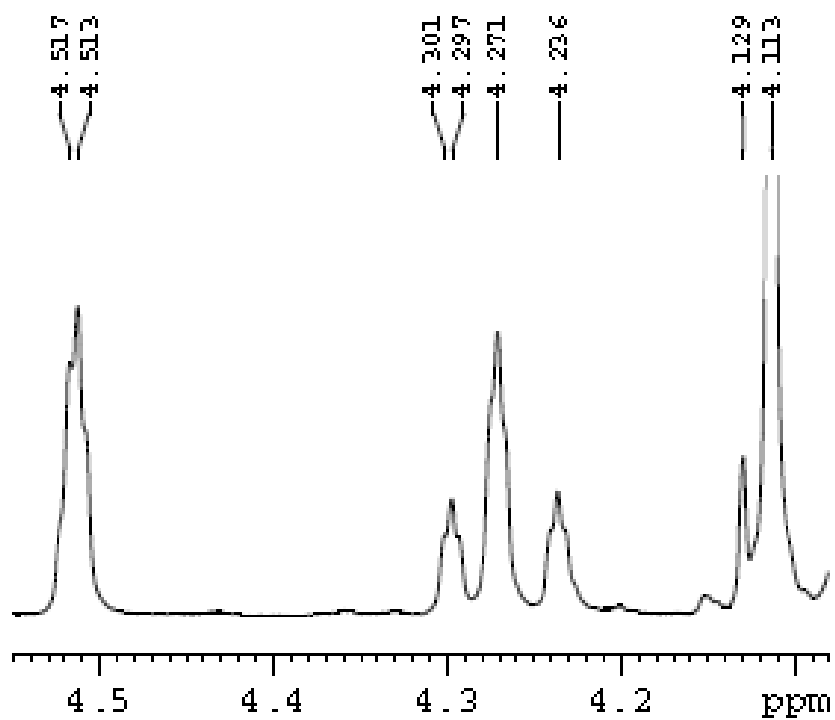


Figure 5.5 ^1H NMR of compound 7

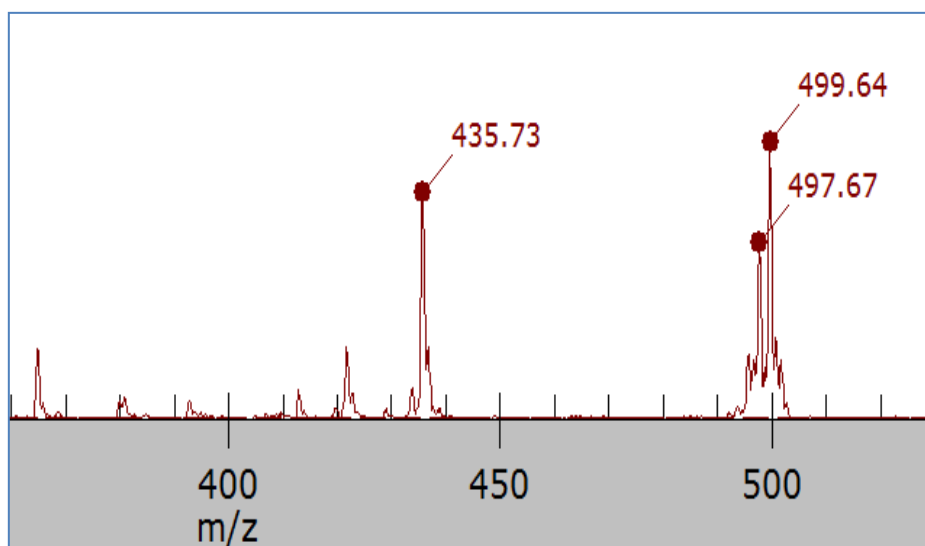


Figure 5.6 ESI-MS spectrum of 7

5.3. EXPERIMENTAL SECTIONS

5.3.1. General Procedures

All reactions and manipulations were carried out under an inert atmosphere of dry, pre-purified argon or nitrogen using standard schlenk line techniques. Solvents were purified, dried and distilled under an argon atmosphere prior to use. Infrared spectra were recorded on a Perkin Elmer Spectrum RX-I spectrometer as dichloromethane solutions and NMR spectra on a 400 MHz Bruker spectrometer in CDCl₃. Elemental analyses were performed on a Vario El Cube CHNS analyser. TLC plates (20x20 cm, Silica gel 60 F254) were purchased from Merck. FcC≡CH⁴² was prepared following the reported procedures and [LM(CO)_n(η²-S₂C)C≡CR] was synthesized by the procedure given in Chapter 4.

5.3.2. Reaction of **1** and **2** with dicobaltoctacarbonyl

In a two necked round bottomed flask, dichloromethane solution of 0.1 mmol of [LM(CO)_n(η²-S₂C)C≡CR]; {L=η⁵-C₅H₅, M = W, R = -C(CH₃)=CH₂, n = 2}(**1**); {L=η⁵-C₅Me₅, M = Fe, R = Ph, n = 1}(**2**) was taken and cooled to 0°C using an ice bath. To the solution mixture equivalent amount of Co₂(CO)₈ was added under inert atmosphere and continuously stirred for 1 hr in cold condition. The reaction was monitored using TLC. After the completion of the reaction, the mixture was dried under vacuum and dissolved in minimum amount of dichloromethane solvent. The solution was subjected to chromatographic workup using preparative TLC in dichloromethane / n-hexane (20:80 v/v) solvent mixture to isolate a dark colored compound [LM(CO)_n(η²-S₂C)CCR(CO₂CO₆)]; {L=η⁵-C₅H₅, M = W, R = -C(CH₃)=CH₂, n = 2}(**3**: 57 mg, 78 %); {L=η⁵-C₅Me₅, M = Fe, R = Ph, n = 1}(**4**: 55 mg, 82 %)).

3: IR(ν_{CO} , cm⁻¹, CH₂Cl₂): 2091 (s), 2057 (vs), 2029 (vs), 1954(vs), 1888 (s). ¹H NMR (δ, CDCl₃): 2.221 (br, 3H, -CH₃), 5.385 (m, 1H, =CH₂), 5.737 (m, 1H, =CH₂), 5.613 (s, 5H, η⁵-C₅H₅).

4: IR(ν_{CO} , cm⁻¹, CH₂Cl₂): 2091.5 (s), 2059 (vs), 2030 (vs), 1933.5(s). ¹H NMR (δ, CDCl₃): 1.58 (s, 15H), 7.25-7.6 (m, 5H, C₆H₅). MS (ESI): m/z 682 (M)⁺.

5.3.3. Reaction of **4** with triphenylphosphine

A dichloromethane solution of $[(\eta^5\text{-C}_5\text{Me}_5)\text{Fe}(\text{CO})(\eta^2\text{-S}_2\text{C})\text{CCPh}(\text{Co}_2\text{CO}_6)]$ (**4**) (0.1 mmol) was reacted with triphenylphosphine (0.1 mmol) at room temperature under continuous stirring condition and argon atmosphere for 20 hours. The reaction was monitored by TLC. On completion of the reaction the solution was dried under vacuum and the residue was dissolved in dichloromethane solvent and subjected to chromatographic work-up using preparative TLC. Elution with dichloromethane / hexane (30:70 v/v) solvent mixture separated the following compounds: unreacted $[(\eta^5\text{-C}_5\text{Me}_5)\text{Fe}(\text{CO})(\eta^2\text{-S}_2\text{C})\text{CCPh}(\text{Co}_2\text{CO}_6)]$ (15 mg), black colored $[(\eta^5\text{-C}_5\text{Me}_5)\text{Fe}(\text{CO})(\eta^2\text{-S}_2\text{C})\text{CCPh}(\text{Co}_2\text{CO}_5\text{PPh}_3)]$ (**5**) (Yield= 46 mg, 72 %). Trace amount of decomposition was also observed during the workup.

5: IR(ν_{CO} , cm^{-1} , CH_2Cl_2): 2061 (vs), 2019 (vs), 2004.6 (vs), 1971 (w), 1919 (s). ^1H NMR (δ , CDCl_3): 1.613 (s, 15H), 6.2-7.3 (m, 20H, C_6H_5). $^{31}\text{P}\{^1\text{H}\}$ NMR(δ): 43.3. MS (ESI): m/z 918 ($\text{M}+2$)⁺.

5.3.4. Synthesis of dithione-thiole heterocycle

An acetonitrile solution of $[(\eta^5\text{-C}_5\text{Me}_5)\text{Fe}(\text{CO})(\eta^2\text{-S}_2\text{C})\text{C}\equiv\text{CPh}]$ (**2**) was taken in a two necked round bottomed flask fitted with a condenser and added an equimolar amount of trimethylamine N-oxide under an inert atmosphere. The reaction mixture was heated to 60 °C under constant stirring condition for 1 hr. The reaction was continuously monitored using TLC. After all the reactant was consumed, the mixture was vacuum dried and dissolved in dichloromethane solvent. The solution was subjected to chromatographic work up using 30 % n-hexane/dichloromethane solvent mixture to isolate a yellow colored compound $[\text{C}(\text{S})\text{C}(\text{H})=\text{C}(\text{Ph})\text{S}_2]$ (**6**). (Yield = 13 mg, 65%).

6: IR(ν_{CO} , cm^{-1} , CH_2Cl_2): 2959 (vs), 2925 (vs), 2854 (vs), 1736 (br, s), 1715 (s), 1463 (s), 1261(m). ^1H NMR (δ , CDCl_3): 7.504 (s, 1H, CH), 7.441-7.70 (m, 5H, Ph).

5.3.5. Photolytic reaction of ferrocenyl alkynes with $[(\text{CO})_8\text{Fe}_3\text{Se}_2(\text{PPh}_3)]$

A mixture of $[\text{Fe}_3\text{Se}_2(\text{CO})_8(\text{PPh}_3)]$ (0.1 mmol) and Ferrocenyl acetylene (0.2 mmol) in n-hexane solution was exposed to UV irradiation at -10°C under an inert atmospheric condition. After 15 minutes the solution color changes to orangish-yellow. The solution was vacuum dried and the residue was subjected to chromatographic work-up using preparative

TLC with dichloromethane / hexane (20:80 v/v) solvent mixture. The compound obtained on subsequent elution is trace amount of the reactants and a pale yellow compound [$\{(\eta^5\text{-C}_5\text{H}_5)_2\text{Fe}\}\text{C}_2\text{H}_2\text{Se}\{(\eta^5\text{-C}_5\text{H}_5)_2\text{Fe}\}$] (**7**). (Yield = 22 mg, 46 %).

7: ^1H NMR (δ , CDCl_3): 4.11 (s, 10H, $\eta^5\text{-C}_5\text{H}_5$), 4.27 (t, 4H, $\eta^5\text{-C}_5\text{H}_4$), 4.51 (t, 4H, $\eta^5\text{-C}_5\text{H}_4$), 6.94 (s, 2H, $\text{CH}=\text{CH}$). ESI (MS): m/z 499.8 (M^+).

5.3.6. Crystal structure determination for **6**.

Single crystal X-ray structural studies of **6**, was performed on a CCD Oxford Diffraction XCALIBUR-S diffractometer equipped with an Oxford Instruments low-temperature attachment. Data were collected at 150(2) K using graphite-monochromated Mo $\text{K}\alpha$ radiation ($\lambda_\alpha = 0.71073 \text{ \AA}$). The strategy for the Data collection was evaluated by using the CrysAlisPro CCD software. The data were collected by the standard 'phi-omega scan techniques, and were scaled and reduced using CrysAlisPro RED software. The structures were solved by direct methods using SHELXS-97 and refined by full matrix least-squares with SHELXL-97, refining on F^2 .⁴³ The positions of all the atoms were obtained by direct methods. All non-hydrogen atoms were refined anisotropically. The remaining hydrogen atoms were placed in geometrically constrained positions and refined with isotropic temperature factors, generally $1.2U_{eq}$ of their parent atoms. The crystallographic details are summarized in Table 5.1.

5.4. CONCLUSIONS

Triiron selenido phosphine cluster have shown to undergo transformation of ferrocenyl alkynes to diferrocenyl selenophene. Although, the exact mechanism for the transformation is difficult to identify, but the involvement of one or more metal is understandable. We have also described the transformation of the carbon-carbon triple bond in alkynyl dithiocarboxylato complex, $[(\text{Cp}^*)\text{Fe}(\text{CO})(\eta^2\text{-S}_2\text{CC}\equiv\text{CPh})]$ by a cobalt cluster and subsequent synthesis of trimetallic-dithiocarboxylate cluster complex. In another transformation study, a dithiole-thione heterocycle has been obtained when metal containing dithiolato-alkyne complexes was exposed to oxidation and other reaction condition. It is worth mentioning that dithiole-thione derivatives are an important class of chemoprotective agents and used for various medicinal purposes.

Table 5.1: Crystal data and structure refinement parameters for compound **6**.

6	
Empirical formula	C ₃₆ H ₂₄ S ₁₂
Formula weight	841.27
Crystal system	Orthorhombic,
Space group	P b c a
<i>a</i> , Å	12.0872(10)
<i>b</i> , Å	7.4386(5)
<i>c</i> , Å	19.9725(15)
<i>α</i> deg	90
<i>β</i> deg	90
<i>γ</i> deg	90
<i>V</i> , Å ³	1795.8(2)
<i>Z</i>	2,
<i>D</i> _{calcd} , Mg m ⁻³	1.556
abs coeff, mm ⁻¹	0.759
<i>F</i> (000)	864
Cryst size, mm	0.33 x 0.29 x 0.23
<i>θ</i> range, deg	3.37 to 25.00
index ranges	-13 ≤ <i>h</i> ≤ 14, -8 ≤ <i>k</i> ≤ 8, -23 ≤ <i>l</i> ≤ 23
reflections collected/ unique	12046 / 1581 [R(int) = 0.1317]
data/ restraints / parameters	1581 / 0 / 109
goodness-of-fit on <i>F</i> ²	1.454
Final R indices [I > 2σ(I)]	R1 = 0.1369, wR2 = 0.1899
R indices (all data)	R1 = 0.1736, wR2 = 0.2025
largest diff peak	0.603
and hole, eÅ ⁻³	-0.622

5.5. REFERENCES

1. P. Mathur, D. Chakraborty, I. J. Mavunkal, *J. Cluster Sci.* 4 (1993) 351.
2. P. Mathur, S. Chatterjee, Y. V. Torubaev, *J. Cluster Sci.* 18 (2007) 505.
3. P. Mathur, S. Chatterjee, V. D. Avasare, *Adv. Organomet. Chem.*, 55 (2008) 201.
4. R. D. Adams, E. Boswell, *Organometallics*, 27 (2008) 2021.
5. P. Mathur, D. Chakraborty, I. J. Mavunkal, *J. Cluster Sci.*, 4 (1993) 351.
6. P. Mathur, V. D. Avasare, A. K. Ghosh, S. M. Mobin, *J. Organomet. Chem.* 689 (2004) 1325.
7. (a) I. R. Whittall, A. M. McDonagh, M. G. Humphrey, M. Samoc, *Adv. Organomet. Chem.* 42 (1998) 291; (b) I. R. Whittall, A. McDonagh, M. G. Humphrey, M. Samoc, *Adv. Organomet. Chem.* 43 (1999) 349; (c) J. Heck, S. Dabek, T. Meyer-Friedrichsen, H. Wong, *Coord. Chem. Rev.* 190_ 192 (1999) 1217; (d) S. Di Bella, *Chem. Soc. Rev.* 30 (2001) 355.
8. (a) T.T.J. Müller, A. Netz, M. Ansorge, E. Schmalzin, C. Brauchle, K. Meerholz, *Organometallics* 18 (1999) 5066; (b) M. Tamm, A. Grzegorzewski, T. Steiner, T. Jentzsch, W. Werncke, *Organometallics* 15 (1996) 4984; (c) I.S. Lee, H. Seo, Y.K. Chung, *Organometallics* 18 (1999) 1091; (d) H. Wong, T. Meyer-Friedrichsen, T. Farrell, C. Mecker, J. Heck, *Eur. J. Inorg. Chem.* 4 (2000) 631.
9. W. Reppe, O. Schlichting, K. Klager, T. Toepel, *J. Liebigs Ann. Chem.* 561 (1948) 1.
10. (a) Hübel, W. In *Organic Synthesis via Metal Carbonyls*; Wender, I., Pino, P., Eds.; Wiley: New York, 1968; Vol. 1, p 273, and references therein. (b) Hübel, W.; Braye, E. H. *J. Inorg. Nucl. Chem.* 10 (1959) 250.
11. J. Cooke, J. Takats, *J. Am. Chem. Soc.* 119 (1997) 11088.
12. F. R. Young, D. H. O'Brien, R. C. Pettersen, R. A. Levenson, D. L. V. Minden, *J. Organomet. Chem.* 114 (1976) 157.
13. A. Efraty, R. Bystrek, J. A. Geaman, M. H. A. Huang, R. H. Herber, *Synthesis* 6 (1971) 305.
14. N. G. Pschirer, W. Fu, R. D. Adams, H. F. Bunz, *Chem. Commun.* (2000) 87.
15. R. D. Adams, J. A. Queisser, J. H. J. Yamamoto, *Am. Chem. Soc.* 118 (1996) 10674.
16. R. D. Adams, J. H. Yamamoto, *Organometallics* 16 (1997) 1430.
17. R. D. Adams, J. L. Perrin, *J. Am. Chem. Soc.* 121 (1999) 3984.
18. C.W. Shiu, Y. Chi, C. Chung, S. M. Peng, G. H. Lee, *Organometallics* 17 (1998) 2970.
19. M. Akita, M. Terada, Y. Moro-oka, *Chem. Commun.* (1997) 265.

20. E. Sappa, *J. Clust. Sci.* 5 (1994) 211.
21. E. Sappa, A. Tiripicchio, P. Braunstein, *Chem. Rev.* 83 (1983) 203.
22. P. Blenkinsop, G. D. Enright, P. J. Low, J. F. Corrigan, N. J. Taylor, Y. Chi, J. Y. Saillard, A. J. Carty, *Organometallics* 17(1998) 2447.
23. M. I. Bruce, M. Ke, P. J. Low, *Chem. Commun.* (1996) 2405.
24. I. M. Irwin, G. Jia, N. C. Payne, R. J. Puddephatt, *Organometallics* 15(1996) 51.
25. O. Lavastre, J. Plass, P. Bachmann, S. Guesmi, C. Moinet, P. H. Dixneuf, *Organometallics* 16 (1997) 184.
26. A. A. Cherkas, S. Doherty, M. Cleroux, G. Hogarth, L. H. Randall, S. M. Breckenridge, N. J. Taylor, A. Carty, *J. Organomet. Chem.* 11 (1992) 1701.
27. (a) S. Houbrechts, K. Calys, A. Persoons, V. Cadierno, M. P. Gamasa, J. Gimeno, *Organometallics* 15 (1996) 5266; (b) I. R. Whittall, M. G. Humphrey, S. Houbrechts, A. Persoons, D. C. R. Hockless, *Organometallics* 15 (1996) 5738; (c) I. R. Whittall, M. P. Cifuentes, M. G. Humphrey, B. Luther-Davies, M. Samoc, S. Houbrechts, A. Persoons, G. A. Heath, D. Begasany, *Organometallics* 16 (1997) 2681; (d) A. M. McDonagh, M. G. Humphrey, M. Samoc, B. Luther-Davies, S. Houbrechts, T. Wada, H. Sasabe, A. Persoons, *J. Am. Chem. Soc.* 121 (1999) 1405; (e) S. K. Hurst, M. P. Cifuentes, J. P. L. Morrall, N. T. Lucas, I. R. Whittall, M. G. Humphrey, I. Asselberghs, A. Persoons, M. Samoc, B. Luther-Davies, A. C. Willis, *Organometallics* 20 (2001) 4664;
28. R. H. Crabtree, *The Organometallic Chemistry of Transition Metals*, 3rd ed., Wiley, New York, 2001, p. 15.
29. I. S. Lee, D. M. Shin, Y. Yoon, S. M. Shin, Y. K. Chung, *Inorg. Chim. Acta.* 343 (2003) 41.
30. M. Periasamy, A. Mukkanti, D. S. Raj, *Organometallics* 13 (2004) 6323.
31. P. Mathur, A. K. Singh, V. K. Singh, P. Singh, R. Rahul, S. M. Mobin, C. Thöne, *Organometallics* 24 (2005) 4793
32. P. Mathur, A. K. Bhunia, S. M. Mobin, V. K. Singh, Ch. Srinivasu, *Organometallics* 23 (2004) 3694.
33. P. Mathur, S. Chatterjee, A. Das, G. K. Lahiri, S. Maji, S. M. Mobin, *J. Organomet. Chem.* 692 (2007) 1601.
34. P. Mathur, S. Chatterjee, A. Das, S. M. Mobin, *J. Organomet. Chem.* 692 (2007) 819.
35. P. Mathur, S. Chatterjee, A. Das, S. M. Mobin, *J. Organomet. Chem.* 692 (2007) 819.
36. M. C. Chung, A. Sakurai, M. Akita, Y. Moro-oka, *Organometallics* 18 (1999) 4684.
37. M. I. Bruce, J. F. Halet, S. Kahlal, P. J. Low, B. W. Skelton, A. H. J. White, J.

Organomet. Chem. 578 (1999) 155.

38. I. S. Lee, D. M. Shin, Y. Yoon, S. M. Shin, Y. K. Chung, Synthesis and non-linear optical properties of (alkyne)dicobalt octacarbonyl complexes and their substitution derivatives,

Inorg. Chim. Acta.343 (2003) 41.

39. C. Moreno, M. L. Marcos, G. Domínguez, A. Arnanz, D. H. Farrar, R. Teeple, A. Lough, J. González-Velasco, S. Delgado, Synthesis and electrochemical study of cobalt carbonyl

complexes of trimethylsilyl-substituted 1,3,5-triethynylbenzene, J. Organomet. Chem. 631 (2001) 19.

40. M. F. D'Agostino, C. S. Frampton, M. J. McGlinchey, Organometallics, 9 (1990) 2972.

41. P. Mathur, V. D. Avasare, A. K. Ghosh, S. M. Mobin, J. Organomet. Chem. 689 (2004) 1325.

42. G. Doisneau, G. Balavonie, T. F. Khan, J. Organomet. Chem. 425 (1992) 113.

43. G. M. Sheldrick, A short history of *SHELX*, Acta Cryst. A 64 (2008) 112.

SUMMARY

Transition metal cluster complexes continues to be a special area of recent organometallic chemistry because of their potential applicability in various fields, from organic synthesis to advanced electronic material. Chapter 1 introduces various aspects of transition metal clusters mainly on the synthesis, reactivity and application of different types of metal cluster and their future scope in chemical sciences. A large variety of organometallic transition metal clusters have been known containing homo or hetero metal atoms, a range of terminal and bridging ligands and with unique structural geometries. Facile synthesis and stability of higher nuclear transition metal clusters with unusual properties have been a key challenge for the development of cluster chemistry. In spite of that, some methodologies for obtaining novel mixed metal clusters of desired structural and reactivity features have been developed in current years. We have been equally interested to explore the reactivity of metal clusters towards cluster growth reactions and recognize the effect of 'naked' chalcogen atoms and other bridging groups in stabilization of the cluster framework.

In Chapter 2, we have described the synthesis of bis(diphenylphosphino)methane coordinated triiron tellurium cluster, $[\text{Fe}_3\text{Te}_2(\text{CO})_8(\mu\text{-dppm})]$ (**2.4**) from a triiron telluride compound using a facile reaction condition. The two-step reaction strategy includes substitution of carbonyl ligands first by a triphenylphosphine group and then using a more basic diphosphine ligand to substitute the PPh_3 moiety. Compound **2.4** has been characterized by FTIR and ^1H and ^{31}P NMR spectroscopy. The molecular structure of **2.4** has been confirmed by single crystal X-ray diffraction technique. In a cluster expansion reaction, two new bis(diphenylphosphino)ethane coordinated clusters $[(\text{CO})_{18}\text{Fe}_6(\mu_3\text{-Te})_4\{\mu\text{-PPh}_2(\text{CH}_2)_2\text{PPh}_2\}]$ (**2.5**) and $[\text{Fe}_3(\mu_3\text{-Te})_2(\text{CO})_8\{\text{PPh}_2(\text{CH}_2)_2\text{PPh}_2\}]$ (**2.6**) were obtained by a room temperature reaction under inert atmospheric condition. Both the clusters have been characterized using FTIR, ^1H NMR, ^{31}P NMR and single crystal diffraction studies. The molecular structures of **2.5** and **2.6** have been established by single crystal X-ray diffraction study and discussed in details with the mention of bond lengths and bond angles.

Chapter 3 describes the synthesis and structural characterization of $[(\text{CO})_6\text{Fe}_2\text{PdY}_2(\text{PPh}_3)_2]$ ($\text{Y} = \text{Se}$ (**3.6**), Te (**3.7**)) from triiron-chalcogenide cluster using trimethylamineoxide. We have also reported the synthesis of four new iron-palladium mixed metal clusters containing diphosphine ligand in different bonding modes. The mixed metal clusters, $[(\text{CO})_{12}\text{Fe}_4\text{Y}_4\text{Pd}_2(\text{dppm})_2]$ ($\text{Y} = \text{Se}$ (**3.8**), Te (**3.9**)), obtained by the reaction of $[(\text{CO})_6\text{Fe}_2\text{PdY}_2(\text{PPh}_3)_2]$ ($\text{Y} = \text{Se}$ (**3.6**), Te (**3.7**)) with bis(diphenylphosphino)methane,

contain two diphosphine units forming a bridge between two cluster framework, while the clusters $[(\text{CO})_6\text{Fe}_2(\mu_3\text{-Y})_2\text{Pd}\{\text{PPh}_2(\text{CH}_2)_2\text{PPh}_2\}]$ ($\text{Y}=\text{Se}$ **(3.10)**; $\text{Y}=\text{Te}$ **(3.11)**) having a chelating type of diphosphine coordination, have been obtained using bis(diphenylphosphino)ethane ligand. The variation in cluster coordination has been attributed to different factors like diphosphine chain length, metallic framework and strain in between the phosphorus atoms of a diphosphine unit. The contrasting results show the difference in reactivity between the cluster species and the influence of phosphines in controlling the cluster synthesis.

Synthesis of metal complexes containing several metal binding sites has been an important strategy to obtain multi-metallic cluster compounds. In an effort to synthesize such molecules, we have described in Chapter 4, the preparation of dithiocarboxylate-alkyne metal complexes by using a renewable source of energy in presence of sunlight reaction condition. We have described the synthesis of a variety of transition metal dithiocarboxylate-alkyne complexes, $[(\eta^5\text{-C}_5\text{H}_5)\text{W}(\text{CO})_3(\eta^2\text{-S}_2\text{C})\text{C}\equiv\text{C-C}(\text{CH}_3)=\text{CH}_2]$ **(4.4)**, $[(\eta^5\text{-C}_5\text{H}_5)\text{Mo}(\text{CO})_3(\eta^2\text{-S}_2\text{C})\text{C}\equiv\text{C-C}(\text{CH}_3)=\text{CH}_2]$ **(4.5)** and $[(\eta^5\text{-C}_5\text{Me}_5)\text{Fe}(\text{CO})_2(\eta^2\text{-S}_2\text{C})\text{C}\equiv\text{CPh}]$ **(4.6)** by the insertion reaction of carbondisulfide into metal-carbon acetylide bond using sunlight as activation agent. Three different dithiocarboxylate-alkyne complexes have been characterized by spectroscopic techniques and structural characterization of the two complexes have been carried out by single crystal X-ray diffraction studies. We have also been able to understand the electronic properties of iron dithiocarboxylate complexes by carrying out DFT calculations and electron charge distribution studies. Frontier molecular orbitals involved in the electronic transition of iron dithiocarboxylate-alkyne complexes was determined by TD-DFT calculation. Electron charge density on different atoms was also calculated to understand the charge distribution.

In Chapter 5, we have focussed our study to understand the behaviour of the synthesized molecules on the metal mediated transformation of different alkynes. Three different types of metal mediated organic transformations have been carried out and their tentative mechanism was discussed. Triiron-selenido phosphine cluster have shown to undergo transformation of ferrocenyl alkynes to diferrocenyl selenophene **(5.7)**. Although, the exact mechanism for the transformation is difficult to identify, but the involvement of one or more metal is understandable. We have also described the transformation of the carbon-carbon triple bond in alkynyl dithiocarboxylate complex, $[(\text{Cp}^*)\text{Fe}(\text{CO})(\eta^2\text{-S}_2\text{CC}\equiv\text{CPh})]$ by dicobaltoctacarbonyl cluster and subsequent synthesis of trimetallic-dithiocarboxylate cluster

complex, $[(\eta^5\text{-C}_5\text{H}_5)\text{W}(\text{CO})_3(\eta^2\text{-S}_2\text{C})\text{CC}\{\text{C}(\text{CH})_3=\text{CH}_2\}\{\text{Co}_2\text{CO}_6\}]$ (**5.3**) and $[(\eta^5\text{-C}_5\text{Me}_5)\text{Fe}(\text{CO})_2(\eta^2\text{-S}_2\text{C})\text{CC}(\text{Ph})\{\text{Co}_2\text{CO}_6\}]$ (**5.4**). In another transformation study, a dithiolethione heterocycle, $[\text{C}(\text{S})\text{C}(\text{H})=\text{C}(\text{Ph})\text{S}_2]$ (**5.6**) has been obtained when metal containing dithiolato-alkyne complexes was exposed to oxidation and other reaction condition. The proposed mechanistic aspects of the transformations have also been discussed in this chapter.

Aknowledgements

First and foremost I would like to thank my supervisor, Professor SauravChatterjee for sharing his knowledge, taking his time to work with me and having the patience to assist me. Without his expertise and guidance, this thesis would not be written.

I am thankful to the Director, National Institute of Technology, Rourkela and the Head, Department of Chemistry, for providing me the use of all infrastructural facilities.

I sincerely thank Professor P. Rath, Professor K. M. Purohit and Professor G. Hota for evaluating my progress reports and seminars, their helpful comments and valuable discussion during the Ph.D programme

I am greatly indebted to Prof. R. K. Patel, Chemistry Department, for his selfless support and advice and for extending the necessary infrastructural facilities when I joined this department as a research scholar.

I would like to thank Dr. S. M. Mobin, IIT, Indore for Single crystal X-ray crystallography and Dr. S. Saha, IIT BHU for D.F.T. studies and related discussion.

It is my great pleasure to thank all my past and present colleagues, Vijayalakshmi, Sagarika, Subhashree, Sasmita, Saswati, Satabdi, Satish, Paresh, Ashis, Deepak, Puspanjali, Abhishek for their help and cooperation during my Ph.D.

I would like to thank all the faculty members and office staff of the Department of Chemistry, for the help they have rendered from time to time.

I take this opportunity to thank Mr. B. K. Panda, Mr. P. C. Naik, Mr. J. K. Sahu, Mr. K. C. Bhoi and all my friends and colleagues in my college who have taken so much interest in my work and have been in my side through the ups and downs of my research.

Lastly but most importantly, I would like to thank my spouse, my kid and my parents for all they have done for me, sacrifice, love, encouragement, unfailing moral support..... What I am today, would not have been possible if it were not for their love, blessings and good wishes.

No words are adequate to express my gratitude to them.....

Sumanta Kumar Patel

Bio-data

Name:- Mr. Sumanta Kumar Patel
Date of Birth:- 21st April 1967
Educational qualification:- M. Sc. in Chemistry, Sambalpur University
Present position:- Lecturer, Department of Chemistry,
Kuchinda college, Kuchinda
Area of research interest :- Synthesis, characterization and reactivity
of transition metal clusters
Address:- 7/7, Rajiv Gandhi Circle, Kuchinda,
Dist.-Sambalpur, Odisha-768222

List of Publications:-

1. Synthesis and characterization of diphosphine bridged homo and heterometallic clusters containing chalcogen as “naked” atoms.
S. Chatterjee , S. K. Patel, S. M. Mobin, J. Organomet. Chem. 696 (2011) 1782.
2. Synthesis and characterization of bridged and chelated diphosphine coordinated transition metal chalcogenide clusters, $[(CO)_{18}Fe_6\mu_3-Te)_4\{\mu-PPh_2(CH_2)_2PPh_2\}]$ and $[(CO)_nFe_2\mu_3-Y)_2M\{PPh_2-R-PPh_2\}]$, [Y = Se, Te; M = Pd, Fe; n = 6, 8; R = $\{(\eta^5-C_5H_4)_2Fe\}$, $\{(CH_2)_2\}$]
S. Chatterjee , S. K. Patel, V. Tirkey, S. M. Mobin, J. Organomet. Chem., 699 (2012) 12.
3. Synthesis of mono- and bi-metallic alkynyldithiocarboxylate complexes from sunlight driven insertion reaction and their biological activity
S.K. Patel, V. Tirkey, S. Mishra, H.R. Dash, S. Das, M. Shukla, S. Saha, S.M. Mobin, S.Chatterjee, J. Organomet. Chem., 749 (2014) 75.
4. Transition metal mediated transformation of organic moieties
S. K. Patel, V. Tirkey, S. M. Mobin, S. Chatterjee, (Manuscript under preparation)
5. Synthesis, characterization and anti-cancer property of Cp based half sandwich complexes
S. Mishra, S. K. Patel, V. Tirkey, S. Bhutia, S. M. Mobin, S. Chatterjee
(Manuscript under preparation)